



ADRIANO REIS PRAZERES MASCARENHAS

**ASSOCIAÇÃO DE MICRO/NANOFIBRILAS CELULÓSICAS
E SILICATOS: ESTUDO DA SUSPENSÃO, FILMES E
PERFORMANCE NO REVESTIMENTO DE PAPEL CARTÃO**

**LAVRAS - MG
2022**

ADRIANO REIS PRAZERES MASCARENHAS

**ASSOCIAÇÃO DE MICRO/NANOFIBRILAS CELULÓSICAS E SILICATOS:
ESTUDO DA SUSPENSÃO, FILMES E PERFORMANCE NO REVESTIMENTO DE
PAPEL CARTÃO**

Tese apresentada à Universidade Federal de Lavras como parte das exigências do Programa de Pós-Graduação em Ciência e Tecnologia da Madeira, área de concentração Ciência e Tecnologia da Madeira, para obtenção do título de Doutor.

Prof. Dr. Gustavo Henrique Denzin Tonoli
Orientador

Dra. Maria Alice Martins
Coorientadora

**LAVRAS - MG
2022**

**Ficha catalográfica elaborada pelo Sistema de Geração de Ficha Catalográfica da Biblioteca
Universitária da UFLA, com dados informados pelo(a) próprio(a) autor(a).**

Mascarenhas, Adriano Reis Prazeres.

Associação de micro/nanofibrilas celulósicas e silicatos: estudo da suspensão, filmes e performance no revestimento de papel cartão / Adriano Reis Prazeres Mascarenhas. - 2022.

171 p. : il.

Orientador(a): Gustavo Henrique Denzin Tonoli.

Coorientador(a): Maria Alice Martins.

Tese (doutorado) - Universidade Federal de Lavras, 2022.

Bibliografia.

1. Biopolímeros. 2. Celulose Microfibrilada (MFC). 3. Nanotecnologia. I. Tonoli, Gustavo Henrique Denzin. II. Martins, Maria Alice. III. Título.

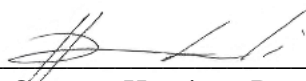
ADRIANO REIS PRAZERES MASCARENHAS

**ASSOCIAÇÃO DE MICRO/NANOFIBRILAS CELULÓSICAS E SILICATOS:
ESTUDO DA SUSPENSÃO, FILMES E PERFORMANCE NO REVESTIMENTO DE
PAPEL CARTÃO**

**ASSOCIATION OF CELLULOSIC MICRO/NANOFIBRILS AND SILICATES:
STUDY OF SUSPENSION, FILMS AND PERFORMANCE IN PAPERBOARD
COATING**

Tese apresentada à Universidade Federal de Lavras como parte das exigências do Programa de Pós-Graduação em Ciência e Tecnologia da Madeira, área de concentração Ciência e Tecnologia da Madeira, para obtenção do título de Doutor.

APROVADA em 2 de setembro de 2022.
Dra. Elaine Cristina Lengowski UFMT
Dr. Francys Kley Vieira Moreira UFSCar
Dr. Pedro Fardim KU Leuven
Dr. Pedro Henrique Gonzalez de Cademartori UFPR



Prof. Dr. Gustavo Henrique Denzin Tonoli
Orientador

**LAVRAS - MG
2022**

AGRADECIMENTOS

À Deus pela minha vida e por permitir que tivesse saúde física e mental para conclusão do doutorado.

À Universidade Federal de Lavras (UFLA) e ao Programa de Pós-Graduação em Ciência e Tecnologia da Madeira (PPGCTM) pela infraestrutura e recursos humanos disponibilizados.

Aos professores do PPGCTM que contribuíram significativamente no aperfeiçoamento de meus conhecimentos.

Ao Conselho Nacional de Desenvolvimento Científico e Tecnológico (CNPq - Código de financiamento 314203/2018-4), Fundação de Amparo à Pesquisa de Minas Gerais (FAPEMIG - Código de financiamento CAG APQ-03248-17) pelo apoio financeiro.

À Embrapa Instrumentação e à Klabin S.A. pela disponibilidade de insumos e equipamentos para a análise dos materiais deste trabalho.

À Universidade Federal de Rondônia (UNIR) pela concessão do afastamento e aos colegas do Departamento Acadêmico de Engenharia Florestal (DAEF) por todo apoio e compreensão, o que me deu mais tranquilidade para vencer esta etapa.

Ao Laboratório de Microscopia Eletrônica (LME) e à Central de Análise e Prospecção Química (CAPQ) da UFLA pela realização de análises e disponibilização de equipamentos.

Ao meu orientador, Prof. Gustavo Henrique Denzin Tonoli, por ser sempre disponível, pelos incentivos e pela ajuda na definição de estratégias para execução da tese e definição das abordagens para escrita dos artigos derivados. Agradeço ainda as conversas e ajuda que prestou desde o início do curso.

À minha coorientadora, Dra. Maria Alice Martins, pelas orientações e contribuições no projeto e intermediação de análises.

Aos membros das bancas de defesa de projeto (Mário Vanoli Scatolino e Maria Alice Martis), qualificação (Iara Demuner, Joabel Raabe e Rafael Rodolfo de Melo) e tese (Elaine Cristina Lengowski, Francys Kley Vieira Moreira, Pedro Fardim e Pedro Henrique Gonzalez de Cademartori) pelas valiosas contribuições.

Ao Mário Vanoli Scatolino, Matheus Cordazzo Dias e Maressa Carvalho Mendonça por toda ajuda nos ensaios e estruturação do texto dos artigos. Agradeço ainda ao Lorrán de Sousa Arantes pela parceria e ajuda para o desenvolvimento desta tese.

À minha esposa, Sabrina Neres Ribeiro, pelo carinho, apoio e motivação em todos os momentos do doutorado nas alegrias e decepções de forma incondicional. Sou muito grato a você por tudo, te amo demais!

Aos meus pais, Everaldo Nunes Mascarenhas e Elcemy de Maria Reis Prazeres Mascarenhas, meu irmão Matheus Reis Prazeres Mascarenhas e familiares que sempre me deram apoio em todas as etapas da minha vida.

Aos meus sogros, Erli Neres Ribeiro e Joãomar Ribeiro, que também são meus pais e me deram apoio e motivação em todo os momentos.

À equipe do Laboratório de Nanotecnologia Florestal por terem me acolhido, pela paciência e disponibilidade em passar os conhecimentos.

Aos membros do Núcleo de Estudos em Nanotecnologia Florestal (NENF) e Núcleo de Estudos em Madeira (NEMAD) pela oportunidade de contribuir na realização de eventos e discussões sobre temas relativos à ciência e tecnologia da madeira. Sem dúvidas isso ajudou em minha evolução profissional.

E, por fim, minha gratidão a todos que diretamente ou indiretamente contribuíram positivamente na minha formação profissional.

“O Senhor é o meu pastor, nada me faltará. Ele me faz repousar em pastos verdejantes. Leva-me para junto das águas de descanso; refrigera-me a alma. Guia-me pelas veredas da justiça por amor do seu nome. Ainda que eu ande pelo vale da sombra da morte, não temerei mal nenhum, porque tu estás comigo, o teu bordão e o teu cajado me consolam. Preparas-me uma mesa na presença dos meus adversários, unges a minha cabeça com óleo, o meu cálice transborda. Bondade e misericórdia certamente me seguirão todos os dias da minha vida, e habitarei na Casa do Senhor para todo o sempre.”

(Bíblia Sagrada, Salmos 23:1-6)

RESUMO GERAL

Pré-tratamentos químicos facilitam a produção de micro/nanofibrilas celulósicas (MFC/NFC) e ampliam as possibilidades de utilização deste material em filmes e revestimento de embalagens. Objetivou-se avaliar o efeito do pré-tratamento com silicato de sódio (Na_2SiO_3) nas propriedades químicas e morfológicas de polpas de *Eucalyptus* sp. e *Pinus* sp. e o consumo energético durante a produção das MFC/NFC utilizando ultra-refinador. Ainda, foram avaliadas as propriedades químicas, morfológicas, físico-mecânicas e índice de qualidade (IQ) das MFC/NFC produzidas. Também objetivou-se avaliar e aplicar MFC/NFC produzidas a partir de polpas de *Eucalyptus* sp. pré-tratadas com silicato de magnésio (MgO_3Si) e silicato de cálcio ($\text{Ca}_2\text{O}_4\text{Si}$) como revestimentos de papel cartão quanto as propriedades de barreira, superfície e mecânicas. A polpa de *Eucalyptus* sp. pré-tratada com 10% de Na_2SiO_3 apresentou a maior retenção de água. Os menores consumos de energia durante a fibrilação foram obtidos para polpa de *Eucalyptus* sp. pré-tratada com 5% de Na_2SiO_3 (~4100 kWh/t). As MFC/NFC pré-tratadas apresentaram maior frequência de diâmetros abaixo de 45 nm. O potencial zeta indicou estabilidade moderada das suspensões (-24 ~ -18 mV). Os pré-tratamentos com Na_2SiO_3 reduziram a transparência dos filmes em ~25% para *Eucalyptus* sp. e ~20% para *Pinus* sp. Os filmes apresentaram barreira adequada à radiação UVC, vapor de água e óleo. A resistência à tração dos filmes foi aumentada em 20% usando 10% de Na_2SiO_3 . Esta concentração de Na_2SiO_3 resultou em IQ de ~70 para as MFC/NFC de *Eucalyptus* sp. Os pré-tratamentos com $\text{Ca}_2\text{O}_4\text{Si}$ e MgO_3Si reduziram o consumo de energia em ~30% na produção de MFC/NFC. As camadas de MFC/NFC adicionadas ao papel cartão reduziram a permeabilidade ao vapor de água, especialmente para as MFC/NFC pré-tratadas com 5% de MgO_3Si (~98 g mm/kPa⁻¹ dia m²). As suspensões de MFC/NFC com 5% e 10% de $\text{Ca}_2\text{O}_4\text{Si}$ aumentaram a dispersão de líquidos e tinta de impressão na superfície do papel. Os revestimentos aumentaram a formabilidade do papel. O Na_2SiO_3 mostrou eficiência para a produção de MFC/NFC devido ao reduzido consumo de energia e permitiu obter filmes com propriedades adequadas para embalagens. As suspensões têm características compatíveis para aplicação como estabilizador de sistemas coloidais e reforço de compósitos. A otimização da aplicação e das técnicas de secagem para formulações de MFC/NFC e revestimento de silicato pode melhorar as propriedades mecânicas e de barreira dos papéis revestidos para embalagens multicamadas.

Palavras-chave: Biopolímeros. Barreira à umidade. Barreira à gases. Consumo energético. Celulose Microfibrilada (MFC). Nanotecnologia. Polissacarídeos. Embalagens secundárias.

GENERAL ABSTRACT

Chemical pretreatments facilitate the production of cellulosic micro/nanofibrils (MFC/NFC) and expand the possibilities of using these materials in coatings and packaging films. The objective was to evaluate the effect of pretreatment with sodium silicate (Na_2SiO_3) on the chemical and morphological properties of *Eucalyptus* sp. and *Pinus* sp. pulps and energy consumption during MFC/NFC production using an ultra-refiner. We also evaluated the chemical, morphological, physical-mechanical properties and the quality index (QI) of the produced MFC/NFC. We also aimed to evaluate and apply MFC/NFC produced from *Eucalyptus* sp. pulps pretreated with magnesium silicate (MgO_3Si) and calcium silicate ($\text{Ca}_2\text{O}_4\text{Si}$) as paperboard coatings regarding barrier, surface and mechanical properties. *Eucalyptus* sp. pulp pretreated with 10% Na_2SiO_3 showed the highest water retention. The lowest energy consumptions during fibrillation were obtained for *Eucalyptus* sp. pulp pretreated with 5% Na_2SiO_3 (~4100 kWh/t). The pretreated MFC/NFC showed higher frequency of diameters below 45 nm. The zeta potential indicated moderate stability of the suspensions (-24 ~ -18 mV). Pretreatments with Na_2SiO_3 reduced the transparency of the films by ~25% for *Eucalyptus* sp. and ~20% for *Pinus* sp. The films showed adequate barrier to UVC radiation, water vapor and oil. The tensile strength of the films was increased by 20% using 10% Na_2SiO_3 . This concentration of Na_2SiO_3 resulted in IQ of ~70 for the MFC/NFC of *Eucalyptus* sp. Pretreatments with $\text{Ca}_2\text{O}_4\text{Si}$ and MgO_3Si reduced energy consumption by ~30% in MFC/NFC production. MFC/NFC layers added to paperboard reduced water vapor permeability, especially for MFC/NFC pretreated with 5% MgO_3Si (~98 g mm/kPa⁻¹-day m²). MFC/NFC suspensions with 5% and 10% $\text{Ca}_2\text{O}_4\text{Si}$ increased the dispersion of liquids and printing ink on the paper surface. The coatings increased the formability of the paper. Na_2SiO_3 showed efficiency for MFC/NFC production due to reduced energy consumption and allowed to obtain films with properties suitable for packaging. The suspensions have compatible characteristics for application as stabilizer of colloidal systems and reinforcement of composites. Optimization of application and drying techniques for MFC/NFC formulations and silicate coating can improve the mechanical and barrier properties of coated papers for multilayer packaging.

Keywords: Biopolymers. Moisture barrier. Gas barrier. Energy consumption. Microfibrillated Cellulose (MFC). Nanotechnology. Polysaccharides. Secondary Packaging.

SUMÁRIO

APRESENTAÇÃO DA TESE	12
PRIMEIRA PARTE	11
1 INTRODUÇÃO	11
2 REFERENCIAL TEÓRICO	14
2.1 Fibrilação mecânica de polpas celulósicas: aspectos gerais e desafios	14
2.2 Pré-tratamentos químicos e fibrilação mecânica de polpas celulósicas	19
2.3 Modificação de fibras e micro/nanofibrilas celulósicas com sílica e silicatos	21
2.4 Aplicações do papel cartão em embalagens	24
2.5 Embalagens primárias, secundárias ou terciárias	26
2.6 Aplicações de micro/nanofibrilas celulósicas em embalagens	28
2.7 Métodos para revestimento de papel	29
3 CONSIDERAÇÕES GERAIS	32
REFERÊNCIAS	33
SEGUNDA PARTE – ARTIGOS	49
ARTIGO 1 – PRODUCTION OF CELLULOSE MICRO/NANOFIBRILS WITH SODIUM SILICATE: IMPACT ON ENERGY CONSUMPTION, MICROSTRUCTURE, CRYSTALLINITY AND STABILITY OF SUSPENSIONS	49
ARTIGO 2 – FIBERS PRE-TREATMENTS WITH SODIUM SILICATE AFFECT THE PROPERTIES OF SUSPENSIONS, FILMS, AND QUALITY INDEX OF CELLULOSE MICRO/NANOFIBRILS	82
ARTIGO 3 – ASSOCIATION OF CELLULOSE MICRO/NANOFIBRILS AND SILICATES FOR CARDBOARD COATING: TECHNOLOGICAL ASPECTS FOR PACKAGING	119
TERCEIRA PARTE - CONCLUSÃO DA TESE	170

APRESENTAÇÃO DA TESE

A tese está subdividida em duas partes. A primeira é composta por uma introdução geral da tese, com a contextualização do tema do trabalho, objetivos gerais e específicos. Além disso, contém uma revisão bibliográfica abordando aspectos referentes ao processo de produção de micro/nanofibrilas celulósicas (MFC/NFC); pré-tratamentos de fibras para fibrilação mecânica; silicatos com potencial para pré-tratamentos de fibras; tipos de embalagem, tipos de papel cartão; e aplicação das MFC/NFC como revestimento de papel. A segunda parte foi estruturada em três artigos. O primeiro é referente ao estudo da produção de micro/nanofibrilas de celulose com silicato de sódio e seu impacto no consumo de energia, microestrutura, cristalinidade e estabilidade das suspensões. As principais contribuições deste artigo foram no sentido de demonstrar a redução dos teores de hemiceluloses das fibras de *Eucalyptus* sp. e *Pinus* sp., diminuição do consumo energético durante a fibrilação mecânica, maior individualização das MFC/NFC e maior estabilidade das suspensões com a utilização do pré-tratamento à base de silicato de sódio. O segundo artigo é referente ao estudo do efeito da alcalinidade do silicato de sódio nas propriedades das suspensões, filmes e índice de qualidade de MFC/NFC. As contribuições deste trabalho são direcionadas à melhoria das propriedades de barreira ao vapor de água e ao óleo dos filmes obtidos a partir das MFC/NFC pré-tratadas com silicato de sódio. As propriedades ópticas e mecânicas dos filmes também foram melhoradas com o pré-tratamento aplicado, isso resultou em valores de índice de qualidade semelhantes aos de MFC/NFC obtidas a partir de pré-tratamentos consagrados na literatura. O terceiro artigo foi desenvolvido com foco na avaliação de revestimentos de papel cartão com MFC/NFC produzidas a partir de polpa de *Eucalyptus* sp. pré-tratadas com silicato de magnésio (MgO_3Si) e silicato de cálcio (Ca_2O_4Si). As principais contribuições deste trabalho foram relacionadas à redução do consumo de energia durante a fibrilação mecânica com adição de silicato de cálcio e de magnésio. Os revestimentos com as MFC/NFC pré-tratadas aumentaram o espalhamento de tinta sobre o papel cartão devido ao aumento da energia livre de superfície. Ocorreu redução da penetração do vapor de água e aumento da ductibilidade dos papéis revestidos com as MFC/NFC pré-tratadas com os silicatos. A terceira parte consiste na conclusão geral da tese abordando os principais resultados encontrados e apresentado sugestões para novos trabalhos.

PRIMEIRA PARTE

1 INTRODUÇÃO

Os polímeros não biodegradáveis à base de petróleo ocasionam efeitos negativos devido ao acúmulo e lenta degradação nos ecossistemas. Estudos reportam a contaminação de água e alimentos por microplásticos (COX et al., 2019); comprometimento de ciclos biogeoquímicos (SEELEY et al., 2020); e prejuízos à saúde dos organismos terrestres e aquáticos (CHIA et al., 2020; JÂMS et al., 2020) e alteração da paisagem (LAVERS et al., 2019).

Assim, o uso de biopolímeros tem sido cada vez mais investigado visando substituir total ou parcialmente o emprego de polímeros não biodegradáveis. Nesse contexto, a celulose é uma alternativa plausível por ser o polímero natural mais abundante da Terra e possuir grande versatilidade de utilização (KIM et al., 2020). Dentre as linhas de pesquisa relativas à celulose, destacam-se os estudos voltados à sua transformação, caracterização e aplicações em escala micro e nanométrica.

Micro/nanofibrilas de celulose (MFC/NFC) são unidades fibrilares resultantes da desconstrução da parede celular e isolamento das cadeias de celulose com dimensões nanométricas (1-100 nm) e baixa densidade ($\sim 1,5 \text{ g cm}^{-3}$) em relação a outros materiais, como metais e vidros (KARIM et al., 2017; ARIFFIN et al., 2018). Por possuir elevada resistência mecânica e superfície específica, baixa toxicidade e alta biodegradabilidade, este material tem sido pesquisado visando aplicações em encapsulamento de fármacos (KUPNIK et al., 2020); embalagens e filmes (BHARIMALLA et al., 2017; AHANKARI et al., 2021); filmes magnéticos (ARANTES et al., 2019); na indústria têxtil (SAREMI et al., 2020); e no reforço para matrizes poliméricas (GUAN et al., 2020a; MÜLLER et al., 2020).

Os processos para obtenção de MFC/NFC de origem vegetal podem ser a partir de processos químicos, por meio de hidrólise ácida, ou por processos mecânicos. Em relação aos processos mecânicos, pode-se citar a microfluidização (PERRIN et al., 2020), sonicação (ZHOU et al., 2020; WU et al., 2021), homogeneização de alta pressão (KARINA et al., 2020) e fibrilação mecânica em moinho de pedras (ZENG et al., 2020; LEAL et al., 2021).

Os desafios no processo de fibrilação mecânica estão relacionados à dificuldade para desconstruir a estrutura cristalina da celulose (KARIM et al., 2017; BIAN et al., 2019; SÁNCHEZ-GUETIÉRREZ et al., 2020). Por sua vez, isso acarreta em elevado consumo energético para desconstrução das paredes celulares das fibras vegetais sem o uso de tratamento químico, que pode variar de 30.000 e 50.000 kWh/t utilizando-se o moinho de pedras (ESPINOSA et al., 2019; DU et al., 2020).

Para reduzir o consumo energético durante o processo de fibrilação mecânica da parede celular, pré-tratamentos químicos às fibras celulósicas têm sido muito utilizados (NECHYPORCHUK et al., 2016; MALUCELLI et al., 2019). Rol et al. (2019) destacaram em suas pesquisas os principais pré-tratamentos visando a modificação da superfície das fibras para produção de MFC/NFC com diferentes propriedades, sendo eles a sulfoetilação (NADERI et al., 2017); carboximetilação (ARVIDSSON et al., 2015; IM et al., 2018); fosforilação (NOGUCHI et al., 2017); e a oxidação mediada por N-oxil-2,2,6,6-tetrametilpiperidina-TEMPO (SAITO et al., 2007).

Apesar de reduzirem consideravelmente o consumo energético durante o processo de fibrilação mecânica da celulose, alguns dos pré-tratamentos apresentados podem elevar custos com reagentes tendo em vista a produção em escala industrial (LONG et al., 2017; HU et al., 2018; BIAN et al., 2020). O uso do TEMPO pode resultar em custos superiores à US\$ 700.000,00/t, levando em conta a quantidade necessária descrita na metodologia de Saito et al. (2007). Além disso, não se pode desconsiderar o risco à saúde decorrente da presença de substâncias químicas aderidas às superfícies das MFC/NFC quando pretende-se empregá-la em embalagens e alimentos (KHARE et al., 2020; STOUDMANN et al., 2020; AIMONEN et al., 2021).

Desse modo, o estudo de pré-tratamentos alternativos pode proporcionar a obtenção de MFC/NFC com redução de consumo energético e propriedades físico-químicas adequadas para aplicação em novos produtos. Uma possibilidade a ser considerada é a sililação da celulose (TRACHE et al., 2020), que pode proporcionar aumento da estabilidade térmica e dimensional, aumento da repelência à água, barreira aos gases e ganhos em resistência mecânica (ANDRESEN et al., 2006; ROBLES et al., 2015; MIRI et al., 2021).

A maioria dos trabalhos reportam a sililação das MFC/NFC e fibras visando aplicações diversas, mas não como pré-tratamento para fibrilação mecânica. Ventura et al. (2020) e Wang et al. (2021) reportaram em suas pesquisas aplicações de MFC/NFC em tratamento de água, filtragem de ar, usos biomédicos, como aditivos em cosméticos, na indústria farmacêutica, para fabricação de dispositivos eletrônicos e produção de embalagens de papel e papel-cartão.

Porém, vale ressaltar que os agentes de sililação mais utilizados – ortossilicato de tetraetila (TEOS); metiltrimetoxissilano (MTMS); isobutiltrimetoxissilano (IBTMS); n-octiltrióxissilano (OTES); clorodimetil isopropilsilano (CDMIPS) e 3-aminopropil trióxissilano (ATS) – apresentam custo elevado e necessidade de reagentes para sua ativação (ANDRESEN et al., 2006; RAABE et al., 2015; ROBLES et al., 2015; MIRI et al., 2021).

A proposta de pré-tratamento da presente tese, baseia-se na impregnação de partículas de sílica na superfície da celulose visando potencializar o mecanismo de fibrilação interna e externa da parede celular pelo aumento da abrasão entre a parede celular e as pedras do moinho. Assim, por apresentarem alta afinidade com os grupos hidroxílicos da celulose, os silicatos podem ser uma fonte de sílica mais barata para este processo (PETERSSON; OKSMAN, 2006; HO et al., 2012a). Por outro lado, considerando os processos mecânicos de fibrilação, a abrasão da sílica pode propiciar desgaste prematuro dos componentes dos equipamentos (moinho de pedras, extrusores e moinho microfluidizador).

Os silicatos de sódio (Na_2SiO_3), magnésio (MgO_3Si) e cálcio ($\text{Ca}_2\text{O}_4\text{Si}$) apresentam-se como opção, pois já são utilizados no processo de tratamento de água potável (LI et al., 2021); branqueamento da celulose (MOGHADDAM; KARIMI, 2020); na indústria alimentícia como agente estabilizante de emulsões (GOULD et al., 2013; YOUNES et al., 2018); e como fonte de nutrientes em suplementos alimentares (MARTIN et al., 2007; KASAAI, 2015).

Em algumas pesquisas é reportado que a adição dos silicatos mencionados em fibras celulósicas e em suspensões de MFC/NFC permitiram obter suspensões, compósitos e filmes com menor permeabilidade à umidade e ao oxigênio; maior resistência mecânica e ao fogo; maior da superfície específica, maior da estabilidade em suspensões e melhor dispersão em matrizes poliméricas (DEMILECAMPS et al., 2014; MÁRMOL et al., 2016; HUANG et al., 2018; ASSAF et al., 2019; LI et al., 2020a; GORGIEVA et al., 2020).

Essas características são desejáveis para aplicação em revestimentos, filmes e embalagens. Apesar de existirem estudos sobre a aplicação das MFC/NFC para esta finalidade, autores relatam que nem sempre é possível obter resultados que indiquem viabilidade técnica (VILARINHO et al., 2018; NAZRIN et al., 2020; SPIESER et al., 2020). Outro aspecto a ser considerado é a possibilidade de realização dos pré-tratamentos utilizando os silicatos por meio da metodologia *in situ one-step*, que são baseados na modificação ou síntese de compostos químicos diretamente na polpa celulósica (LI et al., 2010; LI et al., 2018; AN et al., 2021). No entanto, até o momento, não foram encontradas pesquisas que explorem esta abordagem como pré-tratamento, isso pode aumentar a interação entre silicato-celulose, visto que enquanto as MFC/NFC são extraídas os silicatos já se encontram presentes, dispensando a realização de procedimentos adicionais para impregnação.

Por isso, torna-se necessário a realização de pesquisas voltadas para o estudo das características de MFC/NFC produzidas mediante o pré-tratamento *one-step in situ* com silicatos e seus desdobramentos nas propriedades químicas, físicas e mecânicas visando a aplicação em revestimento de papéis para embalagens. Isso é importante porque o uso dos

silicatos como pré-tratamento pode contribuir para facilitar a individualização das MFC/NFC e reduzir o consumo de energia durante a fibrilação mecânica. Apesar de outros pré-tratamentos serem empregados para essa finalidade, conforme mencionado, os custos de reagentes são muito elevados e podem gerar resíduos químicos de difícil recuperação com grande toxidez. Assim, observa-se que existem oportunidades para otimizar o processo de fibrilação mecânica por meio da utilização de silicatos e também utilizar as MFC/NFC para aplicações em embalagens, filmes e como estabilizante de suspensões.

Diante dos aspectos apresentados, o objetivo do presente trabalho foi (i) avaliar o impacto do Na_2SiO_3 como pré-tratamento alcalino de polpas comerciais branqueadas de *Eucalyptus* sp. e *Pinus* sp. no consumo energético durante a fibrilação mecânica da celulose e nas propriedades das suspensões e filmes de micro/nanofibrilas celulósicas (MFC/NFC); (ii) avaliar o efeito de MgO_3Si e $\text{Ca}_2\text{O}_4\text{Si}$ como pré-tratamento em polpas de *Eucalyptus* sp. e aplicação da MFC/NFC produzidas como revestimentos em papel cartão visando aplicações em embalagens.

Os objetivos específicos desta tese estão listados a seguir:

1. Avaliar a eficiência do pré-tratamento Na_2SiO_3 nas fibras de *Eucalyptus* sp. e *Pinus* sp. e seu efeito em suas propriedades químicas e morfológicas.
2. Avaliar o consumo energético durante o processo de fibrilação das polpas de *Eucalyptus* e *Pinus* pré-tratadas com Na_2SiO_3 .
3. Avaliar as propriedades químicas, morfológicas, físico-mecânicas das MFC/NFC produzidas a partir das polpas de *Eucalyptus* sp. e *Pinus* sp. pré-tratadas com Na_2SiO_3 .
4. Aplicar micro/nanofibrilas celulósicas produzidas a partir de polpas de *Eucalyptus* sp. pré-tratadas com MgO_3Si e $\text{Ca}_2\text{O}_4\text{Si}$ como revestimentos de papel cartão e avaliá-los quanto à sua morfologia, propriedades de barreira de superfície e mecânicas.

2 REFERENCIAL TEÓRICO

2.1 Fibrilação mecânica de polpas celulósicas: aspectos gerais e desafios

As micro/nanofibrilas de celulose (MFC/NFC) consistem em um produto renovável, com dimensões que podem variar de 25 à 100 nm em diâmetro, obtido a partir de fibras vegetais por processos químicos ou mecânicos que visam a desconstrução da parede celular (Figura 1), modificando sua morfologia e propriedades de superfície (KARIM et al., 2017; ARIFFIN et al., 2018; SOLIKHIN et al., 2019; MIRI et al., 2021).

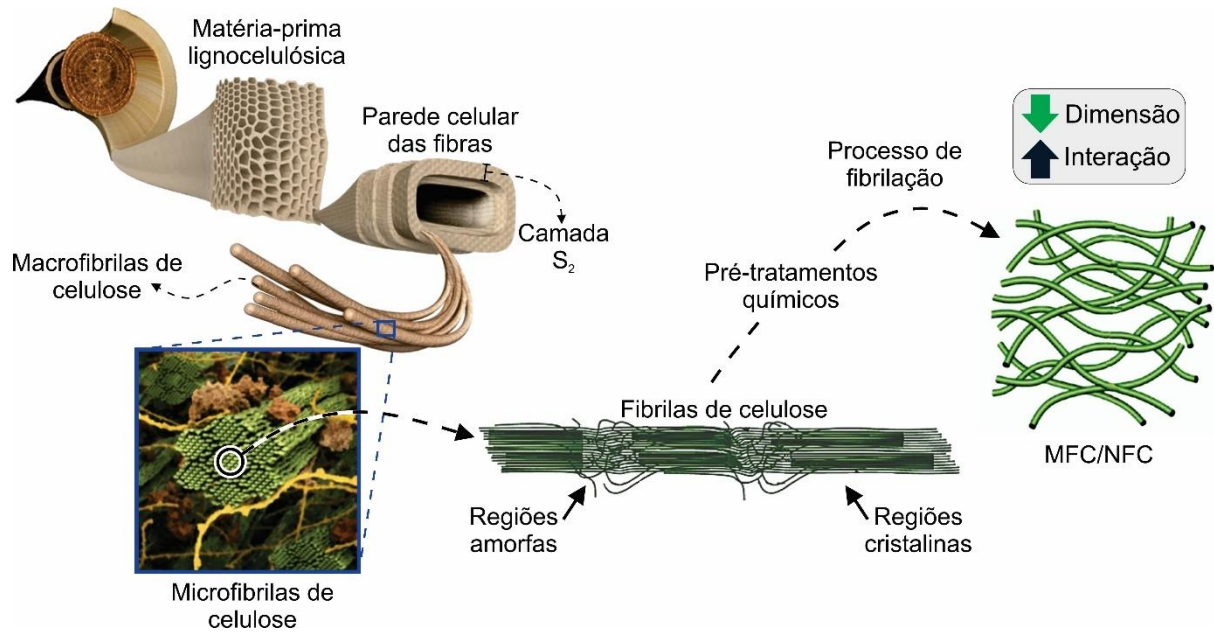


Figura 1 - Esquema geral de obtenção de micro/nanofibrilas de celulose (MFC/NFC) a partir de fibras lignocelulósicas pré-tratadas quimicamente e submetidas ao processo de fibrilação. Fonte: Adaptado de Nishimura et al. (2018).

Conforme a norma ISO/TS 20477:2017 (ISO, 2017), as nanofibrilas celulósicas são compostas por pelo menos uma fibrila elementar, contendo regiões cristalina, paracristalina e amorfa. Além disso, pode conter divisões longitudinais, emaranhamento entre partículas ou estruturas semelhantes a redes. As dimensões das nanofibrilas celulósicas são tipicamente 3-100 nm em seção transversal e normalmente até 100 μm de comprimento.

Os termos celulose nanofibrilada (NFC), celulose microfibrilada (MFC), microfibrila de celulose (MFC) e nanofibra de celulose (CNF) têm sido usados para descrever nanofibrilas de celulose produzidas por tratamento mecânico de materiais vegetais, muitas vezes combinado com etapas de pré-tratamento químico ou enzimático (PENNELS et al., 2020). As nanofibrilas de celulose produzidas a partir de fontes vegetais por processos mecânicos geralmente contêm hemicelulose e, em alguns casos, lignina. Algumas nanofibrilas de celulose podem ter grupos funcionais em sua superfície como resultado do processo de fabricação (ISO, 2017).

Os processos mecânicos mais conhecidos para produção de MFC/NFC são a microfluidização (DIMA et al., 2017; PERRIN et al., 2020), sonicação (ZHOU et al., 2020; WU et al., 2021), homogeneização de alta pressão (KARINA et al., 2020) e fibrilação mecânica (ZENG et al., 2020; LEAL et al., 2021). Para execução da fibrilação mecânica, na maioria das vezes, utiliza-se um “moinho” que induz a fibrilação por meio da descamação externa da parede celular da fibra vegetal, expondo as camadas mais internas (AFRA et al., 2013; KHALIL et al.,

2014; SHARMA et al., 2015). As fibras celulósicas são forçadas em alta velocidade para uma abertura entre um disco de pedra rotativo e outro estático em ciclos sequenciais de stress, e, por abrasão, geram forças de cisalhamento que quebram as ligações de hidrogênio da parede celular. Estes discos em contato com as fibras com auxílio dos sulcos e da pressão emitidos pelo moinho geram a desintegração do material em subcomponentes estruturais. Ao final deste processo, tem-se suspensões aquosas constituídas de redes entrelaçadas e desarranjadas de MFC/NFC (WANG et al., 2012; NAIR et al., 2014a; HE et al., 2017).

Os desafios no processo de fibrilação mecânica estão relacionados à heterogeneidade dos produtos e a dificuldade para degradar a estrutura cristalina da celulose (KARIM et al., 2017; BIAN et al., 2019; SÁNCHEZ-GUETIÉRREZ et al., 2020). Outra grande dificuldade relaciona-se ao elevado consumo energético para desconstrução das paredes celulares das fibras sem uso de tratamento químico. Estudos apontam que utilizando-se o moinho de pedras na fibrilação mecânica, o consumo energético pode atingir valores entre 30.000 e 50.000 kWh/t, dependendo do grau de fibrilação desejado (OSONG et al., 2016; ESPINOSA et al., 2019).

A heterogeneidade dos produtos e variação do consumo energético estão associadas à origem da matéria-prima, tipos e duração de processo de fibrilação, número de passagens no moinho e aplicação de pré-tratamentos à polpa celulósica (KHALIL et al., 2014; NECHYPORCHUK et al., 2015; THOMAS et al., 2020). Esses aspectos foram observados no trabalho de Wang e Zhu (2016), ao verificarem que o tempo e distância entre os discos utilizados no moinho afetaram as características da microfibrilas celulósicas. Os autores observaram que a densidade e a resistência à tração do material foram aumentadas ao passo com que se prolongou o tempo de fibrilação.

Também utilizando o método de fibrilação mecânica, Mihranyan et al. (2012) e Stanislas et al. (2020) demonstraram que os tipos de matéria prima influenciam na cristalinidade, porosidade e resistência mecânica das MFC/NFC. Adicionalmente, Dias et al. (2019) e Durães et al. (2020) verificaram que o número de ciclos de moagem no *grinder* e o efeito de pré-tratamentos alcalinos influenciaram significativamente no deslocamento da parede das fibras, nas propriedades morfológicas das MFC/NFC e no consumo energético durante sua produção.

Essas variações são esperadas, pois existem diferentes mecanismos que explicam a fibrilação mecânica da parede celular vegetal, sendo os mais comuns a fibrilação interna e externa. A fibrilação interna consiste no desempacotamento da estrutura helicoidal das microfibrilas de celulose na camada S₂ da parede celular (CHEN et al., 2014), as quais, em função da ação abrasiva das pedras do moinho, são afrouxadas formando feixes de MFC/NFC (COUTTS, 2005; PHANTHONG et al., 2018; YUAN et al., 2021).

No caso da fibrilação externa da parede celular, o processo de fricção das fibras com as pedras do moinho causa o arrebatamento individual de microfibrilas, porém elas permanecem parcialmente unidas à parede celular (AFRA et al., 2013). Dessa maneira, ocorre o aumento da superfície específica e maior reatividade do material com o meio, sendo esta uma característica desejável para inúmeras aplicações (LIU et al., 2020; KUMAR et al., 2020).

Em relação aos demais mecanismos, estudos apontaram que estão mais relacionados à fibrilação excessiva da polpa celulósica (SCATOLINO et al., 2017; ARÉVALO et al., 2019). Neste caso, ocorre a formação de finos dispersos em função da quebra das MFC/NFC ao longo de seu comprimento reduzindo assim sua razão de aspecto. Este fenômeno acarreta em maior consumo energético, redução do índice de cristalinidade, massa molar e resistência mecânica das microfibrilas (JAISWAL et al., 2021; SERRA-PARAREDA et al., 2021). Na Figura 2 estão apresentados os principais mecanismos de fibrilação da parede celular.

De forma semelhante, Lengowski et al. (2020) constataram que o emprego de diferentes graus de fibrilação das fibras pode influenciar nas propriedades físico-químicas de filmes produzidos com MFC/NFC. Estes autores observaram que quanto maior o grau de fibrilação maior foi a estabilidade térmica e impermeabilidade ao ar e água.

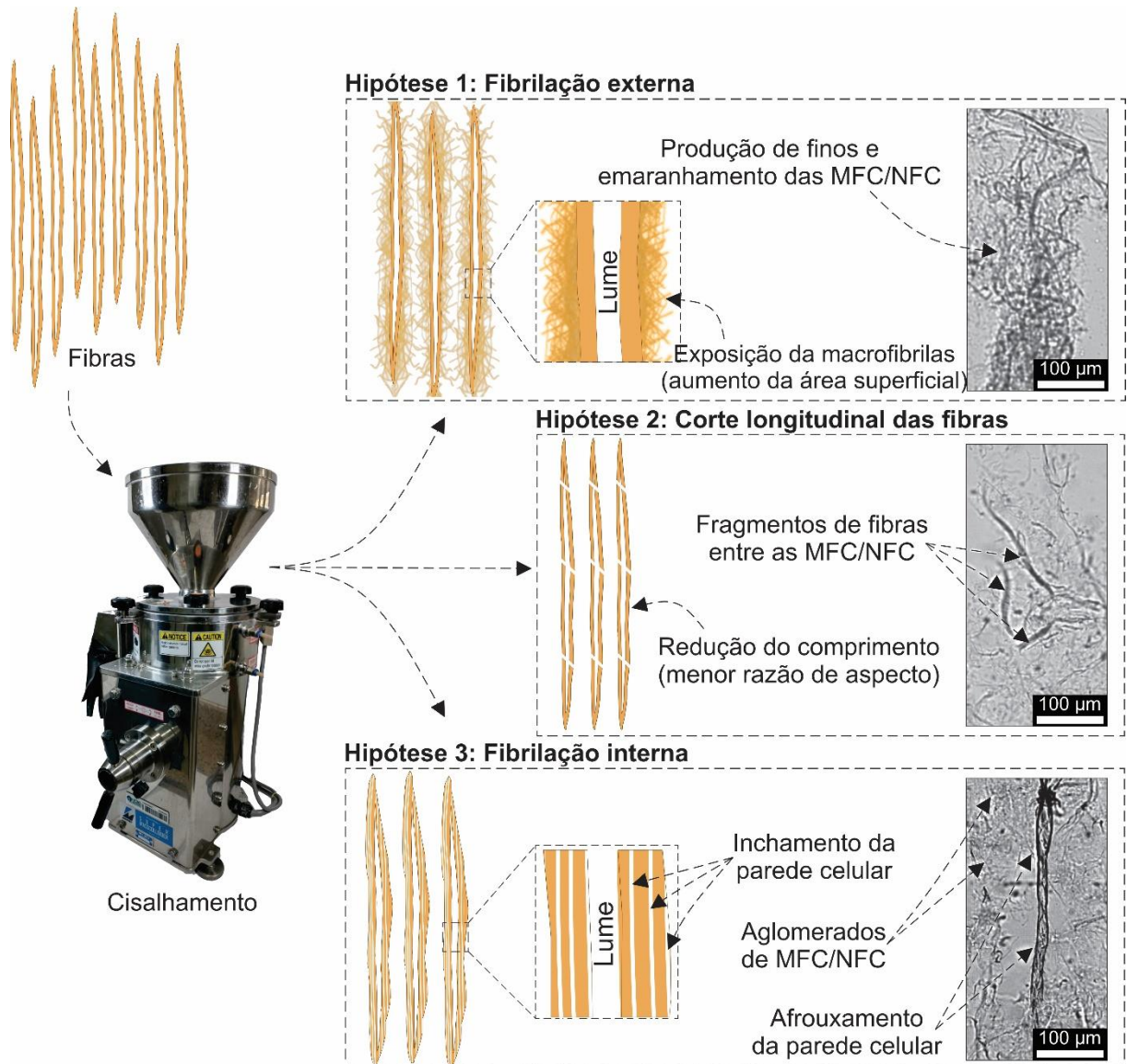


Figura 2 - Esquema dos mecanismos de fibrilação externa e interna e seus impactos nas características das micro/nanofibrilas de celulose (MFC/NFC). Fonte: Do Autor (2022).

Assim, pode-se verificar que ainda existem lacunas a respeito dos fatores que influenciam na fibrilação mecânica e nas propriedades das microfibrilas obtidas por esse processo. Diversos estudos têm apontado que a aplicação de pré-tratamentos nas fibras celulósicas, além de proporcionar a redução do consumo energético, pode resultar na funcionalização das microfibrilas, ampliando sua gama de aplicações e redução do custo de produção (FILIPOVA et al., 2020; ONYIANTA et al., 2020; REN et al., 2020; ZAMBRANO et al., 2020). No próximo tópico serão abordados os principais tipos de pré-tratamentos químicos utilizados nas polpas celulósicas para facilitar o processo de fibrilação mecânica.

2.2 Pré-tratamentos químicos e fibrilação mecânica de polpas celulósicas

Como mencionado, em virtude da estrutura molecular da celulose, o processo de desconstrução mecânica da parede celular é dificultado. Assim, para reduzir o consumo energético desse processo e visando obter MFC/NFC com qualidade desejável, o emprego de pré-tratamentos tem sido amplamente discutido (NECHYPORCHUK et al., 2016; MALUCELLI et al., 2019; DIAS et al., 2020; TRACHE et al., 2020).

Pesquisas realizadas por Rol et al. (2019) apresentam os principais pré-tratamentos para modificação da superfície das fibras e produção de MFC/NFC com diferentes propriedades. Dentre eles, pode-se mencionar a sulfoetilação (NADERI et al., 2017); carboximetilação (ARVIDSSON et al., 2015; IM et al., 2018); fosforilação (NOGUCHI et al., 2017); e a oxidação mediada por N-oxil-2,2,6,6-tetrametilpiperidina - TEMPO (SAITO et al., 2007).

Entre os pré-tratamentos mencionados, cabe destaque à oxidação mediada por TEMPO, devido as características das NFC produzidas. Após empregarem este pré-tratamento na polpa kraft branqueada de coníferas, Saito et al. (2007) obtiveram diâmetros das NFC entre 2 e 5 nm; aumento do índice de retenção de água (IRA) devido à maior superfície específica das NFC; melhoria da estabilidade da suspensão de NFC; aumento da transmitância de luz através da suspensão; aumento da taxa de cisalhamento e viscosidade da suspensão de NFC. Além disso, o uso de TEMPO proporciona a redução do consumo energético e maior velocidade no processo de fibrilação mecânica (ONYIANTA et al., 2018; MENG et al., 2018; LEVANIČ et al., 2020).

Ao estudarem a fibrilação mecânica de polpas kraft branqueadas de coníferas, Isogai et al. (2011) e Filipova et al. (2020) relataram que o uso de TEMPO como pré-tratamento resultou em consumo energético variando entre 13.000 e 19.000 kWh/t utilizando, respectivamente, o *grinder* e homogeneizador de alta pressão na produção de NFC. Comparando-se com os valores de consumo energético apresentados por Osong et al. (2016) e Espinosa et al. (2019), que estão entre 30.000 e 50.000 kWh/t, o uso de TEMPO resulta em uma economia energética em média de 50%. Do ponto de vista industrial, esses resultados são impactantes em relação ao custo de produção de MFC/NFC em escala.

No entanto, o custo de utilização de TEMPO é muito elevado. Considerando-se o protocolo apresentado por Saito et al. (2007) e o custo médio do reagente TEMPO – US\$122,00/g (SIGMA-ALDRICH, 2021). Para cada tonelada seca de polpa celulósica seriam necessários 16 kg do reagente a um custo de US\$1.952.000,00/t. Além disso, tanto o pré-tratamento com TEMPO como os demais citados neste trabalho têm potencial de geração de resíduos quimicamente ativos, havendo necessidade de neutralizá-los para descartá-los no ambiente, adicionando-se mais custos e passivos ambientais (LONG et al., 2017; HU et al.,

2018; BIAN et al., 2020). Outro problema relacionado a isso é que os riscos à saúde em virtude das modificações químicas das MFC/NFC não podem ser totalmente descartados (AIMONEN et al., 2021). Isso pode limitar a aplicação deste material em alimentos e embalagens.

Assim, nota-se que a questão dos pré-tratamentos da polpa celulósica não está totalmente resolvida tornando necessário desenvolver pesquisas para explorar novas soluções. Existem iniciativas de pesquisa visando utilizar reagentes mais baratos para fibrilação mecânica da celulose. Dias et al. (2019) aplicaram diferentes concentrações de NaOH no pré-tratamento da polpa de *Eucalyptus* sp. e *Pinus* sp. obtiveram redução do consumo energético para valores entre 4050 e 10.300 kWh/t, redução do número de ciclos no moinho de pedras e alto grau de fibrilação, utilizando-se uma concentração de NaOH de 5%, temperatura de 80 °C e duração de 2 h. Outros trabalhos apresentaram resultados controversos, indicando que o uso de NaOH não ocasionou redução do consumo energético e tornou as MFC/NFC quebradiças reduzindo sua qualidade e estabilidade (ABE, 2016; MALUCELLI et al., 2019; TRACHE et al., 2020).

Outro caso é a pesquisa de Xu et al. (2020) que também abrange o contexto apresentado. Os autores utilizaram o pré-tratamento hidrotérmico (180 °C/ 30 min) sem aplicações de aditivos na polpa celulósica e após processarem no moinho de pedras obtiveram consumo energético em torno de 8150 kWh/t e diâmetro médio das MFC/NFC de 8,4 nm.

Apesar de ser um processo livre de reagentes, para aplicações da MFC/NFC como reforço de compósitos poliméricos ou como meio para adsorção ou liberação de substâncias, faz-se necessário modificar a superfície da celulose e incluir uma etapa posterior ao processo de fibrilação, visando aumentar a compatibilidade química com a matriz polimérica. Além disso, o pré-tratamento hidrotérmico, em escala industrial, pode se tornar oneroso porque o aquecimento de grandes volumes de água e de polpa depende de fontes energéticas (biomassa, elétrica, fóssil) para execução do processo.

Portanto, a necessidade de se equacionar a redução do consumo energético e a manutenção da qualidade das MFC/NFC, deixando-as compatíveis com usos em que a saúde e o meio ambiente não sejam afetados é um grande desafio. Algumas pesquisas já demonstraram a afinidade entre os grupos hidroxílicos da celulose com fontes de sílica (ANDRESEN et al., 2006; HO et al., 2012b; RAABE et al., 2014; MENDES et al., 2015; LI et al., 2018). Contudo, o potencial de sua utilização como pré-tratamentos da celulose objetivando-se facilitar a fibrilação mecânica não foi abordado. Assim, no próximo tópico serão apresentadas as características dos silicatos mencionados e como sua interação com fibras e MFC/NFC pode modificar suas superfícies.

2.3 Modificação de fibras e micro/nanofibrilas celulósicas com sílica e silicatos

A sililação é o principal método empregado para modificação da superfície da celulose por meio da adição de sílica (TRACHE et al., 2020). Na maioria dos trabalhos observou-se que este método é utilizado para modificação de MFC/NFC e de fibras visando várias aplicações, mas não foram encontradas pesquisas utilizando esta metodologia como pré-tratamento da polpa celulósica visando fibrilação mecânica. O objetivo dessas modificações visa tornar a superfície das MFC/NFC mais hidrofóbica, aumentar sua resistência mecânica e facilitar a miscibilidade das suspensões em matrizes poliméricas (ROL et al., 2019).

Sequeira et al. (2009) produziram compósitos híbridos de celulose e sílica, aplicando ortossilicato de tetraetila (TEOS) às fibras de *Eucalyptus* sp. branqueadas. Estes autores verificaram que o TEOS proporcionou aumento da resistência mecânica dos compósitos e da estabilidade térmica e dimensional, tornando o material apto para utilização em embalagens por apresentar barreira à umidade e isolamento térmico.

Raabe et al. (2015) empregaram o ortossilicato de tetraetila (TEOS) para modificação da superfície de fibras de celulose visando sua aplicação na produção de compósitos com amido termoplástico (TPS). Os pesquisadores verificaram que a adição de SiO_2 promoveu aumento da resistência mecânica, redução da interação com água e maior estabilidade térmica quando se adicionou 10% de fibras modificadas na formulação do compósito.

De forma semelhante, Mendes et al. (2015) empregaram agentes silanos na modificação da polpa de *Eucalyptus* sp. utilizando-se metiltrimetoxissilano (MTMS), isobutiltrimetoxissilano (IBTMS) e n-octiltrietoxissilano (OTES). Os autores verificaram alto grau de substituição nos carbonos 2, 3 e 6 da celulose. Isso resultou em aumento da repelência à água melhorando as propriedades das fibras para aplicações em polímeros compósitos e fibrocimento, principalmente quando se utilizou o OTES.

Em relação às MFC/NFC, Andresen et al. (2006) utilizando-se o clorodimetil isopropilsilano (CDMIPS) como agente de sililação verificaram aumento de hidrofobicidade do material e da rugosidade da superfície. Já Robles et al. (2015), utilizaram o 3-aminopropil trietoxissilano (ATS) para modificação da superfície de nanocristais de nanocelulose (CNC) para utilizá-los como reforço do poli(ácido láctico) (PLA). Na pesquisa foi relatado que houve aumento da hidrofobicidade da celulose com adição do ATS, bem como, melhorias na resistência mecânica e térmica dos compósitos de CNF-PLA, devido a melhor dispersão das CNF na matriz polimérica.

Miri et al. (2021) realizaram a modificação da MFC e da celulose nanofibrilada (NFC) também utilizando-se o ortossilicato de tetraetila (TEOS) em diferentes proporções. Neste

estudo foi observado que o TEOS proporcionou aumento da superfície específica da NFC em relação à MFC. Isso acarretou no aumento do poder de adsorção de componentes químicos pela celulose na forma de aerogel.

As principais vantagens de se utilizar formulações químicas à base de sílica como agente de modificação da superfície da celulose estão ligadas à resistência mecânica e propriedades de barreira. Porém, os reagentes utilizados para sililação mencionados apresentam custo elevado e necessidade de reagentes para sua ativação. Assim, outras fontes de sílica apresentam potencial para tratamento de fibras celulósicas, como os silicatos (PETERSSON; OKSMAN, 2006; HO et al., 2012a).

HO et al. (2012b) utilizaram argilas e micas para produção de compósitos de NFC e silicatos. Os autores verificaram alta impregnação de partículas de silicatos nos grupos hidrofílicos da celulose, o que resultou em menor adsorção do vapor de água, aumento da dureza, da resistência ao cisalhamento e à tração dos compósitos.

Guan et al. (2020b) e Liu e Berglund (2013) ao aplicarem mica e montmorilonita como fontes de silicato para modificação de NFC, obtiveram alta resistência ao fogo, aumento da resistência mecânica, alta barreira à gases e transparência óptica, combinados à baixa densidade global do material produzido. Apesar das vantagens apresentadas, as micas e argilas não são materiais totalmente puros e podem conter substâncias inertes ou indesejáveis no material a ser produzido a depender da aplicação.

Dessa forma, o emprego de fontes de silicatos com alta pureza se faz necessário. Nesta tese, propõe-se utilizar silicatos de sódio (Na_2SiO_3), magnésio (MgO_3Si) e cálcio ($\text{Ca}_2\text{O}_4\text{Si}$) visando potencializar o mecanismo de fibrilação interna e externa da parede celular pelo aumento da abrasão entre a parede celular e as pedras do moinho, considerando-se o poder de adesão dos silicatos à superfície das fibras.

Os silicatos mencionados apresentam disponibilidade e baixo custo quando comparados a outros reagentes utilizados para o pré-tratamento convencional da polpa celulósica. O Na_2SiO_3 é um sal inorgânico alcalino encontrado na forma líquida e sólida, devido à sua homogeneidade, estabilidade química, viscosidade, capacidade de polimerização, alcalinidade e capacidade de modificação de cargas superficiais, tem sido amplamente utilizado em diferentes aplicações industriais (NAHRAWY et al., 2018). Dentre elas, pode-se mencionar a produção de adesivos (SONG et al., 2021), tratamento de madeiras (NEYSES et al., 2017), tratamento de água potável (LI et al., 2021), produção de cerâmicas (EL-DIDAMONY et al., 2020) e o processo de branqueamento da celulose (MOGHADDAM; KARIMI, 2020).

Algumas pesquisas reportam a modificação da superfície da celulose por meio do uso de Na_2SiO_3 . Realizando pesquisas neste contexto, Demilecamps et al. (2014) verificaram que a adição de Na_2SiO_3 proporcionou a redução da superfície específica das fibras celulósicas, inibindo a formação de agregados. Estes autores observaram que houve ganhos consideráveis na resistência mecânica do aerogel de celulose.

Também estudando a produção de aerogéis, empregando o Na_2SiO_3 em NFC de origem vegetal e bacteriana, Sai et al. (2014) e Gorgieva et al. (2020) observaram alta impregnação do reagente na superfície da rede de nanofibrilas, aumento da hidrofobicidade, redução da porosidade, melhoria das propriedades mecânicas e da estabilidade térmica ao passo que se elevou as concentrações de Na_2SiO_3 . Apesar de ser necessário o uso de outros reagentes, os pesquisadores destacaram ainda que o processo gera pouca quantidade de resíduos e é promissor para obtenção de materiais para isolamento térmico.

Quanto ao silicato de magnésio, caracteriza-se por ser adsorvente em forma de pó muito fino, branco ou cinza e inodoros, podendo ser natural ou obtido de forma sintética. Sua aplicação é observada em vários setores da indústria, na forma de carga em tintas conferindo maior resistência à lavabilidade ao revestimento (KRYSZTAFKIEWICZ et al., 2004); na indústria alimentícia como agente estabilizante de emulsões e antiemectante em sais e frutas desidratadas (GOULD et al., 2013; YOUNES et al., 2018); e como fonte de nutrientes em suplementos alimentares (MARTIN et al., 2007; KASAAI, 2015). Outra característica interessante dos silicatos de magnésio naturais está relacionada à baixa porosidade e grande superfície específica (PALEM et al., 2021).

Elsayed et al. (2018) e Assaf et al. (2019) estudaram a combinação do silicato de magnésio e celulose visando a produção de cápsulas para medicamentos. Na pesquisa foi constatado que as cápsulas se mantiveram por mais tempo intactas por conta da proteção à umidade conferida pelo silicato de magnésio, sem necessidade de se utilizar substâncias adicionais. Além disso, verificou-se maior compatibilidade e que o tempo de desintegração e liberação do fármaco foi mais rápido.

Já Huang et al. (2018), desenvolveram filmes porosos com silicato de magnésio visando a adsorção de íons de metal pesado em solução aquosa e destacaram como principais vantagens deste material o baixo custo e grande reatividade do silicato de magnésio na adsorção de metais pesados. Estudando o efeito da adição de silicato de magnésio à superfície de carboximetilcelulose (CMC), Liu et al. (2019) verificaram que a adesão do silicato de magnésio à superfície da celulose depende do pH, sendo que os melhores resultados se encontram para faixa de 4 a 6.

Mármol et al. (2016) estudaram o efeito da adição de silicato de magnésio para modificação da celulose em fibrocimento e observaram que houve ganho expressivo de resistência mecânica do material utilizando-se 30% de silicato de magnésio na mistura, mesmo após 200 ciclos de envelhecimento acelerado após 28 dias. Os autores explicaram que a camada formada na superfície da fibra celulósica reduziu a exposição aos agentes alcalinos do cimento.

Quanto ao silicato de cálcio, trata-se de um material obtido a partir de matérias primas naturais como cal virgem (Richardson, 2008; Dawood et al., 2017). Apresenta alta resistência à abrasão, umidade e temperatura, é atóxico e suas aplicações são muito semelhantes às do silicato de magnésio. Biswas et al. (2019) estudaram a síntese de compósitos de celulose e silicato de cálcio e verificaram que há grande quantidade de ligações entre Ca e Si nas hidroxilas celulósicas, demonstrando a afinidade entre as moléculas. Além disso, concluíram que o material obtido possui alta resistência mecânica sendo indicado para confecção de próteses dentárias e ortopédicas. Li et al. (2020a) produziram nanocompósitos à base de silicato de cálcio e NFC e também verificaram alta interação entre esses componentes. O material produzido apresentou uma rede porosa, alta superfície específica com alta repelência à água.

Li et al. (2018), encontraram resultados semelhantes ao produzirem compósito de silicato de cálcio estruturado com celulose. Nessa pesquisa, os autores constataram que a adição de silicato de cálcio proporcionou aumento significativo da resistência mecânica ao rasgo e à tração e alta interação com as superfícies da celulose. Ouyang et al. (2012) explicaram que essa interatividade proporciona dispersão homogênea do silicato de cálcio na superfície da celulose, pois verificaram por meio da espectroscopia no infravermelho com transformada de Fourier (FTIR) que essas partículas se ligam fortemente aos grupos hidroxílicos da celulose.

Diante do que foi apresentado, verifica-se que os silicatos apresentam grande interação com as superfícies reativas da celulose, isso é a premissa inicial para a possibilidade de se utilizá-los como pré-tratamentos da fibrilação mecânica. Além disso, verificou-se que as modificações resultantes dessas interações são interessantes para aplicações como revestimento de papel e produção de embalagens em aplicações que necessitem de alta barreira à água. Com isso tem-se a oportunidade de se associar essas características às MFC/NFC, que apresentam grande potencial para essa finalidade.

2.4 Aplicações do papel cartão em embalagens

Considerando os diversos tipos de embalagens e suas aplicações (proteção de alimentos, eletrônicos, produtos químicos e outros), o papel é um dos materiais mais utilizados para este fim. Isso se explica em função de suas vantagens em relação a outros materiais utilizados para

embalagens (vidro, plástico e borracha), pois possui menor custo, é biodegradável, reciclável e advém de fontes renováveis, promovendo menores impactos ao meio ambiente (YI et al., 2017; KHEDKAR; KHEDKAR, 2020; MAZIRIRI, 2020).

Entre os tipos de papel, o papel cartão possui grande versatilidade de utilização, sendo o seu uso mais representativo no setor de embalagens (FAO, 2020; IBÁ, 2021a). De forma geral, o papel cartão, ou simplesmente cartão, é o papel fabricado em múltiplas camadas com gramatura superior a 180 g/m², rígido e pode ou não apresentar revestimento superficial. Sua estrutura pode ser simples no caso dos do cartão sólido ou com mais camadas como a cartolina, papelão, papel cartão duplex e triplex (FIEP, 2016; IBÁ, 2021b).

O cartão sólido possui diferentes camadas brancas e é utilizado na composição de embalagens de cosméticos, medicamentos, produtos de higiene pessoal, capas de livro e cartões-postais. A cartolina pode conter uma ou mais camadas e tem variados usos: pastas para arquivos, calendário, etiquetas, encartes escolares, cartões de ponto, capas de livros e cadernos. O papelão tem elevada gramatura e rigidez, trata-se de um cartão fabricado em várias camadas, com utilidade diversa, das caixas à encadernação de livros (FADIJI et al., 2016; IBÁ, 2021c).

O papel cartão duplex é formado por diferentes camadas com aditivos para cor e composições de fibras curtas e longas, conforme demonstrado na Figura 3.

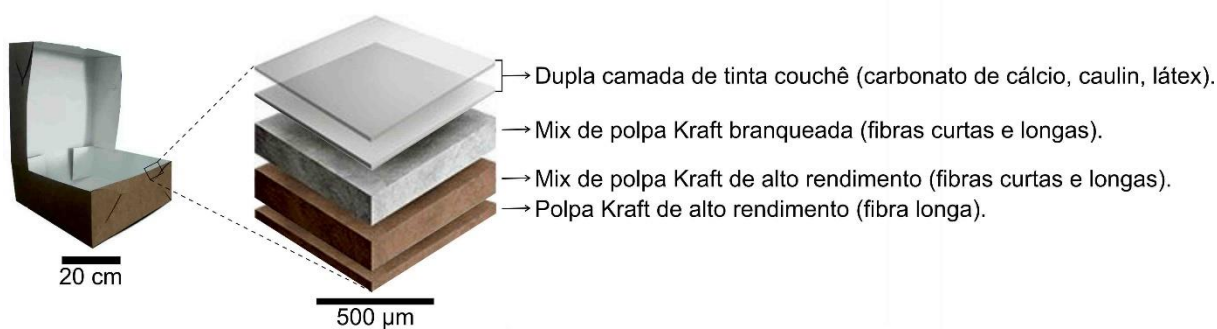


Figura 3 - Esquema da composição das camadas do papel cartão duplex.

Fonte: Adaptado de IBÁ (2021c).

O papel cartão duplex é geralmente aplicado na produção de caixas para chocolates, cosméticos, medicamentos, fast food e bebidas porque possui elevada rigidez, resistência superficial e espessura uniforme. Além disso, caracteriza-se por absorver água e tintas para impressão offset. A diferença do papel cartão triplex é a presença de três ou mais camadas de tinta couchê e fibras em ambas as faces das folhas, sendo suas aplicações muito similares ao do papel cartão duplex (VIDAL; HORA, 2012; IBÁ, 2021c).

Apesar de apresentar elevada resistência mecânica, o papel cartão nem sempre proporcionará barreira à gases, água, gorduras e ácidos (FADIJI et al., 2016; LOMMATZSCH et al., 2016). Isso pode resultar em emissão de odores do conteúdo das embalagens para o ambiente ou entrada de gases através do papel comprometendo as propriedades do conteúdo das embalagens (VERA et al., 2020).

O revestimento de barreira é uma operação de melhoria aplicada ao papel cartão. Como resultado desse processo, embalagens revestidas são utilizadas para embalar produtos alimentícios e não alimentícios. As propriedades de barreira mais estudadas são resistência à umidade, óleo, água, ar, odor e oxigênio. É um grande desafio ter todas essas propriedades em um tipo de papel. Por este motivo o tipo de barreira desejada é definido de acordo com a finalidade de uso do papel (SÖNMEZ; ÖZDEN, 2018).

Diversos estudos reportam a melhora das propriedades de barreira do papel cartão após a aplicação de polímeros em sua superfície. Rovera et al. (2020) observaram redução de 71% na taxa permeabilidade ao vapor de água (TPVA) do papel cartão ao adicionarem revestimentos híbridos produzidos com glúten e sílica de trigo visando aplicações alimentícias. Ottesen et al. (2017) observaram que ao utilizarem MFC/NFC como recobrimento do papel cartão houve redução significativa de sua porosidade, resultando em maior resistência à passagem do ar e do vapor de água.

Bideau et al. (2018) explicaram que esses efeitos são decorrentes do diâmetro diminuto das MFC/NFC, possibilitando preencher os espaços vazios do papel cartão e formando uma camada contínua e mais fechada sobre sua superfície. Além disso, dependendo das características químicas das MFC/NFC esse efeito pode ser potencializado.

Yook et al. (2020) verificaram melhoria da barreira ao vapor de água, do oxigênio e de gorduras através do papel cartão após aplicarem MFC/NFC modificadas pela adição de silanos como recobrimento. Estes autores verificaram ainda uma redução de 90% na absorção de água do papel cartão determinada pelo teste Cobb.

Apesar de ser muito utilizado, o papel cartão pode ter suas propriedades físico-mecânicas melhoradas pela adição de recobrimentos. As MFC/NFC têm potencial para essa finalidade. No entanto, melhores resultados para as propriedades de barreira foram observados após sua modificação pela adição de sílica.

2.5 Embalagens primárias, secundárias ou terciárias

As embalagens têm por função preservar as características dos produtos e garantir o seu prazo de validade (*shelf life*), viabilizando a proteção de sua integridade física e química durante

o transporte, armazenamento e exposição em prateleiras (EMBLEM, 2012). Além disso, em alguns casos, deve ser capaz de fornecer a identificação e divulgação da marca da mercadoria, bem como, apresentar informações a respeito da fabricação ou processamento, constituintes, informações nutricionais, validade e orientações para manuseio dos produtos (KUSWANDI; JUMINA, 2020).

O papel cartão possui características para atender esses requisitos, com a vantagem de ser biodegradável. Porém, os tipos de papel cartão irão variar conforme a aplicação com base na classificação das embalagens.

De forma geral, as embalagens são classificadas em três categorias, sendo elas embalagens primárias, embalagens secundárias e embalagens terciárias. As embalagens primárias caracterizam-se por ficar em contato direto com o produto que envolvem, sejam eles líquidos ou sólidos (RUDRA et al., 2013). Enquadra-se nesse contexto os sacos de papel para pães, caixas para leite ou sucos e caixas para frutas. Fora do setor de alimentos, as embalagens primárias podem ser exemplificadas como as caixas de sabão em pó e caixas para calçados.

As embalagens primárias geralmente apresentam-se construídas por papéis multicamadas de metais ou plásticos para evitar que o conteúdo interaja com a atmosfera ou ainda retenham líquidos e odores oriundos do produto embalado. Além disso, é muito importante que os componentes do papel para este tipo de embalagem não sejam tóxicos ou reativos. Em alguns casos as embalagens primárias devem ser resistentes a baixas temperaturas e a ambientes úmidos (MAHMOUDI; PARVIZIOMRAN, 2020).

As embalagens secundárias caracterizam-se por abrigar uma ou mais embalagens primárias. Outra função das embalagens secundárias é proteger as embalagens primárias de choques mecânicos ou contato com produtos químicos no entorno do local de armazenamento (MEHERISHI et al., 2019). Alguns exemplos deste tipo de embalagem são as caixas de papelão que protegem o creme dental, as caixas que embalam os sacos plásticos com cereais (sucrilhos, aveia, milho) e as caixas de papel cartão que contêm as embalagens plásticas que envolvem medicamentos.

Por fim a embalagem terciária também protege os produtos manufaturados, porém suas principais finalidades estão relacionadas ao transporte de grandes quantidades e manuseio seguro de mercadorias em embalagens secundárias agrupadas (CHUNG et al., 2018).

Os materiais e formato das embalagens terciárias serão definidos com base no tipo de produto, modo de transporte e serviços de armazenamento. Caixas de papelão e sacolas de papel de lojas e supermercado são exemplos de embalagens terciárias (MOLINA-BESCH et al.,

2019). O esquema de organização das embalagens primárias, secundárias e terciárias estão apresentados na Figura 4.

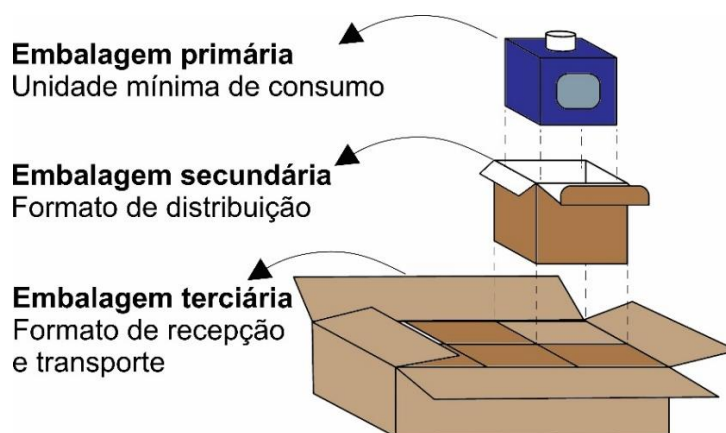


Figura 4 - Representação dos tipos e funções de embalagens primárias, secundárias e terciárias.

Fonte: Do autor (2022).

2.6 Aplicações de micro/nanofibrilas celulósicas em embalagens

O maciço uso de polímeros derivados de petróleo e seu descarte inadequado afetam negativamente os ambientes aquáticos e terrestres, comprometendo a saúde dos organismos e as dinâmicas ecossistêmicas (BAKKE et al., 2013; SEELEY et al., 2020). Lavers et al. (2019) relataram em sua pesquisa que objetos de plástico percorreram mais de 2 mil km de distância e que 28% dos itens encontrados eram de uso único. Por isso, tem-se estudado cada vez mais maneiras de se mitigar esses efeitos utilizando-se biopolímeros, principalmente no âmbito das embalagens (SIRACUSA et al., 2008; DILKES-HOFFMAN et al., 2018; SONAR et al., 2020).

No entanto, há um grande desafio em se desenvolver embalagens biodegradáveis que possuam características para proteção do seu conteúdo com resistência mecânica, barreira ao oxigênio, à umidade, luz e outros fatores que possam afetar as propriedades físico-químicas do produto (ANUKIRUTHIKA et al., 2020). Dentre os principais biopolímeros utilizados para obtenção de embalagens alternativas, pode-se destacar o amido, quitosana, hemiceluloses e celulose (BASUMATARY et al., 2020; LI et al., 2020b; NECHITA et al.; 2020).

No que diz respeito à celulose, diversas pesquisas e patentes apresentam sua aplicação em embalagens, filmes comestíveis, encapsulação de fármacos e revestimentos em micro/nanoescala (LI et al., 2015; GÓMEZ et al., 2016; BHARIMALLA et al., 2017; AHANKARI et al., 2021).

Ferrer et al. (2017) destacaram que os nanocristais de celulose (CNC), celulose nanofibrilada (NFC) e nanocelulose bacteriana (BC) possuem potencial para serem implementados no mercado de embalagens. Além disso, por ser um recurso renovável e não

tóxico, a nanocelulose pode melhorar de forma sustentável as propriedades de barreira ao oxigênio e ao vapor de água quando usados como revestimento, preenchimento em compósitos e como filmes finos autossustentáveis, devido à superfície específica e cristalinidade elevadas e possibilidade de modificação química da superfície (AZEREDO et al., 2017).

Nesse sentido, Spieser et al. (2020) estudaram o emprego de nanofibrilas de celulose com prata para aplicação em embalagens antibacterianas com matriz de poli(ácido láctico) (PLA) e obtiveram maior uniformidade na espessura das camadas e transparência acima de 65%. Os autores verificaram ainda que o uso das nanofibrilas como revestimento do PLA da embalagem reduziu significativamente a permeabilidade ao oxigênio e ao vapor de água.

Nair et al. (2014b) e Vilarinho et al. (2018) constataram que o uso de NFC no revestimento de embalagens ou na forma de filmes podem reduzir substancialmente a permeabilidade ao oxigênio e vapor de água, apresentado resultados superiores a polímeros à base de petróleo. Esta característica explica-se em função da densa rede formada por nanofibrilas com dimensões menores e uniformes. Também estudando embalagens utilizando amido e PLA como matrizes, Nazrin et al. (2020) obtiveram resultados semelhantes aos apresentados anteriormente. Porém, verificaram que a interface entre as MFC/NFC e à matriz polimérica nem sempre é perfeita, havendo necessidade de se modificar as cargas do material para compatibilização entre os componentes.

Em alguns casos essas características podem ser melhoradas, devido a possibilidade de modificação química da superfície das NFC (Spieser et al., 2020). No presente estudo, pretende-se utilizar silicatos para essa finalidade, pois conforme já demonstrado possuem alta afinidade com os grupos hidroxílicos da cadeia de celulose (HO et al., 2012b; ELSAYED et al., 2018; ASSAF et al., 2019).

De forma análoga, Yu et al. (2018) avaliaram filmes biodegradáveis de PVA/quitosana com sílica para embalagens de alimentos e obtiveram ganho de resistência mecânica, redução da permeabilidade à água e oxigênio. Isso demonstra que a adição de sílica pode melhorar a propriedades de biopolímeros, como a celulose, para revestimento de embalagens.

2.7 Métodos para revestimento de papel

A adição de camadas coesas na superfície de papéis para embalagens depende da padronização de parâmetros e emprego de equipamentos para obter a repetibilidade das aplicações visando garantir a homogeneidade de distribuição das formulações empregadas no revestimento.

Assim, técnicas e métodos de recobrimentos são empregados para essa finalidade. Conforme Kogler e Auhorn (2013), os principais métodos para aplicação de formulações na superfície dos papéis consistem na aplicação com rolos e barra dosadora, aplicação por pulverização e aplicação por cortina (TYAGI et al., 2021).

No revestimento por barra dosadora, as formulações são distribuídas na superfície do papel empregando-se aplicadores de rolos. A camada de revestimento é nivelada por barras ou lâminas metálicas pressionadas sobre o papel. A pressão e velocidade de aplicação é definida em detrimento da viscosidade e teor de sólidos da solução ou suspensão utilizada, visando reduzir falhas no recobrimento (KOGLER; AUHORN, 2013).

Ainda conforme estes autores, na sequência do processo de revestimento a folha úmida passa por secadores infravermelhos e depois são expostas à aplicação de ar sob alta temperatura. O tempo de permanência nessas fases de secagem não pode ser prolongado, pois pode ocorrer a queima do revestimento e do papel. Posteriormente, a espessura do papel é medida para se ter o controle de qualidade com base nas especificações de mercado dos produtos. Por fim, alguns tipos de revestimento requerem o alisamento da superfície, por meio de supercalandragem ou calandragem suave.

O método de aplicação por pulverização difere do anterior apenas pela forma de aplicação das suspensões/soluções para revestimento. Neste caso os rolos de aplicação são substituídos por uma pistola (MIRMEHDI et al., 2018; OLIVEIRA et al., 2022). O leque de dispersão, pressão e tempo de aplicação também varia em função da viscosidade e teor de sólidos da solução ou suspensão utilizada. Os detalhes dos métodos apresentados estão representados na Figura 5.

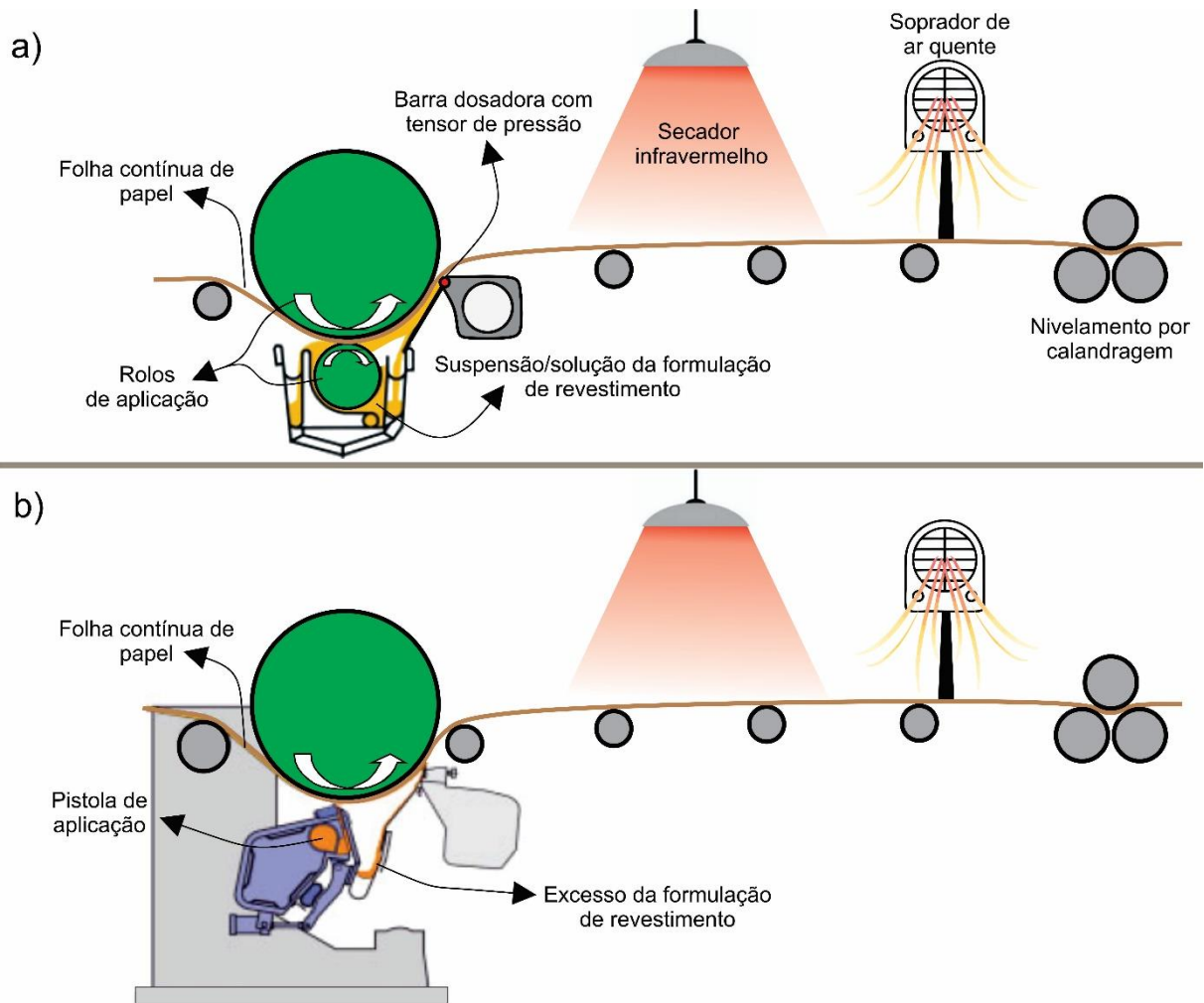


Figura 5 - a) Método de aplicação de revestimento em papéis por meio de rolos com barra dosadora e b) revestimento de papéis por meio de pulverização. Fonte: Adaptado de Kogler e Auhorn (2013).

O revestimento com cortina é usado principalmente para papéis especiais e possui a vantagem de realizar a aplicação das suspensões sem contato de equipamentos com o papel. Estes papéis geralmente possuem alto valor agregado, portanto o método de revestimento com cortina permite adicionar a quantidade mínima absoluta, reduzindo desperdício de material. Isso ocorre porque forma-se uma fina película de meio de revestimento que cai por gravidade sobre a superfície do papel (POPIL; JOYCE, 2008), pois a velocidade dos transportadores e o fluxo de material que é vertido do tanque determinam a espessura do revestimento (TYAGI et al., 2021), conforme ilustrado na Figura 6.

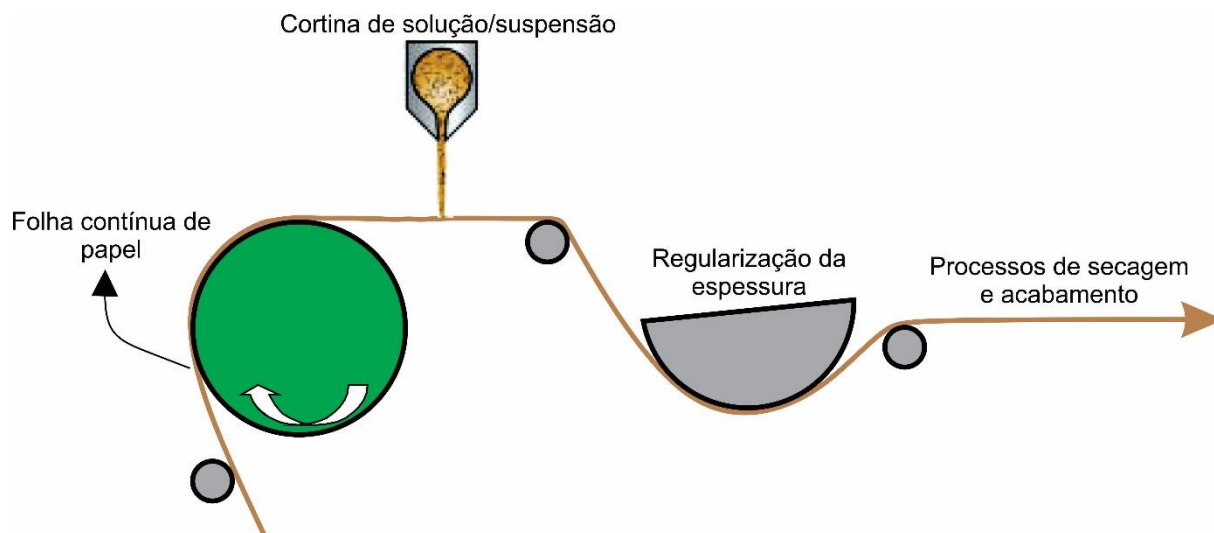


Figura 6 - a) Método de cortina para aplicação de revestimento em papéis. Fonte: Adaptado de Kogler e Auhorn (2013).

Ao final tem-se a deposição de um filme homogêneo sobre papel, isto reduz consideravelmente o risco de quebras e falhas no revestimento, melhorando a qualidade dos produtos e otimizando os processos de aplicação. Khwaldia et al. (2010) e Lee et al. (2018) relataram que este método tem despertado interesse da indústria, pois os revestimentos apresentam maior gramatura e alta barreira à gases.

3 CONSIDERAÇÕES GERAIS

De acordo com os trabalhos apresentados, verificou-se que existe grande potencial de utilização de silicatos como pré-tratamentos de fibras para produção de MFC/NFC, haja vista sua afinidade de interação com a celulose.

O emprego de pré-tratamentos químicos resulta em modificações da celulose reduzindo o consumo energético durante a fibrilação mecânica. O Na_2SiO_3 , por possibilitar obter soluções de elevada alcalinidade pode facilitar a dissociação e inchamento da parede celular das fibras, o que indica potencial para redução do consumo energético.

Quanto aos pré-tratamentos utilizando-se MgO_3Si e $\text{Ca}_2\text{O}_4\text{Si}$ espera-se que a impregnação das fibras resulte em maior abrasividade com as pedras do moinho, facilitando a quebra das fibrilas durante a fibrilação mecânica. Além disso, tendo em vista as aplicações destes silicatos, existe potencial dos mesmos conferirem propriedades interessantes para aplicação das MFC/NFC produzidas em revestimentos de papéis, tais como: repelência à água, repelência à gorduras e incremento da resistência mecânica.

No entanto, as informações sobre o comportamento das suspensões de MFC/NFC produzidas com estes silicatos são incipientes. Devido a isso, foi necessário caracterizá-las para aplicá-las por meio da técnica de recobrimento com barras dosadoras em escala laboratorial. As propriedades de barreira e de superfícies dos papéis também foram avaliadas a fim de se verificar modificações em função do revestimento aplicado.

REFERÊNCIAS

- ABE, K. Nanofibrillation of dried pulp in NaOH solutions using bead milling. **Cellulose**, v. 23, p. 1257-1261, 2016.
- AFRA, E.; YOUSEFI, H.; HADILAM, M. M.; NISHINO, T. Comparative effect of mechanical beating and nanofibrillation of cellulose on paper properties made from bagasse and softwood pulps. **Carbohydrate Polymers**, v. 97, n. 2, p. 725-730, 2013.
- AHANKARI, S. S.; SGHEDAR, A. R.; BHADAURIA, S. S.; DUFRESNE, A. Nanocellulose in food packaging: A review. **Carbohydrate Polymers**, v. 255, 117479, 2021.
- AIMONEN, K.; SUHONEN, S.; HARTIKAINEN, M.; LOPES, V. R.; NORPPA, H.; FERRAZ, N.; CATALÁN, J. Role of surface chemistry in the in vitro lung response to nanofibrillated cellulose. **Nanomaterials**, v. 11, 389, 2021.
- AN, Y.; LIU, H.; LIU, J.; LI, X.; LI, J.; LIN, C.; JIN, X.; XU, Y.; ZHAO, Z.; SONG, S.; HUI, L.; LIU, Z.; HUANG, Y. Effects of calcium silicate synthesized in situ on Fiber loading and paper properties. **Nordic Pulp & Paper Research Journal**, v. 36, p. 443-455, 2021.
- ANDRESEN, M.; JOHANSSON, L. S.; TANEM, B. S.; STENIUS, P. Properties and characterization of hydrophobized microfibrillated cellulose. **Cellulose**, v. 13, p. 665-677, 2006.
- ANUKIRUTHIKA, T.; SETHUPATHY, P.; WILSON, A.; KASHAMPUR, K.; MOSES, J. A.; ANANDHARAMAKRISHNAN, C. Multilayer packaging: Advances in preparation techniques and emerging food applications. **Comprehensive Reviews in Food Science and Food Safety**, v. 19, p. 1156-1186, 2020.
- ARANTES, A. C. C.; SILVA, L. E.; WOOD, D. F.; ALMEIDA, C. G.; TONOLI, G. H. D.; OLIVEIRA, J. E.; SILVA, J. P.; WILIAMS, T. G.; ORTS, W. J.; BIANCHI, M. L. Bio-based thin films of cellulose nanofibrils and magnetite for potential application in green electronics. **Carbohydrate Polymers**, v. 207, p. 100-107, 2019.
- ARÉVALO, R.; SOYKEABKAEW, N.; PEJIS, T. Turning low-cost recycled paper into high-value binder-free all-cellulose panel products. **Green Materials**, v. 8, n. 2, p. 51-59, 2019.

- ARIFFIN, M. N. F. N.; YASIM-ANUAR, T. A. T.; GHAEMI, F.; HASSAN, M. A.; IBRAHIM, N. A.; NGEE, J. L. H.; YUNUS, W. M. Z. Superheated steam pretreatment of cellulose affects its electrospinnability for microfibrillated cellulose production. **Cellulose**, v. 25, p. 3853-3859, 2018.
- ARVIDSSON, R.; NGUYEN, D.; SVANSTRÖM, M. Life cycle assessment of cellulose nanofibrils production by mechanical treatment and two different pretreatment processes. **Environmental Science & Technology**, v. 49, p. 6881-6890, 2015.
- ASSAF, S. M.; KHANFAR, M. S.; FARHAN, A. B.; RASHID, I. S.; BADWAN, A. A. Preparation and Characterization of Co-processed Starch/MCC/Chitin Hydrophilic Polymers onto Magnesium Silicate. **Pharmaceutical development and technology**, v. 24, p. 761-774, 2019.
- AZEREDO, H. M. C.; ROSA, M. F.; MATTOSO, L. H. C. Nanocellulose in bio-based food packaging applications. **Industrial Crops and Products**, v. 97, p. 664-671, 2017.
- BAKKE, T.; KLUNGSØYR, J.; SANNI, S. Environmental impacts of produced water and drilling waste discharges from the Norwegian offshore petroleum industry. **Marine Environmental Research**, v. 92, p. 154-169, 2013.
- BASUMATARY, I. B.; MUKHERJEE, A.; KATIYAR, V.; KUMAR, S. Biopolymer-based nanocomposite films and coatings: recent advances in shelf-life, improvement of fruits and vegetables. **Critical Reviews in Food Science and Nutrition**, aop, p. 1-24, 2020.
- BHARIMALLA, A. K.; DESHMUKH, S. P.; VIGNESHWARAN, N.; PATIL, P. G.; PRASAD, V. Nanocellulose-Polymer composites for applications in food packaging: current status, future prospects and challenges. **Polymer-Plastics Technology and Engineering**, v. 56, 805-823, 2017.
- BIAN, H.; DONG, M.; CHEN, L.; ZHOU, X.; NI, S.; FANG, G.; DAI, H. Comparison of mixed enzymatic pretreatment and post-treatment for enhancing the cellulose nanofibrillation efficiency. **Bioresource Technology**, v. 293, 1122171, 2019.
- BIAN, H.; CHEN, L.; DONG, M.; FU, Y.; WANG, R.; ZHOU, X.; WANG, X.; XU, J.; DAI, H. Cleaner production of lignocellulosic nanofibrils: potential of mixed enzymatic treatment. **Journal of Cleaner Production**, v. 270, 122506, 2020.
- BIDEAU, B.; LORANGER, E.; DANEAULT, C. Nanocellulose-polypyrrole-coated paperboard for food packaging application. **Progress in Organic Coatings**, v. 123, p. 128-133, 2018.
- BISWAS, N.; SAMANTA, A.; MILTRA, S.; BISWAS, R.; PODDER, S.; SANYAL, A.; GHOSH, J.; GHOSH, C. K.; MUKHOPADHYAY, A. K. Synthesis and structure

determination of calcium silicate-cellulose nanograss biocomposite. **Journal of the American Society Ceramic Society**, v. 103, p. 2868-2879, 2019.

CHEN, W.; ABE, K.; UETANI, K.; YU, H.; LIU, Y.; YANO, H. Individual cotton cellulose nanofibers- pretreatment and fibrillation technique. **Cellulose**, v. 21, p. 1517-1528, 2014.

CHIA, W. Y.; TANG, D. Y. Y.; KHOO, K. S.; LUP, A. N. K.; CHEW, K. W. Nature's fight against plastic pollution: Algae for plastic biodegradation and bioplastics production. **Environmental Science and Ecotechnology**, v. 4, 100065, 2020.

CHUNG, S. H.; MA, H. L.; CHAN, H. K. Maximizing recyclability and reuse of tertiary packaging in production and distribution network. **Resources, Conservation and Recycling**, v. 128, p. 259-266, 2018.

COUTTS, R. S. P. A review of Australian research into natural fiber cement composites. **Cement and Concrete Composites**, v. 27, n. 5, p. 518-526, 2005.

COX, K. D.; CONVERNTON, G. A.; DAVIES, H. L.; DOWER, J. F.; JUANES, F.; DUDAS, S. E. Human consumption of microplastics. **Environmental Science & Technology**, v. 53, 12, 2019.

DAWOOD, A. E.; PARASHOS, P.; WONG, R. H. K.; REYNOLDS, E. C.; MANTON, D. J. Calcium silicate-based cements: composition, properties, and clinical applications. **Journal of Investigative and Clinical Dentistry**, v. 8, e12195, 2017.

DEMILECAMPS, A.; RECHENAUER, G.; RIGACCI, A.; BUDTOVA, T. Cellulose-silica composite aerogel from "one-pot" synthesis. **Cellulose**, v. 21, p. 2625-2626, 2014.

DIAS, M. C.; MENDONÇA, M. C.; DAMÁSIO, R. A. P.; ZIDANES, U. L. MORI, F. A.; FERREIRA, S. R.; TONOLI, G. H. D. Influence of hemicellulose content of *Eucalyptus* and *Pinus* fibers on the grinding process for obtaining cellulose micro/nanofibrils. **Holzforschung**, v. 73, n. 11, p. 1035-1046, 2019.

DIAS, O. A. T.; KONAR, S.; LEÃO, A. L.; YANG, W.; TJONG, J.; SAIN, M. Current state of applications of nanocellulose in flexible energy and electronic devices. **Frontier in Chemistry**, v. 8, 240, 2020.

DILKES-HOFFMAN, L. S.; LANE, J. L.; GRANT, T.; PRATT, S.; LANT, P. A.; LAYCOCK, B. Environmental impact of biodegradable food packaging when considering food waste. **Journal of Cleaner Production**, v. 180, p. 325-334, 2018.

DIMA, S. O.; PANAITESCU, D. M.; ORBAN, C.; GHIUREA, M.; DONCEA, S. M.; FIERASCU, R. C.; NISTOR, C. L.; ALEXANDRESCU, E.; NICOLAE, C. A.; TRICA, B.; MORARU, A.; OANCEA, F. Bacterial nanocellulose from side-streams of kombucha

- beverages production: preparation and physical-chemical properties. **Polymers**, v. 9, n. 8, 374, 2017.
- DU, H.; PARIT, M.; WU, M.; CHE, X.; WANG, Y.; ZHANG, M.; WANG, R.; ZHANG, X.; JIANG, Z.; LI, B. Sustainable valorization of paper mill sludge into cellulose nanofibrils and cellulose nanopaper. **Journal of Hazardous Materials**, v. 400, 123106, 2020.
- DURÃES, A. F. S.; MOULIN, J. C.; DIAS, M. C.; MENDONÇA, M. C.; DAMÁSIO, R. A. P.; THYGESES, L. G.; TONOLI, G. H. D. Influence of chemical pretreatments on plant fiber cell wall and their implications on the appearance of fiber dislocations. **Holzforschung**, v. 74, n. 10, p. 949-955, 2020.
- EL-DIDAMONY, H.; EL-FADALY, E.; AMER, A. A.; ABAZEED, I. H. Synthesis and characterization of low cost nanosilica from sodium silicate solution and their applications in ceramic engobes. **Boletín de La Sociedad Española de Cerámica y Vidrio**, v. 59, p. 31-43, 2020.
- ELSAYED, A.; AL-REMAWI, M.; MAGHRABI, I.; HAMAIDI, M.; JABER, N. Evaluation of calcium magnesium silicate-date palm cellulose as potential tablet excipient. **Journal of Excipients and Food Chemicals**, v. 9, p. 106-115, 2018.
- EMBLEM, A. 3 - Packaging functions. In: EMBLEM, A.; EMBLEM, H. (org.) **Packaging Technology: Fundamentals, Materials and Processes**. Amsterdam: Elsevier, 2012. p. 24-29. Disponível em: <https://www.sciencedirect.com/science/article/pii/B9781845696658500032>. Acesso em: 21 jan. 2022.
- ESPINOSA, E.; ROL, F.; BRAS, J.; RODRÍGUEZ, A. Production of lignocellulose nanofibers from wheat straw by different fibrillation methods. Comparison of its viability in cardboard recycling process. **Journal of Cleaner Production**, v. 239, 118083, 2019.
- FAO – Food and Agriculture Organization of the United Nations. **Pulp and paper capacities – Survey 2019-2024**. Roma: FAO, 214p, 2020.
- FADIJI, T.; COETZEE, C.; OPARA, U. L. Compression strength of ventilated corrugated paperboard packages: Numerical modelling, experimental validation and effects of vent geometric design. **Biosystems Engineering**, v. 151, p. 231-247, 2016.
- FERRER, A.; PAL, L.; HUBBE, M. Nanocellulose in packaging: Advances in barrier layer technologies. **Industrial Crops and Products**, v. 95, p. 574-582, 2017.
- FIEP – Federação das Indústrias do Estado do Paraná. **Panorama Setorial: Indústria de Celulose, Papel, Embalagens e Artefatos de Papel**. Curitiba: FIEP, 236p, 2016.

- FILIPOVA, I.; SERRA, F.; TARRÉS, Q.; MUTJÉ, P.; DELGADO-AGUILAR, M. Oxidative treatments for cellulose nanofibers production: a comparative study between TEMPO-mediated and ammonium persulfate oxidation. **Cellulose**, v. 27, p. 10671-10688, 2020.
- GÓMEZ, C.; SERPA, A.; VELÁSKES-COCK, J.; GAÑÁN, P.; VÉLEZ, L.; ZULUAGA, R. Vegetable nanocellulose in food science: A review. **Food Hydrocolloids**, v. 57, p. 178-186, 2016.
- GORGIEVA, S.; JANCIC, U.; HRIBERNIK, S.; FAKIN, D.; KLEINSCHEK, K. S.; MEDVED, S.; FAKIN, T.; BOZIC, M. Processing and functional assessment of anisotropic cellulose nanofibril/allot/sodium silicate: based aerogels as flame retardant thermal insulators. **Cellulose**, v. 27, p. 1661-1683, 2020.
- GOULD, J.; VIEIRA, J.; WOLF, B. Cocoa particles for food emulsion stabilization. **Food & Function**, v. 4, p. 1396-1375, 2013.
- GUAN, Q. F.; YANG, H. B.; HAN, Z. M.; LING, Z. C.; YU, S. H. An all-natural bioinspired structural material for plastic replacement. **Nature Communications**, v. 11, 5401, 2020a.
- GUAN, Q. F.; YANG, H. B.; HAN, Z. M.; ZHOU, L. C.; ZHU, Y. B.; LING, Z. C.; JIANG, H. B.; WANG, P. F.; MA, T.; WU, H. A.; YU, S. H. Lightweight, tough, and sustainable cellulose nanofiber-derived bulk structural materials with low thermal expansion coefficient. **Science advances**, v. 6, eaaz1114, 2020b.
- HE, M.; YANG, G.; CHO, B. U.; LEE, Y. K.; WON, J. M. Effects of addition method and fibrillation degree of cellulose nanofibrils on furnish drainability and paper properties. **Cellulose**, v. 24, p. 5657-5669, 2017.
- HO, T. T.; KO, Y. S.; ZIMMERMANN, T. Processing and characterization of nanofibrillated cellulose/layered silicate systems. **Journal of Material Science**, v. 47, p. 4370-4382, 2012a.
- HO, T. T.; ZIMMERMANN, T.; OHR, S.; CASERI, W. R. Composites of cationic nanofibrillated cellulose and layered silicates: water vapor barrier and mechanical properties. **Applied Materials & Interfaces**, v. 4, n. 9, p. 4832-4840, 2012b.
- HU, J.; TIAN, D.; RENNECKAR, S.; SADDLER, J. N. Enzyme mediated nanofibrillation of cellulose by the synergistic actions of an endoglucanase, lytic polysaccharide monooxygenase (LPMO) and xylanase. **Scientific Reports**, v. 8, 3195, 2018.
- HUANG, R.; HE, L.; ZHANG, T.; LI, D.; TANG, P.; FENG, Y. Novel Carbon Paper@Magnesium Silicate Composite Porous Films: Design, Fabrication, and Adsorption Behavior for Heavy Metal Ions in Aqueous solution. **ACS Applied Materials & Interfaces**, v. 10, p. 22776-22785, 2018.

- IBÁ – Indústria Brasileira de Árvores. **Cenários IBÁ**. Disponível em: [https://www. iba.org/datafiles/publicacoes/cenarios/66cenarios_2.pdf](https://www.iba.org/datafiles/publicacoes/cenarios/66cenarios_2.pdf). Acesso em: 01 out. 2021a.
- IBÁ – Indústria Brasileira de Árvores. **Relatório Anual 2020**. Brasília: IBÁ, 66p, 2021b.
- IBÁ – Indústria Brasileira de Árvores. **Papel Cartão**. Disponível em: [https://www. iba.org/papelcartao](https://www.iba.org/papelcartao). Acesso em: 01 out. 2021c.
- IM, W.; LEE, S.; ABHARI, A. R.; YOUN, H. J.; LEE, H. L. Optimization of carboxymethylation reaction as a pretreatment for production of cellulose nanofibrils. **Cellulose**, v. 25, p. 3873-3883, 2018.
- ISOGAI, A.; SAITO, T.; FUKUZUMI, H. TEMPO-oxidized cellulose nanofibers. **Nanoscale**, v. 3, n. 71, 2011.
- ISO - International Organization for Standardization. **ISO/TS 20477:2017: Nanotechnologies - Standard terms and their definition for cellulose nanomaterial**. Genebra: ISSO, 2017. Disponível em: <https://www.iso.org/obp/ui/#iso:std:iso:ts:20477:ed-1:v1:en>. Acesso em: 08 set. 2022.
- 20477.2017. <https://www.iso.org/standard/68153.html>
- JAISWAL, A. K.; KUMAR, V.; KHAKALO, A.; LAHTINEN, P.; SOLIN, K.; PERE, J.; TOIVAKKA, M. Rheological behavior of high consistency enzymatically fibrillated cellulose suspensions. **Cellulose**, v. 28, p. 2087-2104, 2021.
- JÂMS, I. B.; WINDSOR, F. M.; POUDEVIGNE-DURANCE, T.; ORMEROD, S. J.; DURANCE, I. Estimating the size distribution of plastics ingested by animals. **Nature Communications**, v. 11, 1594, 2020.
- KARIM, Z.; AFRIN, S.; HUSAIN, Q.; DANISH, R. Necessity of enzymatic hydrolysis for production and functionalization of nanocelluloses. **Critical Reviews in Biotechnology**, v. 37, n. 3, p. 355-370, 2017.
- KARINA, M.; SATOTO, R.; ABDULLAH, A. D.; YUDIANTI, R. Properties of nanocellulose obtained from sugar palm (*Arenga pinnata*) fiber by acid hydrolysis in combination with high-pressure homogenization. **Cellulose Chemistry and Technology**, v. 54, n. 2, p. 33-38, 2020.
- KASAAI, M. R. Nanosized particles of silica and its derivates for applications in various branches of food and nutrition sectors. **Journal of nanotechnology**, v. 2015, 852394, 2015.
- KHALIL, H. P. S. A.; DAVOUDPOUR, Y.; ISLAM, M. N.; MUSTAPHA, A.; SUDESH, K.; DUNGANI, R.; JAWAID, M. Production and modification of nanofibrillated cellulose using various mechanical processes: A review. **Carbohydrate Polymers**, v. 99, p. 649-665, 2014.
- KHARE, S.; DELOID, G. M.; MOLINA, R. M.; GOKULAN, K.; COUVILLION, S. P.; BLOODSWORTH, K. J.; EDER, E. K.; WONG, A. R.; HOYT, D. W.; BRAMER, L. M.;

- METZ, T. O.; THRALL, B. D.; BRAIN, J. D.; DEMOKRITOU, P. Effects of ingested nanocellulose on intestinal microbiota and homeostasis in wistar han rats. **NanoImpact**, v. 18, 100216, 2020.
- KHEDKAR, D.; KHEDKAR, R. New innovations in food packaging in food industry. In: THAKUR, M.; MODI, V. K. (eds) **Emerging Technologies in Food Science**. Singapura: Springer, p. 15-36, 2020.
- KHWALDIA, K.; ARAB-TEHRANY, E.; DESOBRY, S. Biopolymer Coatings on Paper Packaging Materials. **Comprehensive Reviews in Food Science and Food Safety**, v. 9, p. 82-91, 2010.
- KIM, S.; SEO, A. Y.; LEE, T. G. Functionalized cellulose to remove surfactants from cosmetic products in wastewater. **Carbohydrate Polymers**, v. 236, 116010, 2020.
- KOGLER, W.; AUHORN, W. J. Coating of Paper and Board. In: HOLIK, H. (org.) **Handbook of Paper and Board**. Shipholweg: Taylor & Francis Books, 2013. p. 332-382.
- KRYSZTAFKIEWICZ, A.; LIPSKA, L. K.; CIESIELCZYK, F.; JESIONOWSKI, T. Amorphous magnesium silicate - synthesis, physicochemical properties and surface morphology. **Advanced Powder Technology**, v. p. 549-565, 2004.
- KUMAR, V.; PATHAK, P.; BHARDWAJ, N. K. Micro-nanofibrillated cellulose preparation from bleached softwood pulp using chemo-refining approach and its evaluation as strength enhancer for paper properties. **Applied Nanoscience**, v. 11, n. 1, p. 101-115, 2020.
- KUPNIK, K.; PRIMOZIC, M.; KOKOL, V.; LEITGEB, M. Nanocellulose in drug delivery and antimicrobially active materials. **Polymers**, v. 12, 2825, 2020.
- KUSWANDI, B.; JUMINA, J. 12 - Packaging functions. In: SIDDIQUI, M. W. (org.) **Fresh-Cut Fruits and Vegetables: Technologies and Mechanisms for Safety Control**. Massachusetts: Academic Press, 2020. p. 243-294. Disponível em: <https://www.sciencedirect.com/science/article/pii/B9780128161845000124#!>. Acesso em: 21 jan. 2022.
- LAVERS, J. L.; DICKS, M. R.; FINGER, A. Significant plastic accumulation on the Cocos (Keeling) Islands, Australia. **Scientific Reports**, v. 9, 7102, 2019.
- LEAL, M. R.; FLORES-SAHAGUN, T. H. S.; FRANCO, T. S.; MUNIZ, I. B. *Ceiba speciosa* St. Hill fruit fiber as a potential source for nanocellulose production and reinforcement of polyvinyl acetate composites. **Polymer composites**, v. 42, n. 1, p. 397-411, 2021.
- LEE, H. L.; KIM, J. D.; LEE, K. H.; KIM, C. H.; YOUN, H. J. Effect of coating formulations and drying methods on the coverage and smoothness of brown grade base papers. **Nordic Pulp & Paper Research**, v. 27, p. 79-85, 2018.

- LENGOWSKI, E. C.; BONFATTI JÚNIOR, E. A.; SIMON, L.; MUÑIZ, G. I. B.; ANDRADE, A. S.; NISGOSKI, S.; KLOCK, U. Different degree of fibrillation: strategy to reduce permeability in nanocellulose-starch films. **Cellulose**, v. 27, p. 10855-10872, 2020.
- LEVANIČ, J.; ŠENK, V. P.; NADRAH, P.; POLJANŠEK, I.; OVEN, P.; HAAPALA, A. Analyzing TEMPO-Oxidized Cellulose Fiber Morphology: New Insights into Optimization of the Oxidation Process and Nanocellulose Dispersion Quality. **ACS Sustainable Chemistry & Engineering**, v. 8, p. 17752-17762, 2020.
- LI, S. M.; JIA, N.; ZHU, J. F.; MA, M. G.; SUN, R. C. Synthesis of cellulose–calcium silicate nanocomposites in ethanol/water mixed solvents and their characterization. **Carbohydrate Polymers**, v. 80, p. 270-275, 2010.
- LI, F.; MASCHERONI, E.; PIERGIOVANNI, L. The potential of nanocellulose in the packaging field: A review. **Packaging Technology and Science**, v. 28, p. 475-508, 2015.
- LI, L.; ZHANG, M.; SONG, S.; YANG, B.; WU, Y.; YANG, Q. Preparation of core/shell structured silicate composite filler and its reinforcing property. **Powder Technology**, v. 322, p. 27-32, 2018.
- LI, J.; ZHANG, J.; WU, X.; ZHAO, J.; WU, M.; HUAN, W. A nanocomposite paper comprising calcium silicate hydrate nanosheets and cellulose nanofibers for high-performance water purification. **RSC Advances**, v. 10, 30304, 2020a.
- LI, T.; ZHAO, L.; WANG, Y.; WU, X.; LIAO, X. Effect of High-Pressure Processing on the Preparation and Characteristic Changes of Biopolymer-Based Films in Food Packaging Applications. **Food Engineering Reviews**, aop, p. 1-11, 2020b.
- LI, B.; TRUEMAN, B. F.; MUNOZ, S.; LOCSIN, J. M.; GAGNON, G. A. Impact of sodium silicate on lead release and colloid size distributions in drinking water. **Water Research**, v. 190, 116709, 2021.
- LIU, A.; LARS, A.; BERGLUND, A. Fire-retardant and ductile clay nanopaper biocomposites based on montmorillonite in matrix of cellulose nanofibers and carboxymethyl cellulose. **European Polymer Journal**, v. 49, p. 940-949, 2013.
- LIU, C.; ZHANG, W.; SONG, S.; LI, H. A novel method to improve carboxymethyl cellulose performance in the flotation of talc. **Minerals Engineering**, v. 131, p. 23-27, 2019.
- LIU, X.; JIANG, Y.; WANG, L.; SONG, X.; QIN, C.; WANG, S. Tuning of size and properties of cellulose nanofibers isolated from sugarcane bagasse by endoglucanase-assisted mechanical grinding. **Industrial Crops and Products**, v. 146, 112201, 2020.
- LOMMATZSCH, M.; RICHTER, L.; BIEDERMANN-BREM, S.; BIEDERMANN, M.; GROB, K.; SIMAT, T. J. Functional barriers or adsorbent to reduce the migration of mineral

- oil hydrocarbons from recycled cardboard into dry food. **European Food Research and Technology**, v. 242, p. 1727-1733, 2016.
- LONG, L.; TIAN, D.; HU, J.; WANG, F.; SADDLER, J. A xylanase-aided enzymatic pretreatment facilitates cellulose nanofibrillation. **Bioresource Technology**, v. 243, p. 898-904, 2017.
- MALUCELLI, L. C.; MATOS, M.; JORDÃO, C.; LOMONACO, D.; LACERDA, L. G.; CARVALHO FILHO, M. A. S.; MAGALHÃES, W. L. E. Influence of cellulose chemical pretreatment on energy consumption and viscosity of produced cellulose nanofibers (CNF) and mechanical properties of nanopapers. **Cellulose**, v. 26, p. 1667-1681, 2019.
- MAHMOUDI, M.; PARVIZIOMRAN, I. Reusable packaging in supply chains: A review of environmental and economic impacts, logistics system designs, and operations management. **International Journal of Production Economics**, v. 228, 107730, 2020.
- MÁRMOL, G.; SAVASTANO JÚNIOR, H.; TASHIMA, M. M.; PROVIS, J. L. Optimization of the MgO-SiO₂ binding system for fiber-cement production with cellulosic reinforcing elements. **Materials and Design**, v. 105, p. 251-261, 2016.
- MARTIN, K. R. The chemistry of silica and its potential health benefits. **The Journal of nutrition, health & aging**, v. 11, 94, 2007.
- MAZIRIRI, E. T. Green packaging and green advertising as precursors of competitive advantage and business performance among manufacturing small and medium enterprises in South Africa. **Cogent Business & Management**, v. 7, 1719586, 2020.
- MEHERISHI, L.; SUSHMITA, A.; RANJANI, K. S. Sustainable packaging for supply chain management in the circular economy: A review. **Journal of Cleaner Production**, v. 237, 117582, 2019.
- MENDES, R. F.; MENDES, L. M.; OLIVEIRA, J. E.; SAVASTANO JUNIOR, H.; GLENN, G.; TONOLI, G. H. D. Modification of *Eucalyptus* pulp fiber using silane coupling agents with aliphatic side chains of different length. **Polymer Engineering and Science**, v. 55, n. 6, p. 1273-1280, 2015.
- MENG, C.; YANG, J.; ZHANG, B.; YU, C. Rapid and energy saving preparation of ramie fiber in TEMPO-mediated selective oxidation system. **Industrial Crops and Products**, v. 126, p. 143-150, 2018.
- MIHRANYAN, A.; ESMAEILI, M.; RAZAQ, A.; ALEXEICHIK, D.; LINDSTRÖM, T. Influence of the nanocellulose raw material characteristics on the electrochemical and mechanical properties of conductive paper electrodes. **Journal of Materials Science**, v. 47, p. 4463-4472, 2012.

- MIRI, S.; RAGHUWANSHI, V. S.; ANDREWS, P. C.; BATCHELOR, W. Composites of mesoporous silica precipitated on nanofibrillated cellulose and microfibrillated cellulose: Effect of fibre diameter and reaction conditions on particle size and mesopore diameter. **Microporous and Mesoporous Materials**, v. 311, 110701, 2021.
- MIRMEHDI, S.; HEIN, P. R. G.; SARANTÓPOULOS, C. I. G. L.; DIAS, M. V.; TONOLI, G. H. D. Cellulose nanofibrils/nanoclay hybrid composite as a paper coating: Effects of spray time, nanoclay content and corona discharge on barrier and mechanical properties of the coated papers. **Food Packaging and Shelf Life**, v. 15, p. 87-94, 2018.
- MOGHADDAM, M. K.; KARIMI, E. The effect of oxidative bleaching treatment on *Yucca* fiber for potential composite application. **Cellulose**, v. 27, p. 9383-9396, 2020.
- MOLINA-BESCH, K.; WILKSTRÖM, F.; WILLIANS, H. The environmental impact of packaging in food supply chains—does life cycle assessment of food provide the full picture? **The International Journal of Life Cycle Assessment**, v. 24, p. 37-50, 2019.
- MÜLLER, L. A. E.; ZIMMERMAN, T.; NYSTRÖM, G.; BURGET, I.; SIQUEIRA, G. Mechanical properties tailoring of 3d printed photoresponsive nanocellulose composites. **Advanced Functional Materials**, v. 30, 2002914, 2020.
- NADERI, A.; KOSCHELLA, A.; HEINZE, T.; SHIH, K. C.; NIEH, M. P; PFEIFER, A.; CHANG, C. C.; ERLANDSSON, J. Sulfoethylated nanofibrillated cellulose: Production and properties. **Carbohydrate Polymers**, v. 169, n. 1, p. 515-523, 2017.
- NAHRAWY, A. M. E.; MOEZ, A. A.; SAAD, A. M. Sol-Gel Preparation and Spectroscopy Properties of Modified Sodium Silicate/Tartrazine Dye Nanocomposite. **Silicon**, v. 10. p. 2117-2122, 2018.
- NAIR, S. S.; ZHU, J. Y.; RAGAUSKAS, A. J. Characterization of cellulose nanofibrillation by micro grinding. **Journal of Nanoparticle Research**, v. 16, 2349, 2014a.
- NAIR, S. S.; ZHU, J. Y.; DENG, Y.; RAGAUSKAS, A. J. High performance green barriers based on nanocellulose. **Sustainable Chemical Processes**, v. 2, 23, 2014b.
- NAZRIN, A.; SAPUAN, S. M.; ZUHRI, M. Y. M.; IYAS, R. A.; SYAFIQ, R.; SHERWANI, F. K. Nanocellulose reinforced thermoplastic starch (TPS), polylactic acid (PLA), and polybutylene succinate (PBS) for food packaging applications. **Frontiers in Chemistry**, v. 8, 213, 2020.
- NECHITA, P.; ROMAN, M. Review on polysaccharides used in coatings for food packaging papers. **Coatings**, v. 10, 566, 2020.

- NECHYPORCHUK, O.; PIGNON, F.; BELGACEM, M. N. Morphological properties of nanofibrillated cellulose produced using wet grinding as an ultimate fibrillation process. **Journal of Materials Science**, v. 50, p. 531-541, 2015.
- NECHYPORCHUK, O.; BELGACEM, M. N.; BRAS, J. Production of cellulose nanofibrils: A review of recent advances. **Industrial Crops and Products**, v. 93, n. 25, p. 2-25, 2016.
- NEYSES, B.; RAUTKARI, L.; YAMAMOTO, A.; SANDBERG, D. Pre-treatment with sodium silicate, sodium hydroxide, ionic liquids or methacrylate resin to reduce the set-recovery and increase the hardness of surface-densified Scots pine. **iForest**, v. 10, p. 857-684, 2017.
- NISHIMURA, H.; KAMIYA, A.; NAGATA, T.; KATAHIRA, M.; WATANABE, T. Direct evidence for α ether linkage between lignin and carbohydrates in wood cells walls. **Scientific Reports**, v. 8, 6538, 2018.
- NOGUCHI, Y.; HOMMA, I.; MATSUBARA, Y. Complete nanofibrillation of cellulose prepared by phosphorylation. **Cellulose**, v. 24, p. 1295-1305, 2017.
- OLIVEIRA, M. L. C.; MIRMEHDI, S.; SCATOLINO, M. V.; GUIMARÃES JÚNIOR, M.; SANADI, A. R.; DAMASIO, R. A. P.; TONOLI, G. H. D. Effect of overlapping cellulose nanofibrils and nanoclay layers on mechanical and barrier properties of spray-coated papers. **Cellulose**, *in press*, 2022.
- ONYIANTA, A. J.; DORRIS, M.; WILLIAMS, R. L. Aqueous morpholine pre-treatment in cellulose nanofibril (CNF) production: comparison with carboxymethylation and TEMPO oxidization pre-treatment methods. **Cellulose**, v. 25, p. 1047-1064, 2018.
- ONYIANTA, A. J.; O'ROURKE, D.; SUN, D.; POPESCU, C. M.; DORRIS, M. High aspect ratio cellulose nanofibrils from macroalgae *Laminaria hyperborean* cellulose extract via a zero-waste low energy process. **Cellulose**, v. 27, p. 7997-8010, 2020.
- OSONG, S. H.; NORGRÉN, S.; ENGSTRAND, P. Processing of wood-based microfibrillated cellulose and nanofibrillated cellulose, and applications relating to papermaking: a review. **Cellulose**, v. 23, p. 23-123, 2016.
- OUYANG, Y.; YIN, N.; CHEN, S.; TANG, L.; WANG, H. Synthesis and characterization of bacterial cellulose/calcium silicate composite. **Advanced Materials Research**, v. 476, p. 863-866, 2012.
- OTTESEN, V.; KUMAR, V.; TOIVAKKA, M.; CHINGA-CARRASCO, G.; SYVERUD, K.; GREGERSEN, O. W. Viability and properties of roll-to-roll coating of cellulose nanofibrils on recycled paperboard. **Nordic Pulp & Paper Research Journal**, v. 32, n. 2, p. 179-188, 2017.

- PALEM, R. R.; RAO, K. M.; SHIMOGA, G.; SARATALE, R. G.; SHINDE, S. K.; GHODAKE, G. S.; LEE, S. H. Physicochemical characterization, drug release, and biocompatibility evaluation of carboxymethyl cellulose-based hydrogels reinforced with sepiolite nanoclay. **International Journal of Biological Macromolecules**, v. 178, p. 464-476, 2021.
- PENNELS, J.; GODWIN, I. D.; AMIRALIAN, N.; MARTIN, D. J. Trends in the production of cellulose nanofibers from non-wood sources. **Cellulose**, v. 27, p. 575-593, 2020.
- PERRIN, L.; GILLET, G.; GRESSIN, L.; DESOBRY, S. Interest of pickering emulsions for sustainable micro/nanocellulose in food and cosmetic applications. **Polymers**, v. 12, 2385, 2020.
- PETERSSON, L.; OKSMAN, K. Biopolymer based nanocomposites: Comparing layered silicates and microcrystalline cellulose as nanoreinforcement. **Composites science and technology**, v. 66, p. 2187-2196, 2006.
- PHANTHONG, P.; REUBROYCHAROEN, P.; HAO, X.; XU, G.; ABUDULA, A.; GUAN, G. Nanocellulose: Extraction and application. **Carbon Resources Conversion**, in press, 2018.
- POPIL, R. E.; JOYCE, M. K. Strategies for economical alternatives for wax replacement in packaging. **Tappi Journal**, v. 4, p. 11-18, 2008.
- RAABE, J.; FONSECA, A. S.; BUFALINO, L.; RIBEIRO, C.; MARTINS, M. A.; MARCONCINI, J. M.; TONOLI, G. H. D. Evaluation of reaction factors for deposition of silica (SiO₂) nanoparticles on cellulose fibers. **Carbohydrate Polymers**, v. 114, p. 424-431, 2014.
- RAABE, J.; FONSECA, A. S.; BUFALINO, L.; CAUE, R.; MARTINS, M. A.; MARCONCINI, J. M.; MENDES, L. M.; TONOLI, G. H. D. Biocomposite of cassava starch reinforced with cellulose pulp fibers modified with deposition of silica (SiO₂) nanoparticles. **Journal of Nanomaterials**, v. 2015, 493439, 2015.
- REN, Y.; LINTER, B. R.; FOSTER, T. J. Cellulose fibrillation and interaction with psyllium seed husk heteroxylan. **Food Hydrocolloids**, v. 104, 105725, 2020.
- RICHARDSON, I. G. The calcium silicate hydrates. **Cement and Concrete Research**, v. 38, p. 137-158, 2008.
- ROBLES, E.; URRUZOLA, I.; LABIDI, J.; SERRANO, L. Surface-modified nano-cellulose as reinforcement in poly(lactic acid) to conform new composites. **Industrial Crops and Products**, v. 71, p. 44-53, 2015.
- ROL, F.; BELGACEM, M. N.; GANDINI, A.; BRAS, J. Recent advances in surface-modified cellulose nanofibrils. **Progress in Polymer Science**, v. 88, p. 241-264, 2019.

ROVERA, C.; TÜRE, H.; HEDENQVIST, M. S.; FARRIS, S. Water vapor barrier properties of wheat gluten/silica hybrid coatings on paperboard for food packaging applications. **Food Packaging and Shelf Life**, v. 26, 100561, 2020.

RUDRA, S. G.; SINGH, V.; JYOTI, S. D.; SHIVHARE, U. S. Mechanical properties and antimicrobial efficacy of active wrapping paper for primary packaging of fruits. **Food Bioscience**, v. 3, p. 49-58, 2013.

SAI, H.; XING, L.; CUI, L.; JIAO, J.; ZHAO, C.; LI, Z.; LI, F.; ZHANG, T. Flexible aerogels with interpenetrating network structure of bacterial cellulose–silica composite from sodium silicate precursor via freeze drying process. **RSC Advances**, v. 4, p. 30453-30461, 2014.

SAITO, T.; KIMURA, S.; NISHIYAMA, Y.; ISOGAI, A. Cellulose nanofibers prepared by TEMPO-Mediated Oxidation of Native Cellulose. **Biomacromolecules**, v. 8, p. 2485-2491, 2007.

SÁNCHEZ-GUETIÉRREZ, M.; ESPINOSA, E.; BASCÓN-VILLEGAS, I.; PÉREZ-RODRIGUES, F.; CARRASCO, E.; RODRÍGUEZ, A. Production of cellulose nanofibers from olive tree harvest – A residue with wide applications. **Agronomy**, v. 10, n. 5, 2020.

SAREMI, R.; BARODINOV, N.; LARADJI, A. M.; SHARMA, S.; LUZINOV, I.; MINKO, S. Adhesion and Stability of Nanocellulose Coatings on Flat Polymer Films and Textiles. **Molecules**, v. 25, 3238, 2020.

SCATOLINO, M. V.; SILVA, D. W.; BUFALINO, L.; TONOLI, G. H. D.; MENDES, L. M. Influence of cellulose viscosity and residual lignin on water absorption of nanofibrils films. **Procedia Engineering**, v. 200, p. 155-161, 2017.

SEELEY, M.; SONG, B.; PASSIE, R.; HALE, R. C. Microplastics affect sedimentary microbial communities and nitrogen cycling. **Nature Communications**, v. 11, 2372, 2020.

SEQUEIRA, S.; EVTUGUIN, D. V.; PORTUGAL, I. Preparation and Properties of Cellulose/Silica Hybrid Composites. **Polymer Composites**, v. 30, n. 9, p. 1275-1282, 2009.

SERRA-PARAREDA, F.; TARRÉS, Q.; PÈLACH, M. A.; MUTJÉ, P.; BALEA, A.; MONTE, M. C.; NEGRO, C.; DELGADO-AGUILLAR, M. Monitoring fibrillation in the mechanical production of lignocellulosic micro/nanofibers from bleached spruce thermomechanical pulp. **International Journal of Biological Macromolecules**, v. 178, p. 354-362, 2021.

SHARMA, S.; NAIR, S. S.; ZHANG, Z.; RAGAUSKAS, A. J.; DENG, Y. Characterization of micro fibrillation process of cellulose and mercerized cellulose pulp. **RSC Advances**, v. 5, 63111, 2015.

SIGMA-ALDRICH. **2,2,6,6-Tetramethyl-1-piperidinyloxy, free radical, 2,2,6,6-Tetramethylpiperidine 1-oxyl, TEMPO.** Disponível em: [https://www. sigmaaldrich.](https://www.sigmaaldrich)

com/catalog/search?term=tempo&interface=All&N=0&mode=match%20partialmax&lang=pt ®ion=BR&focus=product. Acesso em: 23 março 2021.

SIRACUSA, V.; ROCCULI, P.; ROMANI, S.; ROSA, M. D. Biodegradable polymers for food packaging: a review. **Food Science and Technology**, v. 19, p. 634-643, 2008.

SOLIKHIN, A.; HADI, Y. S.; MASSIJAYA, M. Y.; NIKMATIN, S. Production of microfibrillated cellulose by novel continuous steam explosion assisted chemo-mechanical methods and its characterizations. **Waste and Biomass Valorization**, v. 10, p. 275-286, 2019.

SONAR, C. R.; AL-GHAMDI, S.; MARTI, F.; TANG, J.; SABLANI, S. S. Performance evaluation of biobased/biodegradable films for in-package thermal pasteurization. **Innovative Food Science and Emerging Technologies**, v. 66, 102485, 2020.

SONG, L.; LIU, W.; XIN, F.; LI, YINGMIN. Study of adhesion properties and mechanism of sodium silicate blinder reinforced with silicate fume. **International Journal of Adhesion and Adhesives**, v. 106, 102820, 2021.

SÖNMEZ, S.; ÖZDEN, O. Barrier Properties of Paper and Cardboard. In: SALMAN, S. **Academic Researches in Architecture, Engineering Planning and Design**. İskitler: Gece Kitaplığı, p. 171-183, 2018.

SPIESER, H.; DENNEULIN, A.; DEGANELLO, D.; GETHIN, D.; KOPPOLU, R.; BRAS, J. Cellulose nanofibrils and silver nanowires active coatings for the development of antibacterial packaging surfaces. **Carbohydrate Polymers**, v. 240, 116305, 2020.

STANISLAS, T. T.; TENDO, J. F.; OJO, E. B.; NGASOH, O. F.; ONWUALU, P. A.; NJEUGNA, E.; SAVASTANO JUNIOR, H. Production and characterization of pulp and nanofibrillated cellulose from selected tropical plants. **Journal of Natural Fibers**, p. 1-17, 2020.

STOUDMANN, N.; SCHMUTZ, M.; HIRSCH, C.; NOWACK, B.; SOM, C. Human hazard potential of nanocellulose: quantitative insights from the literature. **Nanotoxicology**, v. 14, p. 1241-1257, 2020.

THOMAS, P.; DUOLIKUN, T.; RUMJIT, N. P.; MOOSAVI, S.; LAI, C. W.; JOHAN, M. R. B.; FEN, L. B. Comprehensive review on nanocellulose: Recent developments, challenges and future prospects. **Journal of the Mechanical Behavior of Biomedical Materials**, v. 110, 103884, 2020.

TRACHE, D.; TARCHOUN, A. F.; DERRADJI, M.; HAMIDON, T. S.; MASRUCHIN, N.; BROSSE, N.; HUSSIN, M. H. Nanocellulose: From fundamentals to advanced applications. **Frontiers in Chemistry**, v. 8, 392, 2020.

- TYAGE, P.; SALEM, K. S.; HUBBE, M. A.; PAL, L. Advances in barrier coatings and film technologies for achieving sustainable packaging of food products – A review. **Trends in Food Science & Technology**, v. 115, p. 461-485, 2021.
- VENTURA, C.; PINTO, F.; LOURENÇO, A. F.; FERREIRA, P. J. T.; LOURO, H.; SILVA, M. J. On the toxicity of cellulose nanocrystals and nanofibrils in animal and cellular models. **Cellulose**, v. 27, p. 5509-5544, 2020.
- VERA, P.; CANELLAS, E.; NERÍN, C. Compounds responsible for off-odors in several samples composed by polypropylene, polyethylene, paper and cardboard used as food packaging materials. **Food Chemistry**, v. 309, 125792, 2020.
- VIDAL, A. C. F.; HORA, A. B. **A indústria de papel e celulose**. In.: BNDES. Banco Nacional de Desenvolvimento Econômico e Social. BNDES 60 anos – Perspectivas Setoriais. Rio de Janeiro, 2012.
- VILARINHO, F.; SILVA, A. S.; VAZ, M. F.; FARINHA, J. P. Nanocellulose in green food packaging. **Critical Reviews in Food Science and Nutrition**, v. 58, p. 1526-1537, 2018.
- WANG, Q.; ZHU, J. Y.; GLEISNER, R.; KUSTER, T. A.; BAXA, U.; MCNEIL, S. E. Morphological development of cellulose fibrils of a bleached *Eucalyptus* pulp by mechanical fibrillation. **Cellulose**, v. 19, p. 1631-1643, 2012.
- WANG, Q.; ZHU, J. Y. Effects of mechanical fibrillation time by disk grinding on the properties of cellulose nanofibrils. **Tappi Journal**, v. 15, n. 6, 2016.
- WANG, L.; LI, K.; COPENHAVER, C.; MACKAY, S.; LAMM, M. E.; ZHAO, X.; DIXON, B.; WANG, J.; HAN, Y.; NEIVANDT, D.; JOHNSON, D. A.; WALKER, C. C.; OZCAN, S.; GARDNER, D. J. Review on Nonconventional Fibrillation Methods of Producing Cellulose Nanofibrils and Their Applications. **BioMacromolecules**, v. 22, p. 4037-4059, 2021.
- WU, C.; MCCLEMENTS, D. V.; HE, M.; ZHENG, L.; TIAN, T.; TENG, F.; LI, Y. Preparation and characterization of okara nanocellulose fabricated using sonication or high-pressure homogenization treatments. **Carbohydrate Polymers**, v. 255, 117364, 2021.
- XU, K.; SHI, Z.; LYU, J.; ZHANG, Q.; ZHONG, T.; DU, G.; WANG, S. Effects of hydrothermal pretreatment on nano-mechanical property of switchgrass cell wall and on energy consumption of isolated lignin-coated cellulose nanofibrils by mechanical grinding. **Industrial Crops and Products**, v. 149, 112317, 2020.
- YI, Y.; WANG, Z.; WENNERSTEN, R.; SUN, Q. Life cycle assessment of delivery packages in China. **Energy Procedia**, v. 105, p. 3711-3719, 2017.
- YOOK, S.; PARK, H.; LEE, S. Y.; KWON, J.; YOUN, H. J. Barrier coatings with various types of cellulose nanofibrils and their barrier properties. **Cellulose**, v. 27, p. 4509-4523, 2020.

YOUNES, M.; AGGETT, P.; AGUILAR, F.; CREBELLI, R.; DUSEMUND, B.; FILIPIC, M.; FRUTOS, M. J.; GALTIER, P.; GOTT, D.; GUNDERT-REMY, U.; KUHNLE, G. G.; LEBLANC, J. C.; LILLEGAARD, I. T.; MOLDEUS, P.; MORTENSEN, A.; OSKARSSON, A.; STANKOVIC, I.; WAALKENS-BERENDSEN, I.; WOUTERSEN, R. A.; WRIGHT, M.; BOON, P.; GURTLER, R.; MOSESSO, P.; PARENT-MASSIN, D.; TOBBACK, P.; CHRYSAFIDIS, D.; RINCON, A. M.; TARD, A.; LAMBRÉ, C. Re-evaluation of calcium silicate (E 552), magnesium silicate (E 553a(i)), magnesium trisilicate (E 553a(ii)) and talc (E 553b) as food additives. **EFSA Journal**, v. 16, e05375, 2018.

YU, Z.; LI, B.; CHU, J.; ZHANG, P. Silica *in situ*, enhanced PVA/chitosan biodegradable films for food packages. **Carbohydrate Polymers**, v. 184, p. 214-220, 2018.

YUAN, Y.; JIANG, B.; CHEN, H.; WU, W.; WU, S.; JIN, Y.; XIAO, H. Recent advances in understanding the effects of lignin structural characteristics on enzymatic hydrolysis. **Biotechnology for Biofuels**, v. 14, 205, 2021.

ZAMBRANO, F.; STARKEY, H.; WANG, Y.; ASSIS, C. A.; VENDITTI, R.; PAL, L.; JAMEEL, H.; HUBBE, M. A.; ROJAS, O. J.; GONZALEZ, R. Using micro-and nanofibrillated cellulose as a means to reduce weight of paper products: a review. **BioResources**, v. 15, n. 2, p. 4553-4590, 2020.

ZENG, Z.; WANG, C.; WU, T.; HAN, D.; LUKOVIC, M.; PAN, F.; SIQUEIRA, G.; NYSTRÖM, G. Nanocellulose assisted preparation of ambient dried, large-scale and mechanically robust carbon nanotube foams for electromagnetic interference shielding. **Journal of Materials Chemistry A**, v. 8, n. 35, p. 17969-17979, 2020.

ZHOU, Y.; ONO, Y.; TAKEUCHI, M.; ISOGAI, A. Changes to the contour length molecular chain length, and solid-state structures of nanocellulose resulting from sonication in water. **Biomacromolecules**, v. 21, n. 6, p. 2346-2355, 2020.

SEGUNDA PARTE – ARTIGOS**ARTIGO 1 – PRODUCTION OF CELLULOSE MICRO/NANOFIBRILS WITH
SODIUM SILICATE: IMPACT ON ENERGY CONSUMPTION,
MICROSTRUCTURE, CRYSTALLINITY AND STABILITY OF SUSPENSIONS**

Artigo publicado no periódico Nordic Pulp & Paper Research Journal

DOI: 10.1515/npprj-2022-0052

Production of cellulose micro/nanofibrils with sodium silicate: impact on energy consumption, microstructure, crystallinity and stability of suspensions

Impact of Na₂SiO₃ on the properties of cellulose micro/nanofibrils

Adriano Reis Prazeres Mascarenhas¹, Mário Vanoli Scatolino², Matheus Cordazzo Dias³, Maria Alice Martins⁴, Maressa Carvalho Mendonça³, Rafael Rodolfo de Melo⁵, Renato Augusto Pereira Damasio⁶, Gustavo Henrique Denzin Tonoli³

¹Department of Forest Engineering, Federal University of Rondônia (UNIR), 76940-000, Rolim de Moura, RO, Brazil.

²Department of Production Engineering, State University of Amapá (UEAP), 68900-070, Macapá, AP, Brazil.

³Department of Forest Science, Federal University of Lavras (UFLA), C.P. 3037, 37200-900, Lavras, MG, Brazil.

⁴Embrapa Instrumentation – National Laboratory of Nanotechnology for Agribusiness, 13561-206, São Carlos, SP, Brazil.

⁵Agricultural Sciences Center, Federal University of the Semi-arid (UFERSA), 59625-900, Mossoró, RN, Brazil.

⁶Klabin – Technology Center, Fazenda Monte Alegre, Santa Harmonia, 03, 84275-000, Telêmaco Borba, PR, Brazil.

Abstract

Pre-treatments reduce energy consumption for the production of cellulose micro/nanofibrils (MFC/CNF). The objective of this work was to study sodium silicate (Na₂SiO₃) solutions as pre-treatment for *Eucalyptus* sp. and *Pinus* sp. pulps. The treatments were identified as *EUC SS 5%* and *EUC SS 10%* when 5 and 10% Na₂SiO₃ were used, respectively. The treatments for *Pinus* sp. pulp were identified as *PIN SS 5%* and *PIN SS 10%*, and the untreated pulps as *EUC control* and *PIN control*. The lowest hemicellulose content was obtained for *PIN SS 10%*. *EUC SS 10%* showed the highest water retention values. *EUC SS 5%* (~4100 kWh/t) and *EUC SS 10%* (~4200 kWh/t) showed the lowest energy consumption. The pre-treated MFC/CNF showed diameters below 45 nm. The lowest viscosity was obtained for *EUC SS 5%* (5.5 cP) and the highest for *PIN control* (7.7 cP), respectively. The zeta potential indicated moderate stability of the suspensions (-24 ~ -18 mV). Na₂SiO₃ showed efficiency for MFC/CNF

production due to reduced energy consumption and better individualization. The suspensions have compatible characteristics for application as a stabilizer of colloidal systems and reinforcement of composites.

Keywords: energy consumption, microfibrillated cellulose (MFC), cellulose nanofibrils, nanotechnology, cell wall.

Introduction

Petroleum-based polymers are used in several industrial sectors and their incorrect disposal combined with the long decomposition time cause numerous damages to the environment. It is estimated that 25 to 30% of the items produced with these polymers are single-use (Lavers et al. 2019), contributing to material accumulation in ecosystems and compromising the aquatic and terrestrial organisms health (Häder et al. 2020). The use of biopolymers as a partial or total replacement of these materials is an alternative to mitigate these problems. Among the possibilities, cellulose stands out, being biodegradable and coming from renewable sources, besides being versatile and widely used in composites production, textile industry, food composition, packaging, and personal hygiene items (Mascarenhas et al. 2022).

Researchers have been striving in developing innovative products with this kind of biopolymers, such as cellulose nanomaterials (CNM) (Mokhena and John 2020; Cao et al. 2020). CNM groups together microfibrillated cellulose or cellulose microfibrils (MFC), cellulose nanofibrils (CNF), and cellulose nanocrystals (CNC) (Trache et al. 2020). Due to their high surface area and physical-mechanical performance, cellulosic micro/nanofibrils (MFC/CNF) have been studied in several applications, such as the production of composites (Wang et al. 2019), drug encapsulation (Kupnik et al. 2020), film production (Wang et al. 2020), and paper coating for biodegradable packaging (Jin et al. 2021).

Common processes related in literature to the production of MFC/CNF are microfluidization, sonication, high-pressure homogenization, ball mill, and mechanical fibrillation in a stone mill known as grinder (Nechyporchuk and Belgacem 2016). The challenges in the mechanical fibrillation process are related to the difficulty in deconstructing the crystalline cellulose structure. The non-application of chemical pre-treatments makes the energy consumption for deconstructing the fiber cell walls increase from 30,000 to 50,000 kWh/t using the grinder (Du et al. 2020).

According to Rol et al. (2019), the main pre-treatments aiming to modify the fibers for MFC/CNF production are sulfoethylation, carboxymethylation, phosphorylation, and oxidation mediated by N-oxy-2,2,6,6-tetramethylpiperidine - TEMPO. Despite considerably reducing

energy consumption in fibrillation, considering production on an industrial scale, some of these pre-treatments can generate toxic residues and costs for reagents acquisition, which can be a limiting factor (Long et al. 2017). Therefore, the study of alternative pre-treatments can provide the obtainment of MFC/CNF with reduced energy consumption, lower cost of reagents, and interesting physicochemical properties for application in new products. One of the possibilities is the application of alkaline pre-treatments, which the most common are based on NaOH solutions.

Dias et al. (2019) studied different concentrations of NaOH in the treatment of commercial bleached fibers of *Eucalyptus* sp. and *Pinus* sp. and found that using 5% (w/w) NaOH solution at 80 °C for 2h resulted in a reduction in energy consumption of about 40-60% in mechanical fibrillation, reducing the number of passes through the grinder. Fonseca et al. (2019) found that pretreatment of raw jute fibers with 5% (w/w) NaOH solution at the ratio of 1/20 (fibers/solution; w/v) resulted in greater individualization of MFC/CNF and reduced energy consumption. Other studies show controversial results, indicating that pre-treatment with NaOH did not reduce energy consumption and become MFC/CNF more brittle, reducing the quality and stability of the suspensions (Malucelli et al. 2019). This demonstrates the gaps in scientific knowledge regarding alkaline pre-treatments and the need to study other chemicals for this purpose.

Sodium silicate (Na_2SiO_3) is included in this context as a low-cost material with high alkaline potential (pH ~ 12). This component is used in the water treatment process, gel production, and pulp bleaching because of its cost-effectiveness (Li et al. 2021). Liu and Ott. (2020) reported that Na_2SiO_3 is the most important of the silicates because of its availability in liquid or powder form, has a high solubility in water, and because it is not flammable or explosive. In addition, silicate can remove extractives and substances from the fiber cell wall (Na et al. 2014), which can hinder fibrillation. Wang et al. (2017) indicated the possible Na_2SiO_3 potential for reduction of hemicelluloses amount from cellulosic pulps. Mastalska-Popławska et al. (2017) reported that treatment of cellulose fibers with NaOH can be replaced by Na_2SiO_3 solutions, which are also strongly alkaline. In this context, this study aimed to evaluate the impact of Na_2SiO_3 as alkaline pre-treatment for commercial bleached pulps of *Eucalyptus* sp. and *Pinus* sp. on energy consumption during mechanical fibrillation of the pulps and the properties of MFC/CNF suspensions.

Material and Methods

Fibers pre-treatment with sodium silicate

The raw material of the study was commercial bleached kraft pulps of *Eucalyptus* sp. (EUC) and *Pinus* sp. (PIN). To clarify the understanding, the commercial terminology “fiber” was used for the structural elements of PIN xylem instead of the botanical terminology “tracheids”. Na_2SiO_3 was used in the fibers pre-treatment, composed by 18% of Na_2O and 63% of SiO_2 , purchased by Dinâmica Química LTDA (São Paulo, Brazil). Solutions were prepared using deionized water and Na_2SiO_3 in ratios 5 and 10% (w/w), which were heated in a water bath at a temperature of 80 ± 2 °C. After heating, EUC and PIN pulps were added to the Na_2SiO_3 solutions, obtaining suspensions with a concentration of 2.5% (w/w). The suspensions were kept at a temperature of 80 ± 2 °C under constant stirring of 500 rpm for 2 h (Dias et al. 2019), being subjected to washing with deionized water until reaching pH 7 (Figure 1). Table 1 presents the identifications of the pre-treatments considering the kind of raw material and Na_2SiO_3 concentrations.

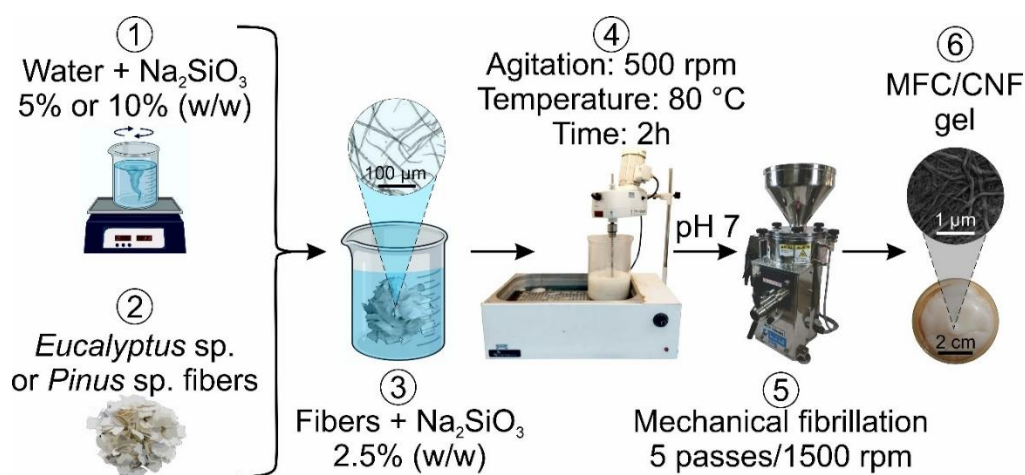


Figure 1: Scheme of pre-treatments with sodium silicate in *Eucalyptus* sp. and *Pinus* sp. until obtaining cellulose micro/nanofibrils (MFC/CNF) through mechanical fibrillation.

Table 1: Identification of pre-treatments with sodium silicate solutions performed for the fibers of *Eucalyptus* sp. and *Pinus* sp.

Raw material	Condition	Identification
<i>Eucalyptus</i> sp.	Untreated	<i>EUC control</i>
	Pre-treatment with 5% Na_2SiO_3	<i>EUC SS 5%</i>
	Pre-treatment with 10% Na_2SiO_3	<i>EUC SS 10%</i>
<i>Pinus</i> sp.	Untreated	<i>PIN control</i>
	Pre-treatment with 5% Na_2SiO_3	<i>PIN SS 5%</i>
	Pre-treatment with 10% Na_2SiO_3	<i>PIN SS 10%</i>

Production of cellulose micro/nanofibril suspensions

The pre-treated fibers were submerged in deionized water in a ratio of 2.0% (w/w) for EUC and 1.5% (w/w) for PIN. The material was stirred for 15 min at 500 rpm to ensure the swelling and fibers dispersion. Suspensions were produced with untreated fibers of EUC and PIN in deionized water in the same proportion presented above, as a control. The hydration procedures were performed as well as for the pre-treated fibers.

The fiber suspensions were mechanically fibrillated in the Supermasscolloider Masuko Sangyo MKGA-80 grinder (Kawaguchi, Japão), obtaining MFC/CNF after 5 passages, with the equipment adjusted to 1500 rpm (Mendonça et al. 2022). The initial distance between the grinder stones was 10 μm , gradually reaching 100 μm as the suspension viscosity increased.

Characterization of the fibers

Chemical composition

The carbohydrate composition of the extractive-free pulp of EUC and PIN, untreated and treated was determined based on Tappi T 249 cm 21 (TAPPI 2021a). The lignin content was obtained according to the standard Tappi T 222 om-02 (TAPPI 2021b). The cellulose content of EUC and PIN pulps was obtained by subtracting the total glucose content from the glucose content associated with mannose since for every 3 mannose units there is one glucose unit (Dias et al. 2019). Therefore, the hemicellulose content was obtained by the sum of galactose, arabinose, xylose, and mannose, with the respective glucose amount (Qaseem et al. 2021).

Fourier transformed infrared spectroscopy

Infrared vibrational spectroscopy analyses were performed for pre-treated and untreated pulps in a Varian 600-IR FT-IR spectrometer with Fourier transformed (FTIR) with a GladiATR accessory from Pike Technologies. Measurements were performed by attenuated total reflectance (ATR) at 45° with zinc selenide crystal. The spectral range analyzed was from 400 to 4000 cm^{-1} , resolution of 2 cm^{-1} , and 32 spectral accumulations.

Water retention value

The water retention value (WRV) was determined based on the Scan C 62:00 standard (SCAN 2000). Fibers suspension (0.5% m/m) was prepared, being the water from the suspension drained in a Thermo Fisher Scientific Heraeus Megafuge 16R centrifuge (Waltham, USA), adjusted with a force of 3000 G for 15 min. Posteriorly, the pulp retained on the sieve was weighed and dried at a temperature of 100 ± 2 °C until constant mass. The WRV was calculated according to Equation (1).

$$\text{WRV (g/g)} = \left(\frac{M_1}{M_2} \right) - 1 \quad (1)$$

Where M_1 is the mass (g) after draining in a centrifuge and M_2 is the mass (g) after drying.

Characterization of cellulose micro/nanofibril suspensions

Energy consumption in mechanical fibrillation

The energy consumption was evaluated for all passes. For this, the average current and time at each pass during fibrillation of the EUC and PIN pulps were recorded. The energy consumption was also calculated for the pass where the suspension obtained gel consistency, as shown in Equation (2).

$$\text{EC (kWh/t)} = \frac{(P \times t)}{m} \quad (2)$$

Where P (voltage \times electrical current) is the equipment potency (kW); t is the time spent for fibrillation (h); and m is the mass of pulp subjected to fibrillation (t).

Microstructural analysis

Suspensions with a concentration of 0.001% (w/w) of MFC/CNF were sonicated at 150 Hz for 2 min (Silva et al. 2020), being small aliquots added on double-sided carbon tape adhered to the aluminum sample holder (stubs). After an overnight period in a desiccator with silica gel, the samples were gold-metalized in a sputtering device. MFC/CNF morphology was observed in ultra-high resolution (UHR) field emission scanning electron microscope (SEM/FEG) TESCAN CLARA (Libušina, Czech Republic), in conditions of 10 KeV, 90 pA, and 10 mm of working distance. MFC/CNF diameters were measured for at least 200 individual structures using the software ImageJ.

X-ray diffraction and crystallinity index

X-ray diffraction (XRD) was performed to verify possible changes in the cellulose crystallinity index due to the removal of amorphous molecules (hemicelluloses) after the pretreatments and as a function of the fibrillation process in the ultra-refiner. Spectra were acquired from intact films produced from MFC/CNF by the “casting” method. The analyses were performed using an x-ray diffractometer Shimadzu Corporation XRD 6000 (Kyoto, Japan), adjusted with Cu K α radiation (1.1540 Å) at 30 kV and 30 mA. Scattered rays were collected in the range of $2\theta = 10\text{-}40^\circ$, a rate of $2^\circ/\text{min}$ (Tonoli et al. 2021). Curve noises were removed by the adjacent average method, with 10 points per window, producing smoothed patterns without compromising peak information. The patterns were deconvoluted using the software Magic Plot (3.0.1), and the peak information was presented in French (2014).

For the amorphous phase, the peak was set to $2\theta = 18^\circ$ and 9 to peak width at half maximum (PWHM) (Figure 2), varying only its intensity, as the literature suggests (French 2020).

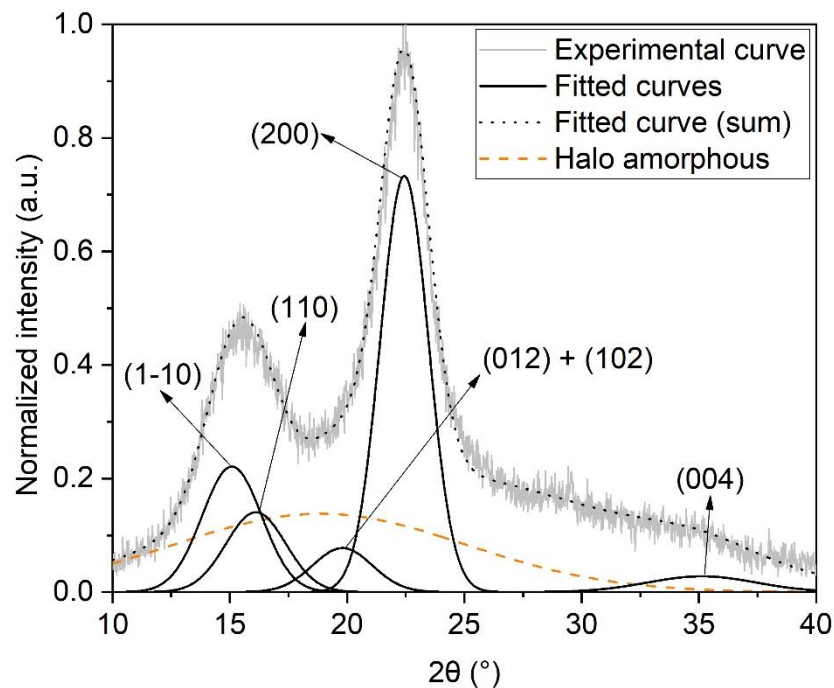


Figure 2: Typical x-ray diffraction pattern with different peaks for cellulose micro/nanofibrils (MFC/CNF).

The crystallinity index (CI) was calculated by Equation (3), where A_c is the sum of areas under the crystalline curves and A_t is the total area under XRD patterns.

$$CI (\%) = \frac{A_c}{A_t} \quad (3)$$

The crystallite size (CS) was estimated by the Scherrer equation (Equation (4)), where CS is the crystallite size in the (200) plane; K is the Scherrer constant that varies according to the crystal symmetry ($K = 0.89$); λ is the incident x-ray wavelength; and β is the peak width at half maximum (PWHM), in radians, θ is the Bragg angle corresponding to the plane peak (200).

$$CS \text{ (nm)} = \frac{K \times \lambda}{\beta \times \cos\theta} \quad (4)$$

Viscosity of suspensions

The viscosity of MFC/CNF suspensions was determined according to the standard TAPPI T 230 om-19 (TAPPI 2019). MFC/CNF suspensions were produced with concentration 0.5% (w/w) and diluted in copper ethylenediamine - CUEN (0.5 M). The suspension flow time was measured in a Cannon-Fenske viscometer n.150 and the viscosity was calculated according to Eq. 5.

$$V \text{ (cP)} = C \times t \times d \quad (5)$$

Where V is the viscosity (cP) of the cupric ethylenediamine solution (25 °C); C is the viscometer constant obtained by calibration; t is the average flow time (s); and d is the density of cellulose suspension (1.052 g/cm³).

Stability and zeta potential of suspensions

The evaluation of suspension stability (St) was carried out according to the methodology presented in Guimarães Júnior et al. (2015). In test tubes, 10 ml of MFC/CNF suspensions were added, with a concentration of 0.25% (w/w), previously homogenized by magnetic stirring at 500 rpm for 1 h. The suspensions were kept at rest and photographed every hour for 8 h. The measurement of total height and suspended height of MFC/CNF was performed by the software ImageJ. The stability (St) was calculated according to Equation 6.

$$St \text{ (\%)} = \left(\frac{SH}{TH} \right) \quad (6)$$

Where SH is the height corresponding to the particles suspended in the tube, and TH is the total height of the suspension present in the recipient.

The effect of pre-treatments on the suspension electrostatic stability was studied by determining zeta potential (ζ). The equipment Nano-ZS90X Malvern Zetasizer (England, UK),

used in the measurements, was switched on 30 min before the use, for suitable calibration. Measurements were performed at 25 °C, using 1 mL of each suspension with a concentration of 0.1% (w/w). For each treatment, 5 measurements were performed.

Statistical analysis

Data were analyzed by graphics (FTIR and XRD) and descriptive statistics, indicating average and standard deviation for the analyzed parameters.

Results and Discussion

Chemical composition of the fibers

The increase in sodium silicate concentration, from 5 to 10%, provided greater hemicellulose removal and an increase in the relative cellulose amount (Table 2). For EUC pulps, there was a slight hemicellulose removal and a slight increase in the relative cellulose amount after silicate application. For *PIN SS 10%*, there was a considerable reduction in the percentage of mannans (~21%). Galactans were not detected in both pulps.

Table 2: Average and standard deviation for the chemical composition of untreated and pre-treated pulps with sodium silicate.

Identification	Glucose	Arabinose	Xylans	Mannose	Galactose	Total lignin	Cellulose	Hemicelluloses
<i>EUC control</i>	79.1 ± 0.3*	ND**	15.7 ± 0.1	ND	ND	0.4 ± 0.1	79.1 ± 0.3	15.7 ± 0.1
<i>EUC SS 5%</i>	80.2 ± 0.2	ND	15.5 ± 0.2	ND	ND	0.5 ± 0.1	80.2 ± 0.2	15.5 ± 0.2
<i>EUC SS 10%</i>	80.1 ± 0.5	ND	15.3 ± 0.3	ND	ND	0.8 ± 0.1	80.1 ± 0.5	15.3 ± 0.3
<i>PIN control</i>	80.0 ± 0.7	0.5 ± 0.1	9.6 ± 0.1	7.5 ± 0.1	ND	0.5 ± 0.1	78.2 ± 0.6	17.6 ± 0.3
<i>PIN SS 5%</i>	79.6 ± 0.2	0.5 ± 0.1	9.4 ± 0.1	7.1 ± 0.1	ND	0.7 ± 0.1	77.9 ± 0.3	17.0 ± 0.3
<i>PIN SS 10%</i>	79.9 ± 1.1	0.4 ± 0.1	9.0 ± 0.1	5.9 ± 0.1	ND	0.4 ± 0.1	78.5 ± 1.1	15.3 ± 0.3

*Standard deviation; **not detected.

These results are explained by the alkaline nature of sodium silicate solutions, which present pH values typically between 11 and 12. Lignocellulosic materials have a high susceptibility to hemicellulose removal under alkaline conditions (Fonseca et al. 2019). The alkaline action occurs more intensely on the fibers surface, where there is a greater amount of xylans. For untreated coniferous fibers, there are generally higher amounts of glucomannans and xylans, while hardwood fibers have mostly xylans and low levels of glucomannans (Borrega et al. 2017). Based on these aspects, and because it is a commercial pulp, glucomannans absence in the EUC pulp is a possible consequence of the cooking and bleaching

processes (Bränvall 2017). This effect may have been intensified by pre-treatment with Na_2SiO_3 . Liu et al. (2018), using NaOH solution (4% m/v) at 50 °C and 80 °C for the treatment of hardwood kraft pulp, obtained a reduction in the hemicellulose content which varied between 6.8% and 7.7%.

The removal of hemicelluloses can facilitate the pulp mechanical fibrillation, since there is a greater OH group exposure of the cellulose chain, facilitating the fibrils interaction with water. The alkaline action of the Na_2SiO_3 solutions probably promoted the loosening of fiber cell walls due to the saponification of intermolecular ester bonds between cellulose and hemicelluloses, which increased fiber swelling capacity and surface area (Noremylia et al. 2022). Further, maintaining certain hemicelluloses amount results in more cell wall swelling, which can favor internal fibrillation.

Fourier transformed infrared spectroscopy

For the treated and untreated pulps, a large absorption was observed in the band between 3500 and 3300 cm^{-1} (Figure 3), in which the vibration stretching of the cellulose OH groups surface is identified (Lopes et al. 2018). *EUC SS 5%* showed an increase in the band intensity in this region when compared to the control. This was assumed to be due to the greater exposure of the -OH groups of the cellulosic chain, due to hemicellulose removal (Kabir et al. 2013). For *PIN SS 5%* and *PIN SS 10%*, the intensity in this band was decreased, probably due to the removal of glucans associated with mannans. The spectral bands between 1647-1638 cm^{-1} are attributed to the angular deformation of OH groups of adsorbed water (Marwanto et al. 2021). Bands corresponding to silica bonds were not verified, indicating the absence of Na_2SiO_3 residues in the fibers.

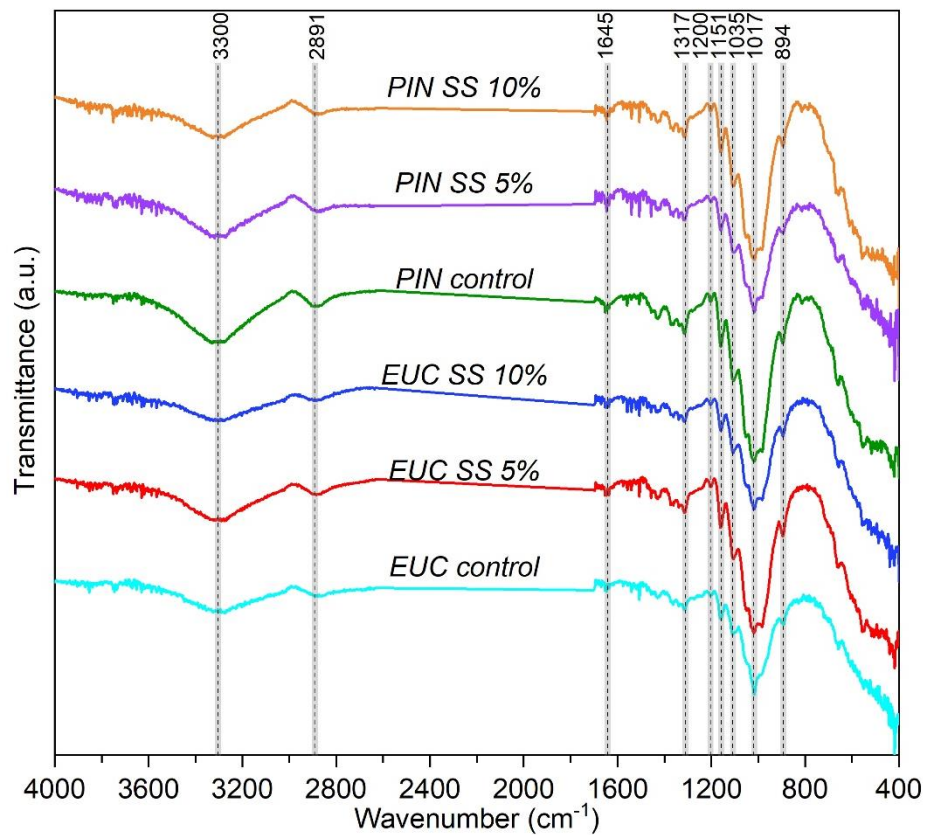


Figure 3: Typical ATR-FTIR spectra for the films from untreated and pre-treated MCF/CNF with sodium silicate.

For all treated pulps, band intensifications were observed in the region of 1017 cm^{-1} in relation to their respective controls, except for *EUC SS 10%* and *PIN SS 5%*. This spectral range is attributed to the stretching vibration of C-O and C-O-C bonds of the cellulosic chain (Qin et al. 2021). The peak intensity in this band is increased when pectin, hemicelluloses, and lignin levels decrease (Salim et al. 2021), confirming the Na_2SiO_3 ability to remove substances from the cell wall. *EUC SS 10%* pulp showed a reduction in peak intensity in the region $810\text{--}896\text{ cm}^{-1}$. In this band are observed the vibrations of C-OH groups related to the β -glycosidic bonds that bind hemicelluloses to cellulose (Özgenç et al. 2017).

Bands located around 1382 cm^{-1} and 1318 cm^{-1} indicate stretching of the C-C ring and C-O-C glycosidic ether bonds, respectively (Ramesh and Radhakrishnan 2019). The adsorption vibrational pattern of asymmetric bonds between C-O and C-O-C of carbons 2, 3, and 6 of glucopyranose, in the region 1171 cm^{-1} , 1110 cm^{-1} , 1060 cm^{-1} , and 1035 cm^{-1} (Sun et al. 2021), was not changed with the treatment of the pulp.

Spectra obtained by FTIR showed that the pre-treatments promoted chemical changes for most of the analyzed pulps. The angular deformations of bonds associated with the exposure

of functional groups of the cellulosic chain were highlighted as a result of the hemicelluloses removal. The Na_2SiO_3 promoted the increase of peak intensity in the bands attributed to the OH groups, which suggests greater water adsorption capacity by the fibers. The vibrational patterns corresponding to the functional groups, characteristic of cellulose I, were maintained, demonstrating that the high silicate alkalinity did not promote excessive chemical modification of pulps.

Water retention value

The WRV for EUC pulp (1.06 to 1.1 g/g) was higher compared with PIN (Figure 4). This fact may be a result of the higher xylans content in EUC pulp, which allowed greater water absorption to the fibers. Xylans are naturally amorphous and have a greater affinity for water than crystalline cellulose. The presence of these molecules reduces the water flow by capillarity in the cell wall and increases the water retention capacity of the fibers (Barbosa et al. 2018). Nahrawy et al. (2018) reported that Na_2SiO_3 can be able to increase the exposure to surface loads, potentiating fibers interactions with water.

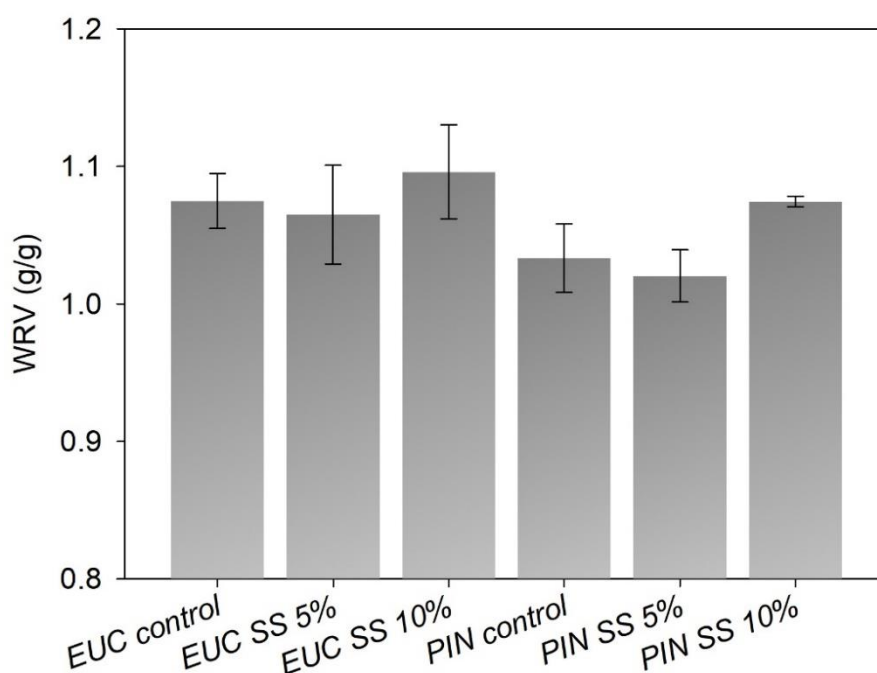


Figure 4: Water retention value (WRV) for the untreated and pre-treated pulps with sodium silicate.

For *EUC SS 5%*, no considerable increase in WRV, compared to *EUC control*, was observed. *EUC SS 10%* obtained an increase of 2% for WRV compared to *EUC control*. This

effect may be related to the swelling of the fibers caused by the Na_2SiO_3 solution alkalinity, which favored the fibers internal fibrillation. This also explains the increase in WRV for *PIN SS 10%* compared to *PIN control* and *PIN SS 5%*. The alkaline treatment promotes greater fiber wall swelling due to osmotic effects and the swelling pressure that breaks the hydrogen bonds between the fibrils (Lund et al. 2012). These characteristics can favor the cell wall deconstruction in the grinder because the reduction of the bonds can increase the shear effect. WRV allows the obtainment of relevant information about the fiber expansion capacity, as it provides indications of the hydrogen bonds with water in the cell wall (González et al. 2022).

For *EUC SS 10%* and *PIN SS 10%*, WRV values were slightly higher than the respective controls. This effect consolidates FTIR results and confirms the pre-treatment ability to promote greater fiber swelling. This effect may favor cell wall deconstruction during mechanical fibrillation, due to increased hydrogen bonds between water and the MFC/CNF network.

Energy consumption in mechanical fibrillation

For both types of fiber, all pre-treatments reduced energy consumption during mechanical fibrillation. For *PIN* pulp, energy consumption was higher compared to the values observed for *EUC* (Figure 5). For the controls, the gel was formed after 4 passes, whereas for *EUC SS 5%* and *PIN SS 5%*, gel formation occurred after 3 passes with energy consumptions of 4166 kWh/t and 4725 kWh/t, respectively. For *EUC SS 10%* (3251 kWh/t) and *PIN SS 10%* (4499 kWh/t), the gel was formed after 2 passes through the grinder.

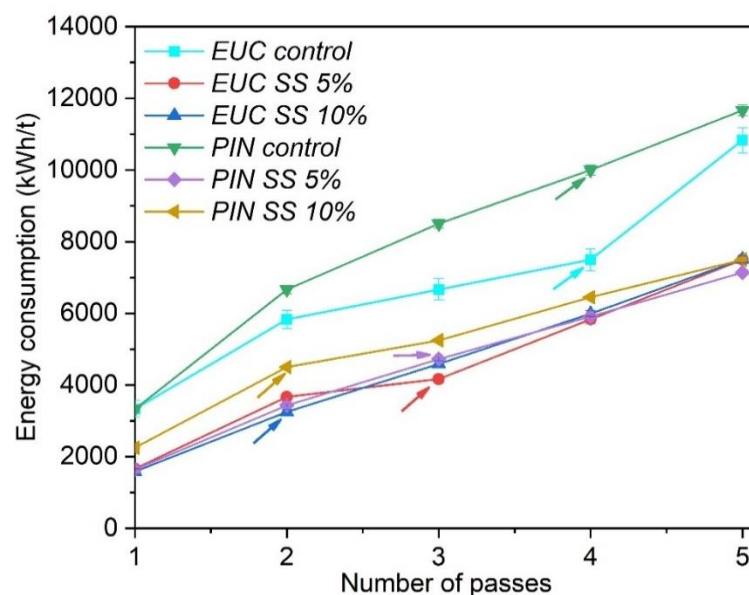


Figure 5: Energy consumption after the mechanical fibrillation of untreated and pre-treated pulps with sodium silicate. Arrows indicate the passage of gel formation.

The treatments *EUC SS 5%* and *EUC SS 10%* reduced energy consumption by 45% and 57%, respectively, compared to the *EUC control*. For *PIN SS 5%* and *PIN SS 10%* the energy consumption in relation to the *PIN control* was reduced by 53% and 55%, respectively. The differences in energy consumption between *EUC SS 5%* - *PIN SS 5%* and between *EUC SS 10%* - *PIN SS 10%* in the passage of gel formation were 559 kWh/t and 295 kWh/t, respectively. The higher energy consumption recorded for PIN pulps can be explained by the fiber morphology (tracheids). PIN tracheids are prone to curling and aggregate formation, favoring material accumulation in the grinder grooves, and increasing the friction between the stones, which increases the time spent for each passage and energy consumption.

This reduction mentioned in energy consumption may have been due to the action of Na_2SiO_3 on the delamination of the fiber cell wall during mechanical fibrillation. The loosening of the cell wall potentiates the shear on the fibril bundles and increases the number of charges on their surfaces. As a result, gel formation is favored due to the strong adhesion of water molecules to the numerous hydroxyl groups available in the MFC/CNF network (Esteves et al. 2020).

Pakutsah and Aht-Ong (2020) explain that the gel appearance of the suspension is a consequence of the viscosity increase. This effect is caused by the ability of MFC/CNF to water retention on their surfaces and internally. As the fibrillation occurs, the contact surface of the MFC/CNF increases, causing greater water retention compared to an original pulp, leading to the higher shear resistance of the suspension (Sarangi et al. 2021). Thus, the greater the suspension viscosity, the greater the energy consumption. These aspects indicate that gel formation for EUC may have been earlier than for PIN. In pulps with higher hemicellulose contents, there is an increase in fibrillation, since the carboxylic groups of these polysaccharides contribute to the electrostatic repulsion between the MFC/CNF in the water (Chen et al. 2020).

The values found for energy consumption are in harmony with results observed for other types of pre-treatments. Martins et al. (2021) observed gel formation on the third passage during mechanical fibrillation of unbleached EUC pulps treated with NaOH (5% m/v), obtaining energy consumption of around 5000 kWh/t. Using the same treatment, Dias et al. (2019) found values of energy consumption around 4000 and 4960 kWh/t for PIN and EUC bleached pulps, respectively, after 5 passages through the grinder.

Pre-treatments with Na_2SiO_3 were presented as an option to reduce energy consumption during mechanical fibrillation of the cellulosic pulp. This was confirmed when comparing the results of this study with works in which other alkaline pre-treatments were used. Abe (2016) reported that NaOH cannot always promote energy consumption reduction. Additionally, the

quality of MFC/CNF was impaired because the alkaline action became the material brittle and with reduced colloidal stability.

Microstructural analysis

EUC control obtained an average diameter for MFC/CNF of 57 ± 30 nm (Figure 6 and Figure 7a). The pre-treatment with 5% of silicate (*EUC SS 5%*) (Figure 7b), the MFC/CNF became more individualized and with an average diameter of 45 ± 10 nm.

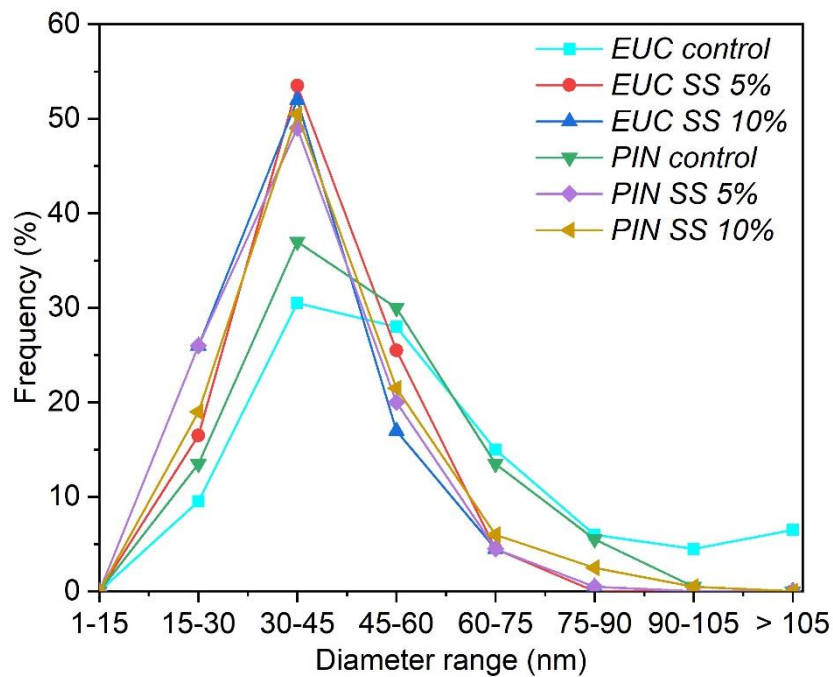


Figure 6: Diametric distribution histograms showing the general occurrence of MFC/NFC for the untreated and pre-treated with sodium silicate.

As observed for *EUC SS 5%*, the MFC/CNF obtained for *PIN SS 5%* were more individualized, with an average diameter of 39 ± 11 nm (Figure 7e). For *PIN control*, MFC/CNF obtained an average diameter of 47 ± 15 nm (Figure 7d).

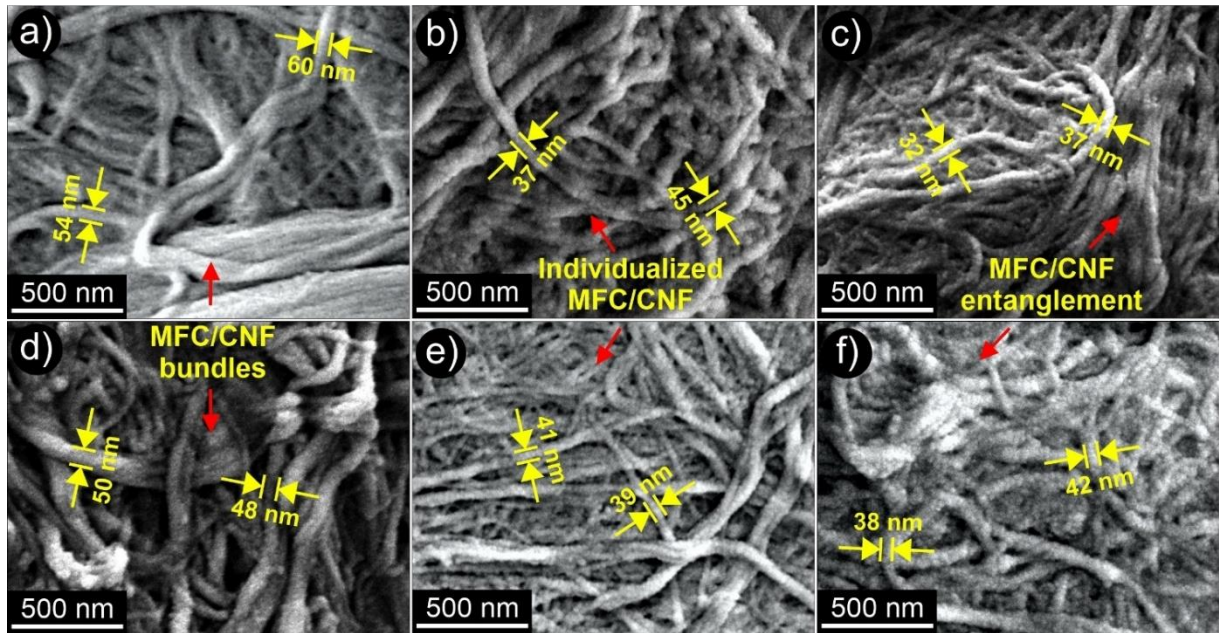


Figure 7: Ultra-high resolution micrographs demonstrating the morphology and arrangement of MFC/CNF; a) *EUC control*; b) *EUC SS 5%*; c) *EUC SS 10%*; d) *PIN control*; e) *PIN SS 5%*; and f) *PIN SS 10%*; arrows indicate typical structures considered for measurements.

EUC SS 10% and *PIN SS 10%* (Figure 7c and Figure 7f) obtained average MFC/CNF diameters of 38 ± 11 nm and 41 ± 13 nm, respectively, whereas more intact microfibril bundles were observed for *EUC* and *PIN* controls (arrows in Figure 7a and Figure 7d). Therefore, it can be said that the pulps pre-treated with Na_2SiO_3 were fibrillated with greater efficiency. These results also explain the higher energy consumption obtained for *PIN* pulps fibrillation about *EUC*. As the MFC/CNF presented smaller diameters, there was a greater intensity in fibrillation to degrade the cellulose crystalline structure, which is one of the factors that contribute to the energy consumption increase (Tonoli et al. 2012). Cruz et al. (2022) found similar results studying mechanical fibrillation of bleached fibers without pre-treatments obtaining MFC/CNF diameters ranging from 20 nm to 40 nm for *EUC*, and from 60 nm to 80 nm for *PIN*.

As observed, *EUC* MFC/CNF presented larger diameters, that is, smaller surface area. Therefore, the gel formation with the same number of passes applied to *PIN* fibers is explained by the presence of xylans in *EUC* pulp, which allowed greater fiber swelling and increased electrostatic repulsion forces between the fibrils during mechanical shear, facilitating gel formation (Afsahi et al. 2018).

The results showed that the pre-treatments, besides allowing the reduction of energy consumption, induced the obtaining of MFC/CNF networks with larger surfaces and aspect ratios, due to the smaller diameters observed for the structures. These characteristics enable the

material produced for applications in which high adsorption capacities are required, such as colloidal stabilizers and emulsions, or as composites reinforcement.

X-ray diffraction and crystallinity index

The diffraction curves of all studied pre-treatments show relatively ordered structures (Figure 8), with a narrow peak at approximately $2\theta = 22.6^\circ$ which corresponds to the plane (200) (Abral et al. 2021). Even with high alkalinity, the use of silicate did not result in the formation of cellulose II, since no peaks in the regions $2\theta = 12.3^\circ$ and $2\theta = 20^\circ$ were observed (French 2014).

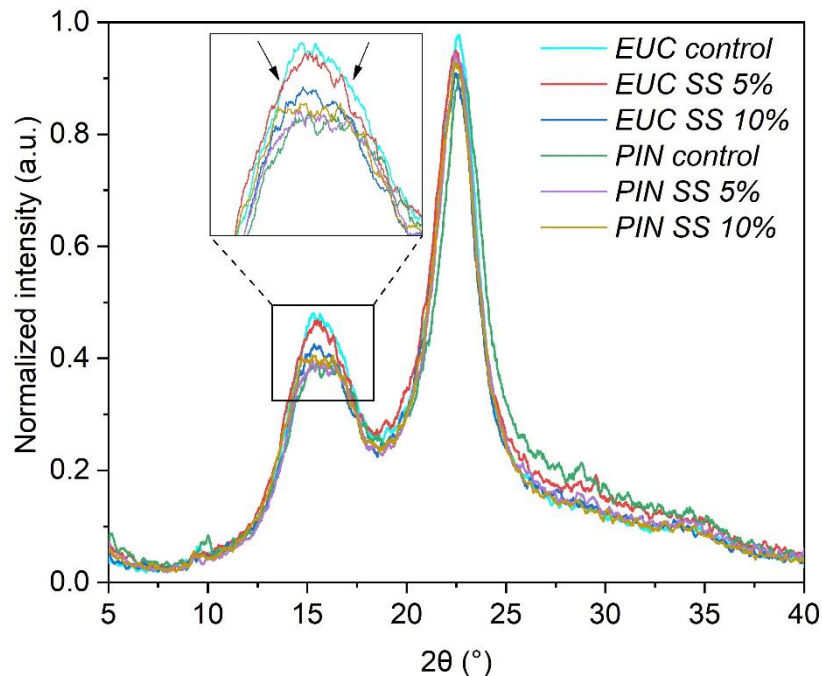


Figure 8: X-ray diffractograms for the films from untreated and pre-treated MFC/CNF with sodium silicate.

Around the region $2\theta = 20.4^\circ$, the planes (012) and (102) were identified (Popescu et al. 2020). This result indicates the absence of preferential orientation of MFC/CNF crystals (French 2014). These crystallographic planes were also observed by Dias et al. (2019) and Silva et al. (2021) for untreated and alkaline-treated MFC/CNF of EUC and PIN. The signal observed in the region close to $2\theta = 35^\circ$, corresponds to the superposition of numerous peaks, led by the crystalline plane (004) (Foster et al. 2018).

The curves deconvolution allowed to estimate the overlapping diffuse peaks located at $2\theta = 14.8^\circ$ and $2\theta = 16.5^\circ$. These peaks correspond to the (1-10) and (110) crystalline planes of

1 β cellulose (monoclinic) overlaid at $2\theta = 15^\circ$ (Lin et al. 2020). French (2020) explained that these peaks are more influenced by the amorphous halo due to the reduction in crystallinity, as can be seen by the distance from the experimental curves, except for *EUC control* and *EUC SS 5%* (see Figure 8). These results can be better observed from the variations in the crystallinity index (CI) (Table 3). *EUC SS 5%* and *EUC SS 10%* presented reductions in CI of 13% and 5.5% in relation to *EUC control*, respectively.

Table 3: Crystallinity index (CI) and crystallite size (CS) for the untreated and pre-treated MFC/CNF with sodium silicate.

Identification	CI (%)	CS (nm)
<i>EUC control</i>	$51.9 \pm 0.01^*$	3.3 ± 0.03
<i>EUC SS 5%</i>	45.1 ± 0.03	3.3 ± 0.01
<i>EUC SS 10%</i>	49.1 ± 0.01	3.1 ± 0.01
<i>PIN control</i>	52.5 ± 0.02	3.5 ± 0.03
<i>PIN SS 5%</i>	52.3 ± 0.05	3.1 ± 0.02
<i>PIN SS 10%</i>	55.7 ± 0.01	3.1 ± 0.02

*Standard deviation.

PIN SS 10% showed an increase of 6% in CI compared to *PIN control*. These results can be explained by the influence of the hemicelluloses removal, which allowed a greater contribution from the crystalline planes due to greater exposure of the cellulosic chain to x-rays. Differences between *PIN SS 5%* and the *PIN control* were very small ($< 0.5\%$). Regarding the crystallite size (CS), pre-treatments applied caused subtle decreases in relation to the respective controls.

The degradation of cellulosic fibers during mechanical fibrillation can change their crystallinity. Costa et al. (2021) explained that CI and CS tend to reduce with increasing MFC/CNF amount because of the breakdown of the crystalline structure of cellulose. For MFC/CNF suspensions with higher amounts of fiber fragments, CI tends to be higher due to the presence of fewer damaged crystals of MFC/CNF.

The variations found are expected because of the fiber shear phenomena involved in the MFC/CNF production. Different mechanisms explain mechanical cell wall fibrillation, such as internal and external fibrillation. In external fibrillation, the friction of fibers between the mill stones causes microfibrils individual burst, however, they remain partially attached to the cell wall (Zhao et al. 2019) (Figure 9a). Further, the specific surface is increased, which is a desirable characteristic for applications aiming composites reinforcement and ions adsorption (Liu et al. 2020).

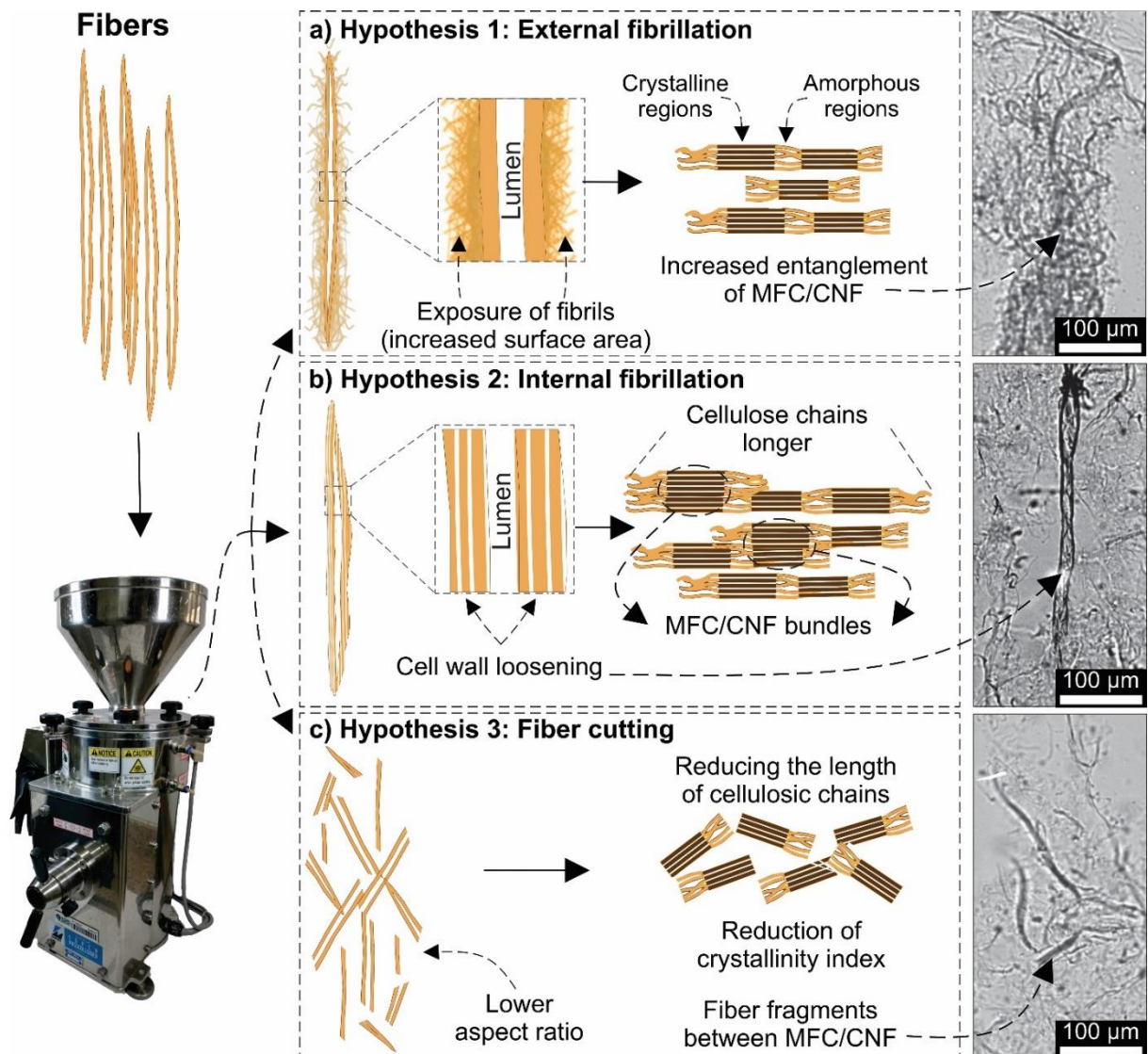


Figure 9: Light microscopy and scheme of the main mechanisms of external and internal fibrillation of MFC/CNF.

Internal fibrillation consists of the unpacking of the helical structure of cellulose microfibrils in the S_2 layer of the cell wall (Chen et al. 2014). Wang and Zhu (2016) explained that the abrasive action of the mill stones promotes the loosening of the cell wall and induces the formation of MFC/CNF bundles (Figure 9b). Regarding the other mechanisms, in general, they are more related to excessive fibrillation of the cellulosic pulp (Scatolino et al. 2017). In this case, the formation of dispersed fines occurs due to the MFC/CNF breaks along its length, reducing its aspect ratio (Figure 9c). This phenomenon leads to a reduction of CI, diameter, molar mass, and lower mechanical resistance of the microfibrils (Serra-Parareda et al. 2021). The last hypothesis may explain the reduction of CI and CS of MFC/CNF of *EUC SS 5%* and

EUC SS 10% because the higher hemicelluloses content results in earlier gel formation. As a result, the number of passes applied until the end of the processing may have reduced the length of the crystalline structures of the cellulosic chains.

Viscosity, stability and zeta potential

Viscosity of *EUC SS 5%* suspensions was reduced by 11% compared to *EUC control*, whereas for *EUC SS 10%*, there was an increase of 16% (Figure 10). This can be explained by the gel formation in *EUC SS 10%* with fewer passes. Due to the higher viscosity, it was necessary to increase the distance between the grinder stones to keep the suspension flow and avoid equipment overheating. Therefore, *EUC SS 10%* cellulose chains may have been subjected to lower abrasion intensities, keeping the greater apparent length and, consequently, greater viscosity.

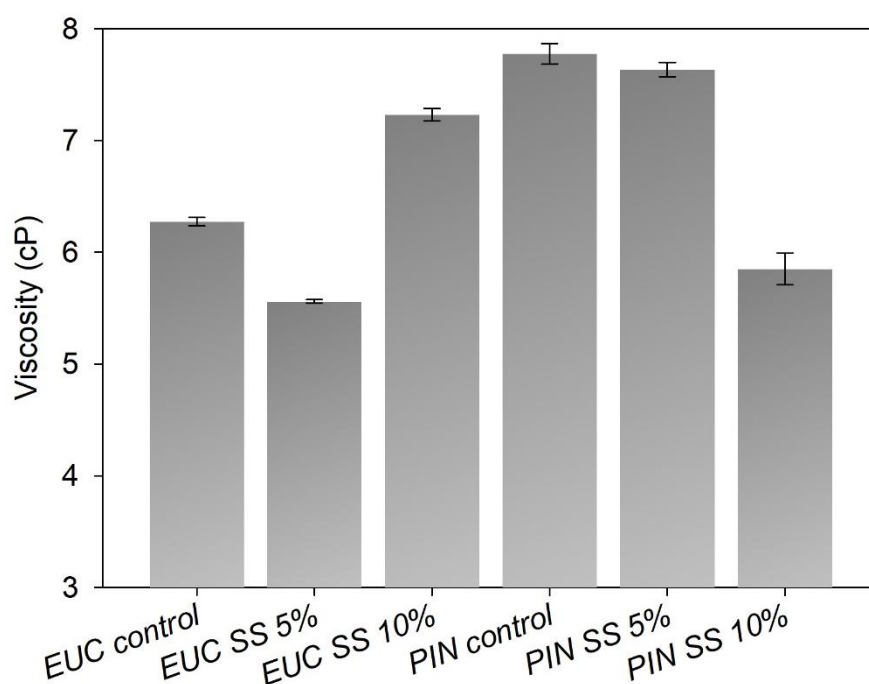


Figure 10: Viscosity for untreated and pre-treated MFC/CNF suspensions with sodium silicate solutions.

The viscosity found for *PIN SS 10%* was reduced by 25% compared to *PIN control*. This fact may be related to excessive fibrillation after gel formation, which reduced the length of the cellulosic chain and suspension viscosity. Viscosity is directly related to the three-dimensional architecture of the MFC/CNF network, which is defined by the increase or

decrease of particles homogeneity, length of cellulosic chains, amount of exposed amorphous regions, and fibrillation degree and hemicelluloses content (Ono et al. 2021).

The reduction in length of the cellulosic chain promotes an increase in electrostatic repulsion, lower interfibrillar interaction, and reduced viscosity (Jia et al. 2014). This effect may explain the results found for *PIN SS 10%*: greater reduction in hemicelluloses content (13%), and a lower reduction in crystallite size (11%) in relation to *PIN control* (see Table 2 and Table 3).

The internal and external fibrillation processes provide better development for the three-dimensional network of MFC/CNF, and higher viscosity for the suspension due to the greater number of hydrogen bonds between OH groups of cellulosic chain (Li et al. 2019). The behavior is opposite when the microfibrils are longitudinally cut. Excessive shear during mechanical fibrillation disrupts parts of the three-dimensional MFC/CNF network and reduces suspension viscosity (Dimic-Misic et al. 2018). This phenomenon reinforces the explanation of viscosity reduction for *EUC SS 5%*, *EUC SS 10%*, and *PIN SS 10%*. All suspensions showed low MFC/CNF sedimentation, indicating high stability (> 90%). In the first 4 h of evaluation, the sedimentation was rapid. After 5 h, *EUC SS 5%* and *PIN SS 10%* suspensions showed a tendency to stabilize (Figure 11a).

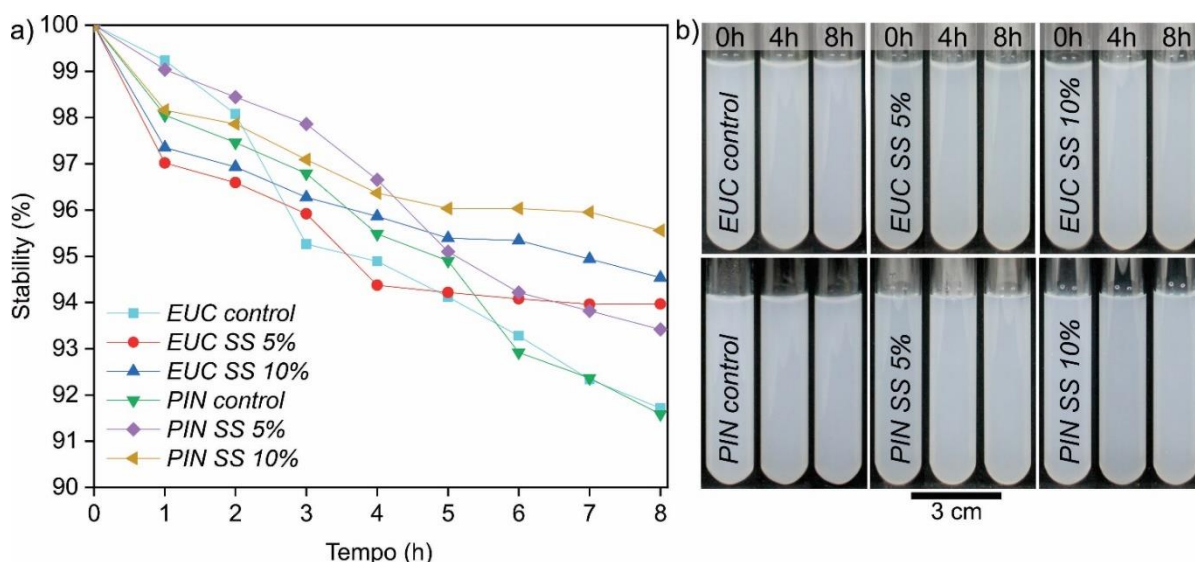


Figure 11: Stability of untreated and pre-treated MFC/CNF suspensions with sodium silicate.

EUC control stability was 2% lower compared to *EUC SS 5%* at the end of the evaluation, and 3% lower compared to *EUC SS 10%*. *PIN SS 5%* stability was 1% higher in relation to the control and 4% higher for *PIN SS 10%*. In general, the pre-treatments resulted in

a slight increase in suspension stability, being difficult to differentiate the sedimented region (Figure 11b). The results obtained for stability are in agreement with the values found for zeta potential (ζ). The values found for all pre-treatments studied ranged from -17 mV to -30 mV (Figure 12).

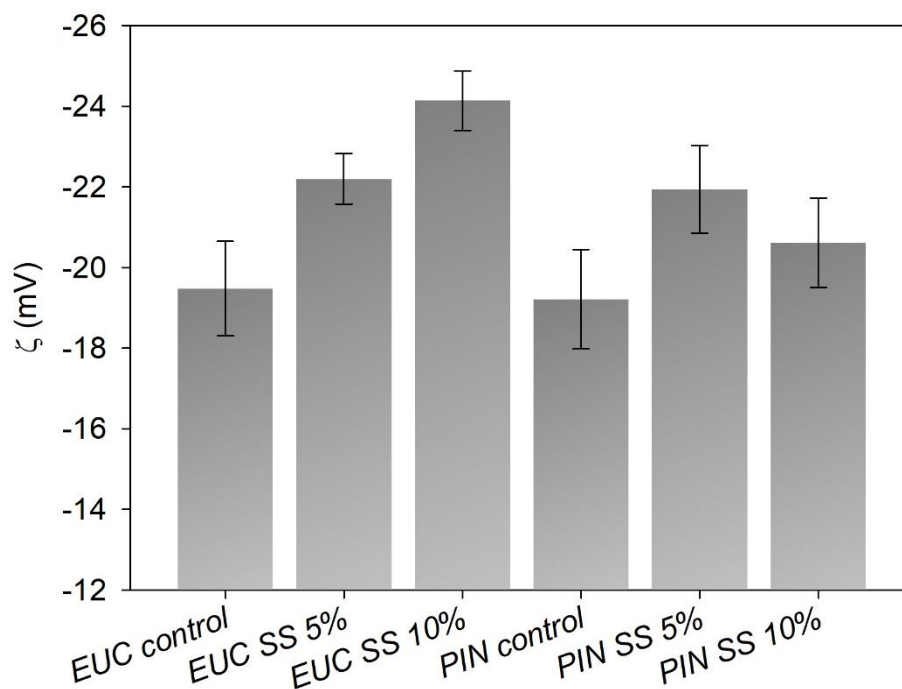


Figure 12: Zeta Potential (ζ) of the untreated and pre-treated MFC/CNF suspensions with sodium silicate.

The average ζ obtained for *EUC control* and PIN control were -19,5 mV and -19 mV, respectively. The characteristic ζ values are between -43 mV and -60 mV for MFC/CNF; -24 mV for CNF; and around -30 mV for cellulose nanocrystals, considering a pH close to 7 (Dimic-Misic et al. 2014).

Values lower than -15 mV indicate that MFC/CNFC show a tendency to agglomerate. On the other hand, when the values found are close to -20 mV and -30 mV, indicates that particles in suspension present sufficient bilateral electrostatic repulsion between them, resulting in greater colloidal stability and maintenance of Brownian motion (Blanco et al. 2018). This explains the difficulty of visual detection of sedimentation in the suspensions studied (see Figure 11b). Values of ζ between ± 10 mV and -20 mV; and between ± 20 mV and -30 mV allow classifying suspensions as relatively stable and moderately stable, respectively (Bhattacharjee 2016).

More stable suspensions (~25 mV) and with high viscosity are possible to be stored for longer periods without the need for additives (salts, polymers, and other ionic stabilizers) to reduce MFC/CNF sedimentation and/or flocculation (Sinquefield et al. 2020). For the application of this material as structural reinforcement in polymeric matrices, this characteristic is also interesting. Higher viscosity prevents major MFC/CNF sedimentation on one side of the composite (Dimic-Misic et al. 2021). This results in a more homogeneous distribution and greater predictability of the physical-mechanical behavior of the material in its application. The use of sodium silicate proved to be feasible as a pretreatment to facilitate the mechanical fibrillation process, which resulted in MFC/CNF with smaller diameters compared to the material not subjected to pretreatment. Furthermore, the reduction in energy consumption by the addition of sodium silicate is an important contribution to the large-scale application of MFC/CNF manufacturing.

Conclusion

In this study, commercial pulps of EUC and PIN were treated with sodium silicate in order to reduce energy consumption. The pre-treatment with Na_2SiO_3 in the concentration of 10% (w/w) increased the WRV for both the pulps studied, indicating greater swelling capacity. The X-ray diffractograms of the pre-treated samples did not reveal the transformation of cellulose to other isomers. However, it was possible to verify crystallinity index reduction for EUC with the 2 concentrations of Na_2SiO_3 tested. The higher content of xylans in EUC seems to have provided gel formation at an early stage. As a result, this material suffered excessive fibrillation concerning other treatments, intensifying the damage to the cellulose crystalline structure. Pre-treatments with 10% Na_2SiO_3 proved to be effective as a facilitator of the fibrillation process because it reduced the energy consumption by around 45% for EUC and 53% for the PIN, considering the gel consistency point. The Na_2SiO_3 alkalinity also contributed to greater efficiency of pulp fibrillation since there was greater individualization of MFC/CNF and the final structures reached the nanoscale. More studies are required to expand the approach on the use of pre-treatments with Na_2SiO_3 , evaluating more variables in the process (duration and temperature), or even application of other alkaline compounds, which could result in a reduction of energy consumption and optimization of the of MFC/CNF production in industrial scale.

Acknowledgments We are especially grateful to the Postgraduate Program in Wood Science and Technology (PPGCTM) of the Federal University of Lavras (UFLA) for providing material

and infrastructure. We would also like to thank Embrapa Instrumentação and Klabin S.A. for the availability of inputs and equipment for the analysis of the materials of this work.

Funding: The research was funded by the National Council for Scientific and Technological Development (CNPq finance code 314203/2018-4) and Fundação de Amparo à Pesquisa do Estado de Minas Gerais (FAPEMIG finance code CAG APQ-03248-17). We also thank the and Fundação de Amparo à Pesquisa do Estado do Amapá (FAPEAP), and the State University of Amapá for the postdoctoral scholarships (financial code: 0022.0279.1202.0016/2021 – PROPESP).

Conflict of interest No potential conflicts of interest.

References

- Abe, K. (2016) Nanofibrillation of dried pulp in NaOH solutions using bead milling. *Cellulose* 23:1257-1261. <https://doi.org/10.1007/s10570-016-0891-4>
- Abral, H., Chairani, M.K., Rizki, M.D., Mahardika, M., Handayani, D., Sugiart, E., Muslimin, A.N., Sapuan, S.P., Ilyas, R.A. (2021) Characterization of compressed bacterial cellulose nanopaper film after exposure to dry and humid conditions. *Journal of Materials Research and Technology* 11:896-904. <https://doi.org/10.1016/j.jmrt.2021.01.057>
- Afsahi, G., Dimic-Misic, K., Gane, P., Budtova, T., Maloney, T., Vuorinen, T. (2018) The investigation of rheological and strength properties of NFC hydrogels and aerogels from hardwood pulp by short catalytic bleaching (H_{cat}). *Cellulose* 25:1637-1655. <https://doi.org/10.1007/s10570-018-1678-6>
- Barbosa, B.M., Lino, A.G., Faria, B.F.H., Aguiar, A.R., Gomes, F.J.B., Silva, J.C., Colodette, J.L. (2018) Addition of corn fiber xylan to *Eucalyptus* and *Pinus* pulp and its effect on pulp bleachability and strength. *Nordic Pulp & Paper Research Journal* 33:414-419. <https://doi.org/10.1515/npprj-2018-3060>
- Bhattacharjee, S. (2016) DLS and zeta potential – What they are and what they are not? *Journal of Controlled Release* 235:337-351. <https://doi.org/10.1016/j.jconrel.2016.06.017>
- Blanco, A., Monte, M.C., Campano, C., Balea, A., Merayo, N., Negro, C. (2018) Nanocellulose for industrial use: cellulose nanofibers (CNF), cellulose nanocrystals (CNC), and bacterial cellulose (BC). In: Hussain, C.M. (eds) *Handbook of Nanomaterials for Industrial Applications*, Elsevier, Amsterdam, pp.74-126.

- Borrega, M., Concha-Carrasco, S., Pranovich, A., Sixta, H. (2017) Hot water treatment of hardwood kraft pulp produces high-purity cellulose and polymeric xylan. *Cellulose* 24:5133-5145. <https://doi.org/10.1007/s10570-017-1462-z>
- Brännvall, E. (2017) The limits of delignification in kraft cooking. *BioResources* 12:2081-2107. <https://doi.org/10.15376/biores.12.1.Brannvall>
- Cao, S., Rathi, P., Wu, X., Ghim, D., Jun, Y.S., Singamaneni, S. (2020) Cellulose nanomaterials in interfacial evaporators for desalination: a “natural” choice. *Advanced Materials* 33:2000922. <https://doi.org/10.1002/adma.202000922>
- Chen, W., Abe, K., Uetani, K., Yu, H., Liu, Y., Yano, H. (2014) Individual cotton cellulose nanofibers- pretreatment and fibrillation technique. *Cellulose* 21:1517-1528. <https://doi.org/10.1007/s10570-014-0172-z>
- Chen, F., Xiang, W., Sawada, D., Bai, L., Hummel, M., Sixta, H., Budtova, T. (2020) Exploring large ductility in cellulose nanopaper combining high toughness and strength. *ASC Nano* 14:11150-11159. <https://doi.org/10.1021/acsnano.0c02302>
- Costa, L.R., Silva, L.E., Matos, L.C., Tonoli, G.H.D., Hein, P.R. (2021) Cellulose nanofibrils as reinforcement in the process manufacture of paper handsheets. *journal of natural fibers*. in press: 1-16. <https://doi.org/10.1080/15440478.2021.1958415>
- Cruz, T.M., Mascarenhas, A.R.P., Scatolino, M.V., Faria, D.L., Matos, L.C., Duarte, P.J., Neto, J.M., Mendes, L.M., Tonoli, G.H.D. (2022) Hybrid films from plant and bacterial nanocellulose: mechanical and barrier properties. *Nordic Pulp & Paper Research Journal* 37:159-174. <https://doi.org/10.1515/npprj-2021-0036>
- Dias, M.C., Mendonça, M.C., Damásio, R.A.P., Zidanes, U.L., Mori, F.A., Ferreira, S.R., Tonoli, G.H.D. (2019) Influence of hemicellulose content of *Eucalyptus* and *Pinus* fibers on the grinding process for obtaining cellulose micro/nanofibrils. *Holzforschung* 73:1035-1046. <https://doi.org/10.1515/hf-2018-0230>
- Dimic-Misic, K., Salo, T., Paltakari, J., Gane, P. (2014) Comparing the rheological properties of novel nanofibrillar cellulose-formulated pigment coating colours with those using traditional thickener. *Nordic Pulp & Paper Research Journal* 29:253-270. <https://doi.org/10.3183/npprj-2014-29-02-p253-270>
- Dimic-Misic, K., Vanhatalo, K., Dahl, O., Gane, P. (2018) Rheological properties comparison of aqueous dispersed nanocellulose derived from a novel pathway-produced microcrystalline cellulose or by conventional methods. *Applied Rheology* 28:64474, 2018. <https://doi.org/10.3933/applrheol-28-64474>

- Dimic-Misic, K., Buffiere, J., Imani, M., Nieminen, K., Sixta, H. (2021) Improved stabilization of graphite nanoflake dispersions using hydrothermally-produced nanocellulose. *Colloids and Surfaces A: Physicochemical and Engineering Aspects* 610:125668. <https://doi.org/10.1016/j.colsurfa.2020.125668>
- Du, H., Parit, M., Wu, M., Che, X., Wang, Y., Zhang, M., Wang, R., Zhang, X., Jiang, Z., Li, B. (2020) Sustainable valorization of paper mill sludge into cellulose nanofibrils and cellulose nanopaper. *Journal of Hazardous Materials* 400:123106. <https://doi.org/10.1016/j.jhazmat.2020.123106>
- Esteves, C.S.V.G., Brännvall, E., Östlund, S., Sevastyanova, O. (2020) Evaluating the potential to modify pulp and paper properties through oxygen delignification. *ACS Omega* 5:13703-13711. <https://doi.org/10.1021/acsomega.0c00869>
- Fonseca, A.S., Panthapulakkal, S., Konar, S.K., Sain, M., Bufalino, L., Raabe, J., Miranda, I.P.A., Martins, M.A., Tonoli, G.H.D. (2019) Improving cellulose nanofibrillation of non-wood fiber using alkaline and bleaching pre-treatments. *Industrial Crops & Products* 131:203-212. <https://doi.org/10.1016/j.indcrop.2019.01.046>
- Foster, E.J., Moon, R.J., Agarwal, U.P., Bortner, M.J., Bras, J., Espinosa, S.C., Chan, K.J., Clift, M.J.D., Cranston, E.D., Eichhorn, S.J., Fox, D.M., Hamad, W.Y., Heux, L., Jean, B., Korey, M., Nieh, W., Ong, K.J., Reid, M.S., Renneckar, S., Roberts, R., Shatkin, J.A., Simonsen, J., Bagby, K.S., Wanasekara, N., Youngblood, J. (2018) Current characterization methods for cellulose nanomaterials. *Chemical Society Reviews* 47:2511-3006. <https://doi.org/10.1039/C6CS00895J>
- French, A.D. (2014) Idealized powder diffraction patterns for cellulose polymorphs. *Cellulose* 21:885-896. <https://doi.org/10.1007/s10570-013-0030-4>
- French, A.D. (2020) Increment in evolution of cellulose crystallinity analysis. *Cellulose* 27:5445-5448. <https://doi.org/10.1007/s10570-020-03172-z>
- González, G., Ehman, N.V., Aguerre, Y.S., Gallegos, S.H., Fonte, A.P.N., Muniz, G.I.B., Pereira, M., Carneiro, M.E., Vallejos, M.E., Felissina, F.E., Area, M.C. (2021) Quality of microfibrillated cellulose produced from unbleached pine sawdust pulp as an environmentally friendly source. *Waste Biomass Valorization*, 13: 1609-1626. <https://doi.org/10.1007/s12649-021-01615-7>
- Guimarães Júnior, M., Teixeira, F.G., Tonoli, G.H.D. (2015) Preparation of cellulose nanofibrils from bamboo pulp by mechanical defibrillation for their applications in biodegradable composites. *Journal of Nanoscience and Nanotechnology* 15:1-18. <https://doi.org/10.1166/jnn.2015.10854>

- Häder, D.P., Banaszak, A.T., Villafaña, V.E., Narvarte, M.A., González, R.A., Helbling, E.W. (2020) Anthropogenic pollution of aquatic ecosystems: emerging problems with global implications. *Science of the Total Environment*, 713:136586.
- Jia, X., Chen, Y., Shi, C., Ye, Y., Abid, M., Jabbar, S., Wang, P., Zeng, X., Wu, T. (2014) Rheological properties of an amorphous cellulose suspension. *Food Hydrocolloids* 39:27-33. <https://doi.org/10.1016/j.foodhyd.2013.12.026>
- Jin, K., Tang, Y., Liu, J., Wang, J., Ye, C. (2021) Nanofibrillated cellulose as coating agent for food packaging paper. *International Journal of Biological Macromolecules* 168:331-338. <https://doi.org/10.1016/j.ijbiomac.2020.12.066>
- Kabir, M.M., Wang, H., Lau, K.T., Cardona, F. (2013) Effects of chemical treatments on hemp fibre structure. *Applied Surface Science* 276:13-23. <https://doi.org/10.1016/j.apsusc.2013.02.086>
- Kupnik, K., Primožic, M., Kokol, V., Leitgeb, M. (2020) Nanocellulose in drug delivery and antimicrobially active materials. *Polymers* 12:2825. <https://doi.org/10.3390/polym12122825>
- Lavers, J.L., Dicks, L., Dicks, M.R., Finger, A. (2019) Significant plastic accumulation on the Cocos (Keeling) Islands, Australia. *Scientific Reports* 9:7102. <https://doi.org/10.1038/s41598-019-43375-4>
- Li, J., Yang, X., Xiu, H., Dong, H., Song, T., Ma, F., Feng, P., Zhang, X., Kozliak, E., Ji, Y. (2019) Structure and performance control of plant fiber-based foam material by fibrillation via refining treatment. *Industrial Crops & Products* 128:186-193. <https://doi.org/10.1016/j.indcrop.2018.10.085>
- Li, B., Trueman, B.F., Munoz, S., Locsin, J.M., Gagnon, G.A. (2021) Impact of sodium silicate on lead release and colloid size distributions in drinking water. *Water Research* 190:116709. <https://doi.org/10.1016/j.watres.2020.116709>
- Lin, Q., Huang, Y., Yu, W. (2020) An in-depth study of molecular and supramolecular structures of bamboo cellulose upon heat treatment. *Carbohydrate Polymers* 241:116412. <https://doi.org/10.1016/j.carbpol.2020.116412>
- Liu, Y., Sun, B., Zheng, X., Yu, L., Li, J. (2018) Integrated microwave and alkaline treatment for the separation between hemicelluloses and cellulose from cellulosic fibers. *Bioresource Technology* 247:859-863. <https://doi.org/10.1016/j.biortech.2017.08.059>
- Liu, S., Ott, W.K. (2020) Sodium silicate applications in oil, gas & geothermal well operations. *Journal of Petroleum Science and Engineering* 195: 107693. <https://doi.org/10.1016/j.petrol.2020.107693>

- Liu, X., Jiang, Y., Wang, L., Song, X., Qin, C., Wang, S. (2020) Tuning of size and properties of cellulose nanofibers isolated from sugarcane bagasse by endoglucanase-assisted mechanical grinding. *Industrial Crops and Products* 146:112201. <https://doi.org/10.1016/j.indcrop.2020.112201>
- Long, L., Tian, D., Hu, J., Wang, F., Saddler, J. (2017) A xylanase-aided enzymatic pretreatment facilitates cellulose nanofibrillation. *Bioresource Technology* 243:898-904. <https://doi.org/10.1016/j.biortech.2017.07.037>
- Lopes, T.A., Bufalino, L., Claro, P.I.C., Martins, M.A., Tonoli, G.H.D., Mendes, L.M. (2018) The effect of surface modifications with corona discharge in *Pinus* and *Eucalyptus* nanofibril films. *Cellulose* 25:5017-5033. <https://doi.org/10.1007/s10570-018-1948-3>
- Lund, K., Sjöström, K., Brelid, H. (2012) Alkali extraction of kraft pulp fibers: influence on fiber and fluff pulp properties. *Journal of Engineered Fibers and Fabrics* 7:30-39. <https://doi.org/10.1177/155892501200700206>
- Malucelli, L.C., Matos, M., Jordão, C., Lomonaco, D., Lacerda, L.G., Carvalho Filho, M.A.S., Magalhães, W.L.E. (2019) Influence of cellulose chemical pretreatment on energy consumption and viscosity of produced cellulose nanofibers (CNF) and mechanical properties of nanopapers. *Cellulose* 26:1667-1681. <https://doi.org/10.1007/s10570-018-2161-0>
- Martins, C.C.N., Dias, M.C., Mendonça, M.C., Durães, A.F.S., Silva, L.E., Félix, J.R., Damásio, R.A.P., Tonoli, G.H.D. (2021) Optimizing cellulose microfibrillation with NaOH pretreatments for unbleached *Eucalyptus* pulp. *Cellulose* 28:11519-11531. <https://doi.org/10.1007/s10570-021-04221-x>
- Marwanto, M., Maulana, M.I., Febrianto, F., Wistara, N.J., Nikmatin, S., Masruchin, N., Zaini, L.H., Lee, S.H., Kim, N.H. (2021) Characteristics of nanocellulose crystals from balsa and kapok fibers at different ammonium persulfate concentrations. *Wood Science and Technology* 55:1319-1335. <https://doi.org/10.1007/s00226-021-01319-0>
- Mascarenhas, A.R.P., Scatolino, M.V., Santos, A.A., Norcino, L.B., Duarte, P.J., Melo, R.R., Dias, M.C., Faria, C.E.T., Mendonça, M.C., Tonoli, G.H.D. (2022) Hydroxypropyl methylcellulose films reinforced with cellulose micro/nanofibrils: study of physical, optical, surface, barrier and mechanical properties *Nordic Pulp & Paper Research Journal* 1-16. <https://doi.org/10.1515/npprj-2022-0006>
- Mastalska-Popławska, J., Pernechele, M., Troczynski, T., Izak, P. (2017) Thermal properties of silica-coated cellulose fibers for increased fire-resistance. *Journal of Sol-Gel Science and Technology* 83:683-691. <https://doi.org/10.1007/s10971-017-4445-5>

- Mendonça, M., Dias, M.C., Martins, C.C.N., Duarães, A.F.S., Damásio, R.A.P., Tonoli, G.H.D. (2022) Alkaline pretreatment facilitate mechanical fibrillation of unbleached cellulose pulps for obtaining of cellulose micro/ nanofibrils (MFC). *Journal of Natural Fibers*, ahead-of-print: 1-16. <https://doi.org/10.1080/15440478.2022.2092252>
- Mokhena, T.C., John, M.J. (2020) Cellulose nanomaterials: New generation materials for solving global issues. *Cellulose* 27:1149-1194. <https://doi.org/10.1007/s10570-019-02889-w>
- Na, B., Wang, Z., Wang, H., Lu, X. (2014) Wood-cement compatibility review. *Wood Research* 59:813-826.
- Nahrawy, A.M.E., Moez, A.A., Saad, A.M. (2018) Sol-gel preparation and spectroscopy properties of modified sodium silicate/tartrazine dye nanocomposite. *Silicon* 10:2117-2122. <https://doi.org/10.1007/s12633-017-9740-9>
- Nechyporchuk, O., Belgacem, M.N., Bras, J. (2016) Production of cellulose nanofibrils: A review of recent advances. *Industrial Crops and Products* 93:2-25. <https://doi.org/10.1016/j.indcrop.2016.02.016>
- Noremylia, M.B., Hassan, M.Z., Ismail, Z. (2022) Recent advancement in isolation, processing, characterization and applications of emerging nanocellulose: A review. *International Journal of Biological Macromolecules* 206:954–976. <https://doi.org/10.1016/j.ijbiomac.2022.03.064>.
- Ono, Y., Takeuchi, M., Zhou, Y., Isogai, A. (2021) TEMPO/NaBr/NaClO and NaBr/NaClO oxidations of cotton linters and ramie cellulose samples. *Cellulose* 28:6035-6049. <https://doi.org/10.1007/s10570-021-03944-1>
- Özgenç, O., Durmaz, S., Boyaci, I.H., Eksi-Kocak, H. (2017) Determination of chemical changes in heat-treated wood using ATR-FTIR and FT Raman spectrometry. *Spectrochimica Acta Part A: Molecular and Biomolecular Spectroscopy* 171:395-400. <https://doi.org/10.1016/j.saa.2016.08.026>
- Pakutsah, K., Aht-Ong, D. (2020) Facile isolation of cellulose nanofibers from water hyacinth using water-based mechanical defibrillation: Insights into morphological, physical, and rheological properties. *International Journal of Biological Macromolecules* 145:64-76. <https://doi.org/10.1016/j.ijbiomac.2019.12.172>
- Popescu, M.C., Dogaru, B.I., Popescu, C.M. (2020) Effect of cellulose nanocrystals nanofiller on the structure and sorption properties of carboxymethyl cellulose–glycerol–cellulose nanocrystals nanocomposite systems. *Materials* 13:2900. <https://doi.org/10.3390/ma13132900>
- Qaseem, M.F., Shaheen, H., Wu, A.M. (2021) Cell wall hemicellulose for sustainable industrial utilization. *Renewable and Sustainable Energy Reviews* 144:110996. <https://doi.org/10.1016/j.rser.2021.110996>

- Qin, D., Ma, X., Zhang, B., Luo, Q., Na, H., Chen, J., Zhu, J. (2021) Ultra-high gas barrier and enhanced mechanical properties of corn cellulose nanocomposite films filled with graphene oxide nanosheets. *Carbohydrate Polymer Technologies and Applications* 2:100066. <https://doi.org/10.1016/j.carpta.2021.100066>
- Ramesh, S., Radhakrishnan, P. (2019) Cellulose nanoparticles from agro-industrial waste for the development of active packaging. *Applied Surface Science* 484:1274-1281. <https://doi.org/10.1016/j.apsusc.2019.04.003>
- Rol, F., Belgacem, M.N., Gandini, A., Bras, J. (2019a) Recent advances in surface-modified cellulose nanofibrils. *Progress in Polymer Science* 88:241-264. <https://doi.org/10.1016/j.progpolymsci.2018.09.002>
- Salim, R.M., Asik, J., Sarjadi, M.S. (2021) Chemical functional groups of extractives, cellulose and lignin extracted from native *Leucaena leucocephala* bark. *Wood Science and Technology* 55:295-313. <https://doi.org/10.1007/s00226-020-01258-2>
- Sarangi, S., Yatirajula, S.K., Saxena, V.K. (2021) Evaluation of linear and nonlinear rheology of microfibrillated cellulose. *Journal of Coatings Technology and Research* 18:1401-1411. <https://doi.org/10.1007/s11998-021-00505-w>
- SCAN Standard (2000) SCAN-C 62:00, Chemical pulp – Water retention value.
- Scatolino, M.V., Silva, D.W., Bufalino, L., Tonoli, G.H.D., Mendes, L.M. (2017) Influence of cellulose viscosity and residual lignin on water absorption of nanofibrils films. *Procedia Engineering* 200:155-161. <https://doi.org/10.1016/j.proeng.2017.07.023>
- Serra-Parareda, F., Tarrés, Q., Pèlach, M.A., Mutjé, P., Balea, A., Monte, M.C., Negro, C., Delgado-Aguillar, M. (2021) Monitoring fibrillation in the mechanical production of lignocellulosic micro/nanofibers from bleached spruce thermomechanical pulp. *International Journal of Biological Macromolecules* 178:354-362. <https://doi.org/10.1016/j.ijbiomac.2021.02.187>
- Silva, L.C.E., Cassago, A., Batirrola, L.C., Gonçalves, M.C., Portugal, R.V. (2020) Specimen preparation optimization for size and morphology characterization of nanocellulose by TEM. *Cellulose* 27:5435-5444. <https://doi.org/10.1007/s10570-020-03116-7>
- Silva, L.E., Santos, A.A., Torres, L., McCaffrey, Z., Klamczynski, A., Glenn, G., Neto, A.R.S., Wood, D., Williams, T., Orts, W., Damásio, R.A.P., Tonoli, G.H.D. (2021) Redispersion and structural change evaluation of dried microfibrillated cellulose. *Carbohydrate Polymers* 252:117165. <https://doi.org/10.1016/j.carbpol.2020.117165>

- Sinquefield, S., Ciesielski, P.N., Li, K., Gardner, D.J., Ozcan, S. (2020) Nanocellulose dewatering and drying: current state and future perspectives. *ACS Sustainable Chemistry & Engineering* 8:9601-9615. <https://doi.org/10.1021/acssuschemeng.0c01797>
- Sun, S.F., Yang, J., Wang, D.W., Yang, H.Y., Sun, S.N., Shi, Z.J. (2021) Enzymatic response of ryegrass cellulose and hemicellulose valorization introduced by sequential alkaline extractions. *Biotechnology for Biofuels* 14:72. <https://doi.org/10.1186/s13068-021-01921-1>
- TAPPI Standard (2019) T 230 om-19, Viscosity of pulp (capillary viscometer method).
- TAPPI Standard (2021a) T 249 cm-21, Carbohydrate composition of extractive-free wood and wood pulp by gas-liquid chromatography.
- TAPPI Standard (2021b) T 222 om-21, Acid-soluble lignin in wood and pulp.
- Tonoli, G.H.D., Teixeira, E.M., Corrêa, A.C., Marconcini, J.M., Caixeta, L.A., Pereira-da-Silva, M.A., Mattoso, L.H.C. (2012) Cellulose micro/nanofibres from *Eucalyptus* kraft pulp: preparation and properties. *Carbohydrate Polymers* 89: 80-88. <https://doi.org/10.1016/j.carbpol.2012.02.052>
- Tonoli, G.H.D., Holtman, K., Silva, L.E., Wood, D., Torres, L., Williams, T., Oliveira, J.E., Fonseca, A.S., Klamczynski, A., Glenn, G., Orts, W. (2021) Changes on structural characteristics of cellulose pulp fiber incubated for different times in anaerobic digestate. *Cerne* 27:e102647. <https://doi.org/10.1590/01047760202127012647>
- Trache, D., Tarchoun, A.F., Derradji, M., Hamidon, T.S., Masruchin, N., Brosse, N., Hussin, M.H. (2020) Nanocellulose: From fundamentals to advanced applications. *Frontiers in Chemistry* 8:392. <https://doi.org/10.3389/fchem.2020.00392>
- Wang, Q., Zhu, J.Y. (2016) Effects of mechanical fibrillation time by disk grinding on the properties of cellulose nanofibrils. *Tappi Journal* 15:2016.
- Wang, X., Chen, J., Chen, H., Lucia, L.A., Yang, G., Wu, Q. (2017) Influence of chemical pretreatment on the dissolved organics in poplar alkaline peroxide mechanical pulping effluent. *Paper and Biomaterials* 2:32-39.
- Wang, J., Liu, X., Jin, T., He, H., Liu, L. (2019) Preparation of nanocellulose and its potential in reinforced composites. *Journal of Biomaterials Science, Polymer Edition* 30:919-946. <https://doi.org/10.1080/09205063.2019.1612726>
- Wang, L., Chen, C., Wang, J., Gardner, D.J., Tajvidi, M. (2020) Cellulose nanofibrils versus cellulose nanocrystals: Comparison of performance in flexible multilayer films for packaging applications. *Food Packaging and Shelf Life* 23:100464. <https://doi.org/10.1016/j.fpsl.2020.100464>

Zhao, D., Deng, Y., Han, D., Tan, L., Ding, Y., Zhou, Z., Xu, H., Guo, Y. (2019) Exploring structural variations of hydrogen-bonding patterns in cellulose during mechanical pulp refining of tobacco stems. *Carbohydrate Polymers* 204:247-254. <https://doi.org/10.1016/j.carbpol.2018.10.024>

**ARTIGO 2 – FIBERS PRE-TREATMENTS WITH SODIUM SILICATE AFFECT
THE PROPERTIES OF SUSPENSIONS, FILMS, AND QUALITY INDEX OF
CELLULOSE MICRO/NANOFIBRILS**

Artigo publicado no periódico Nordic Pulp & Paper Research Journal

DOI: 10.1515/npprj-2022-0037

Fibers pre-treatments with sodium silicate affect the properties of suspensions, films, and quality index of cellulose micro/nanofibrils

Effect of Na₂SiO₃ on the cellulose micro/nanofibril suspensions and films

Adriano Reis Prazeres Mascarenhas¹, Mário Vanoli Scatolino², Matheus Cordazzo Dias³, Maria Alice Martins⁴, Rafael Rodolfo de Melo⁵, Renato Augusto Pereira Damasio⁶, Maressa Carvalho Mendonça³, Gustavo Henrique Denzin Tonoli³

¹Department of Forest Engineering, Federal University of Rondônia (UNIR), 76940-000, Rolim de Moura, RO, Brazil.

²Department of Production Engineering, State University of Amapá (UEAP), 68900-070, Macapá, AP, Brazil.

³Department of Forest Science, Federal University of Lavras (UFLA), C.P. 3037, 37200-900, Lavras, MG, Brazil.

⁴Embrapa Instrumentation – National Laboratory of Nanotechnology for Agribusiness, 13561-206, São Carlos, SP, Brazil.

⁵Agricultural Sciences Center, Federal University of the Semi-arid (UFERSA), 59625-900, Mossoró, RN, Brazil.

⁶Klabin – Technology Center, Fazenda Monte Alegre, Santa Harmonia, 03, 84275-000, Telêmaco Borba, PR, Brazil.

Abstract

The characteristics of cellulose micro/nanofibrils (MFC/CNF) can be improved with pre-treatments of the original fibers. The present work is proposed to study pre-treatment with sodium silicate (Na₂SiO₃) on bleached fibers of *Eucalyptus* sp. (EUC) and *Pinus* sp. (PIN) and its effects on the quality index of MFC/CNF. Particle homogeneity, turbidity, and microstructure of the suspensions were evaluated. Similarly, the physical-mechanical, and barrier properties of the films were studied. With the results obtained for suspensions and films, the quality index (QI) was MFC/CNF calculated. The smallest particle dimension was observed for MFC/CNF of *Pinus* sp. with 10% of Na₂SiO₃, as well as the lowest turbidity (~350 NTU) was obtained for MFC/CNF of *Pinus* sp. with 5% of Na₂SiO₃. The pre-treatments reduced the transparency of the films by ~25% for EUC and ~20% for PIN. The films presented a suitable barrier to UVC radiation, water vapor, and oil. The tensile strength of EUC and PIN films was

increased by 20% using 10% of Na_2SiO_3 . The same concentration of Na_2SiO_3 provided QI 70 for EUC MFC/CNF. The Na_2SiO_3 was efficient to obtain the MFC/CNF with interesting properties and suitable to generate films with parameters required for packaging.

Keywords: biorefinery, cellulose nanofibrils (CNF), cell wall, microfibrillated cellulose (MFC), nanotechnology.

Introduction

Cellulose has been intensively studied to reduce the consumption of materials derived from petroleum through the development of new products because it is abundant, produced by renewable sources, biodegradable, and has great versatility. Among research developed with cellulose, studies on cellulosic nanomaterials (CNM) should be highlighted (Mokhena and John 2020). CNM includes bacterial cellulose (BC), cellulose nanocrystals (CNC), cellulosic nanofibrils (CNF), microfibrillated cellulose (MFC), and cellulose micro/nanofibrils (MFC/CNF) (Tayeb et al. 2018; Balea et al. 2020; Chanda e Bajwa 2021). Additionally, these materials attract interest from the scientific and industrial community due to their properties such as biocompatibility, high surface area, three-dimensional microstructure, unique optical properties, high rigidity, and specific strength (Guan et al. 2020; Mokhena et al. 2021). Other research horizons of MFC/CNF refer to applications in optical and electrical sensors (Teodoro et al. 2021), drug and food encapsulation (Amalraj et al. 2018), paper coatings for packaging (Yook et al. 2020), film production and composite reinforcement (Mascarenhas et al. 2022), emulsion stabilizers (Li et al. 2021), and water treatment processes (Mohammed et al. 2018).

MFC/CNF are produced by chemical methods or processes based on mechanical shearing of fibers' cell walls. The most used mechanical processes include microfluidization (Perrin et al. 2020), sonication (Wu et al. 2021), high-pressure homogenization (Karina et al. 2020), and mechanical fibrillation in ultra-refiner (Berto and Arantes 2019). Nevertheless, the energy demand for cell wall deconstruction is a limiting factor for MFC/CNF production in industrial scaling, as the consumption values range between 20000 kWh/t and 30000 kWh/t (Kumar et al. 2021).

Due to the high energy consumption, enzymatic, mechanical, or chemical pre-treatments are applied to the fibers. Pre-treatments can also modify the cellulose surface, depending on the applications, such as carboxymethylation, silylation, cationization, phosphorylation, sulfoethylation, and TEMPO (2,2,6,6 – tetramethylpiperidine-1-oxyl) mediated oxidation (Rol et al. 2019; Trovagunta et al. 2021). Although pre-treatments can significantly reduce energy

consumption, the reagent cost is high or the process results in the formation of chemical compounds harmful to health and the environment, as observed in TEMPO-mediated oxidation.

Alkaline pre-treatments are studied as an alternative to reduce energy consumption and reagent costs for MFC/CNF production (Sukmawan et al. 2022). Alkaline agents enhance the MFC/CNF individualization because they promote fiber swelling, reduce the degree of cellulose polymerization and remove hemicelluloses by breaking intermolecular ester bonds with cellulose and lignin, enabling the gelation process (Noremylia et al. 2022).

The main alkaline pre-treatments are NaOH-based solutions in concentrations ranging from 2% to 10%. Martins et al. (2021) obtained MFC/CNF with diameters varying between 15 nm and 30 nm and observed a 48% of reduction in energy consumption, using NaOH solution 5% (w/w) as pre-treatment for unbleached *Eucalyptus* sp. fibers. Similarly, Dias et al. (2019) reduced energy consumption for MFC/CNF production by 40% for *Eucalyptus* sp. and 62% for *Pinus* sp. On the other hand, Malucelli et al. (2019) reported that the NaOH does not always reduce energy consumption and can impair the MFC/CNF quality, as the alkaline action can become the fibers more brittle and reduce the colloidal stability. Limitations such as this indicate the need to research other alkaline pre-treatments. Sodium silicate (Na_2SiO_3) can be considered as an alternative for this purpose because of solutions with concentrations greater than 5% (w/w) present pH between 12 and 14 (Hashem et al. 2010). Na_2SiO_3 solutions are applied to remove lignin and hemicelluloses to improve the cellulosic pulp bleaching (Moghaddam and Karimi 2020).

However, the effects of Na_2SiO_3 on MFC/CNF suspensions and derivatives (foam, films, nanopapers, and composites) are little-known and may influence the characteristics of turbidity, transparency, barrier, and mechanical properties, making them different from those obtained by more conventional pre-treatments. Therefore, studies aiming to compare MFC/CNF obtained by different processes and pre-treatments are essential to facilitate decision-making regarding their applications. Desmaisons et al. (2017) developed a quality index using multivariate models with high precision based on characterizations of MFC/CNF in a simplified way. This index is calculated from the properties obtained from the suspension (turbidity, particle homogeneity, and macroscopic dimension) and MFC/CNF films (Young's modulus, porosity, and transmittance).

The research amount using this methodology is incipient, due to the fact of being a relatively new method, as we can see in works such as Desmaisons et al. (2018), Rol et al. (2018), Banvillet et al. (2021a), Banvillet et al. (2021b) and Espinosa et al. (2020). As the database on MFC/NFC produced from pre-treatments with Na_2SiO_3 is very scarce, the present

work proposed to evaluate the pre-treatments of *Eucalyptus* sp. (EUC) and *Pinus* sp. (PIN) pulps with Na_2SiO_3 solutions at concentrations of 5% and 10% (w/w) and its effects on the properties of the suspensions, films, and MFC/NFC quality index.

Material and methods

Fibers pre-treatment with sodium silicate

Commercial bleached kraft pulps of *Eucalyptus* sp. (EUC) and *Pinus* sp. (PIN) were subjected to pretreatment with Na_2SiO_3 (18% Na_2O ; 63% SiO_2) produced by Dinâmica Química LTDA (São Paulo, Brazil). Na_2SiO_3 solutions with concentrations of 5% and 10% (w/w) (Table 1) were prepared with deionized water heated in a water bath at a temperature of 80 °C. After solubilization, EUC and PIN pulps were mixed with Na_2SiO_3 solutions to obtain suspensions of 2.5% consistency (w/w). Pulps were kept at a temperature of 80 °C \pm 2 °C and constant stirring of 500 rpm for 2 h (Dias et al. 2019), being posteriorly washed in deionized water until pH 7.

Table 1: Identification of the pre-treatments with sodium silicate solutions in different concentrations applied to fibers from EUC and PIN.

Pulp	Condition	Identification
EUC	Untreated	<i>EUC control</i>
	Pre-treatment with 5% of Na_2SiO_3	<i>EUC SS 5%</i>
	Pre-treatment with 10% of Na_2SiO_3	<i>EUC SS 10%</i>
PIN	Untreated	<i>PIN control</i>
	Pre-treatment with 5% of Na_2SiO_3	<i>PIN SS 5%</i>
	Pre-treatment with 10% of Na_2SiO_3	<i>PIN SS 10%</i>

Production of cellulose micro/nanofibrils suspensions and films

Suspensions with pre-treated fibers in 2.0% (w/w) for EUC and 1.5% (w/w) for PIN were produced using deionized water. To ensure swelling and dispersion, the fibers were stirred at 500 rpm for 15 min. Suspensions with untreated fibers in the same proportions presented were also produced. The fibrillation process was carried out with 5 passes of suspensions through the grinder - Supermasscolloider Masuko Sangyo MKGA-80 (Kawaguchi, Japan), at 1500 rpm. The initial distance between the grinder discs was 10 μm and was adjusted to 100 μm as the suspension viscosity increased. The energy consumptions of fibrillation were 3000 kWh/t for *EUC SS 5%*, 4100 kWh/t for *EUC SS 10%*, 4000 kWh/t for *PIN SS 5%* and 4500 kWh/t for *PIN SS 10%*. For untreated fibers, energy consumption was 7500 kWh/t for EUC and 10000 kWh/t for PIN until gel formation. Films were produced with MFC/CNF suspensions in

the concentration of 1% (w/w) by the “*casting*” method, which consists of solvent evaporation at room temperature (± 22 °C). Each film was produced from 50 g of suspension poured into acrylic plates with a diameter of 15 cm. Five films were produced for each treatment.

Chemical characterization of the fibers

Contents of extractive-free carbohydrates of treated and untreated EUC and PIN fibers were determined following the TAPPI T 249 cm 21 standard (TAPPI 2021a). Lignin content was obtained according to the procedure described in TAPPI T 222 om-02 (TAPPI 2021b). For both pulps, cellulose content was calculated by subtracting the total glucose content and the glucose content associated with mannose, since for every 3 mannose units there is one glucose unit (Dias et al. 2019). Therefore, hemicellulose content was obtained by the sum of galactose, arabinose, xylose, and mannose, with the respective glucose amount (Zhou et al. 2016; Qaseem et al. 2021).

Dimension and homogeneity of the particles

To estimate the fiber’s residual fraction after the fibrillation process, images were taken using the Olympus BX41 light microscope (Tokyo, Japan). MFC/CNF suspensions were diluted in deionized water in proportion 0.1% (w/w). Suspension drops were deposited on glass slides and covered with a coverslip for observation using an objective of 10x.

The images obtained were transformed into the 8-bit format and analyzed using the “particle analysis” routine to obtain the average area of particles (macroscopic dimension), of the software Image J (Rueden et al. 2017). This procedure was performed using six images per sample. Homogeneity of particles was calculated with the relative frequency observed for visible particles smaller than $5 \mu\text{m}^2$, between 5 and $10 \mu\text{m}^2$, and larger than $10 \mu\text{m}^2$ (Desmaisons et al. 2017). As greater the number of particles included in the same size class, with a smaller standard deviation for each class, the greater the homogeneity.

Turbidity of the suspensions

The turbidity of the MFC/CNF suspensions was determined in a Plus Alfakit turbidimeter (Santa Catarina, Brazil), adjusted to a wavelength of 860 nm. MFC/CNF aliquots were collected, under stirring at 900 rpm, in concentration 0.1% (w/w). Five measurements were done for each sample.

Microstructure of the films

Films samples with 5 x 5 mm were submerged in liquid nitrogen for instant freezing, then fractured and fixed on sample holders (stubs) containing double-sided adhesive tapes. The samples were subjected to metallic coating in a gold evaporator (SCD 050) before the micrographs obtainment in an ultra-high resolution (UHR) scanning electron microscope with a field emission gun (SEM/FEG) TESCAN CLARA (Libušina, Czech Republic), under the conditions of 10 KeV, 90 pA, with a working distance of 10 mm.

Physical properties of films

Before the mentioned tests, the films were conditioned at a temperature of 25 °C and relative humidity of 65%, according to TAPPI T 402 sp -21 (TAPPI 2021c). The thickness of the films was obtained using a digital micrometer (0.001 mm), following the TAPPI T 411 om-15 standard (TAPPI 2015). The grammage was obtained according to TAPPI T 410 om-08 standard (TAPPI 2013), weighing the films in analytical balance and determining their respective areas with a digital caliper (0.001 mm). The grammage (g/m^2) was calculated with the ratio mass/area. The bulk density of the films was calculated by the ratio between the grammage and thickness. The porosity (Φ) was calculated by the ratio between the bulk density of the film and the cellulose density (Eq. 1).

$$\Phi (\%) = 1 - \left(\frac{\rho_f}{\rho_c} \right) \quad (1)$$

Where ρ_f is the bulk density of the films (kg/m^3) and ρ_c is the cellulose density (1540 kg/m^3).

Light transmittance and transparency of films

The light transmittance on the films was obtained in five replications for each treatment, in a Genesys 10S UV-Vis Thermo Scientific spectrophotometer (Massachusetts, USA), adjusted with wavelength ranging between 200 and 800 nm. The transmittance obtained at 600 nm was used to calculate the transparency of the films (Tr), following the procedures presented by Sothornvit et al. (2010) (Eq. 2). The transmittance observed in 550 nm was used to calculate the quality index.

$$\text{Tr} (\%) = \frac{(\log T_{600})}{\text{th}} \quad (2)$$

Where T_{600} = transmittance in 600 nm (%) and th = thickness of the films (mm).

The opacity of the films was obtained following the methodologies presented in Fakhouri et al. (2013) and Lago et al. (2020). A Konica Minolta CM-5 colorimeter (Osaka,

Japan), adjusted with a viewing angle of 10° and D65 illuminant (daylight) was used for the analysis. For obtaining the luminosity values (L^*), the films were evaluated in a black pattern and a white one. These data were used to calculate the apparent opacity (Eq. 3) and the results were expressed on a scale from 0 to 100%. For each treatment, five samples were analyzed.

$$\text{Opacity (\%)} = \frac{Y_b}{Y_w} \times 100 \quad (3)$$

Where Y_b = sample luminosity in the black pattern and Y_w = sample luminosity in the white pattern.

Water vapor barrier and grease resistance of films

Five samples with a diameter of 16 mm were prepared for each treatment and stored in a conditioned room with a temperature of 25 °C and relative humidity of 65% for three days, according to ASTM E96-16 (ASTM 2016a). After this period, the samples were placed in glass capsules partially filled with dry silica. The capsules were placed in desiccators containing saturated KCl solution at 38 °C to create an atmosphere with a relative humidity of 90%, as requested by ASTM E104-02 (ASTM 2012). The capsules with samples were weighed in analytical balance for eight consecutive days. The water vapor transmission rate (WVTR) and water vapor permeability (WVP) were calculated with Eq. 4 and Eq. 5.

$$\text{WVTR (g/m}^2 \text{ day)} = \frac{W}{t \times A} \quad (4)$$

$$\text{WVP (g mm/kPa}^{-1} \text{ day m}^2\text{)} = \frac{(\text{WVTR} \times \text{th})}{(p \times \text{UR}_o - \text{UR}_i)} \quad (5)$$

Where W = capsule weight with sample (g); t = time (days); A = exposed area of sample (m²); th = film thickness (mm); p = water vapor pressure (kPa); UR_o and UR_i are, respectively, the the humidity inside the desiccator (90%) and inside the capsule.

A grease resistance test was conducted following the TAPPI T 559 cm-12 standard (TAPPI 2012). Ten films with dimensions 216 x 279 mm were cut, in which drops of the test solutions were applied. The solutions were classified from 1, less aggressive and composed only of oil, to 12, more aggressive and composed of toluene and n-heptane. One drop of oily solution was applied on the film surface, being removed after 15 s. The film was classified with the highest score (solution from 1 to 12) that permeates the sample.

Mechanical properties of the films

The tensile strength of the films was evaluated according to ASTM D 882-18 (ASTM 2018) using a Stable Micro Systems texturometer, TATX2i, (England, United Kingdom) equipped with a load cell with a capacity of 500 N. To determine the tensile strength, Young's modulus, and elongation at break, 10 specimens were tested for each treatment, with dimensions of 10 x 100 mm. The initial distance between the grips was 50 mm, with a test speed of 0.8 mm/s.

Quality index of the cellulose micro/nanofibrils

The simplified quality index (QI) was determined from the multivariate model developed by Desmaisons et al. (2017), using data of macroscopic dimension, particle homogeneity, turbidity, the transmittance at 550 nm, Young's modulus, and porosity (Eq. 6). The parameters “weights” applied must result in the sum of 10. Therefore, the distribution of weights was carried out according to the application (films for packaging and colloidal stabilizers) of suspensions and films reported in the literature (Desmaisons et al. 2018; Rol et al. 2019).

$$\begin{aligned} \text{QI} = & 1.5 \times [-2.67 \times \ln(x_1) + 12.81] + 1.5 \times [0.18 \times (x_2)] \\ & + 1.5 \times [0.10 \times (x_3) + 11] + 1.5 \times [1.65 \times \ln(x_4) + 2.7] \\ & + 1.5 \times [-0.036 \times (x_5) \times 1.27 \times (x_5)] + 2.5 \times [3.81 - 0.16 \times (x_6)] \end{aligned} \quad (6)$$

Where x_1 = macroscopic dimension (μm^2); x_2 = homogeneity (%); x_3 = turbidity (NTU); x_4 = transmittance in 550 nm; x_5 = Young's modulus (GPa); and x_6 = porosity (%).

Statistical analysis

Data obtained were analyzed using descriptive statistics, using the software R Core Team (2020), indicating average and standard deviation.

Results and discussion

Chemical composition

Regarding *EUC control*, treatments *EUC SS 5%* and *EUC SS 10%* reduced hemicellulose contents by 2.6% and 1.3%, respectively, resulting in a slight increase in relative cellulose contents (Table 2). Compared with the *PIN control*, *PIN SS 5%* obtained a reduction of 3.4% in hemicellulose amount, whereas for *PIN SS 10%*, the reduction was 13.1%. In

addition, for PIN pulp, the type of hemicellulose most affected by the treatment with 10% Na_2SiO_3 was mannose, followed by xylose and arabinose.

Table 2: Average and standard deviation for chemical components of untreated and pre-treated pulps with sodium silicate solutions in concentrations of 5% and 10%.

Identification	Glucose	Galactose	Arabinose	Xylose	Mannose	%		
						Total lignin	Cellulose	Hemicelluloses
<i>EUC control</i>	79.1 ± 0.3*	ND**	ND	15.7 ± 0.1	ND	0.4 ± 0.1	79.1 ± 0.3	15.7 ± 0.1
<i>EUC SS 5%</i>	80.2 ± 0.2	ND	ND	15.5 ± 0.2	ND	0.5 ± 0.1	80.2 ± 0.2	15.5 ± 0.2
<i>EUC SS 10%</i>	80.1 ± 0.5	ND	ND	15.3 ± 0.3	ND	0.8 ± 0.1	80.1 ± 0.5	15.3 ± 0.3
<i>PIN control</i>	80.0 ± 0.7	ND	0.5 ± 0.1	9.6 ± 0.1	7.5 ± 0.1	0.5 ± 0.1	78.2 ± 0.6	17.6 ± 0.3
<i>PIN SS 5%</i>	79.6 ± 0.2	ND	0.5 ± 0.1	9.4 ± 0.1	7.1 ± 0.1	0.7 ± 0.1	77.9 ± 0.3	17.0 ± 0.3
<i>PIN SS 10%</i>	79.9 ± 1.1	ND	0.4 ± 0.1	9.0 ± 0.1	5.9 ± 0.1	0.4 ± 0.1	78.5 ± 1.1	15.3 ± 0.3

*Standard deviation; **non-detected.

These results can be explained by the high Na_2SiO_3 solution alkalinity (pH ~ 12). Na_2SiO_3 is used to increase the capacity to remove lignin and hemicelluloses, improving the pulp bleaching (Hashem et al. 2010; Moghaddam and Karimi 2020). Studies indicate that hydrolysis of alkaline solutions promotes the saponification of intermolecular ester cross-links that link hemicelluloses to cellulose or other components such as lignin (Grigatti et al. 2015; Melati et al. 2019). Removing hemicelluloses from fibers promotes an increase in relative sugar content, allows easier access to cellulose chains, and facilitates cell wall swelling (Shimizu et al. 2016). These effects facilitate the MFC/CNF production by mechanical method, as the cell wall swelling promotes the microfibrils loosening, increases the contact surface of fibers, making them more susceptible to shocks against the grinder stones, intensifying the shear forces on the cell wall (Trovagunta et al. 2021). With more passes through the grinder, the alkaline pre-treatments potentiate the reduction of particle sizes and increase the exposure of the cellulose OH groups. Further, there is an increase in the number of hydrogen bonds between cellulose and water, facilitating gelation (Fonseca et al. 2019). These mechanisms can reduce energy consumption during MFC/CNF production (Martins et al. 2021).

On the other hand, excessive hemicelluloses removal can hinder the obtainment of MFC/CNF gels. Dias et al. (2019) and Albornoz-Palma et al. (2020) explained that hemicelluloses, especially xylans, contribute to gel formation with fewer passes through the grinder. Because they are amorphous molecules, xylans can reduce the water output from fibers and potentiate the establishment of hydrogen bonds between cellulose and water, increasing the suspension viscosity during mechanical fibrillation (Afsahi et al. 2018; Claro et al. 2019).

Moreover, it can be said that pre-treatments with Na_2SiO_3 were able to reduce the hemicellulose contents, but not harm the gel obtainment.

Dimension, homogeneity of particles, and turbidity

In the particles classes with an area smaller than $5 \mu\text{m}^2$ (Figure 1), the frequencies obtained for *EUC SS 5%* and *EUC SS 10%* (~42%) were slightly lower than those observed for *EUC control* (~45%). Regarding this class, the highest frequency among treatments was observed for *PIN SS 10%* (~56%) followed by *PIN control* (~48%) and *PIN SS 5%* (~46%).

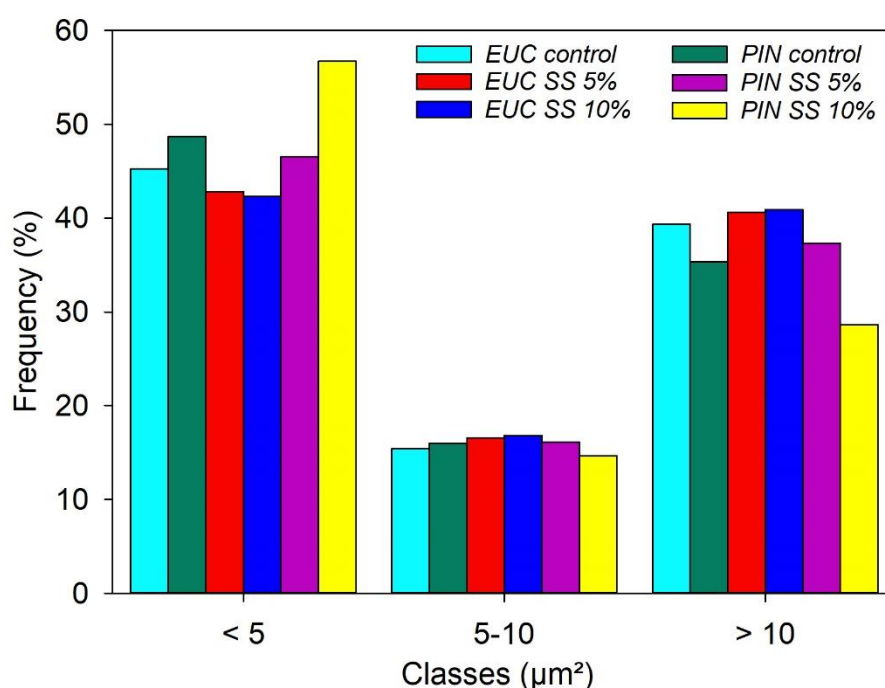


Figure 1: Classes of particles area of MFC/CNF suspensions from untreated and pre-treated pulps with sodium silicate solution in concentrations of 5% and 10%.

For classes with areas between 5 and $10 \mu\text{m}^2$, the frequencies were strongly similar among the pre-treatments studied. Regarding the particles class with areas larger than $10 \mu\text{m}^2$, it was observed that *EUC SS 5%* and *EUC SS 10%* showed similar frequencies (~40%) which were higher in relation to *EUC control* (~35%). Also in this class, *PIN SS 5%* (~37%) presented higher frequencies than *PIN control* (~35) and *PIN SS 10%* (~28%).

For some pre-treatments, the particle area was slightly larger in relation to their respective controls. This indicates that the action of Na_2SiO_3 contributed to the greater efficiency of mechanical fibrillation. Furthermore, it is notable that *EUC control* and *PIN*

control particles are composed of fibrils bundles of partially dissociated and cell wall fragments (arrows in Figure 2A).

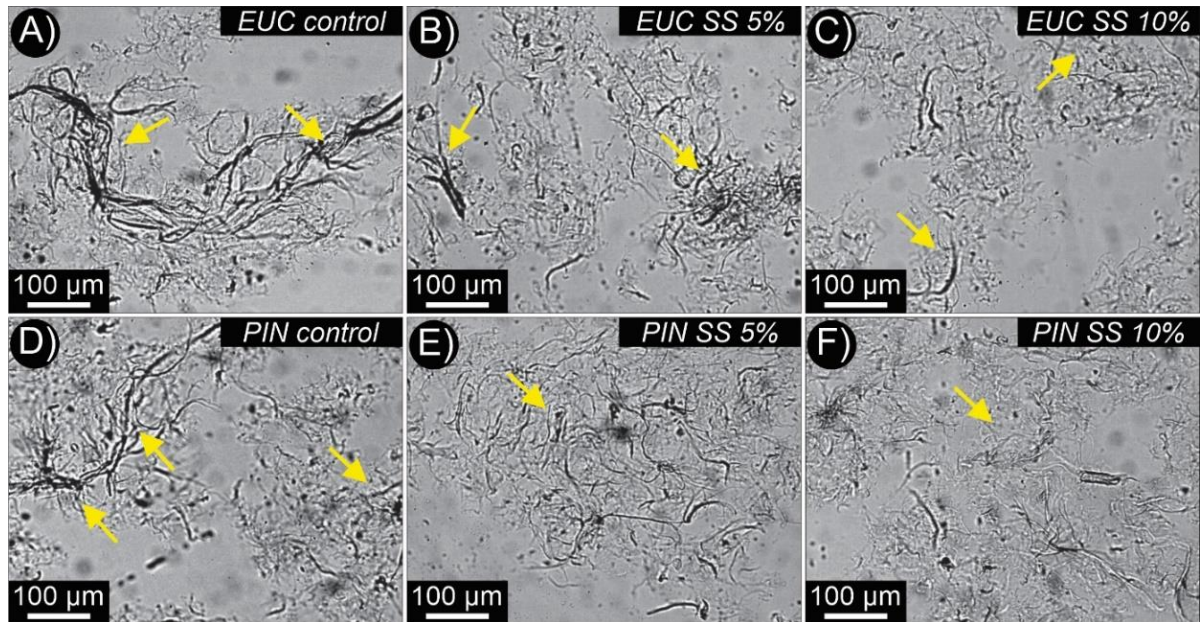


Figure 2: Images of light microscopy of MFC/CNF suspensions from untreated and pre-treated pulps with sodium silicate solution in concentrations of 5% and 10% (10x magnification).

Differently than indicated for controls, the particles with larger dimensions observed for *EUC SS 5%* and *EUC SS 10%* suspensions were formed by the aggregation of fibrils already individualized, much smaller, and thin cell wall fragments (arrows in Figures 2B and 2C). These characteristics were also observed for PIN MFC/CNF (arrows in Figures 2D, 2E, and 2F). Table 3 shows the averages for particle size as a function of the respective area class. Considering only the pre-treated pulps, around 59 and 71% of the particles showed areas smaller than $10 \mu\text{m}^2$ and with low standard deviation ($< 3.4 \mu\text{m}^2$), indicating greater homogeneity of the MFC/CNF suspension (Desmaisons et al. 2017).

Table 3: Average and standard deviation of the particles area MFC/CNF suspensions from EUC and PIN, untreated and pre-treated with sodium silicate solutions in concentrations of 5% and 10%.

Class (μm^2)	Particles area (μm^2)					
	<i>EUC control</i>	<i>EUC SS 5%</i>	<i>EUC SS 10%</i>	<i>PIN control</i>	<i>PIN SS 5%</i>	<i>PIN SS 10%</i>
< 5	$2.3 \pm 0.3^*$	2.4 ± 0.3	2.4 ± 0.3	2.3 ± 0.4	2.3 ± 0.3	2.3 ± 0.3
5-10	7.1 ± 1.2	7.1 ± 1.2	7.1 ± 1.2	7.1 ± 1.2	7.1 ± 1.2	7.0 ± 3.4
> 10	50.9 ± 160.2	47.4 ± 126.6	52.2 ± 139.6	44.9 ± 116.1	52.1 ± 164.9	46.9 ± 133.7
Average	20.1 ± 26.8	19.0 ± 24.7	20.6 ± 27.5	18.1 ± 23.3	20.5 ± 27.5	18.7 ± 24.5

*Standard deviation

Particle sizes affect the properties of MFC/CNF suspensions. Guimarães et al. (2016) and Turpeinen et al. (2020) explained that the viscosity and stability of MFC/CNF suspensions can be increased with a higher aspect ratio and homogeneity of particles. Therefore, it can be said that treatments with Na_2SiO_3 favored the obtainment of suspensions composed of particles with small diameters, greater lengths, and greater homogeneity. This can result in gel formation with fewer passes through the grinder and reduce energy consumption during the fibrillation process (Ang et al. 2019; Jaiswal et al. 2021). This effect is due to the alkaline action of Na_2SiO_3 solutions, which promotes the loosening of the cell walls of the fibers due to the removal of hemicelluloses and saponification of the intermolecular ester bonds, which increase the swelling capacity of the fibers and the surface area (Kamel et al. 2020, Noremylia et al. 2022), this potentiates the dissociation of fibril bundles from the abrasion of the grinder stones.

These results are consistent with other research. Mohtaschemi et al. (2014), when carrying out the mechanical fibrillation of Birch kraft pulp subjected to TEMPO-mediated oxidation, found CNF suspensions with thinner and more homogeneous structures. However, the authors detected the presence of fibers and particle fragments with dimensions in millimeter scales that entangled and formed aggregates, reducing the surface area of the MFC/CNF network. Žepič et al. (2014) and Osong et al. (2016) explained that in MFC/CNF suspensions there are nanofibrils, fibers, fine fibrils, fiber fragments, and fibril bundles, as presented in the present work. As a result, enzymatic or chemical pre-treatments are applied to the fibers before the mechanical fibrillation to facilitate the production of more homogeneous MFC/CNF suspensions, mainly containing nanoscale fragments (Santucci et al. 2016). Based on these aspects and the experimental results of this research, it can be said that this objective was achieved.

Turbidity results reinforce the reasoning presented since all the pre-treatments applied reduced the turbidity values compared to the controls. The lowest turbidity value of EUC MFC/CNF was observed for *EUC SS 10%* pre-treatment. For PIN MFC/CNF, the lowest turbidity was obtained for *PIN SS 5%* (Figure 3).

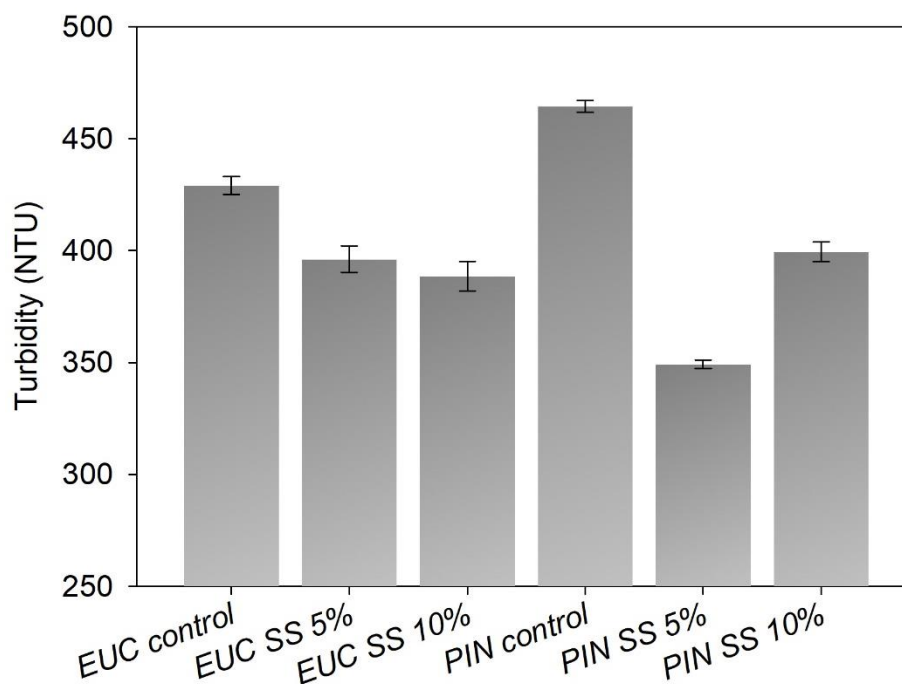


Figure 3: Turbidity of MFC/CNF suspensions from untreated and pre-treated pulps with sodium silicate solution in concentrations of 5% and 10%.

According to Bejoy et al. (2018), the purpose of this test is to measure the scattered light at an incidence angle of 90° , the variation of the readings is related to the shape and refractive index of the dispersed material. The unit NTU from turbidimeter refers to nephelometric turbidity units. If the suspension is composed only of nanoscale particles, the turbidity value is close to zero. On the other hand, the presence of partially deconstructed fibers in the suspension will increase turbidity, as observed in the present work. The experimental results obtained for turbidity were in harmony with values found in other works. Qu et al. (2019) obtained turbidities ranging between 100 NTU and 500 NTU for CNF produced by mechanical fibrillation of kraft pulp from coniferous wood, after TEMPO-mediated oxidation. Moser et al. (2015) found turbidity values around 300 NTU when studying CNF obtained from coniferous pulp produced by fiber steam explosion.

Amini et al. (2020) evaluated the effect of different fine content on the turbidity of CNF suspensions and obtained values ranging between 400 NTU and 500 NTU. These authors observed that for higher fines content in the suspension, the turbidity values increased. These observations corroborate the understanding of the turbidity variation observed in the present study. As shown in Figure 2, different fibrillation conditions favored the different amounts of fines and aggregates in the suspensions.

Microstructure and physical properties of the films

The films obtained were visually homogeneous and malleable, being easily detached from the acrylic plates. Scanning electron microscopy showed a reduction in surface granularity of films with the application of Na_2SiO_3 (Figure 4).

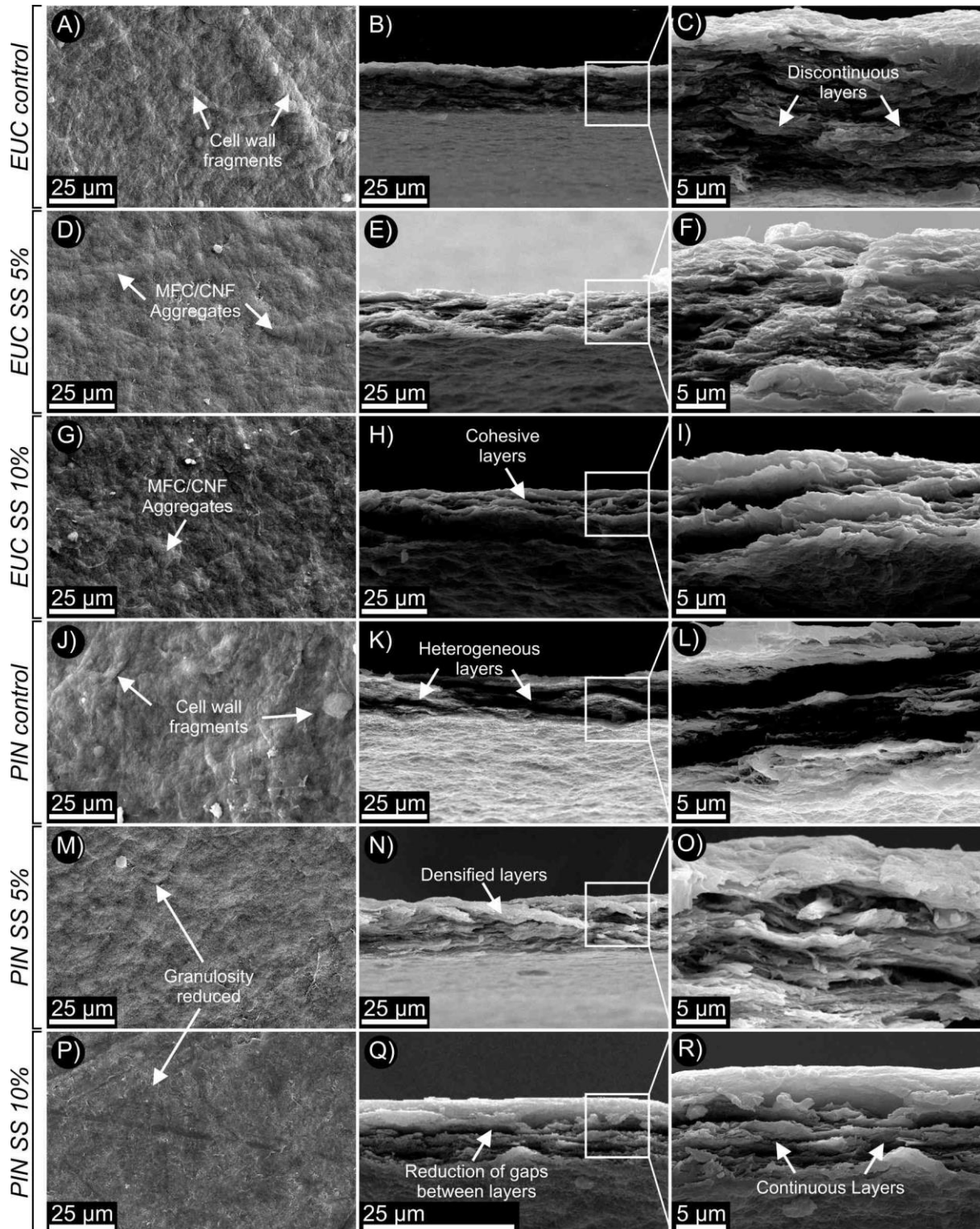


Figure 4: Micrographs of films of MFC/CNF from untreated and pre-treated pulps with sodium

silicate solution in concentrations 5% and 10%; A) *EUC control* – surface; B) *EUC control* – cross section and C) *EUC control* – cross section zoom; D) *EUC SS 5%* - surface; E) *EUC SS 5%* - cross section; F) *EUC SS 5%* - cross section zoom; G) *EUC SS 10%* - surface; H) *EUC SS 10%* - cross section; I) *EUC SS 10%* - cross section zoom; J) *PIN control* – surface; K) *PIN control* - cross section; L) *PIN control* - cross section zoom; M) *PIN SS 5%* - surface; N) *PIN SS 5%* - cross section; O) *PIN SS 5%* - cross section zoom; P) *PIN SS 10%* - surface; Q) *PIN SS 10%* - cross section; and R) *PIN SS 10%* - cross section zoom.

Cell wall aggregates and fragments were observed on the *EUC control* and *PIN control* film surface, indicated by the arrows in figures 4A and 4J, respectively. *EUC SS 5%* and *EUC SS 10%* films (Figures 4D and 4G) showed higher surface granularity in relation to *PIN SS 5%* and *PIN SS 10%* films (Figures 4M and 4P). In cross-sections, *EUC control* (Figures 4B and 4C) and *PIN control* (Figures 4K and 4L) films presented heterogeneous and discontinuous layers, due to the presence of cell wall fragments with different dimensions.

EUC SS 5% (Figures 4E and 4F) and *EUC SS 10%* (Figures 4H and 4I) films presented more cohesive and continuous layers in relation to the control. Similar characteristics were observed for *PIN SS 5%* films (Figures 4N and 4O), in which the layers were vertically and horizontally more homogeneous. For *PIN SS 10%* (Figures 4Q and 4R), there was a gap reduction between the MFC/CNF layers.

Greater granularities and roughness resulted in greater dispersion of incident light on the surface of the film, with a decrease in transparency (From et al. 2020). Films with a more granular surface show a greater contact surface, directly influencing the wettability (Aulin et al. 2009). This characteristic favors greater amounts of hydrogen bonds with water molecules. For this reason, adhesion forces overcome the cohesion forces, increasing the scattering of liquid on the film surface (Dimic-Misic et al. 2019). The thickness ranged between 20 μm and 36 μm (Figure 5A). The average thickness for *EUC control* was 18% lower than *EUC SS 5%* and 6% greater than *EUC SS 10%*. The smallest variation was observed for *EUC SS 5%* films and the largest for *EUC SS 10%*. Film thicknesses of *PIN SS 5%* and *PIN SS 10%* were 23% and 12% superior compared to *PIN control*, respectively.

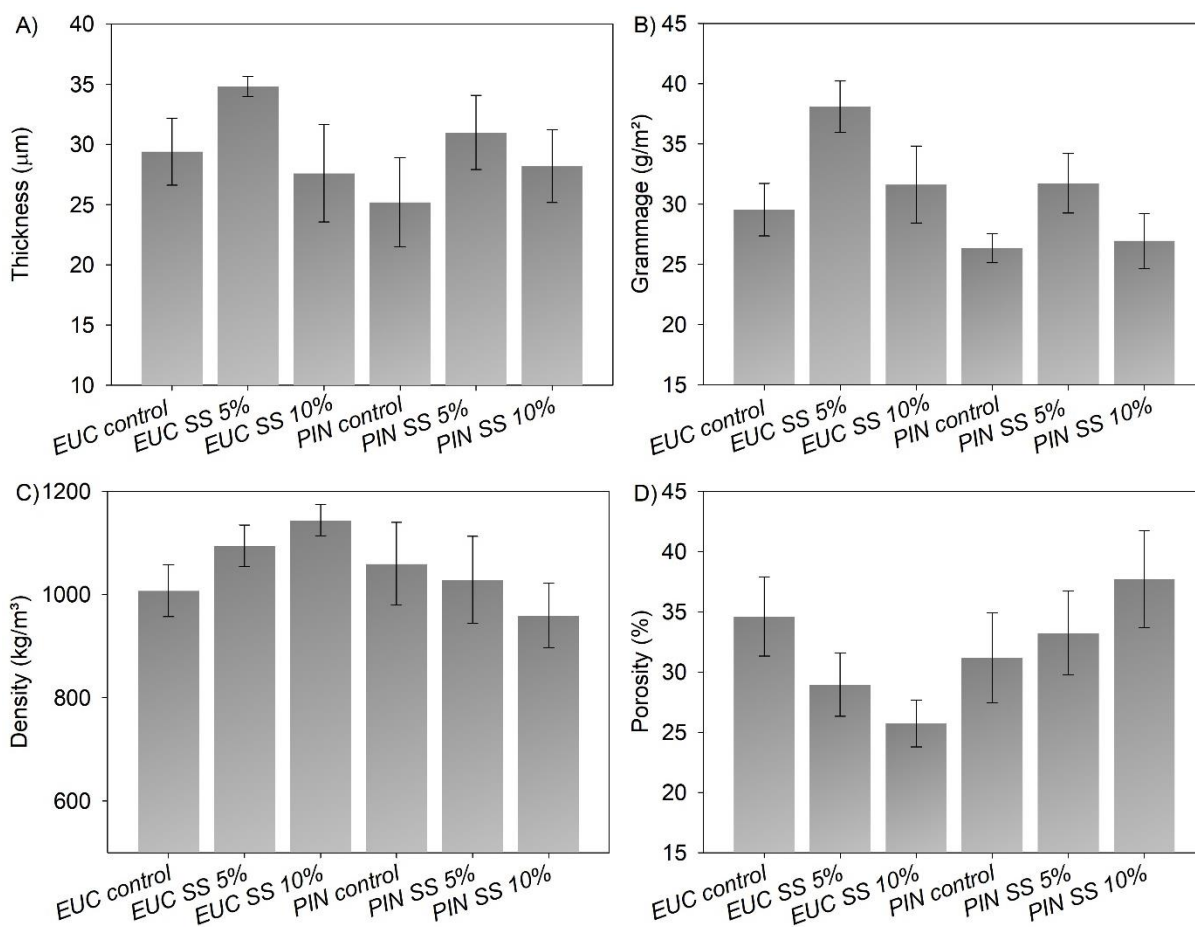


Figure 5: A) Thickness; B) grammage; C) bulk density, and D) porosity of films of MFC/CNF suspensions from untreated and pre-treated pulps with sodium silicate solutions in concentrations of 5% and 10%.

Thickness is strongly influenced by the characteristics of the raw material and the concentration of MFC/CNF suspensions (Kolakovic et al. 2012). In the present study, the films were produced with identical suspension volume and solids content, which indicates that thickness variations observed were due to the effects of pre-treatments with Na_2SiO_3 in the film-forming suspensions. Kim et al. (2021) explained that MFC/CNF suspensions with lower gel formation, lower viscosity, and lower surface area, tend to form thinner films. This effect was observed in the present work because *EUC control* and *PIN control* films obtained the lowest average thickness. These materials presented suspensions with lower particle homogeneity, which indicates lower gel formation and lower surface area due to the larger aggregates of MFC/CNF (see Figure 2). All the films showed increments in grammage compared to the control (Figure 5B), except *PIN SS 10%*. The grammages of *PIN SS 5%* and *EUC SS 10%* were similar ($\sim 31 \text{ g/m}^2$), while the highest average was obtained for *EUC SS 5%*

(~38 g/m²). The lowest grammage averages were obtained for *PIN control*, *PIN SS 10%*, and *EUC control*, respectively.

For bulk density, *EUC SS 5%* and *EUC SS 10%* presented averages, respectively, 8.6% and 13.6% higher in relation to *EUC control* (1007 kg/m³) (Figure 5C). *PIN control*, *PIN SS 5%*, and *PIN SS 10%* showed the greatest variations in bulk density. Variation of the porosity of the film followed an inversely proportional trend in relation to bulk density (Figure 5D), as they are collinear parameters. Porosity varied between 20% and 44%, with the highest average observed for *PIN SS 10%* and the lowest for *EUC SS 10%*. Since the porosity variation was small, due to low standard deviation, the results indicated that the films produced were relatively homogeneous. For suspensions with larger particle sizes, and in which the “gel point” was probably prolonged (*EUC control* and *PIN control*), porosity averages were slightly higher.

Raj et al. (2015) reported that reduced “gel point” results in increased porosity of CNF composites, suggesting that the three-dimensional open/porous structure of cellulose suspension is partially maintained during the formation of the two-dimensional film structure. Research reports that thickness, density, and porosity are determining parameters of the characteristics of the film, as they are strongly related to mechanical, optical, and barrier properties to water vapor and gases (Fukuzumi et al. 2013; Bedane et al. 2015). Additionally, part of the variations observed for the parameters studied can be explained by the characteristics inherent to the *casting* method, which is widely used in research with cellulose, starch, and protein-based films (Suhag et al. 2020). Production of films with larger dimensions is limited, the time of solvent evaporation is prolonged and the films may present heterogeneity in thickness and wrinkling because the method does not apply vacuum (Moraes et al. 2013; Espitia et al. 2014). Even so, the results found are in harmony with other works from the literature. Cruz et al. (2022) found average thicknesses for MFC/CNF films of EUC and PIN around 35 and 32 μm, respectively. For MFC/CNF films of PIN, Mascarenhas et al. (2022) found a thickness value close to 21 μm and bulk density of 1050 kg/m³.

Light transmittance and transparency of the films

The films showed different transmittance intensities across the entire wavelength range, indicating the influence of Na₂SiO₃ pre-treatments (Figure 6A). Most films showed transmittance below 15% and only *PIN SS 5%* and *PIN SS 10%* showed transmittance below 10%. For cellulose films, transmittance values in this range indicate suitable UV light barrier properties (Cazón et al. 2020). This characteristic is interesting for applications in the packaging of products susceptible to degradation by UV light, such as some foods and medicines (Niu et

al. 2018; Bastante et al. 2021). For UVB wavelength from 280 to 315 nm, the highest transmittance was observed for *EUC control* film followed by *PIN control*, *EUC SS 5%*, *EUC SS 10%*, *PIN SS 10%*, and *PIN SS 5%*. The same order was observed for transmittance in the UVA range (315-400 nm). For both UVB and UVA, transmittance rates were low, confirming that the films produced are translucent (Kim et al. 2021).

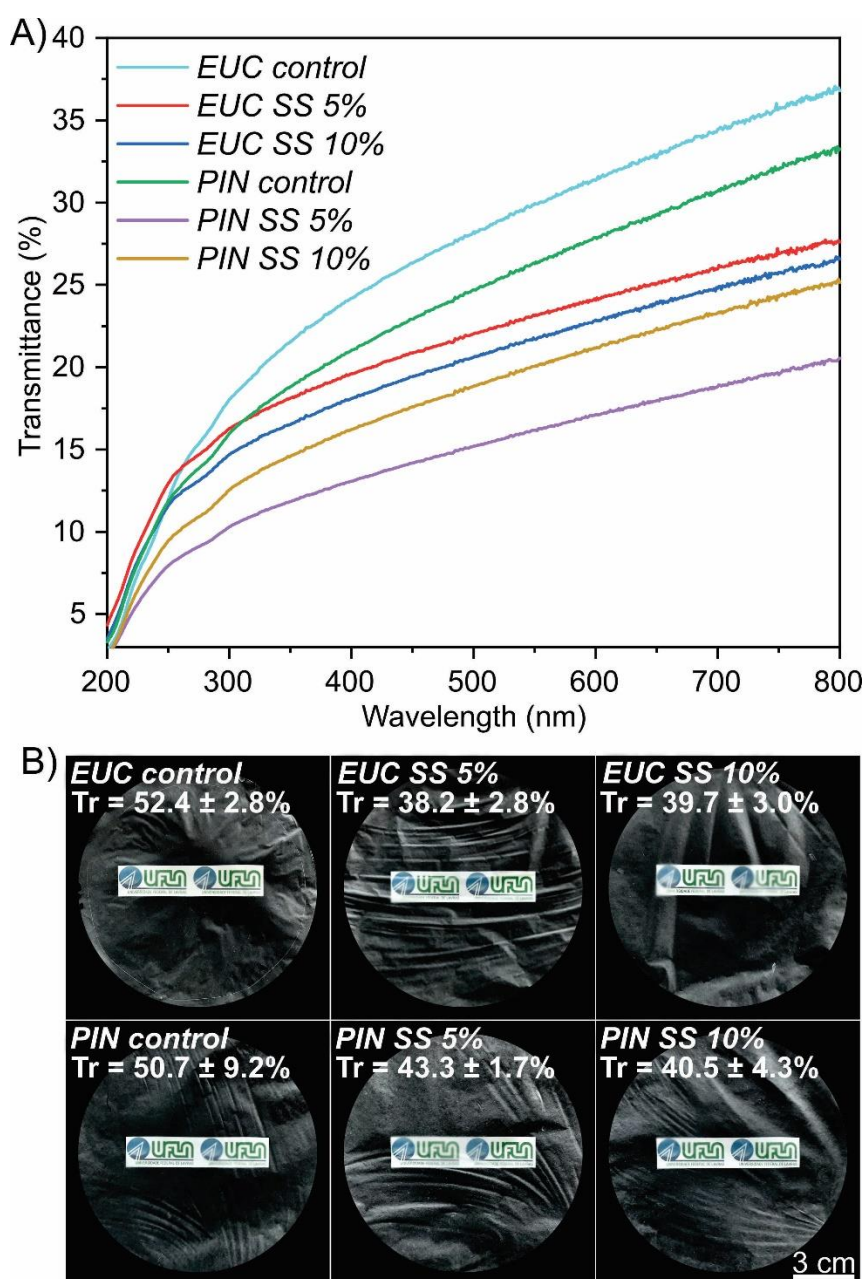


Figure 6: A) Transmittance; and B) transparency (Tr) of films of MFC/CNF suspensions from untreated and pre-treated pulps with sodium silicate solution in concentrations of 5% and 10%.

For the visible light region (400 - 700 nm), the transmittance for *EUC control* and *PIN control* ranged between 21% and 34%. For *EUC SS 5%*, *EUC SS 10%*, and *PIN SS 10%*, the transmittance range was between 16% and 26%, whereas for *PIN SS 5%*, the transmittance ranged from 12% to 19%. The infrared region (> 700 nm), confirmed the same trends described for the visible light region, with increased transmittance intensity with Na₂SiO₃ pre-treatment.

Transmittance values for *EUC SS 5%* and *EUC SS 10%* were 27% and 24% higher than the *EUC control*, respectively. Compared to the *PIN control*, the transmittances for *PIN SS 5%* and *PIN SS 10%* were 15% and 20% higher, respectively. In general, variations for Tr between treatments were low. Considering only MFC/CNF films from pre-treatments, the Tr values obtained for PIN were slightly higher than those found for EUC.

The transparency of MFC/CNF films can be influenced by the dimensions of cellulose fibrils, fiber aggregates, degree of homogenization, and the granularity/roughness of the film surface (Mascarenhas et al. 2022). The granularity was lower for *PIN SS 5%* and *PIN SS 10%* (see Figures 4M and 4P). MFC/CNF diameters are smaller in relation to the wavelength of visible light, as a result, dense packing of cellulose bundles can cause suppression or projection of light scattering, depending on the fibrillation degree (Kumar et al. 2014).

Transparency is also affected by the MFC/CNF crystal structure, therefore, the smaller the dimensions of the crystallites present in the cellulose aggregates, the greater the light scattering, which results in lower transparency (Zhang et al. 2015). The results indicated improvements in the optical properties, mainly regarding the barrier to UVC. This aspect is important for the application of the film, as transparency is configured as an important indicator for the commercial destination, such as packaging (Jing et al. 2022). The highest opacity values were obtained for *EUC control* (~59%) and *PIN SS 5%* (~60%) while the lowest value was found for *EUC SS 5%* (~53%) (Figure 7). Films produced with *EUC SS 10%*, *PIN control*, and *PIN SS 10%* showed intermediate opacity values (~55%).

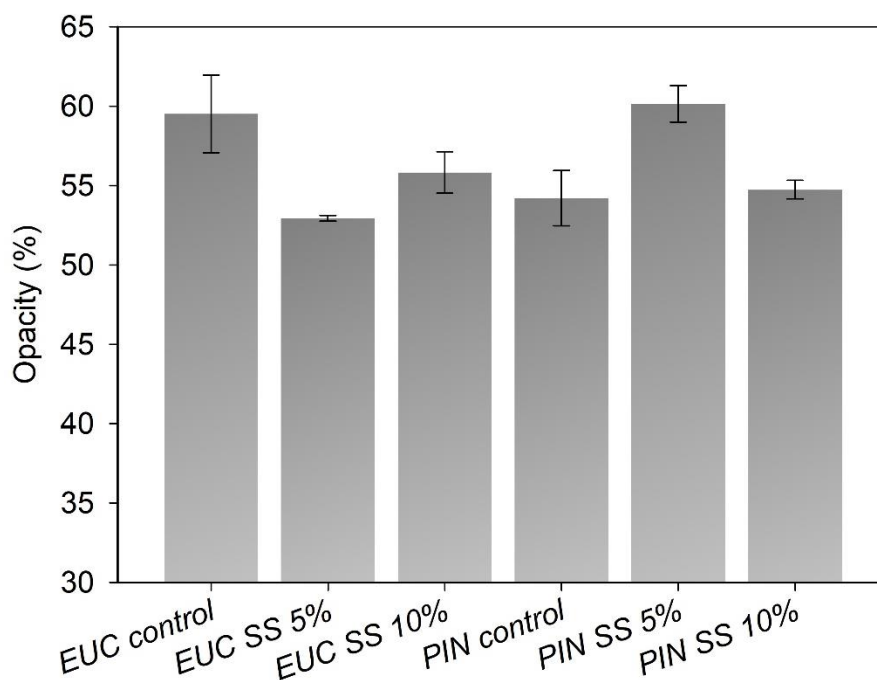


Figure 7: Opacity of films of MFC/CNF suspensions from untreated and pre-treated pulps with sodium silicate solution in concentrations of 5% and 10%.

The higher opacity can be explained by the presence of cell wall particles, bundles of fibrils, and MFC/NFC aggregates in the composition of the films, as seen in Figure 4. Larger fragments offer a greater barrier to the passage of light through the films (Wang et al. 2013), as evidenced by the transmittance results.

The opacity in some cases can more consistently explain aspects related to the influence of the degree of fibrillation and the dimensions of the MFC/NFC in the films. Hsieh et al. (2017) and Xinping et al. (2020) explained that the presence of larger fragments in NFC films/nanopapers from bleached materials may allow the passage of light because they have certain transparency. This may contribute to the overestimation of transparency values, which will not necessarily be associated with a higher degree of fibrillation and may represent higher opacity values (Yang et al. 2019; Hou et al. 2020).

Barrier properties and grease resistance

The highest values of WVTR were observed for *EUC control* and *PIN SS 10%*, whereas the other films presented values ranging from 1170 to 1220 g/m² day (Figure 8A). The WVP averages of the films were decreased in the following order: *EUC SS 5%*, *EUC SS 10%*, *PIN SS 5%*, *EUC control*, *PIN SS 10%*, and *PIN control* (Figure 8B).

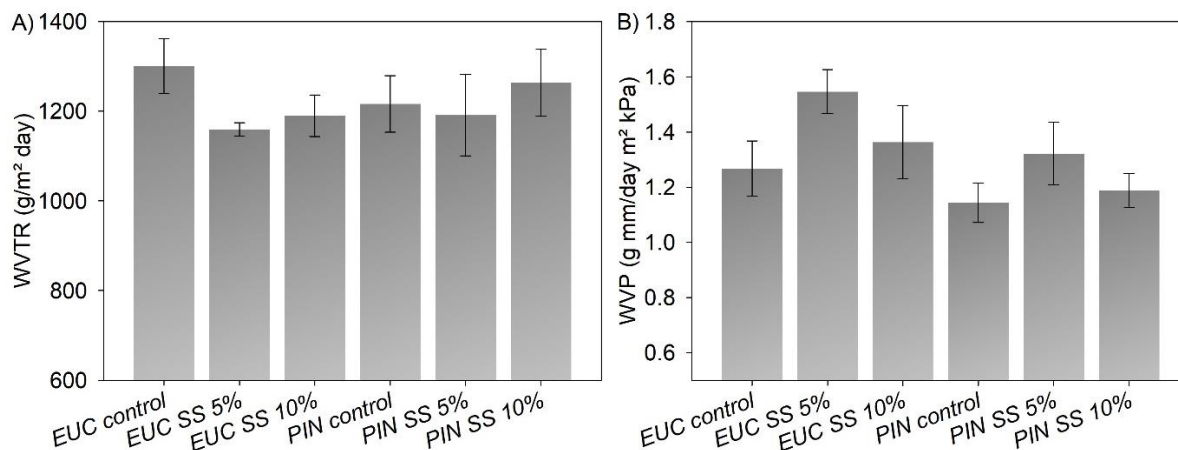


Figure 8: A) Water vapor transmission rate (WVTR) and B) water vapor permeability (WVP) of films of MFC/CNF suspensions from untreated and pre-treated pulps with sodium silicate solution in concentrations 5% and 10%.

For *EUC SS 5%* the WVP was slightly higher because the films were thicker in relation to other treatments. As already mentioned, it is possible that excessive fibrillation affected the three-dimensional structure of the MFC/CNF network, reducing the number of interfibrillar interactions and allowing the formation of isolated aggregates. This results in the appearance of regions with void spaces in the films, facilitating the passage of water vapor (Li et al. 2019).

Based on the TAPPI T 559 cm-12 standard (TAPPI 2012), all the films were resistant to kit 12, which is more aggressive because it contains higher n-heptane and toluene amounts. This indicates that the films present a high barrier to the fats penetration and the ability to retain fine and viscous oils, which can be found in foods, grains, and waxes. This result is in accordance with other research, which reports that films and paper coatings based on MFC/CNF present resistance to oil penetration (Tyagi et al. 2018; Jin et al. 2021).

Cruz et al. (2022) and Mascarenhas et al. (2022) also observed high resistance to oil penetration in MFC/CNF films from *Eucalyptus* sp. and *Pinus* sp. The authors explained that because the MFC/CNF diameters are very small, the layers architecture of the films tends to be strongly closed and difficult for being penetrated by viscous liquid.

According to the classification presented by Wang et al. (2018), it can be considered that all films presented an average barrier to water vapor because the WVP values were between 0.4 g H₂O mm/day m² kPa and 4 H₂O mm/day m² kPa. These authors also reported that films with these characteristics could be used for food packaging, depending on their nature. The films evaluated in the present study meet the WVTR and thickness for package bakery products, fruits, and salads (Wang et al. 2018).

WVP values obtained in the present work were lower than results found in the literature, demonstrating that the pre-treatments performed contributed to the barrier properties improvement. This is an advantage because in general, MFC/CNF are combined with synthetic polymers, proteins, and minerals to improve gas barrier properties (Zhang et al. 2021).

Hasan et al. (2021) found WVP values ranging from 5 mm/day m² kPa to 25 g H₂O mm/day m² kPa when analyzing different techniques for film production obtained from CNF from untreated coniferous fibers by mechanical fibrillation. Wang et al. (2020) found WVP around 5.5 g H₂O mm/day m² kPa and 12 g H₂O mm/day m² kPa for NFC films. Nascimento et al. (2021), studying films composed of cellulose nanocrystals and bacterial nanocellulose, found WVP values ranging from 2.96 g H₂O mm/day m² kPa and 3.57 g H₂O mm/day m² kPa. Evaluation of permeability is important in choosing a better destination for the films. For applications involving foods like fresh vegetables, permeable films could be applied, while poorly permeable films can be indicated for foods and dehydrated products (Lago et al. 2020).

Mechanical properties of the films

EUC SS 10% achieved tensile strength of ~82 MPa, 17% higher compared to *EUC control* (Figure 9A). The strength of *PIN SS 10%* (~70 MPa) was around 20% higher in relation to *PIN control*. The highest values for Young's modulus (Figure 9B) were found for *EUC SS 5%* (~4 GPa) and *PIN SS 10%* (~3.5 GPa), while the lowest value was obtained for *PIN control* (~1.7 GPa). These results indicate that the pre-treatments proposed promoted improvements in mechanical properties, especially for *EUC SS 10%*.

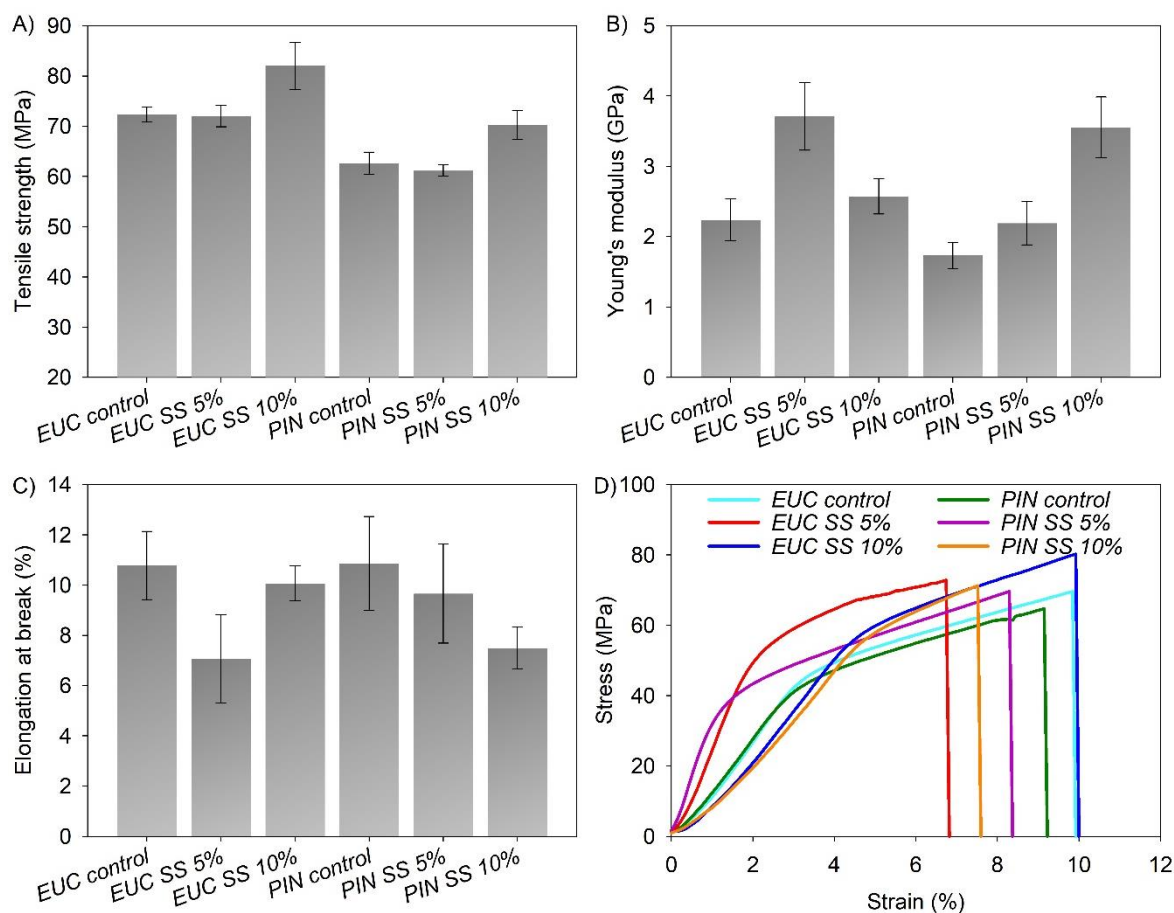


Figure 9: A) Tensile strength; B) Young's modulus; C) elongation at break; and D) stress x strain curves (tensile test) of films of MFC/CNF suspensions from untreated and pre-treated pulps with sodium silicate solution in concentrations 5% and 10%.

Films with higher density showed higher values of tensile strength. Yang et al. (2019) and Liang et al. (2020) explained that MFC/CNF present absolutely small dimensions, which favors the obtainment films with high layer compaction and a great number of hydrogen bonds. As a result, there is an increase in density and greater slipping resistance in the structure of the film, when subjected to tensile stress. Analyzing the results of Young's modulus and elongation at break (Figure 9C), it is possible to note that films with lower strength presented lower elongation (< 8%), lower energy absorption, and presented lower tenacity when compared to films with higher strength (*EUC SS 5%* and *EUC SS 10%*). Verker et al. (2009) explained that films with this characteristic release the highest percentage of energy absorbed in the elastic phase, as observed for *EUC control*, *PIN control*, and *EUC SS 10%* (Figure 9D).

In general, films presented strengths consistent with other studies. Noorbakhsh-Soltani et al. (2018) when studying nanocellulose and chitosan films for food packaging, found tensile strength ranging between 60 and 70 MPa and Young's modulus between 2 and 4 GPa. Wang et

al. (2020) evaluated films produced with different proportions of CNC/CNF for application in packaging and obtained tensile strength around 40 - 80 MPa and Young's modulus ranging from 2 to 7 GPa.

Quality index of the cellulose micro/nanofibrils

The IQ values for MFC/CNF of EUC and PIN were similar, ranging between ~53 and ~58. However, for *EUC SS 10%* (~70), the IQ values were 16% higher in relation to other treatments (Figure 10).

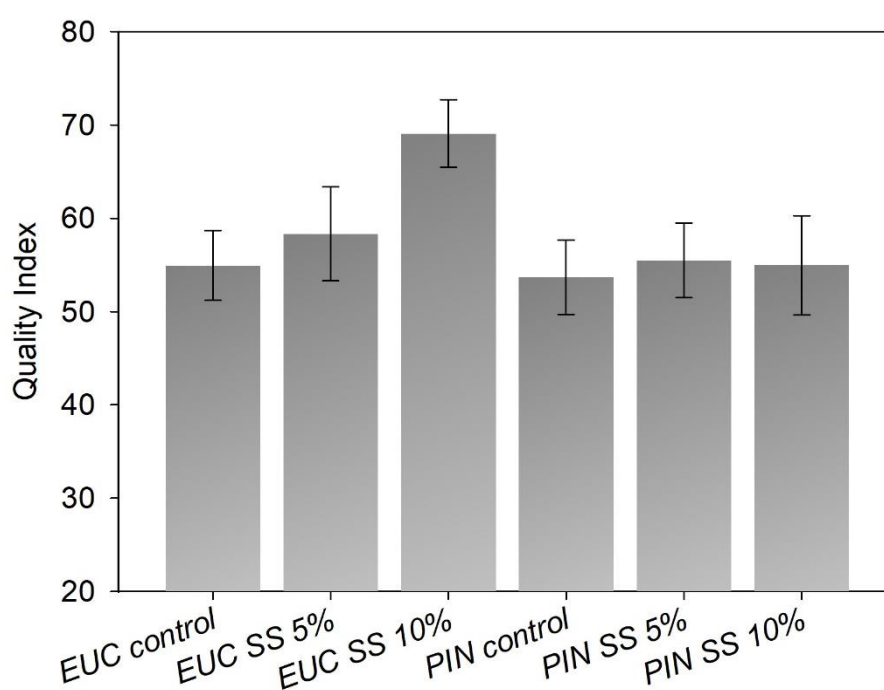


Figure 10: Quality Index (QI) of MFC/CNF suspensions from untreated and pre-treated pulps with sodium silicate solution in concentrations of 5% and 10%.

Research indicates that QI is related to energy consumption during mechanical fibrillation. Desmaisons et al. (2017) reported that QI values between 50 - 70 are characteristic of MFC/CNF produced with energy consumption of around 5000 kWh/t. Banvillet et al. (2021a) found QI values ranging between 40 – 60 when producing CNF from pulps treated with 10% NaOH (w/w). The authors found that these QI values are according to energy consumption between 2000 - 5000 kWh/t during mechanical fibrillation. In the present work, the energy consumption until the gel consistency was between 3000 - 4100 kWh/t for *EUC control* and 4400 - 4500 kWh/t for *PIN control*.

Besides correlating with energy consumption, QI is also calculated based on the suspension properties and resulting film/nanopaper, including particle dimensions in multiple length scales (Desmaisons et al. 2018). Comparing the results obtained in Rol et al. (2019), Banvillet et al. (2021a), and Dias et al. (2022) QI values from the present study were comparable to those obtained for pre-treatments already established and with potential for industrial application, such as pre-treatment with NaOH solution 10% (QI between 54 - 82), oxidation with periodates – sulfonation, NaBH₄, amines, and ClO₂ (~62), carboxymethylation (~66), enzymatic pre-treatments (68 - 75) and pre-treated fibers with deep eutectic solvent (66 - 72).

Given the reduced number of studies addressing QI, the studies mentioned corroborate the results found in the present research, because the QI was in accordance with the same variation presented in the literature. Moreover, it can be said that Na₂SiO₃ proved to be efficient, improving the MFC/CNF individualization, being a low-cost alternative, and with effects similar to other successful pre-treatments.

Conclusion

Fibers from *Eucalyptus* sp. and *Pinus* sp. were treated with Na₂SiO₃ to reduce energy consumption in mechanical fibrillation, evaluating the properties of suspensions, films, and posteriorly, calculating QI. Pre-treatments with Na₂SiO₃ resulted in greater individualization, greater homogeneity, and lower turbidity of the MFC/CNF suspensions. Films properties were strongly influenced by the suspension characteristics. The transparency of the films produced with treated fiber was ~22% lower compared to the controls. Barrier properties to grease were suitable for all the treatments, although the same was not observed for the barrier to water vapor. Young's modulus was increased from 2 to 4 GPa for both pulps with the treatment with 10% of Na₂SiO₃. Considering the greater individualization capacity of MFC/NFC, a greater barrier to UV radiation, less water vapor penetration, and greater tensile strength, the best results were found for MFC/NFC obtained from EUC and PIN pre-treated with 10% Na₂SiO₃. As for the QI, the highest values were found for the PIN MFC/CNF obtained with pre-treatment with 10% Na₂SiO₃ (~70). For EUC fibers, the highest QI values (~58) were found for MFC/NFC obtained from the pre-treatment using 5% Na₂SiO₃. The suspensions showed interesting characteristics for applications in the form of emulsion stabilizers. The films presented microstructural, physical, optical, barrier, and mechanical properties suitable to the parameters required for packaging. The experimental results indicate that the use of Na₂SiO₃ as fibers pre-treatment for production of MFC/CNF has potential for industrial scaling up, with low cost and similar to other pre-treatments already established.

Acknowledgments

We are especially grateful to the Program in Wood Science and Technology (PPGCTM) of the Federal University of Lavras (UFLA) for providing study material and infrastructure. We would also like to thank Embrapa Instrumentação and Klabin S.A. for the availability of inputs and equipment for the analysis required in this work. The authors are also grateful to the Coordination for the Improvement of Superior Education Personnel (CAPES) for providing the research grant.

Funding: The research was funded by the National Council for Scientific and Technological Development (CNPq) (finance code 300985/2022-3).

Conflict of interest: The authors declare that there are no conflicts of interest.

References

- Afsahi, G., Dimic-Misic, K., Gane, P., Budtova, T., Maloney, T., Vuorinen, T. (2018) The investigation of rheological and strength properties of NFC hydrogels and aerogels from hardwood pulp by short catalytic bleaching (Hcat). *Cellulose* 25:1637-1655. <https://doi.org/10.1007/s10570-018-1678-6>
- Albornoz-Palma, G., Ching, D., Valerio, O., Mendonça, R.T., Pereira, M. (2020) Effect of lignin and hemicellulose on the properties of lignocellulose nanofibril suspensions. *Cellulose* 27:10631-10647. <https://doi.org/10.1007/s10570-020-03304-5>
- Amalraj, A., Gopi, S., Thomas, S., Haponiuk, J.T. (2018) Cellulose nanomaterials in biomedical, food, and Nutraceutical Applications: A Review. *Macromolecular Symposia* 380: 1800115. <https://doi.org/10.1002/masy.201800115>
- Amini, E., Hafez, I., Tajvidi, M., Bousfield, D.W. (2020) Cellulose and lignocellulose nanofibril suspensions and films: A comparison. *Carbohydrate Polymers* 250:117011. <https://doi.org/10.1016/j.carbpol.2020.117011>
- Ang, S., Haritos, V., Batchelor, W. (2019) Effect of refining and homogenization on nanocellulose fiber development, sheet strength and energy consumption. *Cellulose* 26:4767-4786. <https://doi.org/10.1007/s10570-019-02400-5>
- ASTM Standard (2012) E-104-02, Standard Practice for Maintaining Constant Relative Humidity by Means of Aqueous Solutions.
- ASTM Standard (2016a) ASTM E-96, Standard Test Methods for Water Vapor Transmission of Materials.

ASTM Standard (2018) ASTM D882-18, Standard Test Methods for Tensile Properties of Thin Plastic Sheeting.

Aulin, C., Yun, S.H., Wagberg, L., Lindström, T. (2009) Design of Highly Oleophobic Cellulose Surfaces from Structured Silicon Templates. *Applied Materials & Interfaces* 1:2443-2452. <https://doi.org/10.1021/am900394y>

Balea, A., Fuente, E., Monte, M.C., Merayo, N., Campano, C., Negro, C., Blanco, A. (2020) Industrial Application of Nanocelluloses in Papermaking: A Review of Challenges, Technical Solutions, and Market Perspectives. *Molecules* 25:256. <http://dx.doi.org/10.3390/molecules25030526>

Banvillet, G., Depres, G., Belgacem, N., Bras, J. (2021a) Alkaline treatment combined with enzymatic hydrolysis for efficient cellulose nanofibrils production. *Carbohydrate Polymers* 255:117383. <https://doi.org/10.1016/j.carbpol.2020.117383>

Banvillet, G., Gatt, E., Belgacem, N., Bras, J. (2021b) Cellulose fibers deconstruction by twin-screw extrusion with in situ enzymatic hydrolysis via bioextrusion. *Bioresource Technology* 327:124819. <https://doi.org/10.1016/j.biortech.2021.124819>

Bastante, C.C., Silva, N.H.C.S., Cardoso, L.C., Serrano, C.M., Ossa, E.J.M., Freire, C.S.R., Vilela, C. (2021) Biobased films of nanocellulose and mango leaf extract for active food packaging: Supercritical impregnation versus solvent casting. *Food Hydrocolloids* 117:106709. <https://doi.org/10.1016/j.foodhyd.2021.106709>

Bedane, A.H., Eic, M., Farmahini-Farahani, M., Xiao, H. (2015) Water vapor transport properties of regenerated cellulose and nanofibrillated cellulose films. *Journal of Membrane Science* 493:46-57. <https://doi.org/10.1016/j.memsci.2015.06.009>

Bejoy, T., Midhun, C.R., Athira, K.B., Rubiyah, M.H., Jithin, J., Audrey, M., Drisko, G.L., Sanchez, C. (2018) Nanocellulose, a Versatile Green Platform: From Biosources to Materials and Their Applications. *Chemical Reviews* 24:11575-11625. <https://doi.org/10.1021/acs.chemrev.7b00627>

Berto, G.L., Arantes, V. (2019) Kinetic changes in cellulose properties during defibrillation into microfibrillated cellulose and cellulose nanofibrils by ultra-refining. *International Journal of Biological Macromolecules* 127:637-648. <https://doi.org/10.1016/j.ijbiomac.2019.01.169>

Bradney, L., Wijesekara, H., Palansooriya, K.N., Obadamudalige, N., Bolan, N.S., Ok, Y.S., Rinklebe, J., Kim, K.H., Kirkham, M.B. (2019) Particulate plastics as a vector for toxic trace-element uptake by aquatic and terrestrial organisms and human health risk. *Environment International* 131: 104937. <https://doi.org/10.1016/j.envint.2019.104937>

- Brännvall, E. (2017) The limits of delignification in kraft cooking. *BioResources* 12:2081-2107. <https://doi.org/10.15376/biores.12.1.Brannvall>
- Cazón, P., Velazquez, G., Vázquez, M. (2020) Characterization of mechanical and barrier properties of bacterial cellulose, glycerol and polyvinyl alcohol (PVOH) composite films with eco-friendly UV-protective properties. *Food Hydrocolloides* 99:105323. <https://doi.org/10.1016/j.foodhyd.2019.105323>
- Chanda, S., Bajwa, D.S. (2021) A review of current physical techniques for dispersion of cellulose nanomaterials in polymer matrices. *Reviews on Advanced Materials Science* 60:325-341. <https://doi.org/10.1515/rams-2021-0023>
- Claro, F.C., Matos, M., Jordão, C., Avelino, F., Lomonaco, D., Magalhães, W.L.E. (2019) Enhanced microfibrillated cellulose-based film by controlling the hemicellulose content and MFC rheology. *Carbohydrate Polymers* 218:307-314. <https://doi.org/10.1016/j.carbpol.2019.04.089>
- Cruz, T.M., Mascarenhas, A.R.P., Scatolino, M.V., Faria, D.L., Matos, L.C., Duarte, P.J., Neto, J.M., Mendes, L.M., Tonoli, G.H.D. (2022) Hybrid films from plant and bacterial nanocellulose: mechanical and barrier properties. *Nordic Pulp & Paper Research Journal* aop: 1-16. <https://doi.org/10.1515/npprj-2021-0036>
- Desmaisons, J., Boutonnet, E., Rueff, M., Dufresne, A., Bras, J. (2017) A new quality index for benchmarking of different cellulose nanofibrils. *Carbohydrate Polymers* 174:318-329. <https://doi.org/10.1016/j.carbpol.2017.06.032>
- Desmaisons, J., Gustafsson, E., Dufresne, A., Bras, J. (2018) Hybrid nanopaper of cellulose nanofibrils and PET microfibers with high tear and crumpling resistance. *Cellulose* 25:7127-7142. <https://doi.org/10.1007/s10570-018-2044-4>
- Dias, M.C., Mendonça, M.C., Damásio, R.A.P., Zidanes, U.L., Mori, F.A., Ferreira, S.R., Tonoli, G.H.D. (2019) Influence of hemicellulose content of *Eucalyptus* and *Pinus* fibers on the grinding process for obtaining cellulose micro/nanofibrils. *Holzforschung* 73:1035-1046. <https://doi.org/10.1515/hf-2018-0230>
- Dias, M.C.; Belgacem, M.N.; Resende, J.V.; Martins, M.A.; Damásio, R.A.P.; Tonoli, G.H.D.; Ferreira, S.R. (2022) Eco-friendly laccase and cellulase enzymes pretreatment for optimized production of high content lignin-cellulose nanofibrils. *International Journal of Biological Macromolecules* 209: 413-425. <https://doi.org/10.1016/j.ijbiomac.2022.04.005>
- Dimic-Misic, K., Kostic, M., Obradovic, B., Kramar, A., Jovanovic, S., Stepanenko, D., Mitrovic-Dankulov, M., Lazovic, S., Johansson, L.S., Maloney, T., Gane, P. (2019) Nitrogen

- plasma surface treatment for improving polar ink adhesion on micro/nanofibrillated cellulose films. *Cellulose* 26:3845-3857. <https://doi.org/10.1007/s10570-019-02269-4>
- Durães, A.F.S., Moulin, J.C., Dias, M.C., Mendonça, M.C., Damásio, R.A.P., Thygeses, L.G., Tonoli, G.H.D. (2020) Influence of chemical pretreatments on plant fiber cell wall and their implications on the appearance of fiber dislocations. *Holzforschung* 74:949-955. <https://doi.org/10.1515/hf-2019-0237>
- Espinosa, E., Rol, F., Bras, J., Rodríguez, A. (2020) Use of multi-factorial analysis to determine the quality of cellulose nanofibers: effect of nanofibrillation treatment and residual lignin content. *Cellulose* 27:10689-10705. <https://doi.org/10.1007/s10570-020-03136-3>
- Espitia, P.J.P., Du, W.X., Avena-Bustillos, R.J., Soares, N.F.F., Mchugh, T.H. (2014) Edible films from pectin: Physical-mechanical and antimicrobial properties - A review. *Food Hydrocolloids* 35:287-296. <https://doi.org/10.1016/j.foodhyd.2013.06.005>
- Fakhouri, F.M., Costa, D., Yamashita, F., Martelli, S.M., Jesus, R.C., Alganer, K., Collares-Queiroz, F.P., Innocentini-Mei, L.H. (2013) Comparative study of processing methods for starch/gelatin films. *Carbohydrate Polymers* 95: 681-689. <https://doi.org/10.1016/j.carbpol.2013.03.027>
- Fonseca, A.S., Panthapulakkal, S., Konar, S.K., Sain, M., Bufalino, L., Raabe, J., Miranda, I.P.A., Martins, M.A., Tonoli, G.H.D. (2019) Improving cellulose nanofibrillation of non-wood fiber using alkaline and bleaching pre-treatments. *Industrial Crops and Products* 131:203-212. <https://doi.org/10.1016/j.indcrop.2019.01.046>
- From, M., Larsson, P.T., Andreasson, B., Medronho, B., Svanedal, I., Edlund, H., Norgren, M. (2020) Tuning the properties of regenerated cellulose: Effects of polarity and water solubility of the coagulation medium. *Carbohydrate Polymers* 236:116068. <https://doi.org/10.1016/j.carbpol.2020.116068>
- Fukuzumi, H., Saito, T., Isogai, A. (2013) Influence of TEMPO-oxidized cellulose nanofibril length on film properties. *Carbohydrate Polymers* 93:172-177. <https://doi.org/10.1016/j.carbpol.2012.04.069>
- Grigatti, M., Montecchio, D., Francioso, O., Ciavatta, C. (2015) Structural and Thermal Investigation of Three Agricultural Biomasses Following Mild-NaOH Pretreatment to Increase Anaerobic Biodegradability. *Waste Biomass Valorization* 6:1135-1148. <https://doi.org/10.1007/s12649-015-9423-y>
- Guan, Q.F., Yang, H.B., Han, Z.M., Zhou, L.C., Zhu, Y.B., Ling, Z.C., Jiang, H.B., Wang, P.F., Ma, T., Wu, H.A., Yu, S.H. (2020) Lightweight, tough, and sustainable cellulose nanofiber-

derived bulk structural materials with low thermal expansion coefficient. *Science Advances* 6: eaaz1114. <https://doi.org/10.1126/sciadv.aaz1114>

Guimarães, I.C., Reis, K.C., Menezes, E.G.T., Rodrigues, A.C., Silva, T.F., Oliveira, I.R.N., Boas, E.V.B. (2016) Cellulose microfibrillated suspension of carrots obtained by mechanical defibrillation and their application in edible starch films. 89:285-294. <https://doi.org/10.1016/j.indcrop.2016.05.024>

Hasan, I., Wang, J., Tajvidi, M. (2021) Tuning physical, mechanical and barrier properties of cellulose nanofibril films through film drying techniques coupled with thermal compression. *Cellulose* 28:11345-11366. <https://doi.org/10.1007/s10570-021-04269-9>

Hashem, M., El-Bisi, M., Sharaf, S., Refaie, R. (2010) Pre-cationization of cotton fabrics: An effective alternative tool for activation of hydrogen peroxide bleaching process. *Carbohydrate Polymers* 79:533-540. <https://doi.org/10.1016/j.carbpol.2009.08.038>

Hsieh, M.C., Koga, H., Suganuma, K., Nogi, M. (2017) Hazy Transparent Cellulose Nanopaper. *Scientific Reports* 7: 41590. <https://doi.org/10.1038/srep41590>

Hou, G., Liu, Y., Li, D.Z.G., Xie, H., Fang, Z. (2020) Approaching Theoretical Haze of Highly Transparent All-Cellulose Composite Films. *ACS Applied Materials & Interfaces* 12:31998-32005. <https://dx.doi.org/10.1021/acsami.0c08586>

Jaiswal, A.K., Kumar, V., Khakalo, A., Lahtinen, P., Solin, K., Pere, J., Toivakka, M. (2021) Rheological behavior of high consistency enzymatically fibrillated cellulose suspensions. *Cellulose* 28:2087-2104. <https://doi.org/10.1007/s10570-021-03688-y>

Jin, K., Tang, Y., Liu, J., Wang, J., Ye, C. (2021) Nanofibrillated cellulose as coating agent for food packaging paper. *International Journal of Biological Macromolecules* 168:331-338. <https://doi.org/10.1016/j.ijbiomac.2020.12.066>

Jing, M., Zhang, L., Fan, Z., Liu, X., Wang, Y., Chuntai, L., Shen, C. (2022) Markedly improved hydrophobicity of cellulose film via a simple one-step aminosilane-assisted ball milling. *Carbohydrate Polymers* 275:119701. <https://doi.org/10.1016/j.carbpol.2021.118701>

Kamel, R., El-Wakil, N.A., Dufresne, A., Elkasabgy, N.A. (2020) Nanocellulose: From an agricultural waste to a valuable pharmaceutical ingredient. *International Journal of Biological Macromolecules* 163: 1579-1590. <https://doi.org/10.1016/j.ijbiomac.2020.07.242>

Karina, M., Satoto, R., Abdullah, A.D., Yudianti, R. (2020) Properties of nanocellulose obtained from sugar palm (*Arenga pinnata*) fiber by acid hydrolysis in combination with high-pressure homogenization. *Cellulose Chemistry and Technology* 54:33-38. <http://dx.doi.org/10.35812/CelluloseChemTechnol.2020.54.04>

- Kim, H.J., Roy, S., Rhim, J.W. (2021) Effects of various types of cellulose nanofibers on the physical properties of the CNF-based films. *Journal of Environmental Chemical Engineering* 9:106043. <https://doi.org/10.1016/j.jece.2021.106043>
- Kolakovic, R., Peltonen, L., Laukkanen, A., Hirvonen, J., Laaksonen, T. (2012) Nanofibrillar cellulose films for controlled drug delivery. *European Journal of Pharmaceutics and Biopharmaceutics* 82:308-315. <https://doi.org/10.1016/j.ejpb.2012.06.011>
- Kumar, V., Bollström, R., Yang, A., Chen, Q., Chen, G., Salminen, P., Bousfield, D., Toivakka, M. (2014) Comparison of nano- and microfibrillated cellulose films. *Cellulose* 21:3443-3456. <https://doi.org/10.1007/s10570-014-0357-5>
- Kumar, V., Pathak, P., Bhardwaj, N.K. (2021) Micro-nanofibrillated cellulose preparation from bleached softwood pulp using chemo-refining approach and its evaluation as strength enhancer for paper properties. *Applied Nanoscience* 11:101-115. <https://doi.org/10.1007/s13204-020-01575-9>
- Lago, C.R., Oliveira, A.L.M., Dias, M.C., Carvalho, E.E.N., Tonoli, G.H.D., Vilas Boas, E.V.B. (2020) Obtaining cellulosic nanofibrils from oat straw for biocomposite reinforcement: Mechanical and barrier properties. *Industrial Crops and Products* 148:112264. <https://doi.org/10.1016/j.indcrop.2020.112264>
- Li, W., Wang, S., Wang, W., Qin, C., Wu, M. (2019) Facile preparation of reactive hydrophobic cellulose nanofibril film for reducing water vapor permeability (WVP) in packaging applications. *Cellulose* 26:3271-3284. <https://doi.org/10.1007/s10570-019-02270-x>
- Li, Q., Wu, Y., Fang, R., Lei, C., Li, Y., Li, Y., Li, B., Pei, Y., Luo, X., Liu, S. (2021) Application of Nanocellulose as particle stabilizer in food Pickering emulsion: Scope, Merits and challenges. *Trends in Food Science & Technology* 110:573-583. <https://doi.org/10.1016/j.tifs.2021.02.027>
- Liang, C., Ruan, K., Zhang, Y., Gu, J. (2020) Multifunctional Flexible Electromagnetic Interference Shielding Silver Nanowires/Cellulose Films with Excellent Thermal Management and Joule Heating Performances. *ACS Applied Materials & Interfaces* 12:18023-18031. <https://dx.doi.org/10.1021/acsami.0c04482?ref=pdf>
- Malucelli, L.C., Matos, M., Jordão, C., Lomonaco, D., Lacerda, L.G., Carvalho Filho, M.A.S., Magalhães, W.L.E. (2019) Influence of cellulose chemical pretreatment on energy consumption and viscosity of produced cellulose nanofibers (CNF) and mechanical properties of nanopapers. *Cellulose* 26:1667-1681. <https://doi.org/10.1007/s10570-018-2161-0>
- Mascarenhas, A.R.P., Scatolino, M.V., Santos, A.A., Norcino, L.B., Duarte, P.J., Melo, R.R., Dias, M.C., Faria, C.E.T., Mendonça, M.C., Tonoli, G.H.D. (2022) Hydroxypropyl

- methylcellulose films reinforced with cellulose micro/nanofibrils: study of physical, optical, surface, barrier and mechanical properties Nordic Pulp & Paper Research Journal 1-16. <https://doi.org/10.1515/npprj-2022-0006>
- Martins, C.C.N., Dias, M.C., Mendonça, M.C., Durães, A.F.S., Silva, L.E., Félix, J.R., Damásio, R.A.P., Tonoli, G.H.D. (2021) Optimizing cellulose microfibrillation with NaOH pretreatments for unbleached *Eucalyptus* pulp. *Cellulose* 28:11519-11531. <https://doi.org/10.1007/s10570-021-04221-x>
- Melati, R.B., Shimizu, F.L., Oliveira, G., Pagnocca, F.C., Souza, W., Sant'Anna, C., Brienzo, M. (2019) Key Factors Affecting the Recalcitrance and Conversion Process of Biomass. *BioEnergy Research* 12:1-20. <https://doi.org/10.1007/s12155-018-9941-0>
- Moghaddam, M.K., Karimi, E. (2020) The effect of oxidative bleaching treatment on Yucca fiber for potential composite application. *Cellulose* 27:9383-9396. <https://doi.org/10.1007/s10570-020-03433-x>
- Mohammed, N., Grishkewich, N., Tam, K.C. (2018) Cellulose nanomaterials: promising sustainable nanomaterials for application in water/wastewater treatment processes. *Environmental Science: Nano*. 5:623-658. <https://doi.org/10.1039/C7EN01029J>
- Mohtaschemi, M., Dimic-Misic, K., Puisto, A., Korhonen, M., Maloney, T., Paltakari, J., Alava, M.J. (2014) Rheological characterization of fibrillated cellulose suspensions via bucket vane viscosimeter. *Cellulose* 21:1305-1312. <https://doi.org/10.1007/s10570-014-0235-1>
- Mokhena, T.C., John, M.J. (2020) Cellulose nanomaterials: new generation materials for solving global issues. *Cellulose* 27:1149-1194. <https://doi.org/10.1007/s10570-019-02889-w>
- Mokhena, T.C., Sadiku, E.R., Mochane, M.J., Ray, S.S., John, M.J., Mtibe, A. (2021) Mechanical properties of cellulose nanofibril papers and their bionanocomposites: A review. *Carbohydrate Polymers* 273:118507. <https://doi.org/10.1016/j.carbpol.2021.118507>
- Moraes, J.O., Scheibe, A.S., Sereno, A., Laurindo, J.B. (2013) Scale-up of the production of cassava starch based films using tape casting. *Journal of Food Engineering* 119:800-808. <https://doi.org/10.1016/j.jfoodeng.2013.07.009>
- Moser, C., Lindström, M.E., Henriksson, G. (2015) Toward Industrially Feasible Methods for Following the Process of Manufacturing Cellulose Nanofibers. *BioResources* 10:2360-2375. <https://doi.org/10.15376/biores.10.2.2360-2375>
- Nascimento, E.S., Barros, M.O., Cerqueira, M.A., Lima, H.L., Borges, M.F., Pastrana, L.M., Gama, F.M., Rosa, M.F., Azeredo, H.M.C., Gonçalves, C. (2021) All-cellulose nanocomposite films based on bacterial cellulose nanofibrils and nanocrystals. *Food Packaging and Shelf Life* 29:100715. <https://doi.org/10.1016/j.fpsl.2021.100715>

- Niu, X., Liu, Y., Fang, G., Huang, C., Rojas, O.J., Pan, H. (2018) Highly Transparent, Strong, and Flexible Films with Modified Cellulose Nanofiber Bearing UV Shielding Property. *Biomacromolecules* 19:4565-4575. <https://doi.org/10.1021/acs.biomac.8b01252>
- Noorbakhsh-Soltani, S.M., Zerafat, M.M., Sabbaghi, S. (2018) A comparative study of gelatin and starch-based nano-composite films modified by nano-cellulose and chitosan for food packaging applications. *Carbohydrate Polymers* 189:48-55. <https://doi.org/10.1016/j.carbpol.2018.02.012>
- Noremylia, M.B., Hassan, M.Z., Ismail, Z. (2022) Recent advancement in isolation, processing, characterization and applications of emerging nanocellulose: A review. *International Journal of Biological Macromolecules* 206:954-976. <https://doi.org/10.1016/j.ijbiomac.2022.03.064>
- Osong, S.H., Norgren, S., Engstrand, P. (2016) Processing of wood-based microfibrillated cellulose and nanofibrillated cellulose, and applications relating to papermaking: a review. *Cellulose* 23:23-123. <https://doi.org/10.1007/s10570-015-0798-5>
- Perrin, L., Gillet, G., Gressin, L., Desobry, S. (2020) Interest of pickering emulsions for sustainable micro/nanocellulose in food and cosmetic applications. *Polymers* 12: 2385. <https://doi.org/10.3390/polym12102385>
- Qaseem, M.F., Shaheen, H., Wu, A.M. (2021) Cell wall hemicellulose for sustainable industrial utilization. *Renewable and Sustainable Energy Reviews* 144:110996. <https://doi.org/10.1016/j.rser.2021.110996>
- Qu, J., Yuan, Z., Wang, C., Wang, A., Liu, X., Wei, B., Wen, Y. (2019) Enhancing the redispersibility of TEMPO-mediated oxidized cellulose nanofibrils in N,N-dimethylformamide by modification with cetyltrimethylammonium bromide. *Cellulose* 26:7769-7780. <https://doi.org/10.1007/s10570-019-02655-y>
- R CORE TEAM (2020). R: A language and environment for statistical computing. <https://www.R-project.org/>. Acessado 15 dez 2020.
- Raj, P., Varanasi, S., Batchelor, W., Garnier, G. (2015) Effect of cationic polyacrylamide on the processing and properties of nanocellulose films. *Journal of Colloid and Interface Science* 447:113-119. <https://doi.org/10.1016/j.jcis.2015.01.019>
- Rol, F., Banvillet, G., Meyer, V., Petit-Conil, M., Bras, J. (2018) Combination of twin-screw extruder and homogenizer to produce high-quality nanofibrillated cellulose with low energy consumption. *Journal of Material Science* 53:12604-12615. <https://doi.org/10.1007/s10853-018-2414-1>

- Rol, F., Belgacem, M.N., Gandini, A., Bras, J. (2019) Recent advances in surface-modified cellulose nanofibrils. *Progress in Polymer Science* 88:241-264. <https://doi.org/10.1016/j.progpolymsci.2018.09.002>
- Rueden, C.T., Schindelin, J., Hiner, M.C., DeZonia, B.E., Walter, A.E., Arena, E.T., Eliceiri, K.W. (2017). ImageJ2: ImageJ for the next generation of scientific image data. *BMC Bioinformatics* 18:529. <https://doi.org/10.1186/s12859-017-1934-z>
- Santucci, B.S., Bras, J., Belgacem, M.N., Curvelo, A.A.S., Pimenta, M.T.B. (2016) Evaluation of the effects of chemical composition and refining treatments on the properties of nanofibrillated cellulose films from sugarcane bagasse. *Industrial Crops and Products* 91:238-248. <https://doi.org/10.1016/j.indcrop.2016.07.017>
- Shimizu, M., Saito, T., Isogai, A. (2016) Water-resistant and high oxygen-barrier nanocellulose films with interfibrillar cross-linkages formed through multivalent metal ions. *Journal of Membrane Science* 500:1-7. <https://doi.org/10.1016/j.memsci.2015.11.002>
- Sothornvit, R., Hong, Si., An, D.J., Rhim, J.W. (2010) Effect of clay content on the physical and antimicrobial properties of whey protein isolate/organo-clay composite films. *LWT - Food Science and Technology* 43:279-284. <https://doi.org/10.1016/j.lwt.2009.08.010>
- Suhag, R., Kumar, N., Petkoska, A.T., Upadhyay, A. (2020) Film formation and deposition methods of edible coating on food products: A review. *Food Research International* 136:109582. <https://doi.org/10.1016/j.foodres.2020.109582>
- Sukmawan, R., Kusmono, Rahmanta, A.P., Saputri, L.H. (2022) The effect of repeated alkali pretreatments on the morphological characteristics of cellulose from oil palm empty fruit bunch fiber-reinforced epoxy adhesive composite. *International Journal of Adhesion and Adhesives* 114:103095. <https://doi.org/10.1016/j.ijadhadh.2022.103095>
- TAPPI Standard (2012) T 559 cm-12, Grease resistance test for paper and paperboard.
- TAPPI Standard (2013) T 410 om-08, Grammage of paper and paperboard.
- TAPPI Standard (2015) T 411 om-15, Thickness of paper, paperboard, and combined board.
- TAPPI Standard (2021a) T 249 cm-21, Carbohydrate composition of extractive-free wood and wood pulp by gas-liquid chromatography.
- TAPPI Standard (2021b) T 222 om-21, Acid-soluble lignin in wood and pulp.
- TAPPI Standard (2021c) T 402 sp-21, Standard conditioning and testing atmospheres for paper, board, pulp handsheets, and related products.
- Tayeb, A.H., Amini, E., Ghasemi, S., Tajvidi, M. (2018) Cellulose Nanomaterials – Binding Properties and Applications: A Review. *Molecules* 23: 2684. <http://dx.doi.org/10.3390/molecules23102684>

- Teodoro, K.B.R., Sanfelice, R.C., Migliorini, F.L., Pavinatto, A., Facure, M.H.M., Correa, D.S. (2021) A Review on the Role and Performance of Cellulose Nanomaterials in Sensors. *ACS Sensors* 6:2473-2496. <https://doi.org/10.1021/acssensors.1c00473>
- Trovagunta, R., Kelley, S.S., Lavoine, N. (2021) Highlights on the mechanical pre-refining step in the production of wood cellulose nanofibrils. *Cellulose* 28:11329-11344. <https://doi.org/10.1007/s10570-021-04226-6>
- Turpeinen, T., Jäsberg, A., Haavisto, S., Liukkonen, J., Salmela, J., Koponen, A.I. (2020) Pipe rheology of microfibrillated cellulose suspensions. *Cellulose* 27:141-156. <https://doi.org/10.1007/s10570-019-02784-4>
- Tyagi, P., Hubbe, M.A., Lucia, L., Pal, L. (2018) High performance nanocellulose-based composite coatings for oil and grease resistance. *Cellulose* 25:3377-3391. <https://doi.org/10.1007/s10570-018-1810-7>
- Wang, Q., Zhu, J.Y., Considine, J.M. (2013) Strong and Optically Transparent Films Prepared Using Cellulosic Solid Residue Recovered from Cellulose Nanocrystals Production Waste Stream. *ACS Applied Materials & Interfaces* 5:7. <https://doi.org/10.1021/am302967m>
- Wang, J., Gardner, D.J., Stark, N.M., Bousfield, D.W., Tajvidi, M., Cai, Z. (2018) Moisture and Oxygen Barrier Properties of Cellulose Nanomaterial-Based Films. *ACS Sustainable Chemistry & Engineering* 6:46-70. <https://doi.org/10.1021/acssuschemeng.7b03523>
- Wang, L., Chen, C., Wang, J., Gardner, D.J., Tajvidi, M. (2020) Cellulose nanofibrils versus cellulose nanocrystals: Comparison of performance in flexible multilayer films for packaging applications. *Food Packaging and Shelf Life* 23:100464. <https://doi.org/10.1016/j.fpsl.2020.100464>
- Wu, C., McClements, D.V., He, M., Zheng, L., Tian, T., Teng, F., Li, Y. (2021) Preparation and characterization of okara nanocellulose fabricated using sonication or high-pressure homogenization treatments. *Carbohydrate Polymers* 255:117364. <https://doi.org/10.1016/j.carbpol.2020.117364>
- Yang, X., Berthold, F., Berglund, L.A. (2019) High-Density Molded Cellulose Fibers and Transparent Biocomposites Based on Oriented Holocellulose. *ACS Applied Materials & Interfaces* 11:10310-10319. <http://dx.doi.org/10.1021/acsami.8b22134>
- Verker, R., Grossman, E., Eliaz, N. (2009) Erosion of POSS-polyimide films under hypervelocity impact and atomic oxygen: The role of mechanical properties at elevated temperatures. *Acta Materialia* 57:1112-1119. <https://doi.org/doi:10.1016/j.actamat.2008.10.054>

- Xinping L., Nan, W., Xin, Z., Hui, C., Yaoyu, W., Zhao, Z. (2020) Optical haze regulation of cellulose nanopaper via morphological tailoring and nano-hybridization of cellulose nanoparticles. *Cellulose* 27:1315-1326. <https://doi.org/10.1007/s10570-019-02876-1>
- Yang, W., Jiao, L., Liu, W., Dai, H. (2019) Manufacture of Highly Transparent and Hazy Cellulose Nanofibril Films via Coating TEMPO-Oxidized Wood Fibers. *Nanomaterials* 9:107. <https://doi.org/10.3390/nano9010107>
- Yook, S., Park, H., Park, H., Lee, S.Y., Kwon, J., Youn, H.J. (2020) Barrier coatings with various types of cellulose nanofibrils and their barrier properties. *Cellulose* 27: 4509-4523. <https://doi.org/10.1007/s10570-020-03061-5>
- Žepič, V., Fabjan, E.S., Kasunic, M., Korosec, M., Hancic, A., Oven, P., Perse, L.S., Polijansek, I. (2014) Morphological, thermal, and structural aspects of dried and redispersed nanofibrillated cellulose (NFC). *Holzforschung* 68:657-667. <https://doi.org/10.1515/hf-2013-0132>
- Zhang, B.X., Azuma, J.I., Uyama, H. (2015) Preparation and characterization of a transparent amorphous cellulose film. *RSC Advances* 4:2900. <https://doi.org/10.1039/C4RA14090G>
- Zhang, W., Zhang, Y., Cao, J., Jiang, W. (2021) Improving the performance of edible food packaging films by using nanocellulose as an additive. *International Journal of Biological Macromolecules* 166:288-296. <https://doi.org/10.1016/j.ijbiomac.2020.10.185>
- Zhou, X., Li, W., Mabon, R., Broadbelt, L.J. (2016) A critical review on hemicellulose pyrolysis. *Energy Technology* 5:52-79. <https://doi.org/10.1002/ente.201600327>

**ARTIGO 3 – ASSOCIATION OF CELLULOSE MICRO/NANOFIBRILS AND
SILICATES FOR CARDBOARD COATING: TECHNOLOGICAL ASPECTS FOR
PACKAGING**

Artigo publicado no periódico Industrial Crops and Products

DOI: [10.1016/j.indcrop.2022.115667](https://doi.org/10.1016/j.indcrop.2022.115667)

**Association of cellulose micro/nanofibrils and silicates for cardboard coating:
Technological aspects for packaging**

Adriano Reis Prazeres Mascarenhas¹, Mário Vanoli Scatolino^{2,5}, Matheus Cordazzo Dias³,
Maria Alice Martins⁴, Rafael Rodolfo de Melo⁵, Maressa Carvalho Mendonça³, Gustavo
Henrique Denzin Tonoli³

¹Department of Forest Engineering, Federal University of Rondônia (UNIR), 76940-000, Rolim de Moura, RO, Brazil.

²Department of Production Engineering, State University of Amapá (UEAP), 68900-070, Macapá, AP, Brazil.

³Department of Forest Science, Federal University of Lavras (UFLA), C.P. 3037, 37200-900, Lavras, MG, Brazil.

⁴Embrapa Instrumentation – National Laboratory of Nanotechnology for Agribusiness, 13561-206, São Carlos, SP, Brazil.

⁵Agricultural Sciences Center, Federal University of the Semi-arid (UFERSA), 59625-900, Mossoró, RN, Brazil.

ABSTRACT

Paper coating with cellulose micro/nanofibrils (MFC/NFC) can improve the performance of paper packaging. However, the process cost is high due to the significant energy consumption. The objective of this work was to produce MFC/NFC with pre-treated fibers using calcium silicate ($\text{Ca}_2\text{O}_4\text{Si}$) and magnesium silicate (MgO_3Si) and evaluate their performance as a coating on cardboard. For the production of MFC/NFC, pre-treatments with $\text{Ca}_2\text{O}_4\text{Si}$ and MgO_3Si reduced energy consumption by ~30%. The layers added to the cardboard reduced the water vapor permeability, mainly for the coating with 5% MgO_3Si (~98 g mm/kPa-1day m²). These characteristics indicate that coated paperboard is suitable for packaging bread, cheese, fruit, and vegetables. Suspensions with 5% and 10% $\text{Ca}_2\text{O}_4\text{Si}$ increased the spread of PVAc, PVOH, and printing ink. The coatings reduced the strength and stiffness of the papers by ~50% compared to the uncoated paper due to the wetting and drying cycles. On the other hand, there was an increase in ductility, which potentiated the paper's formability. Optimizing application and drying techniques for MFC/NFC and silicate coating formulations can improve the mechanical and barrier properties of the coated papers for multilayer packaging.

Keywords: Biopolymers, multilayer packaging, barrier properties, surface energy, tensile strength, paper formability.

1. Introduction

To ensure that packaging shows suitable properties to preserve the characteristics of the products, the industry combines paper with metals and petroleum-based polymers (Otto et al., 2021). However, these materials have considerable degradation time, and their accumulation in the environment risks human health and the life cycle in aquatic and terrestrial ecosystems (Mascarenhas et al., 2022a). It is estimated that around 30% of the packages produced are single-use, mainly composed of non-biodegradable materials (Miller, 2020; Dey et al., 2021). Due to this, biopolymers have been extensively researched in renewable packaging production. Cellulose micro/nanofibrils (MFC/NFC) stand out in this context because they are renewable and have technological advantages. It can be used in packaging paper coatings, such as high contact surface, biodegradability, high tensile strength, and the possibility of obtaining films/composites with a barrier to gases and fats (Mirmehdi et al., 2018a; Yu et al., 2019; Lu et al., 2022).

On the other hand, obtaining MFC/NFC demands high energy consumption to deconstruct the cell wall, therefore chemical or enzymatic pre-treatments are applied to the cellulosic pulp to facilitate the mechanical fibrillation process and obtain more individualized MFC/NFC (Cruz et al., 2022). One of the best-known pretreatments with high efficiency to facilitate fiber deconstruction is 2,2,6,6-tetramethylpiperidine-1-oxyl (TEMPO)-mediated oxidation, but the reagent cost is very high and can generate non-eco-friendly compounds, making it necessary to implement means of effluent recovery and treatment (Rol et al., 2019; Chen et al., 2022a).

This demonstrates the need for the development of new types of pretreatments that can provide individualization of NFC, lower energy consumption, and lower costs. Khadraoui et al. (2022) studied the production of NFC from marine lignocellulosic biomass and observed that combination of steam explosion and twin-screw extrusion associated with pretreatment with NaOH at concentrations of 10 or 20% (w/w) allowed to obtain NFC with lower lignin contents and interesting characteristics for papermaking and biocomposites. Mnasri et al. (2022) employed different deep eutectic solvents for refining *Eucalyptus* and cotton fibers and observed modifications in crystallinity and xylan content. This resulted in increased water retention in the fibers and enhanced internal and external fibrillation of the cell wall. These

authors also observed that the fibers obtained allowed the production of papers with superior mechanical properties, due to the increased amount of bonds and maintenance of fiber length.

Another option to reduce reagent costs is the use of alkaline treatments with NaOH or KOH, these reagents can be used because they can increase fiber swelling and reduce shear forces against the cell wall during fibrillation in ultra-refiners (Ang et al., 2019; Scatolino et al., 2022). Dias et al. (2019) produced NFC from *Eucalyptus* and *Pinus* fibers in ultra-refiners and found that the use of NaOH solutions at concentration of 5% (w/w) under the temperature of 80 °C provided energy consumption reduction of around 40-60%. Moreover, for *Eucalyptus* and *Pinus* fibers, Mascarenhas et al. (2022b) used alkaline solutions of sodium silicate (Na_2SiO_3) at concentrations of 5 and 10% (w/w) and observed improvements in the individualization of MFC/NFC and reduction of energy consumption during mechanical fibrillation in the order of ~50% compared to untreated fibers.

The pretreatments can also be used to modify the cellulose surface, aiming to change the physical, chemical, optical, mechanical, and surface properties of MFC/NFC to broaden their range of applications (Rol et al., 2019). The modification of MFC/NFC for the production or coating of packaging papers has been addressed in many research. This is justified due to the improvements that the MFC/NFC provide in physical, mechanical, and barrier properties to water vapor, gases, and grease (Jin et al., 2021; Morais et al. 2021). To achieve these results, polymers and mineral additives can be added to MFC/NFCs, such as latexes, silanes, and nanoclays (Adibi et al. 2022; Oliveira et al., 2022; Saedi et al., 2021a).

The use of calcium silicate ($\text{Ca}_2\text{O}_4\text{Si}$) and magnesium silicate (MgO_3Si) solutions can be considered for this purpose, as they have a high pH (10~13) and can facilitate swelling, and promote swelling of the fiber cell wall, enhancing mechanical fibrillation. Research reports that these silicates have a high affinity for cellulose, which indicates the possibility of obtaining modified MFC/NFC (Liu et al., 2019; Zhang et al., 2018a). However, no research has been found exploring the possibility of using these silicates as pre-treatments for the production of MFC/NFC aiming at their application in paper coatings for packaging production.

In addition, these silicates allow pulp pretreatments to be performed by one-step *in situ* methods, which may increase the interaction between silicates and pulp, since as MFC/NFC are extracted, silicates are already present around them. However, the few researches exploring this approach are focused only on fiber modification and not as a pretreatment for MFC/NFC production (Li et al., 2010; Li et al., 2018; An et al., 2021). Regarding this gap in scientific knowledge, the objective of the present work was to produce MFC/NFC from fibers pre-treated with calcium silicate and magnesium silicate and to evaluate its performance as a cardboard

coating regarding microstructure, water absorption, and surface properties concerning water, adhesives and printing ink, barrier and mechanical properties.

2. Material and methods

2.1. Pre-treatment of the fibers

Bleached commercial Kraft pulp from *Eucalyptus* sp. (EUC), containing $79 \pm 0.3\%$ of cellulose, $16 \pm 0.1\%$ of hemicelluloses, and $0.4 \pm 0.1\%$ of lignin was used in the study. The pulp was pre-treated with calcium silicate ($\text{Ca}_2\text{O}_4\text{Si}$), composed of 25% CaO and 75% SiO_2 . A pre-treatment with magnesium silicate (MgO_3Si) was also carried out, composed of 64% of SiO_2 and 32% of MgO. The silicates were provided by Dinâmica Química LTDA (São Paulo, Brazil). The calcium and magnesium silicate solutions were prepared with deionized water at concentrations of 5 and 10% (w/w). The EUC fibers were added to the solutions for the obtainment of suspensions with a concentration of 2.5% (w/w). The suspensions were kept at a temperature of 80 ± 2 °C and constant stirring at 600 rpm for 2 h (Dias et al., 2019). Posteriorly, the treated pulps were washed in deionized water until reaching pH 7, in order to stop the reaction and avoid excessive fiber degradation. As a control, suspensions were produced with untreated EUC fibers in deionized water in a proportion of 2.5%.

2.2. Production of the MFC/NFC

Pulps suspensions with and without pre-treatments were adjusted to concentrations of 2% (w/w). The material was stirred for 15 min at 600 rpm to ensure dissociation and fiber swelling. The fibers were processed using a Masuko Sangyo MKGA-80 Supermasscolloider grinder (Kawaguchi, Japan) equipped with a rotating and static stone disc. The suspension was processed with five passes through the equipment at 1500 rpm (Mendonça et al., 2022). The distance between the stones was gradually modulated from 10 μm to 100 μm as the suspension viscosity increased.

In addition to the general suspension characteristics, to give a clear idea about the proportional amount of added additive mineral compound (Ca_2SiO_4 and or MgO_3Si), the authors performed the incineration of the MFC/NFC in a muffle furnace at 525 °C and calculated the residual silicate contents by discounting the average ash content of the untreated samples (Table 1). This characterization was performed using five repetitions employing the TAPPI T 211 om-02 (TAPPI, 2022) standard.

Table 1 Parameters of MFC/NFC suspensions produced for cardboard coating.

Formulation	Viscosity (cP)	pH	MFC/NFC content (%)	Silicate content (%)	Solids content (%)
Control	7323 ± 173*	7.2 ± 0.2	1.40 ± 0.05	ND**	1.40 ± 0.05
Ca ₂ O ₄ Si 5%	2853 ± 61	7.8 ± 0.2	1.20 ± 0.30	1.64 ± 0.40	2.85 ± 0.07
Ca ₂ O ₄ Si 10%	4909 ± 142	7.0 ± 0.4	1.05 ± 0.08	2.99 ± 0.12	4.00 ± 0.20
MgO ₃ Si 5%	2606 ± 50	7.7 ± 0.5	1.30 ± 0.04	1.47 ± 0.06	2.77 ± 0.10
MgO ₃ Si 10%	3166 ± 152	7.1 ± 0.2	1.14 ± 0.06	2.30 ± 0.09	3.50 ± 0.15

* Standard deviation; ** non-detected

The energy consumption was evaluated during the fibrillation process by considering the average electric current of each passage, the equipment voltage, the fibrillation time, and the initial mass of the untreated and pretreated pulps. The energy consumption was calculated for the passage in which the suspension presented gel consistency, according to Eq. 1

$$EC (kWh/t) = \frac{(P \times t)}{m} \quad (1)$$

Where P (voltage × electrical current) is the equipment potency (kW); t is the time spent for fibrillation (h); and m is the mass of pulp subjected to fibrillation (t).

2.3. Cardboard coating with MFC/NFC

Before applying the coatings, the suspension concentrations were adjusted to approximately 1.0% (w/w), according to the solids content of MFC/NFC. A duplex commercial cardboard was used with a thickness of 0.48 ± 0.02 mm, a grammage of ~ 300 g/m², and dimensions of 297×210 mm. In order to obtain homogeneous coatings comparable to other work in the literature, four layers of the coating were applied to add a grammage of 12 ± 2 g/m² to the cardboard. A laboratory coating machine equipped with cylindrical bars with grooves for spreading the liquid was used to apply the suspensions to the paper surface at a 7 m/min speed. Three coats were applied with the grooved bar spaced at 0.5 mm, being the last layer applied with the bar without grooves. For each layer added, the paper was subjected to drying in an oven at 105 ± 2 °C for 10 min (Figure 1).

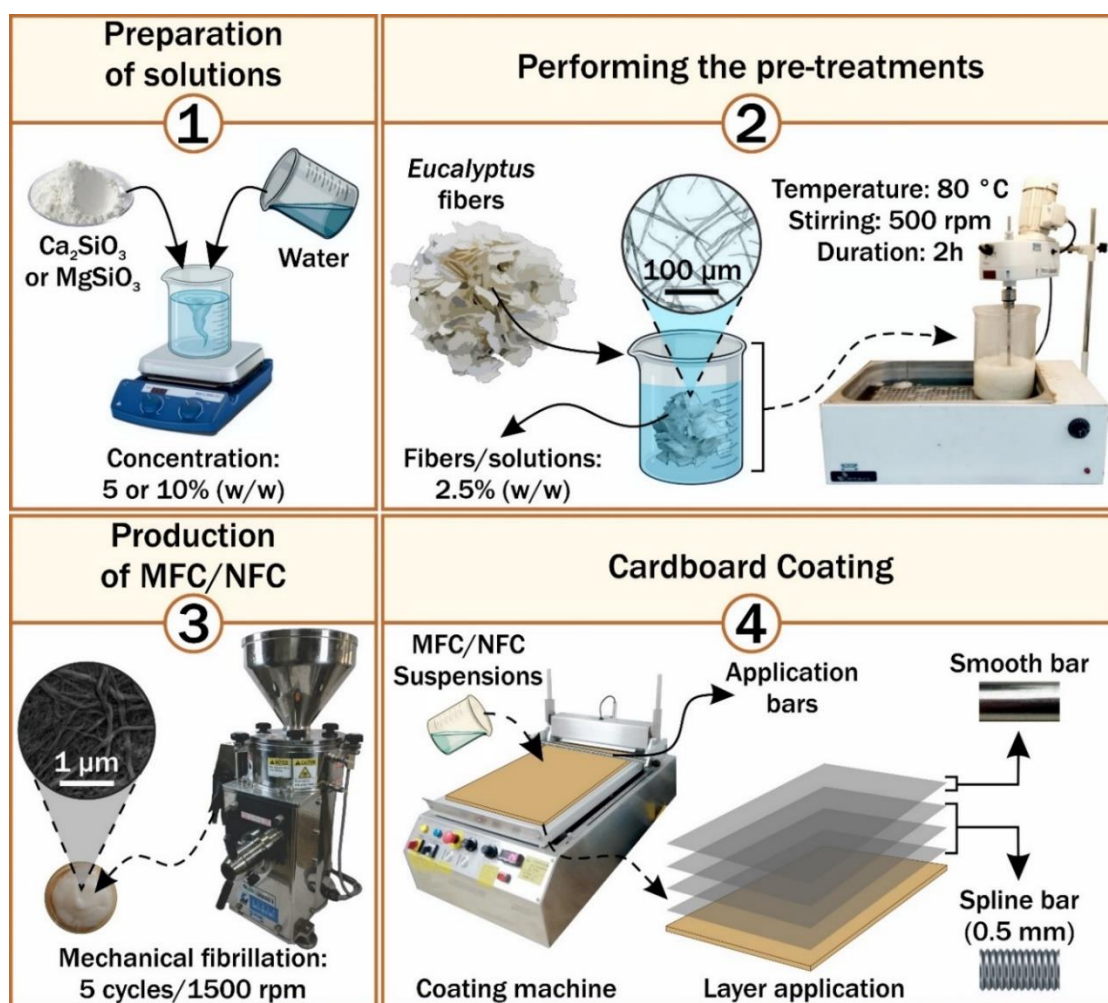


Fig. 1. Scheme of pre-treatments with calcium silicate and magnesium silicate on the EUC fibers; production of MFC/NFC, and cardboard coating.

Cardboard coated only with MFC/NFC without silicates, and uncoated papers were also evaluated. For evaluating the effect of wetting, the cardboards were wetted in a coating machine and subjected to drying, as well as performed for papers coated with several formulations (Figure 2). For each treatment, five samples were evaluated.

Table 2 Characteristics of the coated cardboard with different formulations.

Types of coating	Coating thickness (μm)	Grammage (g/m^2)	Identification
Control paper (uncoated)	-	301 ± 1.5	<i>CP</i>
Wet control paper	-	302 ± 2.5	<i>WCP</i>
MFC/NFC	38.0 ± 3.0	313 ± 1.5	<i>MFC/NFC</i>
MFC/NFC pre-treated with $\text{Ca}_2\text{O}_4\text{Si}$ 5%	40.0 ± 3.6	312 ± 2.2	<i>CS 5%</i>
MFC/NFC pre-treated with $\text{Ca}_2\text{O}_4\text{Si}$ 10%	39.0 ± 4.3	311 ± 2.0	<i>CS 10%</i>
MFC/NFC pre-treated with MgO_3Si 5%	40.8 ± 1.8	311 ± 2.6	<i>MS 5%</i>
MFC/NFC pre-treated with MgO_3Si 10%	38.0 ± 3.3	312 ± 1.4	<i>MS 10%</i>

* Standard deviation

2.4. Characterization of the fibers

2.4.1. Fourier transform infrared spectroscopy

Infrared vibrational spectroscopy analyses were performed on the pulps pre-treated with silicate and untreated pulps. A Varian 600-IR FTIR spectrometer with Fourier transform (FTIR) was used coupled with a GladiATR accessory from Pike Technologies (Santa Clara, USA). The measurements were done by attenuated total reflectance (ATR), at 45° with zinc selenide crystal. The spectral range was analyzed at 400 to 4000 cm⁻¹, resolution of 2 cm⁻¹, and 32 scans.

2.4.2. Water retention index

The water retention index (WRI) was determined based on the Scan C 62:00 standard (SCAN, 2000). Suspensions containing 0.5% (w/w) of treated and untreated fibers were prepared. Subsequently, the water from the suspension was drained in a Thermo Fisher Scientific Heraeus Megafuge 16R centrifuge (Waltham, USA), and adjusted to a force of 3000 G for 15 min. The fibers retained on the sieve were weighed and subjected to drying at a temperature of 100 ± 2 °C until a constant mass. This assay was performed with four repetitions for each pretreatment and the WRI was calculated according to Eq. 2.

$$WRI (g/g) = \left(\frac{M_1}{M_2} \right) - 1 \quad (2)$$

Where M₁ and M₂ are the masses after draining in a centrifuge and after drying, respectively.

2.5. Characterization of the MFC/NFC suspensions

2.5.1. Microstructural analysis of MFC/NFC

For analysis of the particles in the suspensions after the fibrillation process, images were obtained by an Olympus BX41 light microscope (Tokyo, Japan). The MFC/NFC suspensions were diluted in deionized water to a concentration of 0.10% (w/w). Drops of MFC/NFC suspensions were added to glass slides, which were covered with a coverslip for observation using an objective of 10x at a range of 1280 x 1024 pixels.

In addition, samples of the suspensions at a concentration of 0.001% (w/w) MFC/NFC were sonicated at 150 Hz for 2 min (Silva et al., 2020). Subsequently, small aliquots were added to the double-sided carbon tape adhered to the aluminum sample holder (stubs). After an overnight period in a desiccator with silica gel, the samples were gold metalized in a sputtering device (SCD 050). The morphology of the MFC/NFC was observed on an ultra-high resolution (UHR) field emission scanning electron microscope (SEM/FEG) TESCAN CLARA (Libušina,

Czech Republic) using 10 KeV, 90 pA and 10 mm working distance. MFC/NFC diameters were measured for at least 200 individual structures using ImageJ software (Rueden et al., 2017).

2.5.2. Stability and zeta potential of the suspensions

The suspension stability test was conducted according to the methodology presented in Guimarães Júnior et al. (2015). MFC/NFC suspensions (10 mL) with a concentration of 0.25% (w/w) were previously homogenized in a magnetic stirrer at 500 rpm for 1 h and poured into tubes. For each pre-treatment, five samples of the suspensions were photographed every 1 h for a total period of 8 h. The software ImageJ (Rueden et al., 2017) was used to measure the total height of the liquid and the height of the suspended MFC/NFC of each image. The stability was calculated according to Eq. 3.

$$\text{Stability (\%)} = \left(\frac{S}{T}\right) \times 100 \quad (3)$$

Where S corresponds to the height of the suspended particles in the tube, and T corresponds to the total height of the liquid present in the tube.

The zeta potential (ζ) was determined in order to evaluate the effect of pre-treatments on the electrostatic stability of MFC/NFC suspensions. The Nano-ZS90X Malvern Zetasizer equipment (England, United Kingdom) was turned on for 30 min, for calibration, before the measurements. The readings were performed at a temperature of 25 °C, using 1 mL of each coating formulation with a concentration of 0.1% (w/w). Five measurements were performed for each treatment (Zhang et al., 2018a).

2.5.3 X-ray diffraction (XRD) of MFC/NFC

X-ray diffraction (XRD) was performed to verify possible changes in the crystalline structure of the cellulose after the pre-treatments were performed. Spectra were acquired from intact films produced from MFC/CNF by the “casting” method. The analyses were performed using an x-ray diffractometer Shimadzu Corporation XRD 6000 (Kyoto, Japan), adjusted with Cu K α radiation (1.1540 Å) at 30 kV and 30 mA. Scattered rays were collected in the range of $2\theta = 10\text{-}40^\circ$, a rate of $2^\circ/\text{min}$ (Tonoli et al. 2021). Curve noises were removed by the adjacent average method, with 10 points per window, producing smoothed patterns without compromising peak information.

2.6. Characterization of the coated papers

2.6.1. Microstructural analysis of the papers

Samples with 5 x 5 mm of the coated and uncoated papers were submerged in liquid nitrogen for flash freezing, fractured with a scalpel, and fixed on sample holders (stubs) containing double-sided carbon adhesive tapes. Subsequently, the material was subjected to metallic coating in a gold evaporator (SCD 050) and analyzed in a scanning electron microscope with field emission (SEM/FEG) TESCAN CLARA (Libušina, Czech Republic), with ultra-high resolution (UHR), under conditions of 10 KeV, 90 pA, and a working distance of 10 mm. Micrographs of the fracture and the top of the cardboard samples were obtained. The energy dispersive spectroscopy (EDS) analysis was performed to evaluate the penetration of the coatings in the cardboard. The X-Flash6-60 Bruker X-ray detector (Billerica, USA) from the SEM/FEG was calibrated for the element analysis condition. The SEM with EDS with 500x magnification allowed the obtainment of energy spectra of the elements along with the fracture profile (line scan mode). The elements distribution (mapping function) along the samples was studied with a working distance close to 10 mm, Kcps value greater than 30 units, voltage at 20 KeV, and Bean Current around 5 nA.

2.6.2. Contact angle, wettability, and free surface energy

The contact angle and wettability of the cardboards were evaluated according to the TAPPI T 458 cm-14 (TAPPI, 2014). The measurements of the contact angle were performed using a Krüss DSA30 goniometer (Hamburg, Germany). Ten samples with dimensions of 10 × 50 mm were cut, which were fixed on a glass slide. For evaluation, 15 μL of deionized water was dripped on the papers to calculate the average contact angle between the water drop and the surface after 1 s. The wettability of the papers was calculated with the average values of the contact angles measured between 5 and 55 s, according to Eq. 4.

$$Wettability (\text{°/s}) = \frac{(A - a)}{55} \quad (4)$$

Where A is the average contact angle after 5 s (°) and a is the average contact angle after 60 s (°).

To verify the ability to spread adhesives on the surface of coated cardboards, the test was also conducted using polyvinyl acetate - PVAc for industrial use. To evaluate the coated papers as a spreading agent for other industrial coatings, the contact angle and wettability were

evaluated for polyvinyl alcohol (PVOH) diluted in deionized water at a concentration of 5% (w/w) with the agitation of 300 rpm at 90 °C, produced by Kuraray America Inc. (Texas, USA). The spread of ink on the cardboard surface was also evaluated, using the T504 printing ink produced by Epson Brazil Ind. LTDA (São Paulo, Brazil). These tests were performed using 20 samples and adapting some procedures from ASTM D7490-13 (ASTM, 2022). The surface free energy was obtained according to the methodologies presented by Tonoli et al. (2009) and Arantes et al. (2019) using the same goniometer abovementioned. The liquids used for the test are shown in Table 3.

Table 3 Characteristics of liquids used for surface free energy test.

Test liquids	Superficial tension (mJ/m ²)		
	Dispersive	Polar	Total
1-Bromo-2-naphthalene	44.6	0	44.6
Ethylene glycol	29.0	19.0	48.0
Di-iodomethane	48.5	2.3	50.8
Glycerol	37.0	26.4	63.4
Water	21.8	51.0	72.8

2.6.3. Water absorption (Cobb test)

The water absorption test (Cobb Test) was performed according to ASTM D3285-93 (ASTM, 2005). Five samples with dimensions 125 × 125 mm were cut and kept in a desiccator with silica for 72 h at room temperature (25 ± 2 °C), and weighed. The papers were fixed in a Cobb Tester TKB Instruments (São Paulo, Brazil) and 100 mL of deionized water was poured into the equipment ring that delimits a certain area of the paper surface, for 2 min. The excess water was removed from the paper surface. The paper was placed between two sheets of blotting paper and pressed with a cylindrical roller. Finally, the papers were weighed again to calculate the water absorption by Eq. 5.

$$Cobb (g/m^2) = (M_i - M_f) \times 100 \quad (5)$$

Where M_i and M_f are the mass (g) of the paper, before and after the contact with water, respectively.

2.6.4. Water vapor permeability

For each treatment, five circular samples with a diameter of 16 mm were prepared. The samples were stored in an air-conditioned room with a temperature of 25 °C and relative humidity of 65% for 3 days, according to ASTM E96-16 (ASTM, 2016a). The samples were

placed in glass capsules partially filled with silica previously dried at 105 °C, which were placed in desiccators containing a saturated solution of KCl at 38 °C to obtain an atmosphere with a relative humidity of 90%, according to ASTM E104-02 (ASTM, 2012). The capsules with the papers and silica were weighed on an analytical balance for 8 days. The water vapor transmission rate (WVTR) and water vapor permeability (WVP) were calculated using Eq. 6 and Eq. 7.

$$WVTR (g/m^2 day) = \frac{w}{t \times A} \quad (6)$$

$$WVP (g mm/kPa^{-1} day m^2) = \frac{(WVTR \times e)}{(p \times UR_f - UR_d)} \quad (7)$$

Where w is the mass of the capsule with sample (g); t is the time (days); A is the exposed area of the sample (m²); e is the sample thickness (mm); p is the water vapor pressure (kPa) and UR_f - UR_d is the difference between the humidity outside and inside the capsule at 38 °C.

2.6.5. Mechanical characterization of the papers

The mechanical tests were performed with an adaptation of the ASTM D 828-16e1 (ASTM, 2016b). The Stable Micro Systems TATX2i texturometer (Godalming, United Kingdom) equipped with a 500 N load cell was used to determine the strength, Young's modulus, and elongation at break in the tensile test. Ten specimens with dimensions of 10 x 100 mm were tested with an initial distance of 50 mm between the grips and a test speed of 0.8 mm/s.

2.7. Statistical analysis

Data were analyzed using graphic analysis (FTIR and XRD) and descriptive statistics, sketching column graphs with the averages and standard deviation for each property.

3. Results and discussion

3.1. FTIR and WRI

From the spectral curves of the pre-treated pulps, it was possible to observe the presence of bands referring to the functional silicate groups, even after washing and stabilization of the pH. For CS 5% and CS 10%, there was a significant reduction in the vibration bands of C-H and -OH cellulose groups (Figure 2), situated around 2890 and 3350 cm^{-1} (Lopes et al., 2018), indicating a strong interaction of the calcium silicate with the fibers. This behavior was also observed by Li et al. (2010) when studying the synthesis of cellulose and calcium silicate composites using ethanol in their solubilization.

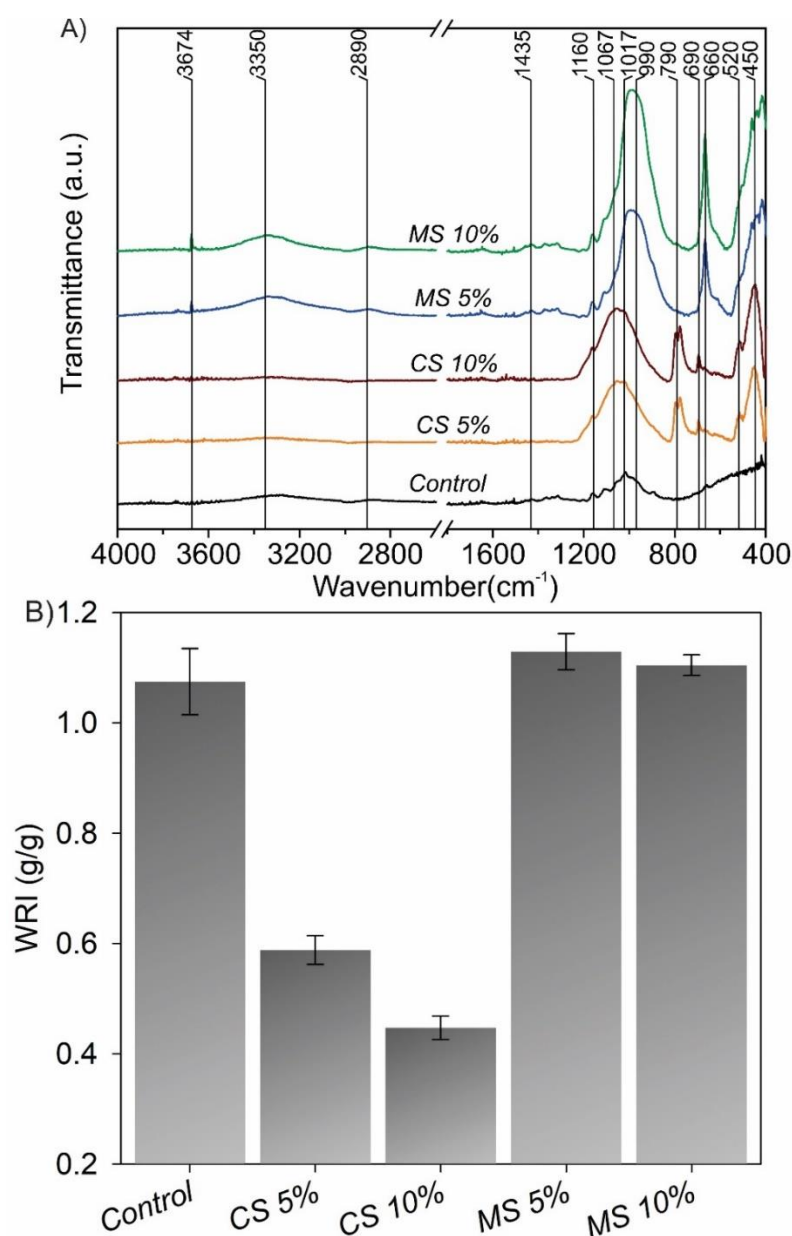


Fig. 2. A) Typical FTIR spectra and B) WRI for untreated and pre-treated fibers with silicates.

To obtain similar results, Li et al. (2018) used hydrochloric acid to facilitate solubilization and exposure of calcium silicate fillers to enhance its interaction with cellulose. From the point of view of industrial scaling, these results highlight the advantages of the process carried out in the present work, because it was not necessary to use additional reagents to increase the impregnation of calcium silicate to cellulose, making the fibers pre-treatment cheaper and more eco-friendly. Another evidence that shows the modification of the fibers pre-treated with calcium silicate is the absorption range between 448 and 457 cm^{-1} , which corresponds to the angular vibration of SiO_4 , and tetrahedral Si-O-Si (Ray et al., 2018; Rotermel et al., 2021). Peaks observed in the range from 980 to 990 cm^{-1} correspond to the stretching of the Si-O, Si-O-Ca, and O-Si-O vibrational modes (Puertas et al., 2004; Li et al., 2010). The increase in peak intensity in the bands 690 and 790 cm^{-1} correspond to the absorptions of Si-O-Si and SiO bonds, respectively (Al-Oweini e El-Rassy, 2009, Gupta et al., 2019).

Fiber modification was also observed when using magnesium silicate, which can be occurred due to the increase in intensity in the band of 473 cm^{-1} and in the absorption bands situated between 540 and 660 cm^{-1} , which correspond to the stretching of the vibrational mode of Mg-O (Selvam et al., 2011; Jeevanandam et al., 2013). An increase in absorption intensity was also observed between the bands of 1420 and 1481 cm^{-1} , corresponding to Mg-OH (Hofmeister and Bowey, 2006). Another point that indicates the fiber modification with magnesium silicate is the peak located around 3674 cm^{-1} , attributed to the -OH group of magnesium ions, located in the octahedral sheets of the mineral (Frost and Mendelovici, 2006). Regarding the peaks referring to the angular vibration of the C-O and C-O-C cellulose bonds (1017 cm^{-1} ~ 1160 cm^{-1}) (Foster et al., 2018; Khan et al., 2020), they were not clearly identified in the fibers pre-treated with magnesium silicate. This occurred because there was an increase in the peak intensity located at 1088, 801, and 456 cm^{-1} , which are attributed to asymmetric stretching, symmetrical stretching, and vibration bending of the Si-O-Si bonds, respectively (Zhu et al., 2017). Another possibility that explains the absence of peaks for C-O, is also related to the overlapping of the asymmetric vibration of O-Si-O located around 1097 cm^{-1} (Jia et al., 2011). The behavior was also observed for fibers pre-treated with calcium silicate. It was also observed in the pre-treated fibers, the suppression of the peak intensity situated between 810 and 896 cm^{-1} . This spectral region corresponds to the angular vibration of the C-OH groups of the β -glycosidic bonds that bind hemicelluloses to cellulose (Ikramullah et al., 2017; Özgenç et al., 2017). The changes can directly influence the surface loads of the cellulose, which affect the interaction with water and physical and colloidal properties.

The greatest reductions in water retention index (WRI) were observed for the fibers pre-treated with calcium silicate. The WRI of the *CS 5%* and *CS 10%* were, respectively, 45% and 58% lower compared to the control (~1.1 g/g) (see Figure 2B). These reductions can be explained by the interaction of the silicate with the -OH cellulose groups. Chen et al. (2019) and Meija-Ballesteros et al. (2021) explained that this effect increases the velocity of capillary water flow out of the cell walls due to the reduction in the number of hydrogen bonds between water and cellulose, reducing the fiber WRI. The fibers pre-treated with magnesium silicate presented a slight increase in the WRI. For *MS 5%*, the increase concerning the control was around 5% and ~2.8% for *MS 10%*. The increase in the WRI occurred due to the Mg-OH groups of the magnesium silicate and little influence on the reduction of the intensity for the -OH cellulose groups. Huan et al. (2018) observed that the addition of magnesium silicate to composites reinforced with carbon sheets resulted in increased porosity and water adsorption capacity.

Even so, the WRI values are in agreement with what has been observed in other works in the literature. Mnasri et al. (2022) verified in *Eucalyptus* fibers WRI values ranging between 1 and 1.35 g/g after application of enzymatic and deep eutectic solvent pretreatments. Using the same pre-treatments, these authors found WRI values for cotton ranging from 0.6 and 0.8 g/g. Similarly, Meija-Ballesteros et al. (2021) studied the effect of hornification on unbleached *Eucalyptus* fibers and obtained WRI values around 1.7 and 1.1 g/g for unhorned fibers and fibers submitted to four hornification cycles, respectively.

3.3. Microstructural analysis, fibrillation energy consumption, stability, zeta potential, and XRD of the suspensions

The untreated fibers resulted in MFC/NFC suspensions with cell wall fragments and bundles of partially joined fibrils (Figure 3). Regarding the suspensions of *CS 5%* and *CS 10%* (Figures 3D e 3G), it was possible to notice that fibrillation occurred more efficiently because the dimensions of the bundles and cell wall fragments were significantly smaller compared to the *Control* (see Figures 3A and 3B). However, it was possible to observe the calcium silicate particles in both suspensions (see Figures 3E e 3H).

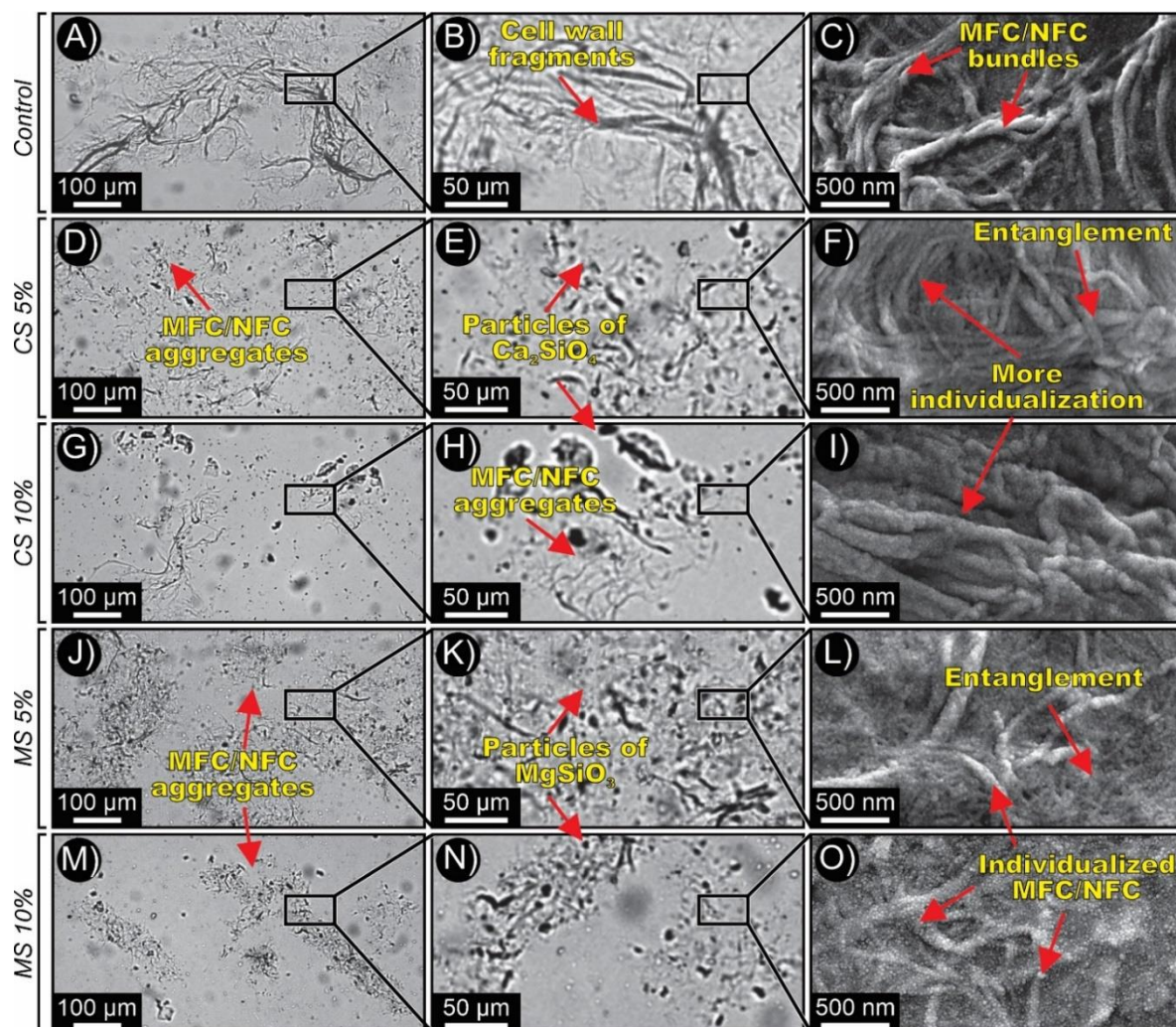


Fig. 3. Light microscopy and SEM images of the EUC MFC/NFC, untreated and pre-treated with calcium silicate and magnesium silicate solutions; A-C) Control; D-F) CS 5%, G-I) CS 10%; J-L) MS 5%; M-O) MS 10%.

The suspensions of MS 5% and MS 10% were more homogeneous among all, showing more cohesive clusters of MFC/NFC and smaller cell wall fragments (see Figures 3J and 3M), which indicates a greater ability to deconstruct fibril bundles. In addition, the residual particles of magnesium silicate are smaller compared to calcium silicate (see Figures 3K and 3N). To better understand the mentioned aspects, Figure 4 shows the frequency distributions as a function of the diametric classes of the MFC/NFC obtained from the SEM images. For the *Control* (Figure 3C), diameters of the MFC/NFC were obtained around ~58 nm. In addition, 68% of the structures had diameters below 60 nm.

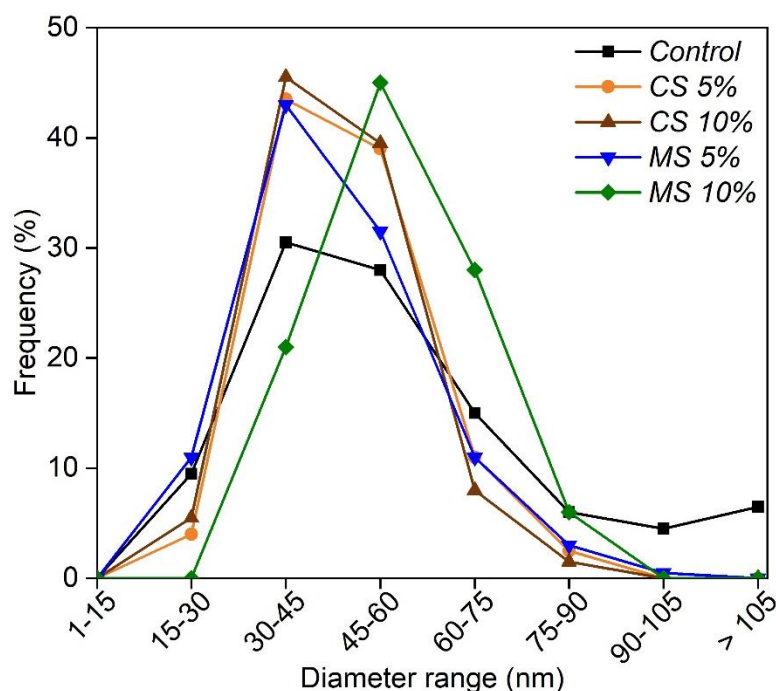


Fig. 4. Diametric distribution histograms showing the general occurrence of MFC/NFC for untreated and pre-treated with calcium silicate and magnesium silicate solutions.

Regarding *CS 5%* and *CS 10%* (Figures 3F and 3I), the average diameters of MFC/NFC were around ~42 nm and ~45 nm, respectively. Considering the frequency of diameters below 60 nm, around ~86% of the structures observed for *CS 5%* presented themselves in this condition and for *CS 10%* the frequency was 90%. The MFC/NFC from *MS 5%* and *MS 10%* had average diameters of ~46 nm and ~55 nm, respectively (Figures 3L and 3O). In *MS 5%*, around ~85% of the structures showed diameters below 60 nm, while for *MS 10%* the frequency of structures in this condition was ~66%. These results indicate that silicate pretreatments improved fibrillation efficiency, especially when calcium silicate was used.

Despite the reduction in the WRI caused by the calcium silicate, which could hinder the MFC/NFC obtainment, the mechanical fibrillation may have been favored by the initial fiber swelling due to the high pH (10~13) during the pre-treatment. The cell wall swelling potentiates the shear against the grinder stones, increases the surface area of the three-dimensional MFC/NFC network during the dissociation of the fibril bundles, and promotes the "gel" obtainment with fewer passes (Gorur et al., 2020, Martins et al., 2021). The magnesium silicate (pH~10.5) promotes fiber swelling, and the presence of Mg-OH groups increases the water entry capacity between the cellulose fibrils (Dimic-Misic et al., 2013; Dias et al., 2019).

The energy consumption to obtain the MFC/NFC reinforces this reasoning. For the *Control*, around 7500 ± 308 kWh/t were required to obtain the gel. Considering the *CS 5%*

and *CS 10%* pre-treatments, the energy consumption was around 6166 ± 94 kWh/t and 5833 ± 71 kWh/t, respectively. Concerning *MS 5%* and *MS 10%*, approximately 7000 ± 119 kWh/t and 5850 ± 58 kWh/t were needed to obtain gel, respectively. Both calcium silicate and magnesium silicate are insoluble in water, nonetheless, when dispersed in an aqueous medium, they have a great capacity for gel formation (Wang et al., 2019; Tang et al., 2021). Mascarenhas et al. (2022b), using sodium silicate solutions at concentrations of 5% and 10% (w/w), found energy consumption for fibrillation of *Eucalyptus* and *Pinus* bleached pulps in the range of 3000-4100 kWh/t and 4000-4500 kWh/t, respectively. Mendonça et al. (2022) studied alkaline pre-treatments with NaOH to facilitate mechanical fibrillation and found reductions in energy consumption of ~31% for *Eucalyptus* and ~28% for *Pinus*. In the present work, the reductions in energy consumption were on the order of ~22% and ~27% for *CS 5%* and *CS 10%*, respectively. For *MS 5%* and *MS 10%*, the reductions in energy consumption for fibrillation were ~12.5% and ~27%, respectively.

These results are unprecedented and meet part of the objectives of this work. This demonstrates that the silicates, in addition to favoring individualization and increasing the MFC/NFC homogeneity, promoted a significant reduction in energy consumption, making the process more efficient. This effect was assumed to be due to the silicate alkalinity and also by the intensification of the shear of the fiber cell walls. The impregnation of the silicate particles on the fiber surfaces may have increased the abrasion of the cell walls with the grinder stones, which may explain the smaller dimensions of the fibril bundles and fragments in the suspensions.

Scatolino et al. (2022) explained that the alkaline pre-treatments in fibers contribute to the reduction of the hemicellulose content and increase fiber swelling. Furthermore, they can facilitate the MFC/NFC obtainment in the grinder with a reduction in energy consumption of more than 45% during mechanical fibrillation (Ang et al., 2019). The results are interesting for applying these suspensions as a coating on the paper using bars and considering the possibility of industrial scaling. Particles with smaller dimensions allow an optimized distribution of the suspensions on the paper surface, reducing the appearance of discontinuities between the applied layers (Tyagi et al., 2021).

After 8h, the stabilities of the *CS 5%* and *CS 10%* suspensions were 46% and 70% lower compared to the control (92%), respectively (Figure 5A).

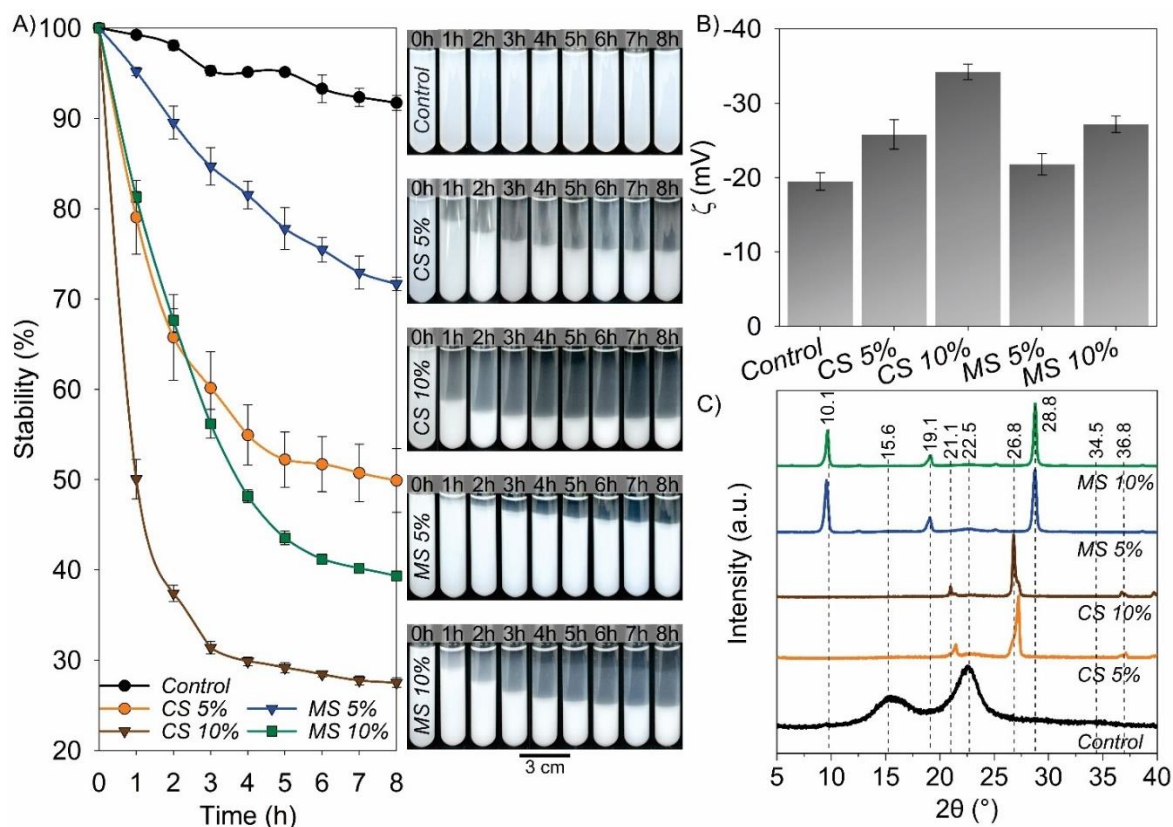


Fig. 5. A) Stability, B) zeta potential (ζ) C) x-ray diffractograms of EUC MFC/NFC suspensions untreated and pre-treated with calcium silicate and magnesium silicate solutions.

Regarding CS 5%, in the first 4 h of evaluation, the stability of the suspensions was abruptly reduced. From 5 h to 8 h of testing, the sedimentation of MFC/NFC suspensions was small (2%). For CS 10%, the stability reduced by 2/3 of the original condition during the first 4 h of testing. From this moment to the end of the test, the variation was not notorious (~1.7%). The MS 5% suspension showed a reduction of the stability of around 22% compared to the control. For the MS 10% suspension, this reduction was around 57%. MS 5% showed no tendency to stabilize the sedimentation of the particles because the stability was reduced until the end of the test. On the other hand, the MS 10% had its stability reduced by 2/3 after 6 h of testing. Posteriorly, the sedimentation was increased by ~4%.

The reduction in the stability of suspensions obtained from fibers pre-treated with silicates is related to the impregnation of the -OH cellulose groups, which are the main ones responsible for the electrostatic repulsion of MFC/NFC in aqueous media (Li et al., 2021). This effect was more intense for calcium silicate. For magnesium silicate, as already demonstrated, the presence of Mg-OH groups may have contributed to the maintenance of particles in suspension. Calcium silicate and magnesium silicate are insoluble in water and have positive

charges on their surfaces (Ca^{2+} and Mg^{2+}) besides different configurations of amorphous silica (Spinthaki et al., 2018; Tipper et al., 2021). This contributes to the impregnation of cellulose by silicates, interruption of the repulsion of charges in the water, and reduction of the dynamics of random movement of particles (Brownian movement), enhancing the sedimentation of MFC/NFC (Yang et al., 2021). Silva et al. (2021) also observed similar behavior when they submitted bleached *Eucalyptus* MFC to drying and redispersion cycles. These authors found that drying promoted the formation of MFC aggregates that limited the electrostatic repulsion capacity, which increased the sedimentation of the suspensions by ~50%. Thinking about industrial scales, this information is critical. If the stability of suspensions is low, measures can be taken to keep the particles dispersed by constant agitation.

The results for the zeta potential of the suspensions reinforce the explanations presented (see Figure 5B). The values for CS 5% and CS 10% were around -25 and -34 mV, which were 32% and 76% lower than the control, respectively. For MS 5%, the results for ζ were around -21 mV, being ~8% lower compared to the control. For MS 10%, the ζ values were around -27 mV, which represented a 40% of reduction in relation to the control. According to Patel and Agrawal (2011) and Bhattacharjee (2016), colloidal suspensions can be classified according to ζ as highly unstable (0 to -10 mV), relatively stable (± 10 to -20 mV), moderately stable (± 20 to -30 mV), and highly stable ($> \pm 30$ mV). Blanco et al. (2018) showed that ζ values lower than -15 mV indicate that MFC/NFC suspensions may show a tendency to agglomeration and sedimentation. In addition, suspensions with ζ values lower than 25 mV, or greater than -25 mV may eventually agglomerate, due to interparticle interactions, including van der Waals forces and hydrogen bonds (Predoi et al., 2020). This behavior was also observed in the present work.

The stability of suspensions is one of the main technological variables involved in the context of paper coating (Pawlowski, 2009). Maintaining the viscosity of the formulations is essential for obtaining paper coatings with uniform surface and interlayer distribution (Liu et al., 2017). Shenoy and Shetty (2022) showed that ζ and surface tension are correlated. These authors found that clay-based suspensions with ζ values around -30 mV resulted in increased surface free energy of the coating, improving fixation and transfer of ink onto cardboard.

These results can be explained by the modification of the crystalline pattern of the cellulose with the pre-treatments (Figure 5C). In the sample referring to the *Control*, the diffraction peaks located at $2\theta = 14.9\text{-}16.5^\circ$, 22.5° , and 34.5° are clearly presented, attributed to the crystalline planes (1-10), (110), (200) and (004) of type I cellulose, respectively (French, 2014). When observing the diffractograms of CS 5% and CS 10% it is possible to notice that the intensity of the cellulose crystalline peaks was suppressed due to the appearance of peaks

located at $2\theta = 21.1^\circ$, 26.8° , and 36.8° which are referring to the typical crystallographic pattern of $\text{Ca}_2\text{O}_4\text{Si}$ and $\text{Ca}_2\text{O}_4\text{Si} \cdot x\text{H}_2\text{O}$ (Meiszterics et al., 2010). Li et al. (2010) and Jia et al. (2011) obtained similar results to the present work and found that this effect is due to the strong interaction between calcium silicate and cellulose.

For *MS 5%* and *MS 10%*, the typical crystallographic pattern of cellulose I was also not identified. Classic diffraction peaks of MgO_3Si were observed with values of $2\theta = 19\text{-}30^\circ$ and $2\theta = 32\text{-}38^\circ$, which were consistent with results obtained in the literature (Wang et al., 2010; Zhao et al., 2015). Between $2\theta = 10^\circ$ and 19.1° peaks referring to the presence of MgO_3 and $\text{Mg}(\text{OH})_2$ were observed (Jin and Al-Tabbaa, 2013; Zhang et al., 2018b). High-intensity peaks located at $2\theta = 28.8^\circ$, on the other hand, indicate the presence of residual silica from magnesium silicate (Darghouth et al., 2021), strongly adhered to cellulose. These results corroborate the behavior observed for stability and zeta potential, confirming the strong interaction of silicates even after the mechanical fibrillation process, proving the occurrence of modifications in the chemical structure of cellulose.

These aspects allow the predictability of the coating parameters (e.g. weight, gas barrier, strength) according to the purpose of the paper application (Tyagi et al., 2021; Jin et al., 2021). With the knowledge of viscosity and stability, it is possible to make decisions regarding the need to implement suspension agitation, speed of application, and the dimension of the amount of material to be prepared for use in the production line.

3.4. Microstructural analysis, contact angle, wettability, and surface energy of the papers

SEM micrographs allowed us to observe that the wetting and drying of the paper resulted in surface modification in relation to control paper (*CP*) (Figure 6). It was possible to notice greater amounts of void spaces on the wet control paper (*WCP*) surface (Figure 6D) due to the swelling and contraction of the fibers resulting from the adsorption and desorption of water (Hubbe et al., 2007). These modifications also occurred between the layers of the paperboard. Compared with *CP* (Figures 6B and 6C), in the *WCP* the cell walls collapsed, and the fibers rearranged (Figure 6E). This induced the formation of more gaps and micro galleries in relation to the original paper (Figure 6F). This effect was also described by Thébault et al. (2017) when presenting the main factors involved in the process of coating paper with phenolic resins. Regarding the coating with MFC/NFC, it was possible to observe that the irregularities and the number of voids on the paper surface were significantly reduced. However, fragments of the cell wall of the suspension were observed distributed on the paper surface (Figure 6G).

In the cross-section, voids were also formed between the layers of paperboard due to the effect of wetting and successive drying (Figure 6H). Oliveira et al. (2022) explained that many cycles of wetting and drying during the application of the coatings cause the hornification of the fibers, inducing the formation of voids in the paper structure. On the other hand, the MFC/NFC coating layer has strongly adhered to the paperboard surface (Figure 6I).

For the *CS 5%* and *CS 10%* coatings (Figures 6J and 6M), the surface was more homogeneous than the MFC/NFC. In addition, calcium silicate particles measuring around 2.6 μm , in cube format were observed surrounded by MFC/NFC. The coating layers applied to both *CS 5%* and *CS 10%* have strongly adhered to the paperboard, without delamination (Figures 6L and 6O).

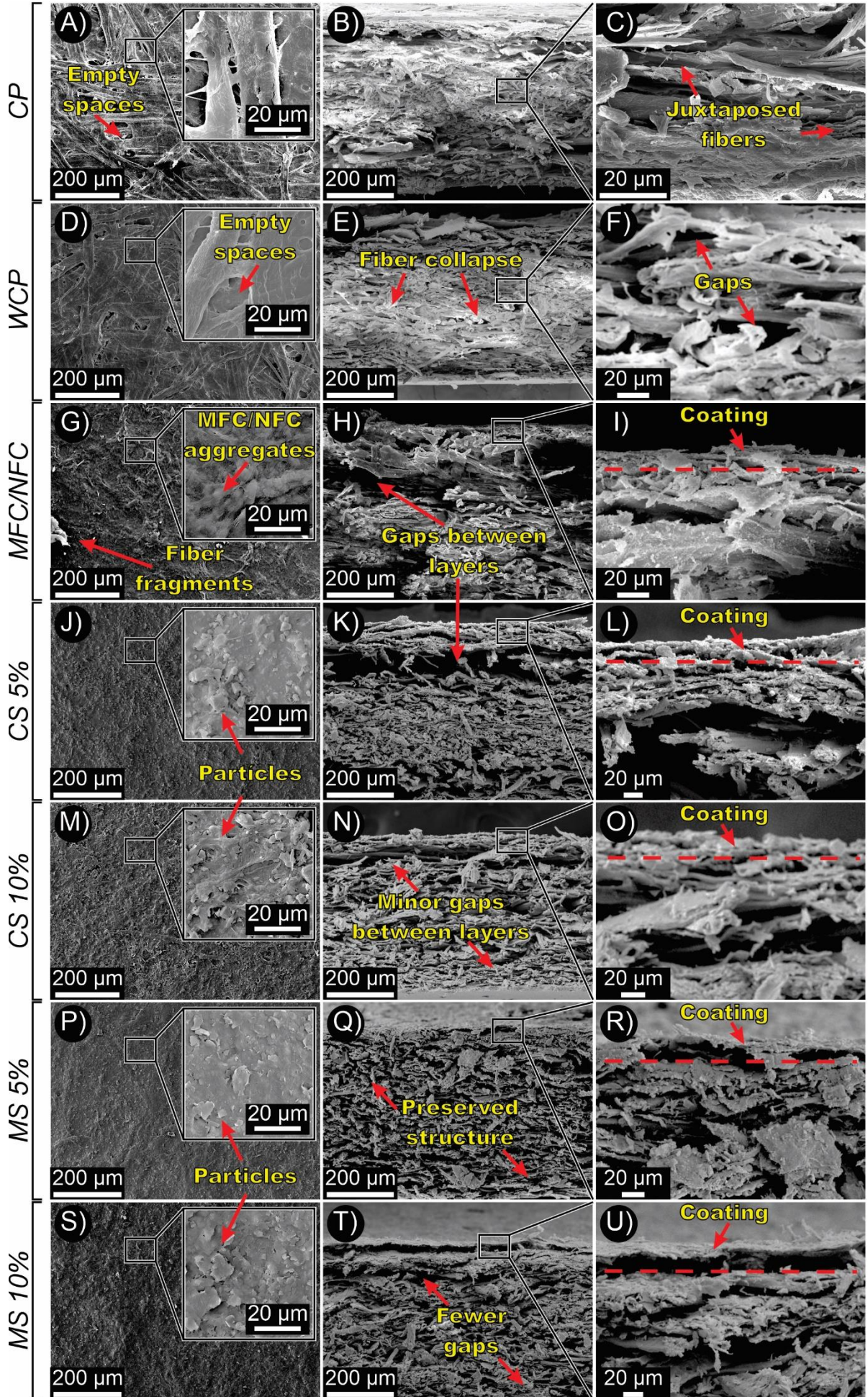


Fig. 6. SEM micrographs of the EUC MFC/NFC coated cardboard from *Eucalyptus* sp. untreated and pre-treated with calcium silicate and magnesium silicate solutions; A) *CP* surface; B) *CP* cross-section; and C) *CP* cross-section zoom; D) *WCP* surface; E) *WCP* cross-section; F) *WCP* cross-section zoom; G) MFC/NFC surface; H) MFC/NFC cross-section; I) MFC/NFC section zoom; J) *CS 5%* surface; K) *CS 5%* cross-section; L) *CS 5%* cross-section zoom; M) *CS 10%* surface; N) *CS 10%* cross-section; O) *CS 10%* cross-section zoom; P) *MS 5%* surface; Q) *MS 5%* cross-section; and R) *MS 5%* cross-section zoom; S) *MS 10%* surface; T) *MS 10%* cross-section; and U) *MS 10%* cross-section zoom.

Figures 5P and 5S show that *MS 5%* and *MS 10%* coatings reduced irregularities and the number of void spaces on the cardboard surface. Particles of magnesium silicate measuring around 9.2 μm with an aspect of blades were also observed. This corroborates the results obtained in the FTIR, in which the band of 3674 cm^{-1} was verified, attributed to the -OH group of the octahedral sheets of magnesium silicate (Frost and Mendelovici, 2006). Regarding the cross-section, the layer structure of the papers coated with *MS 5%* and *MS 10%* was less affected and with smaller gaps concerning the coatings described above (see Figures 6Q and 6T). Some gaps were also detected between the most superficial layers of the coating, as can be seen in Figures 6R and 6U. However, these crevices present a lower potential to increase the water absorption than the gaps observed in the layers below the surface, as described for *WCP*, MFC/NFC, and calcium silicate-containing coatings.

The irregularities observed for the papers submitted to wetting and application of coatings can contribute to greater dispersion of water and adhesives on the paper. In general, more irregular surfaces combined with the large amounts of available fillers potentiates the reduction of the contact angle with the surface (Cruz et al., 2022; Mascarenhas et al., 2022a). This effect was observed in the present work. It is possible to verify that the wetting and drying of the paperboard (*WCP*) promoted a reduction of the contact angle with water by around 9.6% concerning *CP* ($\sim 110^\circ$) (Figure 7). However, the wettability was very similar to cardboard in its original condition ($\sim 0.01^\circ/\text{s}$) (Figure 7B).

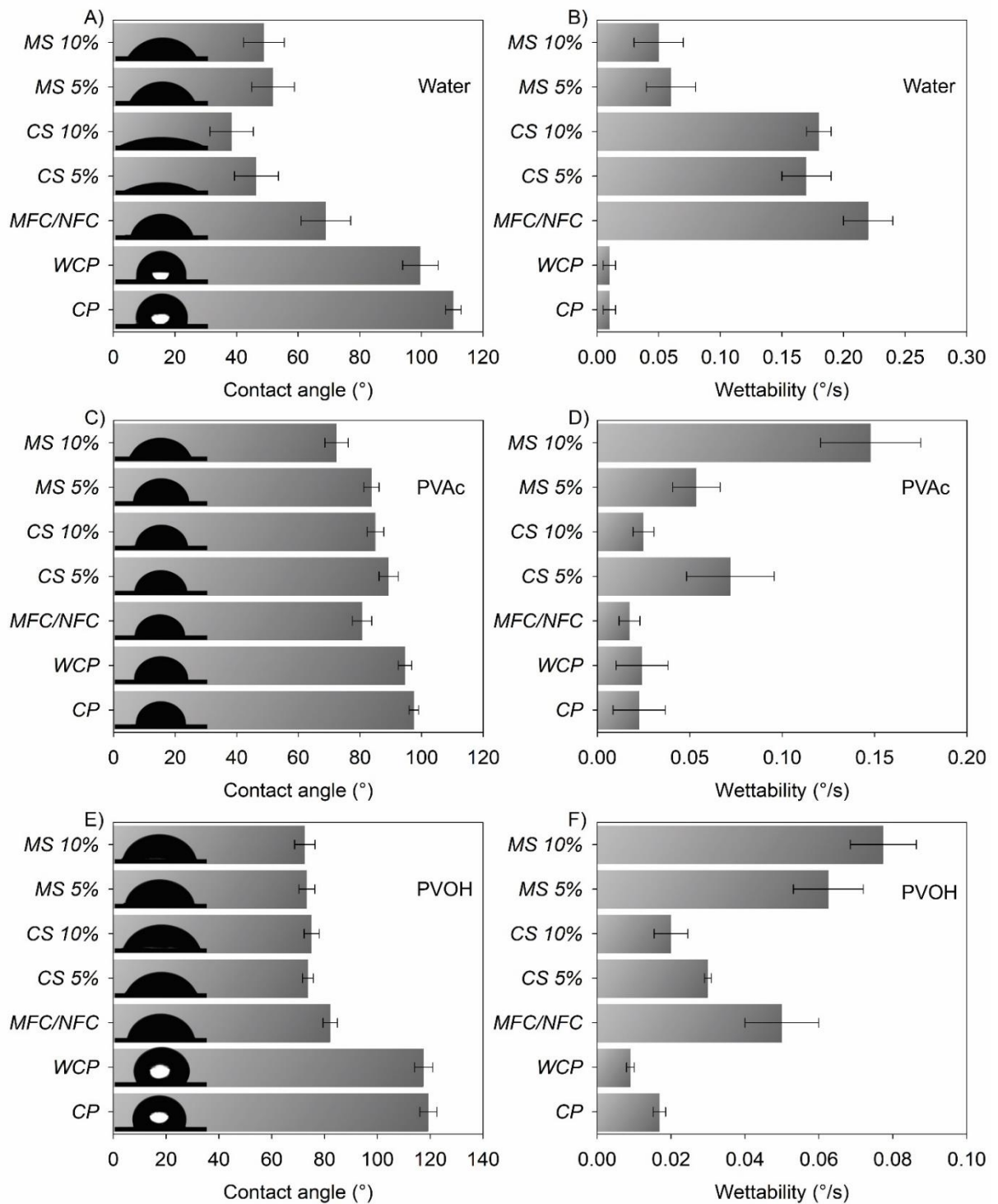


Fig. 7. A) Contact angle with water; B) wettability with water; C) contact angle with PVAc; D) wettability with PVAc; E) contact angle with PVOH; F) PVOH wettability on untreated EUC MFC/NFC coated board and pretreated with calcium silicate and magnesium silicate solutions; The drop images are on the same scale.

The coating composed only of MFC/NFC had a reduced contact angle of about $\sim 37^\circ$, and wettability increased around 20 times about *CP* ($0.01^\circ/\text{s}$), which can be due to the greater contact surface of MFC/NFC and greater exposure of -OH groups (Chen et al., 2022b). The contact angle for *CS 5%* was around 46° and around 38° for *CS 10%*. The wettability for these coatings was very close and varied between 0.17 and $0.18^\circ/\text{s}$. Regarding the *MS 5%* and *MS 10%* coatings, the contact angle values were similar and $\sim 45\%$ lower than *CP*. The wettability followed the same trend, with values varying around $0.05^\circ/\text{s}$.

Regarding the test performed with PVAc, *WCP* presented a contact angle very close to those of *CP* ($\sim 110^\circ$). All the coatings presented a reduction in the contact angle of PVAc with the paper (see Figure 7C). The highest reduction was observed for *MS 10%* ($\sim 26\%$), and the lowest was obtained for *CS 5%* ($\sim 8\%$). As for wettability, the highest increases were also observed for *MS 10%* ($\sim 0.14^\circ/\text{s}$) and *CS 5%* ($\sim 0.07^\circ/\text{s}$) in relation to *CP* ($0.02^\circ/\text{s}$) (Figure 7D). For the PVOH test, the contact angle for *CS 5%*, *CS 10%*, *MS 5%*, and *MS 10%* were around $73 \pm 1.1^\circ$ (see Figure 7E). For *CP* and *WCP* the values were around $\sim 119^\circ$ and $\sim 117^\circ$, respectively. The contact angles for MFC/NFC were around 10% higher than those observed for the coated papers. The highest wettability values were obtained for *MS 10%* ($\sim 0.07^\circ/\text{s}$) and *MS 5%* ($0.06^\circ/\text{s}$), followed by *MFC/NFC* ($0.05^\circ/\text{s}$), *CS 5%* ($0.03^\circ/\text{s}$) and *CS 10%* ($0.02^\circ/\text{s}$) (see Figure 7F). The wettability values of *CP* and *WCP* were in the same range ($\sim 0.01^\circ/\text{s}$).

The reduction of the contact angles for the conditions evaluated occurred due to the wrinkling of the paper surface. This effect was caused by the swelling and contraction of the fibers due to the adsorption and desorption of water, a consequence of the drying process and application of the coatings (Drelich, 2019). This phenomenon can form pores and expose the macrofibrils, increasing the contact surface with water (Abdelouahab et al., 2021). It can be said that the paper in the original condition had a hydrophobic surface ($> 90^\circ$), favoring wetting and causing droplet scattering (Zhao and Jiang, 2018). On the other hand, all the coatings applied made the papers more hydrophilic, as the contact angles reduced and the wettability increased, especially for the calcium silicate coatings.

Tsai et al. (2019) observed that the addition of 20% to 50% of calcium silicate in composites reinforced with chitosan and titanium alloy promoted the reduction of the contact angle to values below 10° . Kotp et al. (2017) studied the performance of polyamide membranes, concluding that the addition of magnesium silicate nanoparticles reduced the contact angle from $\sim 70^\circ$ to $\sim 45^\circ$, corroborating the results found in this work. These authors explained that calcium and magnesium silicate present many external loads that contribute to greater hydration of the surface and interior of the composite matrices. Another important aspect being considered is

that the use of silicates promotes more efficient fibrillation (see Figure 3). Further, MFC/NFC have a greater surface area and exposure of -OH groups, which contributed to the increase in the number of hydrogen bonds with water, increasing wettability (Lengowski et al., 2020; Xu et al., 2020).

In the context of packaging, reducing the contact angle with PVA can be interesting because it is one of the main adhesives used in the industry. The application of cardboard in multi-layer packaging depends on its ability to spread the adhesive, otherwise, failures in gluing and layer delamination may occur (Antón et al., 2020). In the present work, the coatings showed the potential to improve the distribution of the adhesive and increase the adhesion with other layers (plastics, metals, or other papers). Chen et al. (2022b) observed results similar to this work. These authors verified that the application of MFC/NFC modified with nano-silica for coating paper improved the mechanical strength of multilayer packaging due to the greater interaction of bonds with the other materials that compose the layers. This explanation can be applied to the PVOH, as the applied coatings acted as a kind of primer and favored its spread on the paper surface. Consequently, due to many hydrogen bonds established, the adhesion of PVOH can be potentiated. Thus, the behavior observed for coated papers in this work becomes interesting from an industrial point of view because it can provide better fixation of other coatings without the need for additional surface treatments.

For primary and secondary packaging, used for direct storage with the product and the stock organization (Mahmoudi and Parviziomran, 2020), it can be said that in some applications (drugs, footwear, cereals) high wettability will not always be harmful due to the shorter residence time until reaching the final consumer. These kinds of packaging contain the manufacturer's logo, identification, and information about the composition of the products printed directly on the paper. A higher wettability can contribute to this purpose (Lourenço et al., 2020).

The test of contact angle using printer ink can be interesting in this context. The coating containing only MFC/NFC presented a contact angle 36% smaller in relation to *CP* ($\sim 34.4^\circ$), while the values for *WCP* showed differences around $\sim 3\%$ (Figure 8A).

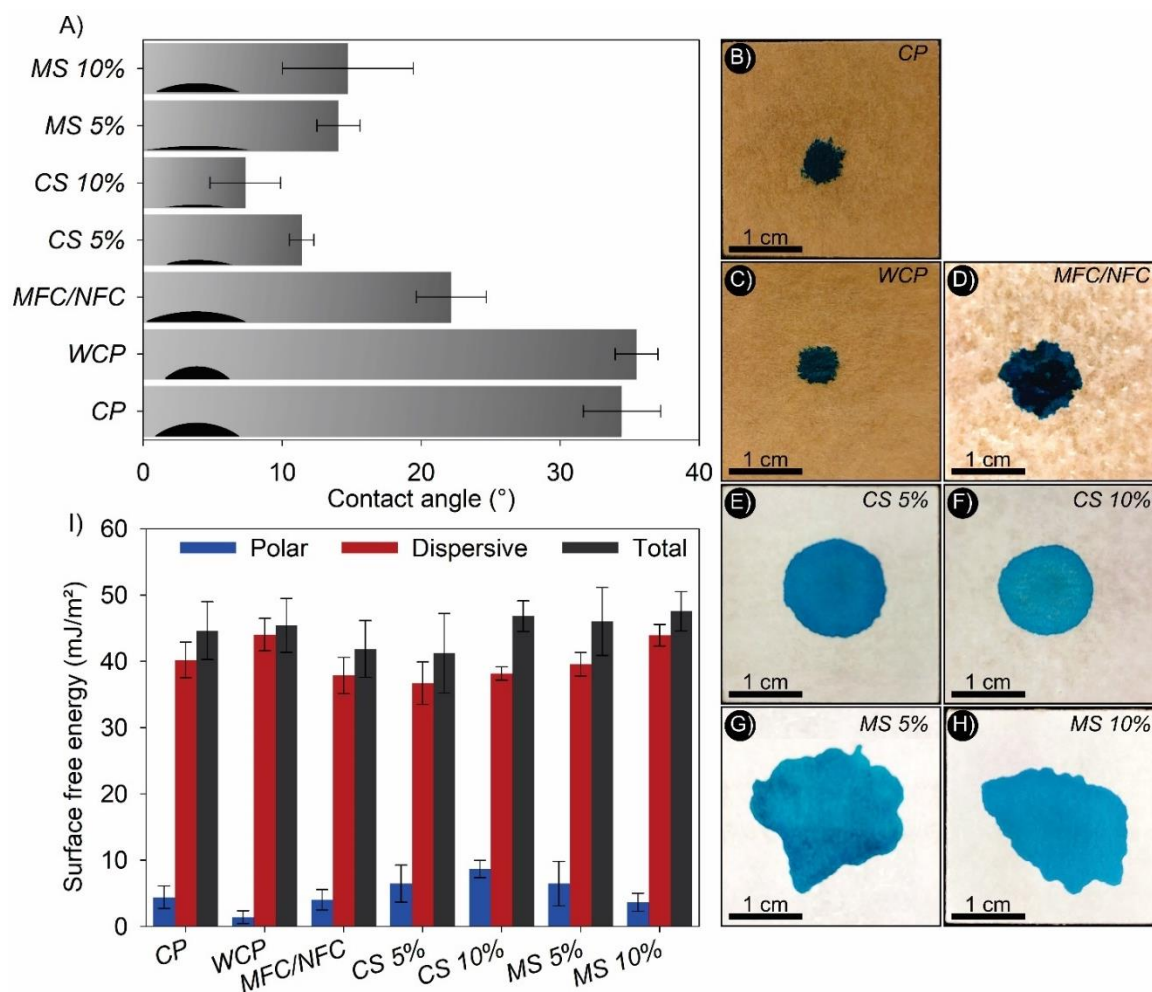


Fig. 8. A) Contact angle, images of the ink spreading on the paper: B) *CP*; C) *WCP*; D) *MFC/NFC*; E) *CS 5%*; F) *CS 10%*; G) *MS 5%*; H) *MS 10%*, and I) free energy of surface coated with EUC *MFC/NFC* untreated and pre-treated with calcium and magnesium silicate solutions.

The values obtained for *CS 5%* and *CS 10%* were ~67 and ~79% lower concerning *CP*, respectively. On the other hand, *MS 5%* presented contact angles ~59% smaller than *CP*, while for *MS 10%* the reduction was ~57%. These results indicate a greater ability to spread and fix the ink on the surface, considering the same volume of ink applied. For *CS 5%* and *CS 10%*, the spreading was more uniform (see Figures 8E and 8F). For *MS 5%* and *MS 10%* (see Figures 8G and 8H), the distribution was more irregular in relation to *CP*, *WCP*, and *MFC/NFC* (see Figures 8B, 8C, and 8D).

Paper wettability has a high correlation with printability (Aydemir et al., 2020; Ozcan et al., 2021). If the wettability is low, the ink fixation on the paper can be impaired during the handling of boxes and bags, due to friction, ultraviolet radiation (UV), pH variations, and contact with humidity or cleaning products in the gondolas (Ozcan e Kandirmaz, 2020; Zołek-

Tryznowska et al., 2020; Genç et al., 2021). Mirmehdi et al. (2018a) observed that the use of MFC/NFC as a coating improved the properties for writing and printing on the paper surface. In addition, coatings act to reduce the surface tension to control and restrict the expansion of ink drops (Mielonen et al., 2015). These characteristics were observed, mainly for coatings containing calcium silicate. The surface free energy also helps to understand these results, as all coated papers showed low surface tension and high surface energy ($> 45 \text{ mJ/m}^2$) (see Figure 8I). The *CS 10%*, *MS 5%*, and *MS 10%* coatings resulted in increases in surface free energy, which were around 4.7, 3.2, and 6.6% over *CP* ($\sim 45 \text{ mJ/m}^2$), respectively. No considerable increase in surface-free energy was observed when evaluating *WCP*. The *CS 10%* coating increased the polar component energy by approximately 96% compared to *CP* ($\sim 4.4 \text{ mJ/m}^2$). The *CS 5%* and *MS 5%* coatings resulted in increases in the polar component of around 47%, explaining the higher wettability values and the greater spread of ink on the surface of the papers.

Surface free energy allows determining the excess energy on the surface of a solid and can be correlated with the adhesion between different materials as a function of the proportions between polar or dispersive energy (Tanzadeh and Shafabakhsh, 2020; Yongabi et al., 2020). The increase in the surface free energy is related to the presence of hydroxyl groups, responsible for the interaction with polar liquids (Zołek-Tryznowska and Kałuzna, 2021). Higher surface energy favors a more efficient distribution of ink and adhesives in coated papers. This aspect is interesting for the industry, as it can contribute to reducing the amount of paint applied and favoring its drying after application (Shenoy and Shetty, 2022). Generally, the industry uses corona treatment to improve the adhesion capacity of the paper (Lopes et al., 2018), the evaluated coatings have the potential to dispense this step, depending on the desired application.

Ozcan et al. (2021) studied the printability with water-based inks and observed that a surface free energy between 40 and 44 mJ/m^2 increased the wettability and printability of the paper. Madeira et al. (2018) reported that surface free energy is also correlated with adhesion strength and can be a tool to assess the quality of multilayer gluing on the packaging.

3.5. Water absorption of the papers

All the coatings provided an increase in Cobb values compared to *CP* ($\sim 38 \text{ g/m}^2$) (Figure 9A). It was also possible to identify a slight increase in water absorption in *WCP* ($\sim 5\%$). The Cobb values found for the coating containing only MFC/NFC were $\sim 65\%$ higher than those observed in *PC*. This can be explained by the greater exposure of hydroxyl groups, which

avored the water absorption and the swelling of the paperboard fibers (Mascarenhas et al., 2022a).

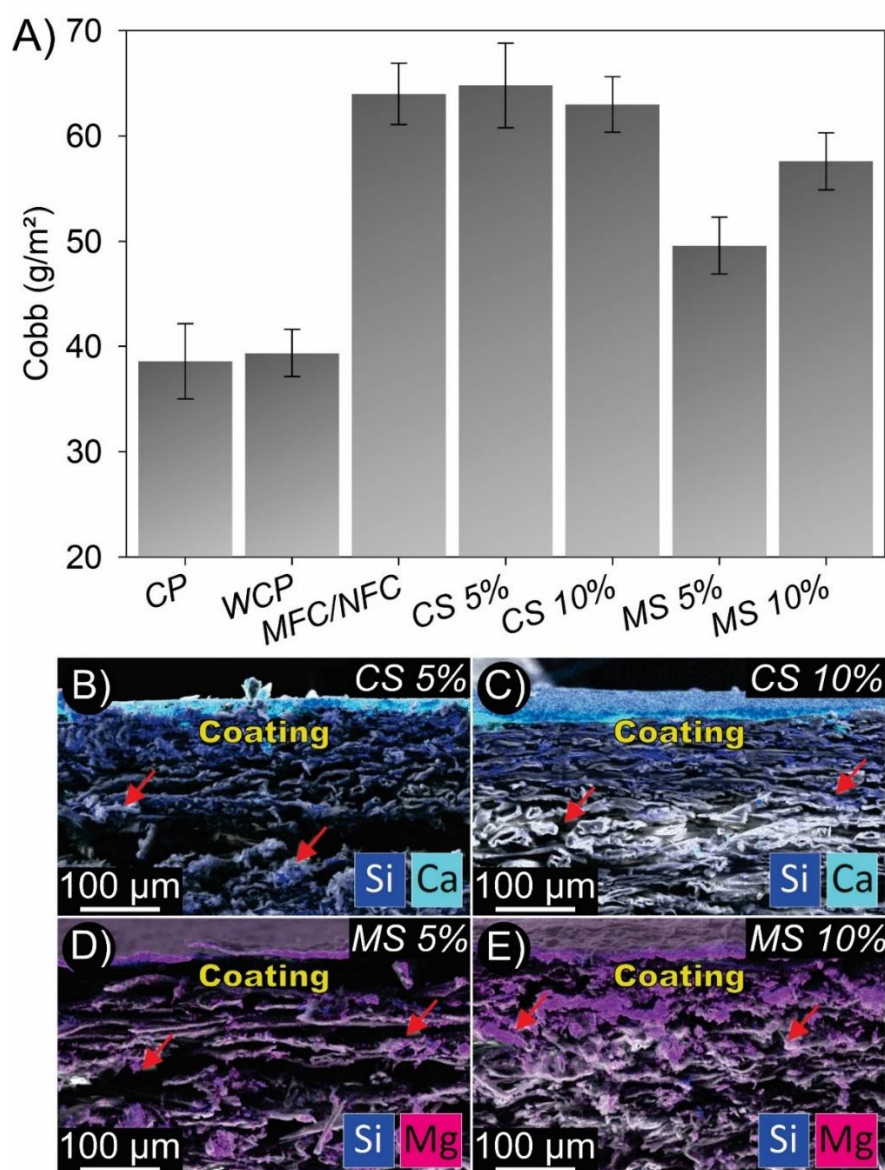


Fig. 9. A) Water absorption (Cobb) and SEM micrographs with EDS of the cardboards cross-sections coated with EUC MFC/NFC untreated and pre-treated with calcium and magnesium silicate solutions; B) CS 5%; C) CS 10%; D) MS 5%; and E) MS 10%.

For CS 5%, the Cobb values were increased by ~68%, while for CS 10%, the increase was around 63%. Considering the MS 5% and MS 10% coatings, the increments in the Cobb values were around 28.5 and 49.2%, respectively. The increases in Cobb can be explained by forming a complex network of microgalleries in the paper layers as a function of the wetting caused by the addition of coatings and by the drying steps (see Figure 6). The results found are in harmony with other studies. Jeong and Yoo (2020) evaluated cardboard coated with sucrose

suspension, beeswax, and whey protein and obtained Cobb values between 60 and 85 g/m². Similarly, Shen et al. (2021) obtained Cobb values between 40 and 100 g/m² for papers coated with PVA and nanoclay.

Further, as explained above, these coatings increased the wetting and surface energy of the paperboard. However, employing EDS scanning electron microscopy, the presence of Si (blue) and Ca (cyan) was verified, indicating the penetration of silicates in the layers of paperboard at depths ranging from 100 to 150 μm for *CS 5%* and *CS 10%* (see Figures 9B and 9C). Due to the lower viscosity (2600-3300 cP), the *MS 5%* and *MS 10%* suspensions penetrated between 250 and 350 μm deep into the paper, as highlighted for Si (blue) and Mg (magenta) in Figure 9D and Figure 9E. This potentiated the entry of water into the microgalleries (red arrows in Figure 9), increasing water absorption in the papers. Adibi et al. (2022) described this behavior when evaluating paper coating with alpha-1-3 glucan and latex. These authors explained that adding the wet layer to the paper surface promotes the swelling of the fibers, which rearrange themselves and form empty spaces between them.

As a result, part of the coating solids was transported along with the solution to the paper's subsurface layers (Figure 10). After drying, they remain impregnated due to the contraction of the fibers and the establishment of bonds with the cellulose (Thébault et al., 2017). This process can be intensified by adding more layers and performing new drying steps, as observed in the present work.

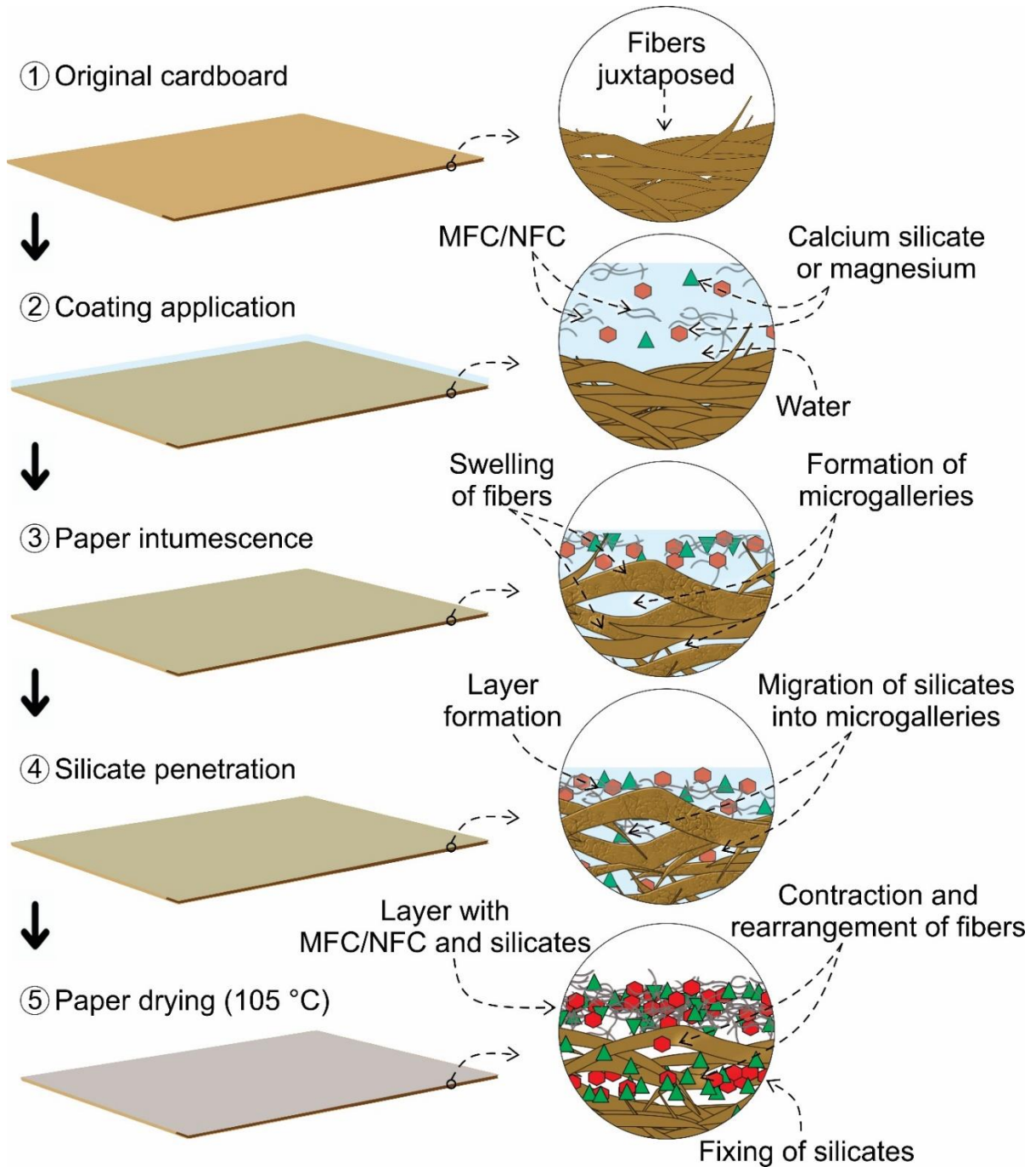


Fig. 10. Steps and mechanisms of penetration of silicate suspensions in the cardboard.

The amount of research using silicates as a paper coating is minimal, but the application of this material in other conditions can contribute to understanding the results found. Calcium and magnesium silicate are widely used as additives to improve the hydration and cohesion of particles dispersed in cementitious matrices (Cho et al., 2020). These silicates have large amounts of charges available to establish electromagnetic interactions (Sadek et al., 2016; Saedi et al., 2021b), which can be potentiated with MFC/NFC.

Kumar et al. (2011) explained that the retention of calcium-based minerals, sodium silicate, and aluminum silicate on the surface and in the lumen of the fibers could increase the paper's water absorption. By analogy, these hypotheses could be applied to explain the increase in water absorption in paperboard. Another aspect to consider is that both calcium silicate and magnesium silicate exhibit the ability to form lamellar structures (Minet et al. 2004; Prati and Gandolfi, 2015; Roosz et al., 2015). With this, it is possible that some of the water has been lodged in the spaces between the lamellae, where they may contain adhered MFC/NFC. This may cause the water to be retained more in the coating and not in the paper structure, explaining the higher absorption values of the coated papers compared to *PC*.

It should be noted that the Cobb test is not only used to assess water absorption in the paper. It is also used to determine the ability of glue penetration (Gok and Akpınar, 2020). For papers with low surface energy and Cobb values, some types of adhesives cannot penetrate, leading to the reduced anchorage between the bonded faces. On the other hand, high Cobb values result in excessive adhesive consumption, which can harm bonding and increase production costs. This variable is crucial in the production of multilayer packaging, as the paper must promote adequate adhesion to the other layers (metals or plastics) to guarantee the barrier to gases and mechanical resistance. Dohr and Hirn (2022) found that adhesive penetration is strongly related to the strength of Kraft sack paper. The authors explained that surface sizing could result in delamination problems between the layers due to the smaller chemical and physical anchorages in the voids located in the subsurface layers of the paper.

3.6. Water vapor permeability and mechanical properties of the papers

For *WCP*, the wetting and drying stages contributed to a slight increase in the values of WVTR and WVP in the order of 2.5 and 5%, respectively, concerning *CP* (Figures 11A and 11B). This was assumed to be due to the increase in the number of empty spaces and microgalleries between the layers of the paperboard, facilitating the passage of water vapor.

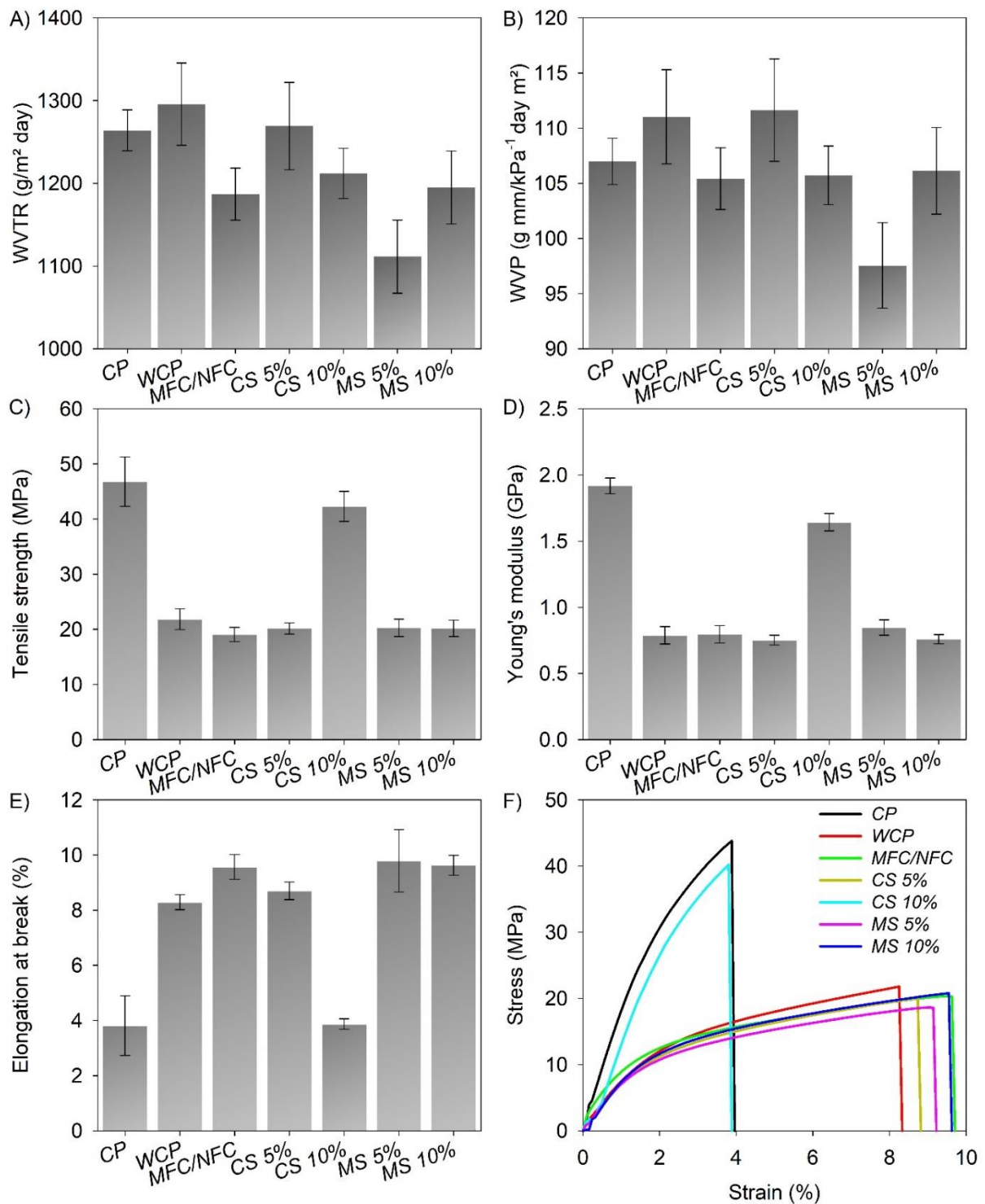


Fig.11. A) WVTR; B) WVP; C) tensile strength; D) Young's modulus; E) elongation at break; and F) stress x strain curves in the tensile test of cardboard coated with EUC MFC/NFC untreated and pre-treated with calcium and magnesium silicate solution.

The coating of cardboard with MFC/NFC resulted in a reduction of WVTR by ~6%, and for the WVP, it was very similar to that observed for CP (~105 g mm/kPa⁻¹ day m²). The

reduction in WVTR is related to the characteristics of the MFC/NFC film on the paper surface, which has a structure with organized layers, very tangled, and higher density, making it difficult for the passage of gases (Wang et al., 2020; Hashemzahi et al., 2022).

About *CS 5%*, the WVTR was very close to the observed for *CP* (~1265 g/m² day), while for *CS 10%*, a reduction of ~4.2% was observed. For WVP, a slight increase (~4.7%) of the values for the *CS 5%* coating was observed. The best barrier properties were obtained using the *MS 5%* and *MS 10%* coatings, for which WVTR obtained reductions of ~12% and ~5.5% in relation to *CP*, respectively. As for WVP, *MS 5%* promoted a reduction of ~14%, while for *MS 10%*, no substantial differences were observed with the other coatings.

Despite the formation of microgalleries, the reductions observed for the calcium and magnesium silicate coatings are due to the impregnation of subsurface layers of the cardboard, as shown in Figures 9 and 10. The silicate particles occupied a large part of the void spaces between the fibers, and in the MFC/NFC network, reducing the flow of water vapor through the layers of the paper. Similarly, Kumar et al. (2011) explained that adding minerals (aluminum silicate and limestone fillers) promotes the occupation of pits, lumen, and mesopores with dimensions of 2-100 nm in diameter present in the fibers and between the fibers. This effect was most prominent for magnesium silicate due to the blade shape of the particles (see Figure 6).

Huang et al. (2018) explained that this feature contributes to better dispersing particles in paper microgalleries. Rastogi and Samyn (2015) explained that the barrier properties of a silicate composite coating depend on its state of aggregation, dispersion, and layer orientation. In general, the results are in harmony with other works in the literature. Chen et al. (2022b) obtained WVTR between 1200 and 2000 g/m² day for MFC and nano-silica coated papers.

Wang et al. (2022) obtained WVTR ranging between 1200 and 1500 g/m² day for paperboard, with a basis weight of 300 g/m², coated with carboxymethyl cellulose sodium and carboxymethyl chitosan. Marzbani et al. (2021), on the other hand, obtained WVP values ranging from 108 to 573 g mm/kPa⁻¹ day m² when evaluating paperboard coating with different concentrations between polyethylene wax and soy protein-based. Considering possible applications for coated papers, Wang et al. (2018) showed that WVTR values between 1000 and 10000 g/m² day indicate that the film/paper can be applied in packaging bakery products and cheeses, fruits, and vegetables.

The values of tensile strength and Young's modulus for *WCP* were ~53 and ~59% lower than *CP*, respectively, which indicates that wetting and drying contributed to the reduction of the mechanical strength of the papers (Figures 11C and D). The tensile strength and Young's

modulus for MFC/NFC, *CS 5%*, *MS 5%*, and *MS 10%* were very similar and were in the range of 20.2 ± 0.06 MPa and 0.79 ± 0.05 GPa, respectively. For *CS 10%*, the results for tensile strength (~42 MPa) and Young's modulus (~1.6 GPa) were slightly lower than those observed for CP. Cataldi et al. (2019) and Wohler et al. (2022) explained that over time water can plasticize (soften) and hydrolyze cellulose and its derivatives. These two phenomena alter and destabilize the cellulosic structures in the paper. Roig et al. (2011) found that this effect is due to the physical aging of the paper and the relaxation of cellulose β 1-4 bonds.

Salmén and Larsson (2018) exposed that temperature and humidity induce the softening of lignocellulosic fibers. The action of water in this context is known as "hygroplastication", which consists of reducing the glass transition temperature and the stiffness of the cell wall after being subjected to different steps of water sorption. Haslach Junior (2000) pointed out that paper mechanical properties significantly depend on the responses to applied loads, humidity, and temperature. The authors explained that successive wetting and drying processes cause the fibers to move apart and reduce the interactions between the cellulose molecules, as the hydrogen bonds become very weak. This is due to the effect of hysteresis that prevents the fibers from returning to their original condition after drying-induced contraction (Salmén and Larsson, 2018).

These explanations clarify the results, as the wetting and drying process during the coatings possibly promoted accelerated aging, intensifying the action of water in breaking hydrogen bonds and reducing the adhesion between the fibers. For the case of *CS 10%*, the low reduction in mechanical strength can be explained by the higher viscosity (~4900 cP), lower water penetration, and stronger anchorage of the coating on the paper surface, as seen in Figure 8C. In higher concentrations, MFC/NFC and calcium silicate formed larger tangles (see Figure 6M). This increased the amount of substances with higher hygroscopic potential, favoring the retention of water on the surface, preventing the swelling of the deeper layers, and preserving the structure of the paper.

Tensile strength indicates the strength of paper and paperboard, which depends on factors such as sizing, fiber length, and fiber strength (Aboura et al., 2004). Assessing the deformation, ductility, and tensile energy absorption in the tensile test can help predict the cardboard performance, particularly when the material is subjected to unequal stresses (Fadiji et al., 2018). The coatings made the paper more malleable due to the greater deformation capacity (see Figures 11E and 11F). Except for PC (3.8%) and *CS 10%* (3.9%), the other coatings showed elongation at break ranging between 8.5 and 9.8%.

Mirmehdi et al. (2018b) also found that increasing nanoclay contents in MFC/NFC suspensions in paper coating resulted in a reduction of mechanical strength in the order of 33% compared to those without nanoclays. Similar results were obtained by Oliveira et al. (2022), which attributed this effect to the hornification of the fibers due to the wetting and drying cycles of the paper during the application of the coatings with NFC and silica. Franke et al. (2020) evaluated paperboard coated with plastic multilayers and obtained improvements in paperboard formability, as observed in the present work. The authors found that the coated papers showed a reduction in tensile strength from 70 MPa to 30 MPa and Young's modulus was reduced from 6.5 GPa to 2.5 GPa.

The ductility is an interesting feature in the packaging (Marsh and Bugusu, 2007), as it allows the paper to be folded to produce boxes of different formats or transport in the form of reels without breaking the fibers. Fadiji et al. (2018) pointed out that when low ductility is detected in a tensile test, the low fracture strength of paperboard under other loading forms is often observed. Vishtal and Retulainen (2012) exposed that ductility is related to formability, which is the ability of the material to undergo plastic deformation without damage. These authors explain that this feature is crucial for cardboard-based materials, as it enables the production of paper trays, cups, paper plates, paper tubes, food containers, and various consumer packaging using the *deep-drawing* method.

Considering the characteristics presented, the coated papers have more interesting properties for application in multilayer packaging than uncoated paper. In addition to mechanical properties, papers coated with calcium and magnesium silicates improved the ability to spread and absorb adhesives, other coating layers, and ink on the paperboard, which can increase the adhesion capacity with other materials or printability. Furthermore, it was observed that there was an improvement in the performance of the paper's ability to prevent the passage of water vapor.

4. Conclusion

The pre-treatments with calcium silicate reduced water retention in the fibers. The FTIR observed new functional groups in cellulose (O-Si-O, Mg-OH, Si-O-Ca, Si-O-Si). Pre-treatments reduced energy consumption in the production of micro/nanofibrils (~30%). Coatings with the suspensions reduced the amount of void space on the surface of the paperboard. In the cross-section, microgalleries were formed due to the paper wetting and drying cycles, especially for MFC/NFC, CS 5%, and CS 10%. The formation of layers with micro/nanofibrils without and with silicates on the surface and subsurface of the paperboard

improved the barrier properties, making them suitable for application in bread, cheese, fruits, and vegetable packaging. MFC/NFC, *CS 5%*, and *CS 10%* increased the water spread on the paperboard's surface. The highest degrees of wettability were observed for *CS 5%* and *MS 10%* in the assay conducted with PVAc. For PVOH, the highest wettability was obtained for MFC/NFC, *MS 5%*, and *MS 10%*, suggesting improvements in adhesive anchoring and adhesion with other coating layers. The coatings increased the spread of ink on the surface of the paper. The strength and stiffness of the papers were reduced due to wetting and drying during the application of the coatings. There was an increase in elasticity, which enhances the formability of paperboard for applications in packaging with different formats. Optimizing application and drying techniques for MFC/NFC and silicate coating formulations can improve the coated packaging papers' mechanical and barrier properties.

CRedit authorship contribution statement

A.R.P.M.: Investigation, Visualization/Data presentation, Writing – original draft. M.V.S., M.C.D., and M.C.M.: Visualization/ Data presentation, Investigation, Writing – original draft. R.R.M.: Conceptualization, Visualization/Data presentation, Writing – review & editing. M.A.M. and G.H.D.T.: Resources, Project administration, Funding acquisition, Supervision.

Declaration of Competing Interest

The authors declare that they have no known competing financial interests or personal relationships that could have appeared to influence the work reported in this paper.

Acknowledgment

We are especially grateful to the Graduate Program in Wood Science and Technology (PPGCTM) of the Federal University of Lavras (UFLA) for providing study material and infrastructure. We thank the Electronic Microscopy Laboratory (LME) of UFLA for obtaining scanning images. The authors are also grateful to the Coordination for the Improvement of Higher Education Personnel (CAPES) for providing research grants. The research was funded by the National Council for Scientific and Technological Development (CNPq finance code 314203/2018-4) and Fundação de Amparo à Pesquisa do Estado de Minas Gerais (FAPEMIG finance code CAG APQ-03248-17). We also thank the and Fundação de Amparo à Pesquisa do Estado do Amapá (FAPEAP), and the State University of Amapá for the postdoctoral scholarships (financial code: 0022.0279.1202.0016/2021 – PROPESP).

5. References

- Abdelouahab, NB, Gossard, A, Ma, X, Dialla, H, Maillet, B, Rodts, S, Coussot, P, 2021. Understanding mechanisms of drying of a cellulose slurry by magnetic resonance imaging. *Cellulose*, 28, 5321-5334. <https://doi.org/10.1007/s10570-021-03916-5>
- Aboura, Z, Talbi, N, Allaoui, S, Benzeggagh, ML, 2004. Elastic behavior of corrugated cardboard: experiments and modeling. *Composite Structures*, 63, 53-62. [https://doi.org/10.1016/S0263-8223\(03\)00131-4](https://doi.org/10.1016/S0263-8223(03)00131-4)
- Adibi, A, Valdesueiro, D, Mok, J, Behabtu, N, Lenges, C, Simon, L, Mekonnen, TH, 2022. Sustainable barrier paper coating based on alpha-1,3 glucan and natural rubber latex. *Carbohydrate Polymers*, 282, 119121. <https://doi.org/10.1016/j.carbpol.2022.119121>
- Al-Oweini, R, El-Rassy, H, 2009. Synthesis and characterization by FTIR spectroscopy of silica aerogels prepared using several $\text{Si}(\text{OR})_4$ and $\text{R}''\text{Si}(\text{OR}')_3$ precursors. *Journal of Molecular Structure*, 919, 140-145. <https://doi.org/10.1016/j.molstruc.2008.08.025>
- An Y, Liu H, Liu J, Li X, Li J, Lin C, Jin X, Xu Y, Zhao Z, Song S, Hui L, Liu Z, Huang Y. 2021. Effects of calcium silicate synthesized in situ on Fiber loading and paper properties. *Nordic Pulp & Paper Research Journal*, 36, 443-455. <https://doi.org/10.1515/npprj-2020-0106>
- Ang, S, Haritos, V, Batchelor, W, 2019. Effect of refining and homogenization on nanocellulose fiber development, sheet strength, and energy consumption. *Cellulose*, 26, 4767-4786. <https://doi.org/10.1007/s10570-019-02400-5>
- Antón, N, González-Fernandez, A, Villarino, 2020. Reliability and Mechanical Properties of Materials Recycled from Multilayer Flexible Packages. *Materials*, 13, 3992. <http://dx.doi.org/10.3390/ma13183992>
- Arantes, ACC, Silva, LE, Wood, DF, Almeida, CG, Tonoli, GHD, Oliveira, JE, Silva, JP, Williams, TG, Orts, WJ, Bianchi, ML, 2019. Bio-based thin films of cellulose nanofibrils and magnetite for potential application in green electronics. *Carbohydrate Polymers*, 207, 100-107. <https://doi.org/10.1016/j.carbpol.2018.11.081>
- ASTM Standard, 2005. ASTM D3285-93, Standard Test Method for Water Absorptiveness of Nonbibulous Paper and Paperboard (Cobb Test).
- ASTM Standard, 2012. E-104-02, Standard Practice for Maintaining Constant Relative Humidity by Means of Aqueous Solutions.
- ASTM Standard, 2016a. ASTM E-96, Standard Test Methods for Water Vapor Transmission of Materials.
- ASTM Standard, 2016b. ASTM D828-16^{e1}, Standard Test Method for Tensile Properties of Paper and Paperboard Using Constant-Rate-of-Elongation Apparatus.

ASTM Standard, 2022. ASTM D7490-13, Standard Test Method for Measurement of the Surface Tension of Solid Coatings, Substrates, and Pigments using Contact Angle Measurements.

Aydemir, C, Altay, BN, Akyol, M, 2020. Surface analysis of polymer films for wettability and ink adhesion. *Color Research Application*, 46, 489-499. <https://doi.org/10.1002/col.22579>

Blanco, A, Monte, MC, Campano, C, Balea, A, Merayo, N, Negro, C, 2018. Nanocellulose for Industrial Use: Cellulose Nanofibers (CNF), Cellulose Nanocrystals (CNC), and Bacterial Cellulose (BC). In: Hussain CM (ed), *Handbook of Nanomaterials for Industrial Applications* (pp. 74-126). Amsterdam: Elsevier.

Bhattacharjee, S, 2016. DLS and zeta potential – What they are and what they are not? *Journal of Controlled Release*, 235, 337-351. <https://doi.org/10.1016/j.jconrel.2016.06.017>

Cataldi, P, Profaizer, M, Bayer, IS, 2019. Preventing Water-Induced Mechanical Deterioration of Cardboard by a Sequential Polymer Treatment. *Industrial Engineering Chemistry Research*, 58, 6456-6465. <http://dx.doi.org/10.1021/acs.iecr.9b00712>

Chen, M, Li, L, Zhao, P, Wang, S Lu, L, 2019. Paper sludge functionalization for achieving fiber-reinforced and low thermal conductivity calcium silicate insulating materials. *Journal of Thermal Analysis and Calorimetry*, 136, 493-503. <https://doi.org/10.1007/s10973-018-7682-0>

Chen, S, Yue, N, Cui, M, Penkova, A, Huang, R, Qi, W, He, Z, Su, R, 2022a. Integrating direct reuse and extraction recovery of TEMPO for production of cellulose nanofibrils. *Carbohydrate Polymers*, 294, 119803. <https://doi.org/10.1016/j.carbpol.2022.119803>

Chen, H, Wang, B, Li, J, Ying, G, Chen, K, 2022b. High-strength and super-hydrophobic multilayered paper based on nano-silica coating and micro-fibrillated cellulose. *Carbohydrate Polymers*, 288, 119371. <https://doi.org/10.1016/j.carbpol.2022.119371>

Cho, BH, Chung, W, Nam, BH, 2020. Molecular Dynamics Simulation of Calcium-Silicate-Hydrate for Nano-Engineered Cement Composites - A Review. *Nanomaterials*, 10, 2158. <http://dx.doi.org/10.3390/nano10112158>

Cruz, TM, Mascarenhas, ARP, Scatolino, MV, Faria, DL, Matos, LC, Duarte, PJ, Moreira Neto, J, Mendes, LM, Tonoli, GHD, 2022. Hybrid films from plant and bacterial nanocellulose: mechanical and barrier properties. *Nordic Pulp Paper Research Journal* 37, 159-174. <https://orcid.org/0000-0001-6623-5310>

Darghouth, A, Aouida, S, Bessais, B 2021. High Purity Porous Silicon Powder Synthesis by Magnesiothermic Reduction of Tunisian Silica Sand. *Silicon*, 13, 667-676. <https://doi.org/10.1007/s12633-020-00433-1>

- Dey, A, Dhumal, CV, Sengupta, P, Kumar, A, Pramanik, NK, Alam, T, 2021. Challenges and possible solutions to mitigate the problems of single-use plastics used for packaging food items: a review. *Journal of Food Science and Technology*, 58, 3251-3269. <https://doi.org/10.1007/s13197-020-04885-6>
- Dias, MC, Mendonça, MC, Damásio, RAP, Zidanes, UL, Mori, FA, Ferreira, SR, Tonoli, GHD, 2019. Influence of hemicellulose content of *Eucalyptus* and *Pinus* fibers on the grinding process for obtaining cellulose micro/nanofibrils. *Holzforschung* 73, 1035-1046, 2019.
- Dimic-Misic, K, Puisto, A, Gane, P, Nieminen, K, Alava, M, Paltakari, J, Maloney, T, 2013. The role of MFC/NFC swelling in the rheological behavior and dewatering of high consistency furnishes. *Cellulose* 20, 2847-2861. <https://doi.org/10.1007/s10570-013-0076-3>
- Dohr, CA, Hirn, U, 2020. Influence of paper properties on adhesive strength of starch gluing. *Nordic Pulp Paper Research Journal*, 37, 120-129. <https://doi.org/10.1515/npprj-2021-0039>
- Drelich, JW, 2019. Contact angles: From mistakes to new developments through liquid-solid adhesion measurements. *Advances in Colloid And Interface Science*, 267, 1-14. <https://doi.org/10.1016/j.cis.2019.02.002>
- Fadiji, T, Berry, TM, Coetzee, CJ, Opara, UL, 2018. Mechanical design and performance testing of corrugated paperboard packaging for the postharvest handling of horticultural produce. *Biosystems Engineering*, 171, 220-224. <https://doi.org/10.1016/j.biosystemseng.2018.05.004>
- Foster, EJ, Moon, RJ, Agarwal, UP, Bortner, MJ, Bras, J, Espinosa, SC, Chan, KJ, Clift, MJD, Cranston, ED, Eichhorn, SJ, Fox, DM, Hamad, WY, Heux, L, Jean, B, Korey, M, Nieh, W, Ong, KJ, Reid, MS, Renneckar, S, Roberts, R, Shatkin, JA, Simonsen, J, Bagby, KS, Wanasekara, N, Youngblood, J, 2018. Current characterization methods for cellulose nanomaterials. *Chemical Society Reviews* 47, 2511-3006. <https://doi.org/10.1039/C6CS00895J>
- Franke, W, Leminen, V, Groche, P, Varis, J, 2020. The effects of pretreatment and coating on the formability of extrusion-coated multilayer paperboard-plastic composites. *Packaging Technology and Science*, 34, 105-116. <https://doi.org/10.1002/pts.2542>
- French, AD, 2014 Idealized powder diffraction patterns for cellulose polymorphs. *Cellulose*, 21, 885-896. <https://doi.org/10.1007/s10570-013-0030-4>
- Frost, RL, Mendelovici, E, 2006. Modification of fibrous silicate surfaces with organic derivatives: An infrared spectroscopic study. *Journal of Colloid and Interface Science*, 294, 47-52. <https://doi.org/10.1016/j.jcis.2005.07.014>

- Genç, HYG, Sönmez, S, Öznur, Ö, Akgül, A, Çetiner, BN, 2021. Printability of bio-composite sheets made from paper mill and cardboard mill waste sludge. *Ahead of print*, 1-9. <http://dx.doi.org/10.1108/PRT-06-2021-0060>
- Gok, B, Akpınar, D, 2020. Investigation of Strength and Migration of Corrugated Cardboard Boxes. *Hittite Journal of Science and Engineering*, 7, 163-168. <http://dx.doi.org/10.17350/HJSE19030000185>
- Gorur, YC, Larsson, PA, Wagberg, L, 2020. Self-Fibrillating Cellulose Fibers: Rapid In Situ Nanofibrillation to Prepare Strong, Transparent, and Gas Barrier Nanopapers. *Biomacromolecules*, 21, 1480-1488. <https://dx.doi.org/10.1021/acs.biomac.0c00040?ref=pdf>
- Guimarães Júnior M, Teixeira, FG, Tonoli, GHD, 2015. Preparation of cellulose nanofibrils from bamboo pulp by mechanical defibrillation for their applications in biodegradable composites. *Journal of Nanoscience and Nanotechnology* 15, 1-18. <https://doi.org/10.1166/jnn.2015.10854>
- Gupta, P, Verma, C, Maji, PK, 2019. Flame retardant and thermally insulating clay-based aerogel facilitated by cellulose nanofibers. *The Journal of Supercritical Fluids*, 152, 104537. <https://doi.org/10.1016/j.supflu.2019.05.005>
- Haslach Junior, HW, 2000. The Moisture and Rate-Dependent Mechanical Properties of Paper: A Review. *Mechanics of Time-Dependent Materials*, 4, 169-210. <https://doi.org/10.1023/A:1009833415827>
- Hashemzahi, M, Mesic, B, Sjöstrand, B, Naqvi, M, 2022. A Comprehensive Review of Nanocellulose Modification and Applications in Papermaking and Packaging: Challenges, Technical Solutions, and Perspectives. *BioResources*, 17, 1-63.
- Hofmeister, AM, Bowey, JE, 2006. Quantitative Infrared Spectra of Hydrosilicates and Related Minerals. *Monthly Notices of The Royal Astronomical Society*, 367, 577-591. <https://doi.org/10.1111/j.1365-2966.2006.09894.x>
- Huang, R, He, Li, Zhang, T, Li, D, Tang, P, Feng, Y, 2018. Novel Carbon Paper@Magnesium Silicate Composite Porous Films: Design, Fabrication, and Adsorption Behavior for Heavy Metal Ions in Aqueous Solution. *ACS Applied Materials Interfaces*, 10, 22776-22785. <http://dx.doi.org/10.1021/acsami.8b01557>
- Hubbe, MA, Venditti, RA, Rojas, OJ, 2007. What happens to cellulosic fibers during papermaking and recycling? a review. *BioResources*, 2, 739-788.
- Ikramullah, SR, Thalib, S, Huzni, S, 2014. Hemicellulose and lignin removal on typha fiber by alkali treatment. *IOP Publishing* 352, 012019. <https://doi.org/10.1088/1757-899X/352/1/012019>

- Jeevanandam, J., Chan, Y.S., Danquah, M.K, 2017. Biosynthesis and characterization of MgO nanoparticles from plant extracts via induced molecular nucleation. *New Journal of Chemistry*, 00, 1-3. <https://doi.org/10.1039/x0xx00000x>
- Jeong, S, Yoo, SR, 2020. Whey protein concentrate-beeswax-sucrose suspension-coated paperboard with enhanced water vapor and oil-barrier efficiency. *Food Packaging and Shelf Life*, 25, 100530. <https://doi.org/10.1016/j.fpsl.2020.100530>
- Jia, N, Li, SM, Ma, MG, Zhu, JF, Sun, RC, 2011. Synthesis and characterization of cellulose-silica composite fiber in ethanol/water mixed solvents. *Bioresources* 6, 1186-1195.
- Jin, F, Al-Tabbaa, A, 2013. Thermogravimetric study on the hydration of reactive magnesia and silica mixture at room temperature. *Thermochimica Acta*, 566, 162-168. <https://doi.org/10.1016/j.tca.2013.05.036>
- Jin, K, Tang, Y, Liu, J, Wang, J, Ye, C, 2021. Nanofibrillated cellulose as coating agent for food packaging paper. *International Journal of Biological Macromolecules*, 168, 331-338. <https://doi.org/10.1016/j.ijbiomac.2020.12.066>
- Khadraoui, M, Khiari, R, Bergaoui, L, Mauret, E, 2022. Production of lignin-containing cellulose nanofibrils by the combination of different mechanical processes. *Industrial Crops & Products*, 183, 114991. <https://doi.org/10.1016/j.indcrop.2022.114991>
- Khan, A, Rehmat, U, Shah, LA, Usman, M, 2020. Effect of experimental variables on the physicochemical characteristics of multi-responsive cellulose-based polymer microgels. *Colloid Chemistry and Electrochemistry* 94, 1503-1541. <https://doi.org/10.1134/S003602442007016X>
- Kotp, YH, Shelb, YA, El-Deab, MS, El-Anadouli, BE, Sawky, HA, 2017. Performance Enhancement of PA-TFC RO Membrane by Using Magnesium Silicate Nanoparticles. *Journal of Inorganic and Organometallic Polymers and Materials*, 27, 201-214. <https://doi.org/10.1007/s10904-017-0667-9>
- Kumar, P, Negi, YS, Singh, SP, 2011. Filler loading in the lumen or/and cell wall of fibers – a literature review. *BioResources*, 6, 3526-3546.
- Lengowski, EC, Bonfatti Júnior, EA, Simon, L, Muñoz, GIB, Andrade, AS, Nisgoski, S, Klock, U, 2020. Different degree of fibrillation: strategy to reduce permeability in nanocellulose-starch films. *Cellulose*, 27, 10855-10872. <https://doi.org/10.1007/s10570-020-03232-4>
- Li, SM, Jia, N, Zhu, JF, Ma, MG, Sun, RC, 2010. Synthesis of cellulose-calcium silicate nanocomposites in ethanol/water mixed solvents and their characterization. *Carbohydrate Polymers* 80, 270-275. <http://dx.doi.org/10.1016/j.carbpol.2009.11.024>

- Li, L, Zhang, M, Song, S, Yang, B, Wu, Y, Yang, Q., 2018. Preparation of core/shell structured silicate composite filler and its reinforcing property. *Powder Technology* 332, 27-32. <https://doi.org/10.1016/j.powtec.2018.03.037>
- Li, MC, Wu, Q, Moon, RJ, Hubbe, MA, Bortner, MJ, 2021. Rheological Aspects of Cellulose Nanomaterials: Governing Factors and Emerging Applications. *Advanced Materials*, 33, 2006052. <https://doi.org/10.1002/adma.202006052>
- Liu, C, Du, H, Dong, L, Wang, X, Zhang, Y, Yu, G, Li, B, Mu, X, Peng, H, Liu, H, 2017. Properties of Nanocelluloses and Their Application as Rheology Modifier in Paper Coating. *Industrial Engineering Chemistry Research*, 56, 8264-8273. <http://dx.doi.org/10.1021/acs.iecr.7b01804>
- Liu, C, Zhang, W, Song, S, Li, H, 2019. A novel method to improve carboxymethyl cellulose performance in the flotation of talc. *Mineral Engineering*, 131, 23-27. <https://doi.org/10.1016/j.mineng.2018.11.003>
- Lopes, TA, Bufalino, L, Claro, PIC, Martins, MA, Tonoli, GHD, Mendes, LM, 2018. The effect of surface modifications with corona discharge in *Pinus* and *Eucalyptus* nanofibril films. *Cellulose*, 25, 5017-5033. <https://doi.org/10.1007/s10570-018-1948-3>
- Lourenço, AF, Gamelas, JAF, Sarmiento, P, Ferreira, PJT, 2020. Cellulose micro and nanofibrils as coating agents for improved printability in office papers. *Cellulose*, 27, 6001-6010. <https://doi.org/10.1007/s10570-020-03184-9>
- Lu, P, Zhao, H, Zheng, L, Duan, Y, Wu, M, Yu, X, Yang, Y, 2022. Nanocellulose/Nisin Hydrogel Microparticles as Sustained Antimicrobial Coatings for Paper Packaging. *ACS Applied Polymer Materials*, 4, 2664-2673. <https://doi.org/10.1021/acsapm.2c00001>
- Madeira, DMF, Vieira, O, Pinheiro, LA, Carvalho, BM, 2018. Correlation between Surface Energy and Adhesion Force of Polyethylene/Paperboard: A Predictive Tool for Quality Control in Laminated Packaging. *International Journal of Chemical Engineering*, 2018, 2709037. <https://doi.org/10.1155/2018/2709037>
- Mahmoudi, M, Parviziomran, I, 2020. Reusable packaging in supply chains: A review of environmental and economic impacts, logistics system designs, and operations management. *International Journal of Production Economics*, 228, 107730. <https://doi.org/10.1016/j.ijpe.2020.107730>
- Marsh, K, Bugusu, B, 2007. Food Packaging—Roles, Materials, and Environmental Issues. *Journal of Food Science*, 72, 39-55. <https://doi.org/10.1111/j.1750-3841.2007.00301.x>
- Martins, CCN, Dias, MC, Mendonça, MC, Durães, AFS, Silva, LE, Félix, JR, Damásio, RAP, Tonoli, GHD, 2021. Optimizing cellulose microfibrillation with NaOH pretreatments for

unbleached Eucalyptus pulp. *Cellulose*, 28, 11519-11531. <https://doi.org/10.1007/s10570-021-04221-x>

Marzbani, P, Azadfallah, M, Yousefzadeh, M, Najafi, F, Pourbabae, AA, Koivula, H, Ritala, M, 2021. Effect of polyethylene wax/soy protein-based dispersion barrier coating on the physical, mechanical, and barrier characteristics of paperboards. *Journal of Coatings Technology and Research*, 18, 247-257. <https://doi.org/10.1007/s11998-020-00403-7>

Mascarenhas, ARP, Scatolino, MV, Santos, AA, Norcino, LB, Duarte, PJ, Melo, RR, Dias, MC, Faria, CET, Mendonça, MC, Tonoli, GHD, 2022a. Hydroxypropyl methylcellulose films reinforced with cellulose micro/nanofibrils: study of physical, optical, surface, barrier and mechanical properties. *Nordic Pulp Paper Research Journal*, ahead of print, 1-19. <https://doi.org/10.1515/npprj-2022-0006>

Mascarenhas, ARP, Scatolino, MV, Dias, MC, Martins, MA, Melo, RR, Damásio, RAP, Mendonça, MC, Tonoli, GHD, 2022b. Fibers pre-treatments with sodium silicate affect the properties of suspensions, films, and quality index of cellulose micro/nanofibrils. *Nordic Pulp & Paper Research Journal*, ahead-of-print, 1-19. <https://doi.org/10.1515/npprj-2022-0037>

Mejia-Ballesteros, JE, Rodier, L, Filomeno, R, Savastano Jr, H, Fiorelli, J, Rojas, MF, 2021. Influence of the fiber treatment and matrix modification on the durability of eucalyptus fiber reinforced composites. *Cement and Concrete Composites*, 124, 104280. <https://doi.org/10.1016/j.cemconcomp.2021.104280>

Meiszterics, A, Rosta, L, Peterlik, H, Rohonczy, J, Kubuki, S, Henits, P, Sinkó, K, 2010. Structural Characterization of Gel-Derived Calcium Silicate Systems. *The Journal of Physical Chemistry*, 114, 10403–10411. <https://doi.org/10.1021/jp1053502>

Mendonça, M, Dias, MC, Martins, CCN, Durães, AFS, Damásio, RAP, Tonoli, GHD, 2022. Alkaline Pretreatment Facilitate Mechanical Fibrillation of Unbleached Cellulose Pulps for Obtaining of Cellulose micro/nanofibrils (MFC). *Journal of Natural Fibers*, ahead-of-print, 1-17. <https://doi.org/10.1080/15440478.2022.2092252>

Mielonen, K, Geydt, P, Österberg, M, Johanasson, LS, Backfolk, K, 2015. Inkjet ink spreading on polyelectrolyte multilayers deposited on pigment coated paper. *Journal of Colloid and Interface Science*, 438, 179-190. <http://dx.doi.org/10.1016/j.jcis.2014.09.077>

Miller, SA, 2020. Five Misperceptions Surrounding the Environmental Impacts of Single-Use Plastic. *Environmental Science Technology*, 54, 14143-14151. <https://dx.doi.org/10.1021/acs.est.0c05295?ref=pdf>

- Minet, J, Abramson, S, Bresson, B, Sanchez, Montouillout, V, Lequeux, N, 2004. New layered calcium organosilicate hybrids with covalently linked organic functionalities. *Chemistry of Materials*, 16, 3955-3962. <https://doi.org/10.1021/cm034967o>
- Mirmehdi, S, Oliveira, MLC, Hein, PRG, Dias, MV, Sarantópoulos, CIGL, Tonoli, GHD, 2018a. Spraying Cellulose Nanofibrils for Improvement of Tensile and Barrier Properties of Writing Printing (WeP. Paper. *Journal of Wood Chemistry and Technology*, 1-13. <https://doi.org/10.1080/02773813.2018.1432656>
- Mirmehdi, S, Hein, PRG, Sarantópoulos, CIGL, Dias, MV, Tonoli, GHD, 2018b. Cellulose nanofibrils/nanoclay hybrid composite as a paper coating: Effects of spray time, nanoclay content and corona discharge on barrier and mechanical properties of the coated papers. *Food Packaging and Shelf Life*, 15, 87-94. <https://doi.org/10.1016/j.fpsl.2017.11.007>
- Mnasri, A, Dhaouadi, H, Khiari, R, Halila, S, Mauret, E, 2022. Effects of Deep Eutectic Solvents on cellulosic fibres and paper properties: Green “chemical” refining. *Carbohydrate Polymers*, 292, 119606. <https://doi.org/10.1016/j.carbpol.2022.119606>
- Morais, FP, Carta, AMMS, Amaral, ME, Curto, JMR, 2021. Micro/nano-fibrillated cellulose (MFC/NFC) fibers as an additive to maximize eucalyptus fibers on tissue paper production. *Cellulose*, 28, 6587-6605. <https://doi.org/10.1007/s10570-021-03912-9>
- Oliveira, MLC, Mirmehdi, S, Scatolino, MV, Guimarães Júnior, M, Sanadi, AR, Damásio, RAP, Tonoli, GHD, 2022. Effect of overlapping cellulose nanofibrils and nanoclay layers on mechanical and barrier properties of spray-coated papers. *Cellulose*, 29, 1097-1113. <https://doi.org/10.1007/s10570-021-04350-3>
- Otto, S, Strenger, M, Maier-Nöth, A, Schmid, M, 2021. Food packaging and sustainability – Consumer perception vs. correlated scientific facts.: A review. *Journal of Cleaner Production*, 298, 126733. <https://doi.org/10.1016/j.jclepro.2021.126733>
- Ozcan, A, Kandirmaz, EA, 2020. Natural ink production and printability studies for smart food packaging. *Color Research Application*, 45, 495-502. <https://doi.org/10.1002/col.22488>
- Ozcan, A, Sonmez, S, Tutak, D, 2021. Effect of coating pigment type on paper printability with water-based inks. *Journal of Coatings Technology and Research*, ahead of print, 1-9. <https://doi.org/10.1007/s11998-021-00593-8>
- Özgenç, O, Durmaz, S, Boyaci, IH, Eksi-Kocak, H, 2017. Determination of chemical changes in heat-treated wood using ATR-FTIR and FT Raman spectrometry. *Spectrochimica Acta Part A: Molecular and Biomolecular Spectroscopy* 171, 395-400. <https://doi.org/10.1016/j.saa.2016.08.026>

- Patel, VR, Agrawal, YK, 2011. Nanosuspension: An approach to enhance solubility of drugs. *Journal of Advanced Pharmaceutical Technology Research*, 2, 81-87. <https://dx.doi.org/10.4103%2F2231-4040.82950>
- Pawlowski, L, 2009. Suspension and solution thermal spray coatings. *Surface Coatings Technology*, 203, 2807-2829. <http://dx.doi.org/10.1016/j.surfcoat.2009.03.005>
- Prati, C, Gandolfi, MG, 2015. Calcium silicate bioactive cements: Biological perspectives and clinical applications. *Dental Materials*, 31, 351-370. <https://doi.org/10.1016/j.dental.2015.01.004>
- Predoi, D, Iconaru, SL, Predoi, MV, Motelica-Heino, M, Buton, N, Megier, C, 2020. Obtaining and Characterizing Thin Layers of Magnesium Doped Hydroxyapatite by Dip Coating Procedure. *Coatings*, 10, 510. <http://dx.doi.org/10.3390/coatings10060510>
- Puertas, F, Fernández-Jiménez, A, Blanco-Varela, MT, 2004. Pore solution in alkali-activated slag cement pastes. Relation to the composition and structure of calcium silicate hydrate. *Cement and Concrete Research*, 34, 139-148. [https://doi.org/10.1016/S0008-8846\(03\)00254-0](https://doi.org/10.1016/S0008-8846(03)00254-0)
- Rastogi, VK, Samyn, P, 2015. Bio-Based coatings for paper applications. *Coatings*, 5, 887-930. <https://doi.org/10.3390/coatings5040887>
- Ray, S, Dash, J, Devi, N, Sasmal, S, Pesala, B, 2018. Comparative Study of Hydration Kinetics of Cement and Tricalcium Silicate Using Terahertz Spectroscopy and Density Functional Theory Simulations. *Journal of Infrared, Millimeter, and Terahertz Waves*, 39, 651-666. <https://doi.org/10.1007/s10762-018-0501-7>
- Roig, F, Dantras, E, Dandurand, J, Lacabanne, C, 2011. Influence of hydrogen bonds on glass transition and dielectric relaxations of cellulose. *Journal of Physics D: Applied Physics*, 44, 045403. <http://dx.doi.org/10.1088/0022-3727/44/4/045403>
- Rol, F, Belgacem, MN, Gandini, A, Bras, J, 2019. Recent advances in surface-modified cellulose nanofibrils. *Progress in Polymer Science*, 88, 241-264. <https://doi.org/10.1016/j.progpolymsci.2018.09.002>
- Roosz, C, Grangeon, S, Blanc, P, Montouillout, V, Lothenbach, B, Henocq, P, Giffaut, E, Vieillard, P, Gaboreau, S, 2015. Crystal structure of magnesium silicate hydrates (M-S-H): The relation with 2:1 Mg-Si phyllosilicates. *Cement and Concrete Research*, 73, 228-237. <https://doi.org/10.1016/j.cemconres.2015.03.014>
- Rotermel, MV, Samigullina, RF, Ivanova, IV, Baklanova, IV, Krasnenko, TI, (2021). Synthesis of the Synthesis of the $Zn_{1.9}Cu_{0.1}SiO_4$ pigment via the sol-gel and coprecipitation methods. *Journal of Sol-Gel Science and Technology*, 100, 404-413. <https://doi.org/10.1007/s10971-021-05648-1>

- Rueden, CT, Schindelin, J, Hiner, MC, DeZonia, BE, Walter, AE, Arena, ET, Eliceiri, KW, 2017. ImageJ2: ImageJ for the next generation of scientific image data. *BMC Bioinformatics* 18, 529. <https://doi.org/10.1186/s12859-017-1934-z>
- Sadek, DM, El-Attar, MM, Ali, HA, 2016. Reusing of marble and granite powders in self-compacting concrete for sustainable development. *Journal of Cleaner Production*, 121, 19-32. <http://dx.doi.org/10.1016/j.jclepro.2016.02.044>
- Saedi, S, Garcia, CV, Kim, JT, Shin, GH, 2021a. Physical and chemical modifications of cellulose fibers for food packaging applications. *Cellulose*, 28, 8877-8897. <https://doi.org/10.1007/s10570-021-04086-0>
- Saedi, A, Jamshidi-Zanjani, A, Darban, AK, 2021b. A review of additives used in the cemented paste tailings: Environmental aspects and application. *Journal of Environmental Management*, 289, 112501. <https://doi.org/10.1016/j.jenvman.2021.112501>
- Salmén, L, Larsson, PA On the origin of sorption hysteresis in cellulosic materials., 2018. *Carbohydrate Polymers*, 182, 15-20. <http://dx.doi.org/10.1016/j.carbpol.2017.11.005>
- SCAN Standard, 2000. SCAN-C 62:00, Chemical pulp – Water retention value.
- Scatolino, MV, Bufalino, L, Dias, MC, Mendes, LM, Silva, MS, Tonoli, GHD, Souza, TM, Alves Junior, FTA, 2022. Copaiba oil and vegetal tannin as functionalizing agents for açai nanofibril films: valorization of forest wastes from Amazonia. *Environmental Science and Pollution Research*, in press, p. 1-16.
- Selvam, NCS, Kumar, RT, Kennedy, LJ, Vijaya, JJ, 2011. Comparative study of microwave and conventional methods for the preparation and optical properties of novel MgO-micro and nano-structures. *Journal of Alloys and Compounds*, 509, 9809-9815. <https://doi.org/10.1016/j.jallcom.2011.08.032>
- Shen, Z, Rajabi-Abhari, A, Oh, K, Yang, G, Youn, HJ, Lee, HL, 2021. Improving the Barrier Properties of Packaging Paper by Polyvinyl Alcohol Based Polymer Coating—Effect of the Base Paper and Nanoclay. *Polymers*, 13, 1334. <https://doi.org/10.3390/polym13081334>
- Shenoy, R, Shetty, P, 2022. New Eco-friendly Coating Formulations for Recycled Paperboards: Effect on Print Quality and Ink Volume Consumption. *Progress in color, colorants and coatings*, 15, 175-189. <https://dx.doi.org/10.30509/pccc.2021.166804.1110>
- Silva, LCE, Cassago, A, Batirrola, LC, Gonçalves, MC, Portugal, RV, 2020. Specimen preparation optimization for size and morphology characterization of nanocellulose by TEM. *Cellulose*, 27, 5435-5444. <https://doi.org/10.1007/s10570-020-03116-7>
- Silva, LE, Santos, AA, Torres, L, McCaffrey, Z, Klamczynski, A, Glenn, G, Sena Neto, AR, Wood, D, Williams, T, Orts, W, Damásio, RAP, Tonoli, GHD, 2021. Redispersion and

- structural change evaluation of dried microfibrillated cellulose. *Carbohydrate Polymers*, 252,117165. <https://doi.org/10.1016/j.carbpol.2020.117165>
- Spinthaki, A, Petratos, G, Matheis, J, Hater, W, Demadis, KD, 2018. The precipitation of “magnesium silicate” under geothermal stresses. Formation and characterization. *Geothermics*, 74, 172-180. <https://doi.org/10.1016/j.geothermics.2018.03.001>
- Tanzadeh, R, Shafabakhsh, G, 2020. Surface free energy and adhesion energy evaluation of modified bitumen with recycled carbon black (micro-nano. from gases and petrochemical waste. *Construction and Building Materials*, 245, 118361. <https://doi.org/10.1016/j.conbuildmat.2020.118361>
- TAPPI Standard, 2002. T 211 om-02, Ash in wood, pulp, paper and paperboard: combustion at 525 °C.
- TAPPI Standard, 2014. T 458 cm-14, Surface wettability of paper (angle of contact method).
- Tang, S, Wang, Y, Geng, Z, Xu, X, Yu, W, Hubao, A, Chen, J, 2021. Structure, Fractality, Mechanics and Durability of Calcium Silicate Hydrates. *Fractal and Fractional*, 5, 47. <https://doi.org/10.3390/fractalfract5020047>
- Thébault, M, Kandelbauer, A, Müller, U, Zikulnig-Rusch, E, Lammer, H, 2017. Factors influencing the processing and technological properties of laminates based on phenolic resin impregnated papers. *European Journal of Wood and Wood Products*, 75, 785-806. <https://doi.org/10.1007/s00107-017-1205-8>
- Tonoli, GHD, Rodrigues Filho, UP, Savastano Júnior, H, Bras, J, Belgacem, MN, Lahr, FAR, 2009. Cellulose modified fibres in cement-based composites. *Composites Part A: Applied Science and Manufacturing*, 40: 2046-2053. <https://doi.org/10.1016/j.compositesa.2009.09.016>
- Tonoli, GHD, Holtman, K, Silva, LE, Wood, D, Torres, L, Williams, T, Oliveira, JE, Fonseca, AS, Klamczynski, A, Glenn, G, Orts, W, 2021. Changes on structural characteristics of cellulose pulp fiber incubated for different times in anaerobic digestate. *Cerne*, 27, e102647. <https://doi.org/10.1590/01047760202127012647>
- Tsai, CF, Hung, CH, Kuo, CN, Chen, CY, Peng, YN, Shie, MY, 2019. Improved Bioactivity of 3D Printed Porous Titanium Alloy Scaffold with Chitosan/Magnesium-Calcium Silicate Composite for Orthopaedic Applications. *Materials*, 12, 203. <http://dx.doi.org/10.3390/ma12020203>
- Tyagi, P, Salem, KS, Hubbe, MA, Pal, L, 2021. Advances in barrier coatings and film technologies for achieving sustainable packaging of food products – A review. *Trends in Food Science Technology*, 115, 461-485. <https://doi.org/10.1016/j.tifs.2021.06.036>

- Wang, Y, Wang, G, Wang, H, Liang, C, Cai, W, Xhang, L, 2010. Chemical-Template Synthesis of Micro/Nanoscale Magnesium Silicate Hollow Spheres for Waste-Water Treatment. *Chemistry A European Journal*, 15, 3497-3503. <http://dx.doi.org/10.1002/chem.200902799>
- Wang, J, Gardner, DJ, Stark, NM, Bousfield, DW, Tajvidi, M, Cai, Z, 2018. Moisture and oxygen barrier properties of cellulose nanomaterial-based films. *ACS Sustainable Chemistry Engineering*, 6, 49-70. <http://dx.doi.org/10.1021/acssuschemeng.7b03523>
- Wang, L, Chen, L, Cho, DW, Tsang, DCW, Yang, J, Hou, D, Baek, K, Kua, HW, Poon, CS, 2019. Novel synergy of Sci-rich minerals and reactive Mg. for stabilization/solidification of contaminated sediment. *Journal of Hazardous Materials* 365, 695-706. <https://doi.org/10.1016/j.jhazmat.2018.11.067>
- Wang, L, Chen, C, Wang, J, Gardner, DJ, Tajvidi, M, 2020. Cellulose Nanofibrils versus Cellulose Nanocrystals: comparison of performance in flexible multilayer films for packaging applications. *Food Packaging and Shelf Life*, 23, 100464. <https://doi.org/10.1016/j.fpsl.2020.100464>
- Wang, FJ, Wang, LQ, Zhang, XC, Ma, SF, Zhao, ZC, 2022. Study on the barrier properties and antibacterial properties of cellulose-based multilayer coated paperboard used for fast food packaging. *Food Bioscience*, 46, 101398. <https://doi.org/10.1016/j.fbio.2021.101398>
- Wohlert, M, Bensefelt, T, Wagberg, L, Furó, I, Berglund, LA, Wohlert, J, 2022. Cellulose and the role of hydrogen bonds: not in charge of everything. *Cellulose*, 29, 1-23. <http://dx.doi.org/10.1016/j.carbpol.2017.11.005>
- Xu, K, Deng, J, Lin, R, Zhang, H, Ke, Q, Huang, C, 2020. Surface Fibrillation of Para-aramid Nonwoven as a Multi-functional Air Filter with Ultralow Pressure Drop. *Journal of Materials Chemistry A*, 1-13. <https://doi.org/10.1039/D0TA07886G>
- Yongabi, D, Khorshid, M, Gennaro, A, Jookan, S, Duwé, S, Deschaume, O, Losada-Pérez, P, Dedecker, P, Bartic, C, Wübbernhorst, M, Wagner, P, 2020. QCM-D Study of Time-Resolved Cell Adhesion and Detachment: Effect of Surface Free Energy on Eukaryotes and Prokaryotes. *ACS Applied Materials Interfaces*, 12, 18258-18272. <https://dx.doi.org/10.1021/acsmi.0c00353>
- Yu, Z, Dhital, R, Wang, W, Sun, L, Zeng, W, Mustapha, A, Lin, M, 2019. Development of multifunctional nanocomposites containing cellulose nanofibrils and soy proteins as food packaging materials. *Food Packaging and Shelf Life*, 21, 100366. <https://doi.org/10.1016/j.fpsl.2019.100366>
- Zhang, K, Zhang, Y, Yan, D, Zhang, C, Nie, S, 2018b. Enzyme-assisted mechanical production of cellulose nanofibrils: thermal stability. *Cellulose* 25, 5049-5061. <https://doi.org/10.1007/s10570-018-1928-7>

- Zhang, T, Zou, J, Wang, B, Wu, Z, Jia, Y, Cheeseman, CR, 2018b. Characterization of Magnesium Silicate Hydrate (MSH) Gel Formed by Reacting MgO and Silica Fume. *Materials*, 11, 909. <https://doi.org/10.3390/ma11060909>
- Zhao, Z, Li, Z, Cui, P, Li, S, Kong, L, 2015. Adsorption of Basic Brown and Chrysophenine from Water Solution by Magnesium Silicate Gel. *Journal of Chemistry*, 2015, 1-7. <http://dx.doi.org/10.1155/2015/374190>
- Zhao, T, Jiang, L, 2018. Contact angle measurement of natural materials. *Colloids and Surfaces B: Biointerfaces*, 161, 324-330. <https://doi.org/10.1016/j.colsurfb.2017.10.056>
- Zołek-Tryznowska, Z, Prica, M, Pavlovic, Z, Cveticanin, Annusik, T, 2020. The influence of aging on surface free energy of corona treated packaging films. *Polymer Testing*, 89, 106629. <https://doi.org/10.1016/j.polymertesting.2020.106629>
- Zołek-Tryznowska, Z, Kałuza, A, 2021. The Influence of Starch Origin on the Properties of Starch Films: Packaging Performance. *Materials*, 14, 1146. <https://doi.org/10.3390/ma14051146>

TERCEIRA PARTE - CONCLUSÃO DA TESE

Ocorreu redução do índice de cristalinidade para as MFC/NFC de *Eucalyptus* com o uso de 5% e 10% de silicato de sódio. O uso de 10% de silicato de sódio mostrou-se eficaz como facilitador do processo de fibrilação devido à maior individualização das MFC/NFC e redução do consumo energético em, no mínimo, 45% para *Eucalyptus* sp. e em 53% para *Pinus* sp (Artigo 1).

O maior índice de qualidade foi encontrado para as MFC/NFC de *Pinus* sp. obtidas a partir do pré-tratamento com 10% de silicato de sódio (>70). Os demais pré-tratamentos resultaram em MFC/NFC com índices de qualidade semelhantes (~60). Os pré-tratamentos com silicato de sódio influenciaram quase todas as propriedades das suspensões e dos filmes resultantes, melhorando as propriedades de barreira à luz, vapor de água e óleo e propriedades de físicas e mecânicas dos filmes (Artigo 2).

Os pré-tratamentos com silicato de cálcio reduziram a retenção de água nas fibras e o consumo de energia por volta de ~30% na produção de MFC/NFC em relação às fibras não tratadas. A formação de camadas com micro/nanofibrilas com silicatos na superfície e abaixo da superfície do papel cartão reduziram a difusão de vapor de água, tornando o papel adequado para aplicação em embalagens de pão, queijo, frutas e vegetais. As MFC/NFC sem pré-tratamentos, pré-tratadas com 5% e 10% de silicato de cálcio aumentaram o espalhamento de água na superfície do papel. Os revestimentos também aumentaram a dispersão de agentes colantes e tintas na superfície do papel. Os revestimentos aumentaram a formabilidade do papel, o que potencializa a formabilidade do material para aplicações em embalagens com diferentes formatos (Artigo 3).

O uso do silicato de sódio não foi interessante para produção de MFC/NFC visando sua aplicação no revestimento de papel cartão, pois foi observado que os filmes se tornaram muito hidrofílicos e isso poderia prejudicar as propriedades do papel. O silicato de cálcio e o silicato de magnésio permitiram obter MFC/NFC funcionalizadas devido à maior impregnação destes materiais na superfície da celulose (Artigo 3), enquanto que para silicato de sódio a impregnação foi baixa, o que destaca sua aplicação como agente alcalino (Artigo 1).

Sugere-se a realização de trabalhos visando otimizar as técnicas de aplicação e secagem para formulações de MFC/NFC e silicatos visando melhorar as propriedades mecânicas e de barreira dos papéis de embalagem. Neste trabalho não foram estudadas as propriedades técnicas dos papéis revestidos. O silicato de cálcio e o silicato de magnésio são empregados como isolantes térmicos, assim seria interessante avaliar se os papéis revestidos apresentaram redução

da condução de calor através das fibras, sendo esta uma característica interessante para embalagens.

Estudos mais aprofundados sobre os mecanismos químicos envolvidos no processo de interação dos silicatos com a celulose também são necessários para melhor entendimento das variações dos parâmetros das suspensões e revestimentos do papel cartão com MFC/NFC. Um estudo a ser feito neste sentido seria a adição estequiométrica dos silicatos com base na capacidade de saturação dos grupos -OH da celulose. Outro estudo interessante a ser realizado seria a produção de aerogel com as MFC/NFC obtidas neste trabalho.

O estudo da mistura das MFC/NFC obtidas com outros polímeros biodegradáveis (álcool polivinílico, látex, amido, proteína de soja, hidroxipropilmetilcelulose, carboximetil celulose, quitosana e poli(ácido láctico)) seria uma possibilidade importante tendo em vista a necessidade de aumentar o teor de sólidos das formulações visando reduzir a quantidade de camadas no revestimento de papel. Além disso, estudos voltados para avaliar outros métodos de secagem dos revestimentos utilizando, por exemplo, infravermelho ou ultravioleta são importantes para se reduzir o efeito de higroplastificação do papel devido ao processo de umectação e secagem com temperaturas acima de 100 °C. Para isso, seria interessante investigar diferentes temperaturas, velocidade de aplicação da radiação infravermelho ou ultravioleta e também o tempo de exposição.

O estudo de outros métodos de aplicação das formulações de MFC/NFC para revestimento de papel também pode ser realizado. Algumas possibilidades que poder ser exploradas seriam o *bird film applicator*, *wire bar*, aplicação por spray e aplicação pelo método de cortina. Com essas opções é possível estudar a aplicação de menos camadas com maior conteúdo de suspensão para revestimento. Considerando a máquina para revestimento laboratorial utilizada neste estudo, também existem possibilidades de explorar mais alternativas. Por exemplo, outras combinações de barras de espalhamento com estrias mais espaçadas podem viabilizar a obtenção de revestimentos mais espessos, com maior gramatura e com menos camadas.

Outra sugestão seria aplicar as suspensões de MFC/NFC produzidas no presente trabalho em outros tipos de papel e utilizar os papéis revestidos como substituto de camadas de polímeros à base de petróleo em embalagens multicamadas. Ou ainda, analisar se os revestimentos aplicados ao papel cartão apresentam capacidade de encapsulamento de outras moléculas no papel (óleos, ácidos, minerais) com vistas à obtenção de embalagens funcionalizadas para inibir maturação de frutos, eliminar vírus e bactérias, liberação lenta de compostos químicos, entre outras possibilidades.